The *Bacillus anthracis* two-component system signaling response to host stressors.

By

Clare Lynn Laut

Dissertation

Submitted to the Faculty of the

Graduate School of Vanderbilt University

in partial fulfillment of the requirements

for the degree of

DOCTOR OF PHILOSOPHY

In

Microbe-Host Interactions

May 14, 2021

Nashville, Tennessee

Approved:

James E. Crowe Jr., M.D.

David M. Aronoff, M.D.

James E. Cassat, M.D., Ph.D.

Maria Hadjifrangiskou, Ph.D.

C. Henrique Serezani, Ph.D.

Eric P. Skaar, Ph.D., M.P.H

ACKNOWLEDGMENTS

My appreciation must first be shared with my thesis mentor, Dr. Eric Skaar. The opportunity to work with such an intelligent and creative scientist is something that I will always value. Both at the bench and beyond it, you have taught me the value of taking a moment to think and the importance of a thorough plan. Under your guidance, I was able to grow from a scattered student wanting all the answers into a scientist with an appreciation for the important ones. Thank you for always providing clear feedback on countless pieces of data, abstracts and presentations. Thank you for never once pushing me into something that I am not and accepting the goals I have strived for. You have taught me to never be okay with the minimum and to continuously push yourself and those around you to just be better. I have learned to face each new challenge with a stubborn determination, especially those that have impact beyond the bench. I will always look back fondly on our conversations in your office that started out just plain intimidating, but ended up entirely motivating and reassuring. Thank you for all of this and for building us a community of people full of support and curiosity. I will always be appreciative.

Thank you to all members of the Skaar laboratory, past and present. Each of you have contributed to this body of work through your experimental guidance, critical feedback, and thoughtful questions. Without the opportunity to discuss my scientific progress with you all, this Thesis would not be what it has become. A massive thanks goes to Nichole Lobdell and Nichole Maloney for your guidance and support. You both work so hard to keep our laboratory functional and organized. Thank you to all of the staff; Valeria Garcia, Amber Petoletti, Anderson Miller and Sydney Drury, for working with these incredible managers to provide the resources for the lab that

allows the science to progress. Thank you to Jacob Choby, Monique Bennett, Reece Knippel, and Zach Lonergan who set the example for how to be a successful student in this lab. To Hualiang Pi, my *Bacillus* bud, thank you for always being there to listen to my crazy theories and provide sound advice. To the postdocs who have supported me, challenged me, questioned me, and taught me – thank you Chris Lopez, Jessica Sheldon, Andy Weiss, Erin Green, Joe Zackular, Lauren Palmer, Caroline Grunenwald, Dillon Kunkle, Cait Murdoch, Aaron Wexler, Valeria Reyes Ruiz, Andrew Monteith, and Will Beavers. Thank you to my graduate student peers Matt Munneke, Catherine Leasure, and Jeanette Miller for the comradery. All of you collectively have been a wonderful source of laughter and intense motivation, something I will always remember.

Beyond the members of the Skaar laboratory who I have been fortunate enough to work alongside, I also need to thank some alumni. Thank you to Laura Mike for laying the foundation for an excellently challenging project; you started a puzzle that I have worked on carefully and one that I look forward to someday seeing solved. Thank you for all of the strains and tools that I inherited that helped me to get my start at the bench. Additionally, is not an overstatement to say that this Thesis would not have been possible without the help of Devin Stauff. Thank you, Devin, for sharing your expertise, clones, students and kindness with me. Starting back at the basics of *B. anthracis* biology on to the nuances of your genetics strategies, you have taught me so much. Thank you to your students Sam Ivan, Michelle Chu, Allen Toth, Alexander Metzger, Jonathan Mathes, Michelle Chu, Amber Leston, Alexis Schmid, Brandy Ndirangu, Amanda Hasley, Betsy Ysais, Hannah Lin, Gideon Hillebrand, Sophia Carlin, Colleen Yi, Xinjie Yi, and Lurena Stewart for their time and dedication to mutant generation and the screening of our selection strains.

Thank you to Chris Aiken, Lorie Franklin, and Liz Roelofsz for the personal support you provided and for the general management of the Microbe-Host Interactions training program.

Beyond the PMI department, I need to thank the leaders of the Office of Biomedical Research Education & Training for the career development support, guidance and assistance getting started here at Vanderbilt. Special thanks also to Starr Hollyfield, Helen Chomicki, and Zeon Sayni along with the administrative team at VI4. None of who have ever hesitated to help me when I come looking for assistance; you are a valuable resource to the trainees in our community.

Thank you to my Thesis Committee, which includes Chair Jim Crowe, Dave Aronoff, Jim Cassat, Henrique Serezani, and Maria Hadjifrangiskou. I appreciate the attention, feedback and advice you have each provided me. Thank you for the letters of recommendation and references you have provided in my support. I recognize the time commitment that must be made by each of you, and I am grateful your willingness to support my graduate training and my career dreams.

Next I need to thank all of the collaborators who I have worked with during my tenure at Vanderbilt. Already mentioned above is Devin Stauff and his lab who have provided me with countless *B. anthracis* mutants utilized in Chapters II-IV, I am indebted to this team as they also performed the screening that identified the proteins TCS accessory proteins ClpX and DnaJ discussed in Chapter III. Will Perry directly contributed to Chapter II through the quantification of cardiolipin. Thank you to Microbial Genome Sequencing Center at the University of Pittsburgh for the whole genome sequencing performed in Chapter III. Thank you to Nick Mignemi for the countless hours of microscopy image collection and data analysis as presented in Chapter IV. The compounds targocil and ‘205 presented in Chapters II, III and IV were synthesized by Brendan Dutter from Vanderbilt University and Mary MacDonald and Scott Joseph at Walter Reed Army Institute of Research, respectively. Thank you to Terry Koehler at The University of Texas Health Science Center at Houston for generously sharing your expression vectors and transposon system for *Bacillus anthracis* as discussed in Chapter III. Daniel Hassett from University of Cincinnati

College of Medicine shared the constitutively fluorescent strains of *B. anthracis* utilized repeatedly in Chapter IV. The precision lung slices presented in Chapter IV were provided by Jen Sucre and Chris Jetter. A special thanks must go to Andrew Monteith for his assistance in all work involving the primary macrophages in Chapter IV, especially the macrophage infection experiments.

Thank you to the funding sources that supported this Thesis work. I was funded using the National Institute of Health (NIH) training program in environmental toxicology T32 ES007028. Eric Skaar was supported through the NIH via R01 AI101171-09, R01 AI073843-11, R01 AI50701-01, R01 AI069233-15, and R01 AI138581-02. Additional funding was provided by the Ernest W. Goodpasture professorship to Eric Skaar. The Department of Defense BA160565 funded Eric Skaar, Sydney Drury, and Anderson Miller. Devin Stauff and his students were funded by Grove City College Swezey Fund and the Jewell, Moore, and MacKenzie Fund. Will Perry was funded by NIH/National Institute of General Medical Sciences 2P41 GM103391-07. Imaging experiments, data analysis, and were performed in part through the use of the Vanderbilt Cell Imaging Shared Resource that is supported by NIH grants CA68485, DK20593, DK58404, DK59637 and EY08126.

Lastly I would like to thank my family and friends. To Mike and Josi, thank you for becoming my family since I started this Thesis and providing me with endless support, joy and love. To my parents, you have shaped me and guided me into the woman who earned this degree. I am forever grateful to you and our whole family, all the aunts and uncles and cousins, for always welcoming me home. To Nicole Brodzik, girl, you are the best friend a girl could ever ask for. Thank you for always listening, building me back up, and making me smile. Thank you to my lifelong friends Kevin Kramer, Megan Kechner, Kali Allis, and Marissa Hur for always being there for me. To everyone, thank you.

TABLE OF CONTENTS

LIST OF TABLES

LIST OF FIGURES

Figure Page

LIST OF ABBREVIATIONS

BMMφs	bone marrow-derived macrophages
CFU	colony forming unit
CL	cardiolipin
Clp	caseinolytic protease
EF	edema factor
EtBR	ethidium bromide
GFP	green fluorescent protein
HK	histidine kinase
LC-MS/MS	liquid chromatography with tandem mass spectrometry
LF	lethal factor
MGM	modified G medium
MOI	multiplicity of infection
OD	optical density
PA	protective antigen
RNS	reactive nitrogen species
ROS	reactive oxygen species
RR	response regulator
SIM	structured illumination microscopy
SOPi	scanned oblique plane illumination microscopy
TCS	two-component system
WTA	wall teichoic acid

CHAPTER I

INTRODUCTION

Bacillus anthracis is the causative agent of anthrax.

The zoonotic pathogen *Bacillus anthracis* is a Gram-positive, spore-forming bacilli. *B. anthracis* is found globally within soil environments. Though nearly two billion people live in regions where this pathogen can be found, the chance of exposure is low [1]. The most at-risk groups, primarily humans and livestock, are concentrated in rural areas of Eurasia, Africa, and North America where the climate is arid and temperate. In these regions, where agricultural systems rely on rainwater for irrigation purposes, low vaccination frequency compounded with mixing of soil with water sources results in an increased infection opportunity [1-5]. The growing public health threat of anthrax in sub-saharan Africa resulted in the placement of *B. anthracis* as the highest priority zoonotic disease for which advancements need to be made by local governments in collaboration with the Global Health Security Agenda [6, 7]. Despite the low global rate of natural infection, *B. anthracis* is a well-known risk to human health as it has been used as a bioterror weapon [8-11]. In September of 2001, at least four letters containing *B. anthracis* spores were shipped through the United States Postal Service, making this pathogen one of only two biologics successfully used as a weapon in the United States [12, 13]. This attack, later termed the Amerithrax Attack, resulted in the infection of 22 individuals, five of whom succumbed to anthrax [13, 14].

There are three infectious syndromes that can result from exposure to *B. anthracis* spores: cutaneous anthrax, gastrointestinal anthrax, and inhalation anthrax [8, 10, 15]. The severity of infection directly correlates with the route of spore introduction. Cutaneous anthrax comprises

95% of reported anthrax cases and is by far the least severe clinically [16]. In less than 1% of untreated cases, mortality occurs after formation of a characteristic black edema [17]. In contrast to this, exposure of the spores to the internal cavities of the body poses a greater risk of death to the patient with mortality for inhalation anthrax approaching 90% in untreated cases [18].

B. anthracis carries two plasmids, pXO1 and pXO2, which encode for the primary virulence factors produced by the pathogen. pXO1 encodes for the three anthrax toxins used for dissemination, tissue destruction, and disruption of central host immune signaling pathways. The toxins consist of three proteins that come together as a binary complex to target host cells. Protective antigen (PA) complexes with either lethal factor (LF) or edema factor (EF) and acts as a delivery system for the associated toxic factor (Fig. 1-1). Upon interaction with either capillary morphogenesis protein 2 (CMG2) or tumor endothelial marker 8 (TEM8) on the host cell, PA will undergo proteolysis-activated conformational changes that result in receptor-mediated endocytosis of LF and EF into the cell [10]. LF is a zinc metalloprotease that disrupts mitogen-activated protein-kinase (MAPK) signaling through the specific cleavage of mitogen-activated protein-kinase-kinase (MAPKK) (Fig. 1-1) [10]. EF is an adenylate cyclase that rapidly increases levels of cAMP, a key second messenger in eukaryotic cells, resulting in cellular edema (Fig. 1-1) [10]. Intoxication with LF and EF distorts intracellular signaling, often leading to cellular apoptosis [19-21]. The second plasmid, pXO2, encodes the poly γ-D-glutamic acid capsule which functions in immune evasion, particularly in shielding the bacilli from phagocytosis [10, 22, 23]. To study this professional pathogen, the Sterne strain, which is lacking pXO2 and is therefore attenuated for virulence, can be used in Biosafety Level 2 conditions without compromising standard bacterial physiology [24]. Since its discovery in the 1930s, *B. anthracis* strain Sterne has been used for the vaccination of livestock [25]. Sterne and corresponding isogenic mutants were used in all studies

presented in this dissertation. The activity of these virulence factors, in combination with optimized adaptation mechanisms, supports uncontrolled systemic growth and prevents host killing of *B. anthracis* leading to hypotension, shock, and death [8].

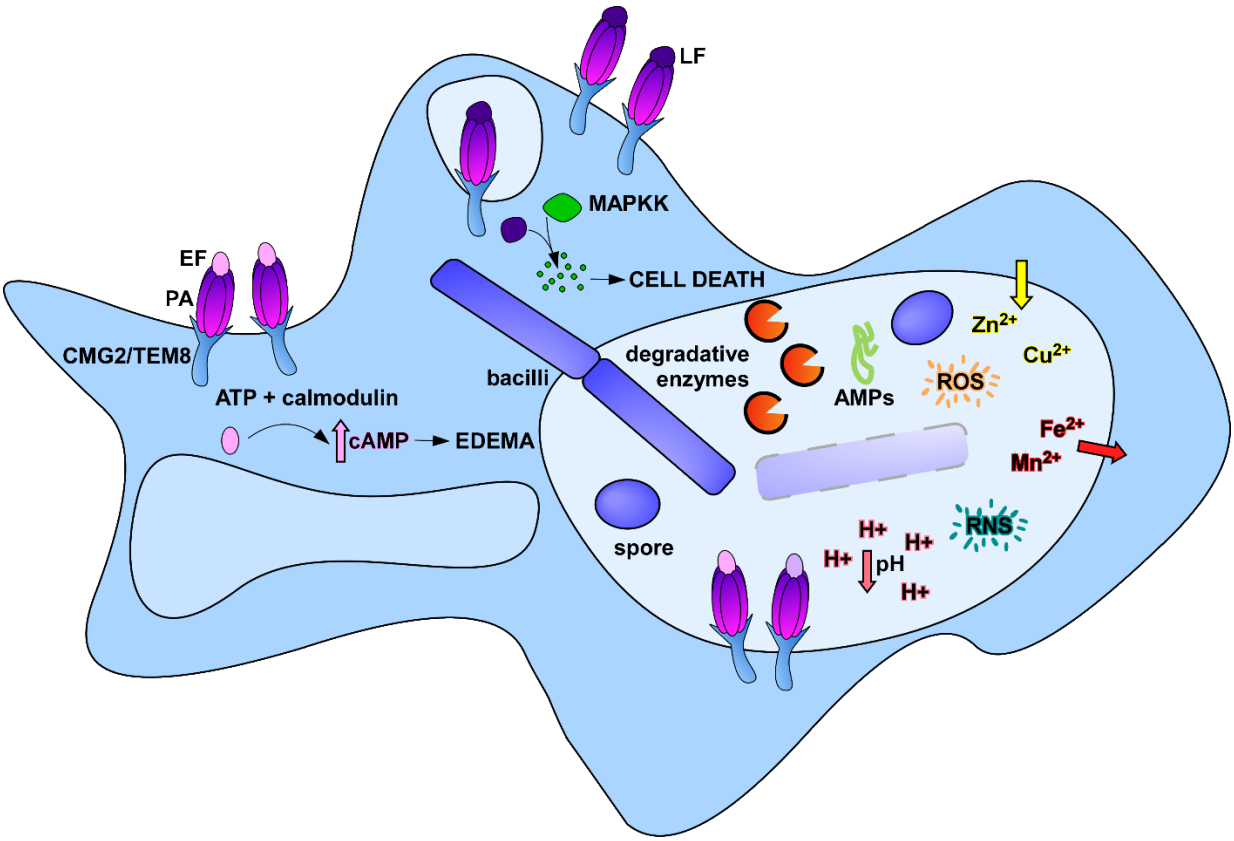

Figure 1-1. The host-pathogen interface for *B. anthracis* and phagocytic cells. A representation of the interactions between *B. anthracis* and phagocytic cells. Within the phagolysosome, antibacterial strategies include decreased pH, production of reactive oxygen and nitrogen species (ROS, RNS), metal starvation (decreased iron and manganese), metal intoxication (influx of zinc and copper), and production of antimicrobial peptides and degradative enzymes (proteases, glycanases, and lipases). The anthrax toxins exert damaging effects by increasing cellular cAMP levels (edema factor, EF) and cleaving MAPKK (lethal factor, LF). LF and EF are delivered by protective antigen (PA) which interacts with host receptors (CMG2 and TEM8) to trigger receptor-mediated endocytosis.

Host innate immune response facilitates *B. anthracis* systemic infection.

The innate immune response is critical for host survival during *B. anthracis* infection. Immune cell depletion models of anthrax highlight the importance of macrophages and neutrophils in controlling disease severity and impacting survival outcomes [26, 27]. Innate immunity is activated by the presence of pathogen-associated molecular patterns (PAMPs) through the activity of Toll-like receptors (TLRs) on the surface of cells. *B. anthracis* PAMPs include the well characterized Gram-positive components such as teichoic acid and lipoteichoic acid, but peptidoglycan is the primary driver of immune activation [28-30]. Detection of pathogens by TLRs triggers uptake of the invader as well as the production of proinflammatory cytokines and chemokines. Upon detection of *B. anthracis,* the p38, ERK, and SAP/JNK pathways are activated within macrophages and resident epithelial cells [31, 32]. The immunomodulatory products that are produced recruit circulating immune cells to the site of infection where *B. anthracis* spores are efficiently phagocytosed (Fig. 1-2). Phagocytic cells then immediately begin the process of pathogen clearance.

B. anthracis spores are highly resistant to desiccation, heat, and UV treatment [33]. The phagolysosome, where spores are localized, is effective at controlling early infection to reduce disease progression despite the vigor of this pathogen (Fig. 1-1) [34]. Maturation of the phagolysosome begins with a decrease in pH through the activity of V-ATPases [35]. The acidic environment, though damaging to the pathogen, functions to promote activation of hydrolytic enzymes such as cathepsins, proteases, lysozymes, and lipases [36]. Additional stress is exerted on the bacteria through the depletion of nutrients, such as essential metals, by scavenger molecules such as lactoferrin and lipocalin or export pumps such as NRAMP1 [34]. Damage to the pathogen exterior is driven primarily by antimicrobial peptides and the production of reactive oxygen species

(ROS) by NADPH oxidase and myeloperoxidase [34, 37-39]. Collectively, these mediate bacterial killing (Fig. 1-1). 90% of internalized *B. anthracis* are killed *in vitro* by immune cells [40, 41]. The remaining bacterial spores that withstand the initial attack will germinate into vegetative cells inside the phagocytes [42-46]. Intracellular expression of anthrax toxins affects MAPK and cAMP signaling pathways which alters chemotaxis and activation of immune cells [47, 48]. During inhalation anthrax, *B. anthracis* that persist beyond phagocytic attack are capable of hijacking host phagocytes such as macrophages and dendritic cells while e*n route* to the lymph nodes right with nutrients such as lipids and plasma proteins [49-54](Fig. 1-2). *B. anthracis*-containing dendritic cells downregulate tissue homing receptors and upregulate lymph node homing receptors, a process that is enhanced by ET and PA activity [52, 55, 56]. After initial infection, *B. anthracis* bacilli are first detected in the lymph nodes prior to hematogenous spread [54, 57, 58]. The bacilli are capable of intracellular replication as the anthrax toxins exert their damaging effects to alter key signaling pathways as described above [42, 45, 46, 52]. Dissemination studies demonstrated the requirement for the capsule, anthrax toxins, and bacterial proteases for sepsis [59, 60]. After escaping into the bloodstream, the toxin-producing bacilli grow to high bacterial titers, resulting in systemic infection that overwhelms the host within a matter of days (Fig. 1-2) [11].

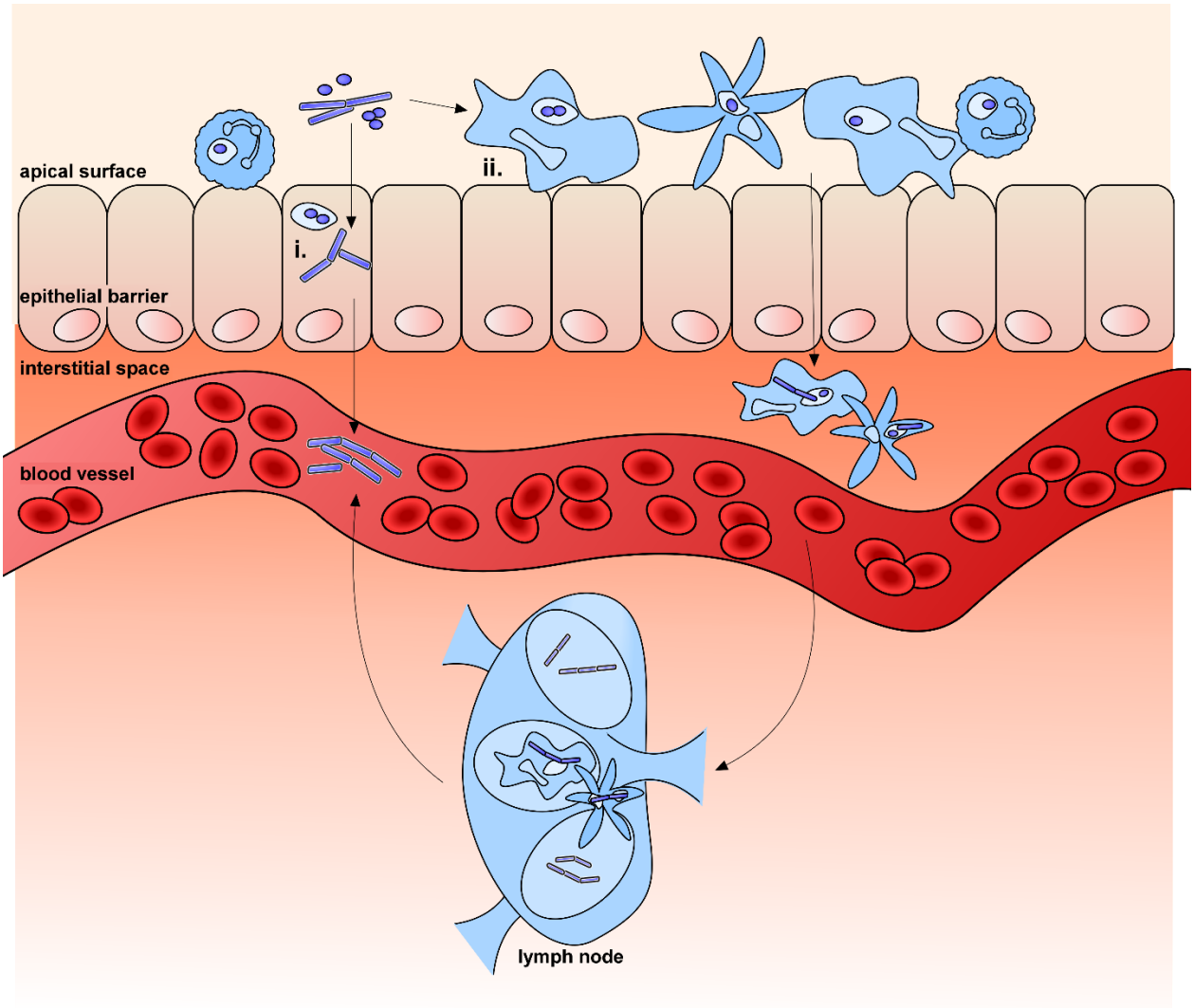

Figure 1-2. **Model for dissemination of *B. anthracis*.** The site of *B. anthracis* infection can include the epithelial layer at the skin surface, in the lung, and in the gastrointestinal tract. Spores are phagocytosed by immune cells and other resident tissue cells. Possible models of dissemination include (i) intracellular germination of spores followed by toxin-mediated translocation of bacilli to the bloodstream, and (ii) transport of intracellular bacilli to the regional lymph node by antigen presenting cells prior to escape to the bloodstream as encapsulated bacteria.

Pathogens must resolve the heme paradox during infection.

Iron is an essential nutrient to almost all bacterial pathogens during infection [61, 62]. Iron readily fluctuates between redox states providing a strong advantage as a catalyst and electron carrier within proteins [63]. Pathogens seek out iron to populate oxidoreductase, nitrogenase, hydrogenase, dehydrogenase, and hydratase enzymes with iron or iron-sulfur clusters [64]. 75% of the iron in the human body is stored as a heme cofactor within hemoproteins [65]. To successfully infect the host, pathogens evolved mechanisms to scavenge heme from hemoglobin, the oxygen-carrying component of red blood cells, as their preferred iron source [66-69]. This is particularly advantageous for *B. anthracis*, as systemic anthrax infection results in cell densities as high as 10^9 colony forming units per milliliter of blood, suggesting the requirement for host heme-iron is substantial [8]. During infection at this magnitude, anthrax toxin-mediated destruction of erythrocytes releases large amounts of heme [20]. The contribution of heme as a source of nutrient iron for the bacterium must be balanced with its toxicity at high concentrations due to its redox potential, referred to as the heme paradox [64, 70-72]. An overabundance of heme results in elevated levels of free iron within the bacterial cell via heme degradation by heme oxygenase enzymes or through reaction with ROS in the cell. Both of these pathways culminate in the cycling of iron between ferric and ferrous iron states, increasing the intracellular levels of ROS [64]. The resulting ROS damages cellular macromolecules and is thought to largely drive the toxicity of heme to bacteria, though the complete mechanism for this is not defined. As such, bacterial pathogens that use heme as an iron source have multiple strategies to alleviate this redox stress.

Heme toxicity can be alleviated via efflux systems that pump the excess heme from the cell, sequestration of heme within hemoproteins, degradation of heme through catabolic enzyme

activity, or the enzymatic detoxification of resulting reactive species. *B. anthracis* uses combinations of each of these strategies to avoid the heme toxicity observed during the course of anthrax infection [72]. Heme accumulates in mutants of the ABC transporter, HrtAB, which is required for growth in high heme concentrations [70, 72, 73]. This system is largely conserved across Gram-positive pathogens, including within *B. anthracis* [72]. Heme can be loaded into hemoproteins as a necessary cofactor for cytochromes in the electron transport system as well as within catalases, peroxidases, and myeloperoxidases to hydrolyze peroxide [64, 74]. *B. anthracis* utilizes IsdG, HmoA, and HmoB for the cytoplasmic degradation of heme [75, 76]. If these strategies are ineffective and an accumulation of reactive species occurs, pathogens rely on the activity of antioxidant enzymes. The genome of *B. anthracis* encodes for multiple copies of each superoxide dismutases (SODs), catalases, and peroxidases for the prevention of oxidative destruction [77]. Collectively these systems enhance the heme tolerance of *B. anthracis* preventing potential damage to cellular structures and macromolecules.

The bacterial cell envelope is essential for structural and functional integrity.

As with all Gram-positive pathogens, the cellular barrier of vegetative *B. anthracis* is a single phospholipid bilayer membrane, surrounded by the peptidoglycan cell wall [78, 79]. Embedded within the cell wall are the short chain wall polysaccharides (SCWP) that exist as anchors for the proteinaceous S layer [80]. The S layer is an array of one of two proteins, Ea1 or Sap, in a paracrystalline coat on the surface of the cell [81]. Coating the S layer is the highly antiphagocytic poly γ-D-glutamic acid capsule encoded on one of the major *B. anthracis* virulence plasmids [82]. Collectively, these five layers make up the *B. anthracis* cell envelope. Each of these protective layers houses distinct, vital protein complexes essential for pathogenesis [83]. The

machinery required to maintain membrane potential for energy generation, lipid synthesis, secretion of effectors, and regulation of cell division, among others, depends on membrane-localized proteins. Nutrient acquisition occurs through the transport of nutrients mediated by selective transporters or substrates binding to specialized receptors found in the membrane and wall of Gram-positive species. Notably, for *B. anthracis,* BslA is abundant on the cell surface and is required for adhesion to host cells and crossing of the blood-brain barrier thus making it essential for bacterial pathogenesis [84, 85] . The cell envelope is the interface between *B. anthracis* and the surrounding environment. Alterations in barrier integrity or the activity of detector complexes on the cell surface allow this pathogen to adapt to changes in environmental stimuli.

Two-component systems (TCSs) alter bacterial gene expression in response to stress.

Two component systems (TCSs) are used by bacteria to detect chemical or physical changes in their environment. These signal transduction systems make up the largest family of multi-step signal pathways, and are important for sensing, responding, and adapting to the environment around them. TCSs are found in nearly all sequenced bacterial genomes. The number of unique systems, 20-30 on average, in each species is proportional to the number of distinct environments encountered by the bacterium. [86]. Classically, TCS signal transduction begins with detection of a stimulus by a membrane-localized histidine kinase (HK) (Fig. 1-3). Autophosphorylation of HK occurs at conserved histidine residue and then the HK transfers this phosphate to a partner response regulator (RR). The RR is activated by phosphorylation of a conserved aspartate and undergoes conformational changes that often support interaction with conserved promoter regions to regulate gene expression (Fig. 1-3). Transcriptional changes, which

often include upregulation of the TCS itself, are the classical output of TCS activation, though modulatory effects have been observed at the mRNA and protein level [87, 88].

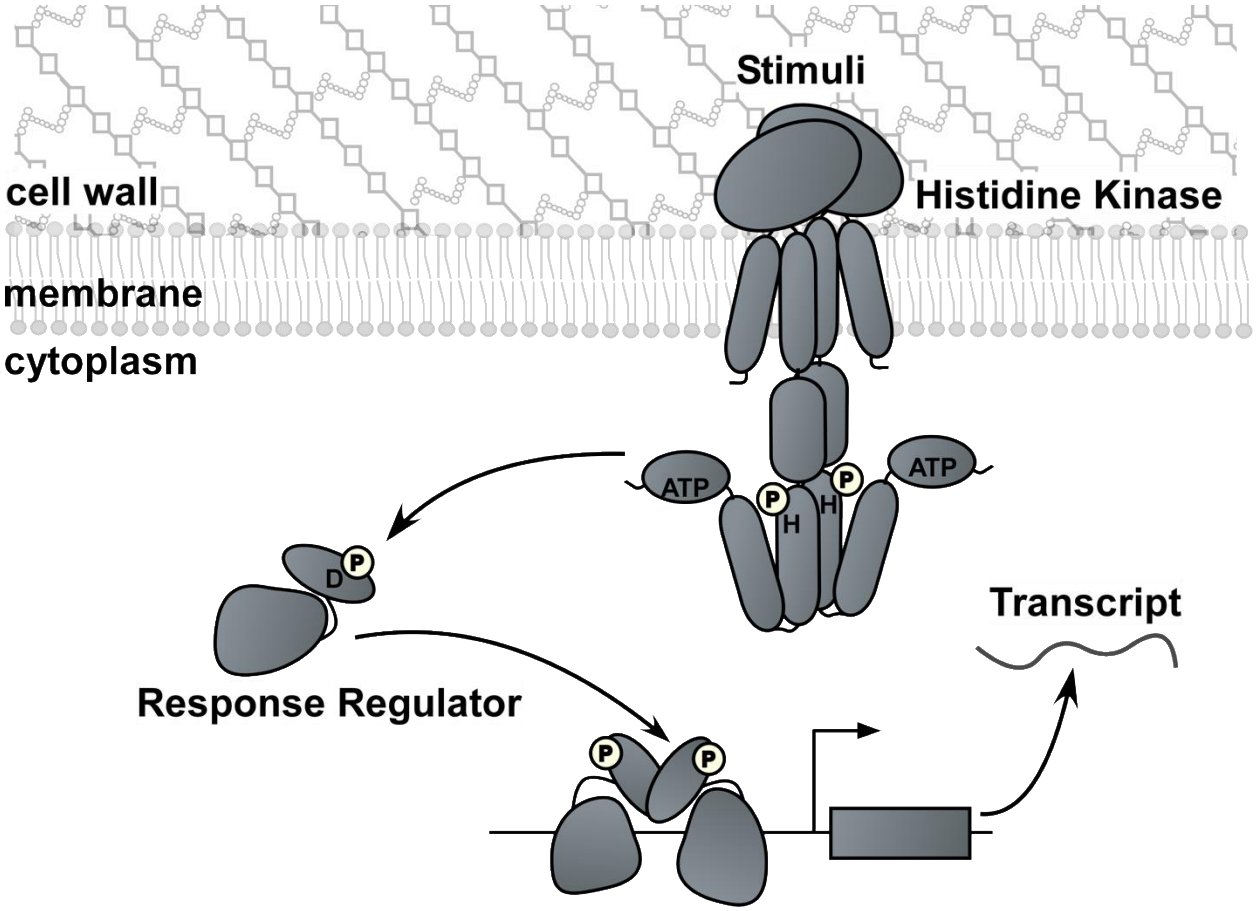

Figure 1-3. **Two-component system (TCS) signal transduction pathway.** A model of TCS signaling beginning with activation of the membrane-localized histidine kinase (HK) in the presence of stimuli via autophosphorylation at a conserved histidine residue. The partner response regulator (RR) is activated upon phosphorylation of an aspartate residue by the HK. This triggers dimerization of the RR leading to conformational changes that reveal DNA-binding residues. The DNA-binding RR acts as a transcriptional regulator that induces changes in gene expression relevant to the initial stimulus that was sensed.

***B. anthracis* responds to heme and membrane stress via TCSs.**

In many Gram-positive pathogens, including *B. anthracis*, heme toxicity is monitored by HssRS, a heme-dependent TCS (Fig. 1-4) [69]. Sensing of elevated heme concentrations leads to transcriptional activation of genes encoding an ABC-type efflux pump, HrtAB, which alleviates heme stress [72]. HssRS activation by low levels of heme primes *B. anthracis* to tolerate increased heme concentrations through the induced expression of HrtAB. The precisely tuned mechanism regulated by HssRS and HrtAB ensure that *B. anthracis* resolves the heme paradox by maintaining heme concentrations at sufficient concentration for growth, but non-toxic levels [72, 89, 90].

Phagocytes employ antimicrobial effectors to limit intracellular pathogen growth, including ROS, reactive nitrogen species (RNS), antimicrobial peptides or degradative enzymes, which are all aimed at the bacterial envelope. The HitRS TCS is activated by cell envelope-damaging agents such as nordihydroguaiaretic acid, chlorpromazine, and targocil (Fig. 1-4) [91-99]. This suggests that HitRS senses and responds to insults to the cell barrier. The *hit* operon encodes the histidine kinase (*hitS)*, the response regulator (*hitR*), and a potential efflux pump (*hitP*). These studies suggest that HitRS functions to alter gene expression in *B. anthracis* in response to specific host stressors targeting the bacterial envelope and could therefore be essential for the initial stages of anthrax infection.

How bacteria coordinate multiple signals is a pressing question in the field of microbiology. TCS are capable of signaling with each other using a process known as signal integration. This can lead to physiologically significant interactions that are beneficial in distinct environmental niches. Instances of signal integration have been described in *Bacillus subtilis, Pseudomonas aeruginosa, Bordetella pertussis,* and *Escherichia coli* [100-106]. Of the 45 TCS encoded by *B. anthracis*, HssRS and HitRS were previously identified as a pair that are capable of

cross-signaling [91]. HssRS responds to increases in available heme and engages in reciprocal cross-regulation with HitRS, which senses cell envelope stress. These results suggests that *B. anthracis* coordinates a single response to these host-related stressors through signaling interactions [72, 91]. Based on these findings, a model is proposed whereby the individual systems are important under unique conditions, and cross-regulation is vital for dissemination between conditions of high heme and membrane stress. Responsiveness to host factors in this cooperative manner may provide significant insight into how this organism contends with the overt stresses initially presented by phagocytes and additionally mechanisms behind infection severity.

Antimicrobial stress on the cell envelope activates TCS signaling.

In addition to activation of HitRS, targocil also activates a previously undescribed TCS in *B. anthracis* named EdsRS (Fig. 1-4) [98]. Targocil is a toxic inhibitor of cell barrier biosynthesis in *Staphylococcus aureus* [94-97]. Bacterial pathogens signal through TCS in response to antibiotic compounds in addition to host derived stimuli [107, 108] . These activators can be both natural products and synthetic compounds, but the changes in gene expression profile of the bacterial cell in response to TCS activation are typically linked to the barrier assault. For example, treatment of *Vibrio* species with β-lactam antibiotics leads to β-lactamase expression via VbrKR TCS signaling [109]. Additionally, the CpxAR TCS is associated with resistance to polymyxin B, fosfomycin, aminoglycosides, β-lactam antibiotics, and others [110-114]. The QseBC and PmrAB systems in *E. coli* cross-regulate to mediate resistance to polymyxin B (PMID: 28074004). In *Klebsiella* and *Salmonella,* active forms for CpxR bind to the genome to induce expression of members of the Omp protein family, which are directly linked to antibiotic resistance [110, 111, 113]. Beyond facilitation of drug resistance, TCS systems repair damage caused to the barriers of

bacterial cells. Activation of DesKR in *B. subtilis* leads to expression of Des, a lipid dehydrogenase [115-120]. When the barrier of *B. subtilis* is compromised, Des desaturates membrane phospholipids to restore membrane fluidity. This system is tightly regulated via a negative feedback loop whereby the synthesis of unsaturated fatty acids via Des acts as a repressor of *des* expression [118, 121].

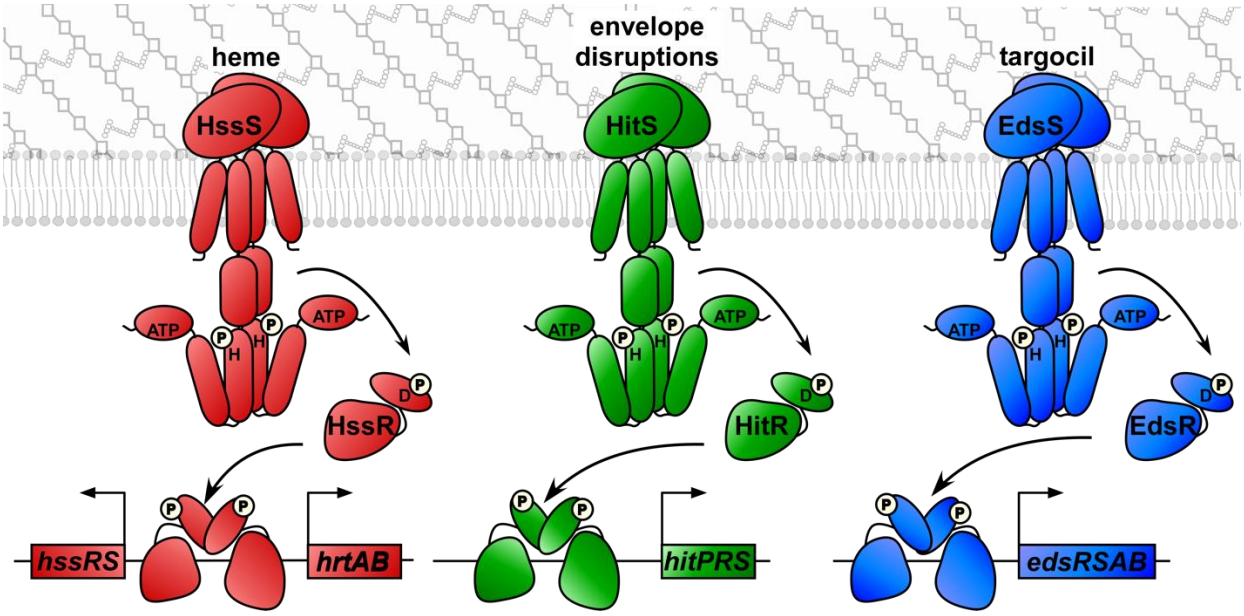

Figure 1-4. **TCS signaling response to host-derived and antimicrobial stressors in *B. anthracis*. B.** HssRS is activated by heme to increase expression of *hssRS* and *hrtAB*. HitRS is activated by envelope disruptions to increase expression of *hitPRS*. EdsRS is activated by targocil to increase expression of *edsRSAB*.

***B. anthracis* TCSs facilitate response to stress and regulate virulence.**

HssRS, HitRS, and EdsRS are three of eight TCSs that have been studied in *B. anthracis.* These TCSs respond to known environmental changes that induce stress to the bacilli. The same can be said for BAS1213-BAS1214. This TCS is activated when *B. anthracis* is exposed to ROS [122]. Following stress sensing, there is increased production of detoxification mediators such as catalase and the Mn importer, MntH, as well as metabolic enzymes [122]. Additionally, phosphate metabolism in *B. anthracis* is regulated through the activity of the highly conserved TCS, PhoPR [123]. During periods of phosphate starvation, PhoPR stimulates expression of uptake systems, which are central to pathogenesis in mice [123]. TCS regulation of *B. anthracis* virulence factors occurs directly via WalRK, BrrAB, and BAS2108-BAS2109 [124-128]. WalRK is a TCS utilized in *Staphylococcus* and *Streptococcus* species for the regulation of virulence genes [129-131]. In *B. anthracis*, WalRK is expressed throughout both exponential and stationary phase growth, and controls expression of the proteinaceous S layer, cellular division proteins and a regulator of sporulation [124-126]. BrrAB shares homology to the SrrAB TCS in *S. aureus* and controls expression of the anthrax toxins via the master virulence regulator AtxA [127]. Lastly, BAS2108-BAS2109, which has no known activating condition, is a regulator of *B. anthracis* protease activity that is required for sporulation [128]. Though the remaining 37 TCSs in *B. anthracis* have yet to be investigated, these systems exemplify the central role of stress sensing and signaling to the maintenance of *B. anthracis* viability and anthrax pathogenesis.

Bacterial protein homeostasis is maintained through conserved mechanisms of stabilization and degradation.

Protein homeostasis is controlled through a delicate balance of protein structural support and degradation that is targeted at maintaining the cellular proteome through one of the following strategies (i) synthesis of novel peptides, (ii) prevention of unfolded protein aggregation, or (iii) degradation or solubilization of damaged proteins. During periods of stress, such as exposure to reactive species or extreme temperatures, bacterial cells employ protein chaperones to preserve protein strucutre. The most conserved of these chaperone systems is trigger factor (TF), GroEL/GroES, and DnaK/DnaJ/GrpE [132-134]. TF functions in support of the ribosome to fold newly translated peptides prior to their release into the cell [135, 136]. GroEL and GroES oligomerize through ATP hydrolysis into a cylindrical structure with two cavities that surround protein substrates [137, 138]. The internal cavity serves as an encasement whereby substrates can refold shielded from the aggregation-inducing conditions of the cytoplasm [139]. Dissassociation of GroES from GroEL then releases the re-folded protein [138, 140]. The DnaJK chaperone is another ATP-dependent protein chaperone [141]. DnaK cycles ATP with the help of co-chaperones DnaJ and GrpE to refold proteins and return them to their native conformation [142]. Substrate binding to DnaK is facilitated by DnaJ and prompts ATP hydrolysis [143]. The substrate is then released with simultaneous replacement of ADP with ATP after interaction with GrpE [144]. The DnaJK complex is broadly used to protect proteins from irreversible aggregation during cellular stress. As the key to the heat shock response, DnaJK is associated with nearly all of the major cellular pathways including DNA replication and protein translation and translocation.

The activity of chaperone systems are largely contrasted by the activity of protease complexes. ATP-dependent proteases are key for the degradation of proteins that are structurally

damaged. Lon proteases are present in both bacterial and eukaryotic species [145, 146]. This protease is a tetrameric complex that targets the products of premature termination of protein translation, abnormal peptides, and regulatory proteins with short half-lives [145, 147, 148]. Lon function is directly linked to the maintenance of homeostasis via cell division, cell barrier elaboration, and the heat shock response, among others [148]. The caseinolytic proteases (Clp) family proteases are comprised of heterodimers which include a nucleotide-binding protein (ClpA, ClpX, ClpC, ClpB) and a protease component (ClpP) [132, 149]. The ATP-binding subunits are thought to be required for binding of protein substrates at distinct peptide tags [149]. The peptide's quaternary structure is subsequently unfolded and translocated to ClpP for degradation [149]. Clp proteases are used by bacterial species to degrade unfolded proteins in stress conditons. During starvation stress, *B. subtilis* ClpCP degrades metabolic proteins as the cells transition to a lower growth rate [150] or degrades SpoIIAB to remove repression of the sporulation pathway [151]. In *Salmonella* Typhimurium, Clp proteases are responsible for appropriate regulation of flagella and other virulence factors for survival in mouse models of infection [152, 153]. During anthrax infection, ClpX is required for β-hemolytic activity and extracellular degradation of the innate immune effector, cathelicidin anitmicrobial peptides, targeted at the bacilli barrier [154]. Regulation of native and exogenous peptides is maintained through a balance of degradation and stabilization to efficiently utilize the resources available to the bacteria in changing conditions.

TCSs are regulated by accessory modulators of protein function.

The activating conditions of TCSs are often changes in the environment that stress the bacteria. This is particularly true in the case of pathogens such as *B. anthracis.* Stresses such as ROS in the phagolysosome or molecules targeting the barrier architecture can directly compromise

the ability of TCS to signal. Though the simplicity of the interaction between the HK and RR facilitates tight regulation of downstream gene products, some TCS are supported by accessory or connector proteins. These proteins are continuing to emerge as important modulators of HK and RR activity that serve to increase the regulatory capability of the TCS [155]. In *B. subtilis*, Sda, KipI, and the Rap family of proteins all affect TCS phoshorylation cascades [155]. Abx1 is a multi-spanning membrane protein in Group B Streptococci that regulates the HK of the CovRS TCS via direct interaction with the protein [156]. The PhoPQ system in *Salmonella* regulates the activation of the PmrAB TCS via the connector protein PmrD, increasing the activty of PmrA [157, 158]. These exemplify how TCS accessory proteins can be specific for an individual TCS, ensuring specifity of the response by preventing unwanted TCS cross-signaling. However, TCS accessory proteins and connectors can also involve conserved systems that maintain cellular function during stress conditions.

The signaling integrity of TCS is not only dependent on accessory proteins specific to each system, but also on the overall maintenance of protein homeostasis within the cell. RcsBC is an *E. coli* TCS that requires DnaK and DjlA, another J-domain containing protein, for signaling to occur [159, 160]. In *Pseudomonas putida*, biofilm maturation is regulated by putisolvin. The GacAS TCS regulates putisolvin biosynthesis and is positively regulated by DnaJK/GrpE chaperone activity [161]. Modulation of TCS signal function has been previously shown to require Clp protease activity in bacterial pathogens. Under osmotic stress, active VgrS, a HK in *Xanthomonas campestris*, is controlled by protease activity to temper activation level [162]. The active form of *S. aureus* SaeR, a RR, is a known binding partner of ClpXP [163]. Also, in *S. aureus*, transcript abundance of AgrAC-regulated genes depends on ClpX [164]. In *B. subtilis*, Clp specifically degrades the active form the RR, DegU [165]. In an example of combining TCS accessory proteins

with proteolytic regulation, the *E. coli* stress response protein RpoS is degraded by ClpXP in a manner that is dependent on the RssB response regulator [166]. Additionally, the *B. subtilis* protein, Sda, mentioned above as being an negative regulator of HKs, is degraded by ClpXP to initiate the sporulation phosphorelay [167-169]. The delicate coordination of TCS modulatory proteins, cellular protein stability, and TCS signaling is critical to ensure the proper response to any environmental stimulus. To date, there are no clearly defined mechanisms for these links between TCS protein function and protein chaperones.

Conclusions

B. anthracis remains a threat both to national security and public health due to the devastating disease caused by anthrax. It is capable of growing within the mammalian host to extreme densities despite the onslaught of toxic conditions generated by the immune response. The ability to persevere in diverse environments indicates that *B. anthracis* harbors a range of gene products that sense and respond to distinct alternations in the environment. TCSs are key modulators of bacterial responses both within and outside the host. As has been shown in the literature, tight signaling control must be maintained by the bacteria to ensure requisite gene expression, including the regulation of the regulatory systems themselves. The requirement for growth within a host during *B. anthracis* infection, indicates that TCSs assist in survival by sensing and enabling a response to host effectors. However, the specific system and regulatory mechanisms that support the TCSs discussed here are not yet defined.

This dissertation further defines the importance of TCS signaling to the response to host effectors. I hypothesized that distinct TCSs are activated by host-derived stimuli to trigger relevant changes in bacterial physiology with the support of conserved homeostasis systems. In the following chapters, I highlight three particular TCSs (EdsRS, HssRS, and HitRS) that coordinate

the *B. anthracis* response to envelope damage and high levels of heme. I identify EdsRS as a TCS activated by an antimicrobial targeting the barrier of *B. anthracis* and subsequently increases synthesis of the phospholipid cardiolipin to repair the damage. I expand on what is known about the HitRS and HssRS response to envelope perturbations and heme toxicity by identifying a potentially conserved strategy to maintain bacterial signaling integrity in fluctuating environments. I define DnaJ and ClpX, components of the protein homeostasis maintenance network, as being required for HitRS and HssRS TCS activity through the use of a unique and unbiased mutant selection strategy. DnaJ provides a balance by reducing HitR levels and increasing HitS. In contrast, ClpX is only required for the maintenance of HitS abundance. Using a model of inhalation anthrax infection and follow up studies in bone marrow derived macrophages, I uncover that HitRS is specifically activated during intracellular germination within macrophages. Finally, I develop a CRISPR screen to identify host factors that activate HitRS signaling in *B. anthracis*. Collectively, the work in this dissertation suggests that TCS signal integrity is required for *B. anthracis* defense against host attack during infection.

A version of the following section (*Chapter II, Bacillus anthracis responds to targocil-induced envelope damage through EdsRS activation of cardiolipin synthesis*) was previously published in

mBio 11 (2)

e03375-19 (March 2020)

doi: 10.1128/mBio.03375-19

CHAPTER II

BACILLUS ANTHRACIS RESPONDS TO TARGOCIL-INDUCED ENVELOPE DAMAGE THROUGH EDSRS ACTIVATION OF CARDIOLIPIN SYNTHESIS

Introduction

Bacillus anthracis is one of the few organisms that has been used as a bioterror weapon [8-11]. Four infectious syndromes can result from exposure to *B. anthracis* spores: cutaneous, gastrointestinal, inhalation, and injectional anthrax [8, 10, 15, 170, 171]. Inhalation anthrax is the most severe with mortality rates approaching 90% [18]. Upon exposure to host tissues, spores are phagocytosed by immune cells in an attempt to eliminate the pathogen. Spores that survive phagocytic attack germinate into vegetative cells that avoid immune-mediated clearance and cause life-threatening disease. Accordingly, *B. anthracis* is well-equipped to respond to a range of stressors experienced during vertebrate colonization.

The infectivity of bacteria that colonize mammals, such as *B. anthracis,* is dependent upon the ability to sense and respond to the host environment. Pathogens can rapidly alter gene expression in response to environmental stimuli using two-component systems (TCSs). TCSs typically consist of a membrane-embedded sensor histidine kinase and cognate response regulator. The sensor kinase becomes activated upon exposure to a specific signal(s), resulting in autophosphorylation. The kinase activates the regulator via phosphotransfer, and the regulator, in turn, commonly acts as a transcription factor resulting in gene expression changes to support survival and growth. Although genes encoding TCSs are often readily identifiable, the activating signals for TCSs are not well defined. Some TCSs, such as the TCS PhoPQ, respond to multiple

signals. This TCS is conserved between gram-positive and gram-negative species, and can be activated by antimicrobial peptides or altered metal levels to provide resistance to antimicrobial peptides [172-175]. Others, like *Staphylococcus aureus* AgrCA, are activated by binding a single ligand such as the quorum sensing molecule, autoinducing peptide (AIP) [176]. Disruption of the phospholipid membrane can be sensed by TCSs. For instance, DesKR in *B. subtilis* is a thermosensor that is activated at low temperatures when the cellular membrane condenses to reveal the linker domain in the sensor kinase and promote autokinase activity [115, 117-121, 177-179]. Activation of DesKR results in the synthesis of unsaturated fatty acids that maintain membrane fluidity in colder conditions [115]. These are some of the few known examples of TCSs with a defined stimulus and response that is vital for the stability of the cell.

In gram-positive species, the cell is protected by a single phospholipid bilayer and the peptidoglycan cell wall [78, 79]. In some cases, there is an additional proteinaceous S-layer and antiphagocytic capsule [180-182]. Maintenance of an intact cell envelope is required for bacterial survival including during growth within vertebrates. The bacterial cell envelope provides protection from environmental assaults to maintain redox state, preserve nutrient pools, and defend against antimicrobial attack, among other activities. Targocil is an example of an antibacterial that inhibits elaboration of wall teichoic acid (WTA) in *S. aureus*. Targocil inhibits TarG, the permease component of the ATP binding cassette (ABC) transporter responsible for the export of fully synthesized WTA to the surface of *S. aureus* [95]. However, not all gram-positive pathogens synthesize WTA; one WTA-negative species is *B. anthracis* [183, 184]. These findings prompted the hypothesis that targocil activity against *B. anthracis* must occur in a WTA-independent manner.

In this study, we demonstrate that targocil treatment of *B. anthracis* activates a previously unstudied TCS, EdsRS. Upon activation, EdsRS upregulates self-expression and expression of an additional operon, *BAS1661-BAS1663clsT*. Elevated expression of *clsT* is required for the protection of *B. anthracis* against alterations in barrier permeability caused by targocil treatment, which are heightened in defined media media and during spore germination. *clsT* encodes a newly identified cardiolipin synthase that is responsible for increasing the abundance of cardiolipin that restores envelope damage caused by targocil. This work describes how antimicrobial-mediated activation of a two-component system in *B. anthracis* initiates a membrane remodeling response to maintain bacterial fitness.

Materials and Methods

Bacterial strains and growth conditions. The bacterial strains (Table 1), plasmids (Table 2), and primers (Table 3) used in this study are listed in their indicated tables below. *Bacillus anthracis* strain Sterne was used in all experiments under BSL2 conditions [24]. Cultures were streaked from glycerol freezer stocks on LB agar (LBA) plates and grown at 30°C for 16 h. LB was inoculated using a single colony from these plates. Cultures were grown at 30°C shaking at 180 rpm with aeration for all overnight growth or anything over 8 h. For growth assays performed for 8 h or less, growth occurred at 37°C. As noted, experiments were performed in RPMI (Thermo Fisher Scientific) plus 1% (w/v) casamino acids to serve as a defined media. Plasmids were constructed using *E. coli* DH5α or TOP10 strains. Plasmids were then moved from *E. coli* to *B. anthracis* after first transforming them into *E. coli* K1077 or *S. aureus* RN4220. Antibiotic concentrations used were 50 μg/mL carbenicillin for *E. coli* (reporter and complementation vectors), 10 μg/mL chloramphenicol for *S. aureus* and *B. anthracis* (reporter and complementation vectors), and kanamycin at 20 μg/mL in *B. anthracis* and 40 μg/mL in *E. coli* (genetic manipulation vector).

Preparation of compound stocks. Carbenicillin stocks (50 mg/mL) were prepared in H_2O and stored at -20°C. Chloramphenicol stocks (10 mg/mL) were made in 70% EtOH and stored at -20°C. Targocil stocks (10 mg/mL) were made in DMSO and stored at -20°C. A stock of cardiolipin sodium salt (10 mg/mL) was made in 100 % EtOH and stored at -20°C. All chemicals were purchased from Sigma Aldrich unless otherwise noted.

Genetic manipulation of *B. anthracis*. Genetic manipulation was performed as previously described [72, 91]. Electroporations were performed, with modifications as described previously

[72, 91, 185]. The generation of knockout strains was performed by inserting the flanking sequences for genes of interest in the mutagenesis plasmid pLM4. Briefly, flanking sequences were amplified using a distal primer containing a restriction enzyme site and a proximal primer containing a short sequence overlapping the adjacent flanking region. PCR-amplified DNA was fused using PCR sequence overlap extension (PCR-SOE) as described previously [186]. *BAS5207* was selected as a *B. anthracis* strain Sterne pseudogene based on NCBI RefSeq annotation (genomic sequence NC_005945). In other strains including *B. cereus* ATCC *14597* and *B. thuringiensis BMB181*, *BAS5207* orthologues are annotated as predicted LPXTG cell wall anchor domain-containing proteins with homology to collagen adhesion proteins. However, in Sterne, *BAS5207* is interrupted by two frameshift mutations (a single-basepair insertion corresponding to nucleotide 1805 and a 14-basepair insertion between nucleotides 5040 and 5041 in the *BAS5207* ORF) and multiple deletions at the C-terminus, leading us to conclude that *BAS5207* is likely a pseudogene in this strain. To construct a chromosomal insertion of *edsRS* into the pseudogene locus *BAS5207*, the plasmid pLM4-*5207* was constructed as described above with the exception that the flanking region overlap site contained recognition sequences for the restriction nucleases NheI and KpnI. The *edsRS* genes were fused to the *eds* promoter by PCR-SOE and the resulting product was inserted between the NheI and KpnI sites of pLM4-*5207* to generate a plasmid for chromosomal complementation of *edsRS*, pLM4-*edsRScomp*. Mutagenesis was performed using this vector as described previously [84] and confirmed by PCR and Sanger sequencing.

Expression studies. *B. anthracis* cultures were grown in LB at 37°C with shaking for 6 h (mid-log phase). Cultures were divided in half and then dosed with either DMSO control or 10 μg/mL targocil. Cultures were returned to 37°C for 10 min. Cultures were mixed at a 1:1 ratio with 1:1

mixture of cold acetone and EtOH and stored at -80 °C until RNA isolation. RNA was isolated using the RNeasy kit (Qiagen) and DNA was removed using the Turbo DNA-free kit (Invitrogen, Thermo Scientific). Quantification of RNA was performed using a Thermo Scientific Spectophotometer NanoDrop before cDNA was synthesized using the iScript cDNA Synthesis kit (Bio-Rad). RNA sequencing was performed by HudsonAlpha as described previously. [187]. qRT-PCR was performed as previously described using the $\Delta\Delta^{CT}$ method using the iQ SYBR Green Supermix (BioRad) [188].

Targocil toxicity growth curves. Strains of interest were streaked on LBA and grown at 30°C for 16-18 h. Single colonies were used to start cultures containing the same media used for the assay as annotated and were grown for 16 h at 30°C with shaking. Cultures were diluted 1:100 into fresh media and grown with shaking for 6 h at 37°C. One microliter of each culture was added to 99 µl of LB or RPMI plus 1% casamino acids, as annotated, containing 0 to 100 µg/mL targocil in a 96-well flat-bottomed plate. Growth was monitored over time at 37°C by measuring the optical density at 600 nm in a BioTek Epoch2 spectrophotometer and analyzed with BioTek Gen5 software.

XylE Assay. To monitor *eds* promoter activity, a XylE reporter plasmid was generated. In the pOS1 vector [189], the *eds* promoter (P_{eds}) sequence was fused to *xylE* using PCR-SOE as described previously [70]. This vector was carried through the cloning strains described above followed by electroporation into *B. anthracis.* Strains containing the P_{eds}*xylE* reporter plasmid were grown at 37°C in LB containing chloramphenicol and 0 to 1 µg/mL targocil. After 6 h, the abundance of the XylE enzyme present in *B. anthracis* cellular lysates was assessed by measuring

the rate at which catechol was converted to 2-hydroxymuconic acid using a spectrophotometer as described previously [72].

Spore preparation. Modified G Medium (MGM) sporulation media were used for spore preparation [190]. A single colony of *B. anthracis* was used to inoculate LB and grown for 4 h at 37°C with shaking. This culture was then back-diluted 1:20 into flask containing MGM at a volume that provides maximum aeration. Cultures were then grown at 37°C for 72 h. The bacterial pellet was collected using centrifugation and washed repeatedly using sterile diH_2O. After washing the spores a minimum of 4 times, culture suspension was incubated at 65°C for 30 min. Samples were washed with sterile diH_2O again and then diluted and plated onto LB for quantification.

Spore outgrowth curves. Spores were prepared as described above. Enumerated spores were diluted to a concentration of $1x10^8$ using diH_2O. One microliter of each spore preparation was added to 99 µl media containing 0 or 25 µg/mL targocil in a 96-well flat-bottomed plate. Growth was monitored over time at 37°C by measuring the optical density at 600 nm in a BioTek Epoch2 spectrophotometer and analyzed with BioTek Gen5 software.

Quantification of spore germination. Spores were prepared as described above. Enumerated spores were diluted to a concentration of $1x10^6$ in LB broth containing a vehicle control 100 µg/mL targocil. Cultures were incubated in at 37°C for 5 min. Samples were dilution plated onto LB agar to enumerate the total bacterial density. The same samples were then incubated at 65°C for 30 min to lyse vegetative cells. The boiled suspension was dilution plated to enumerate spore counts.

Disc diffusion assay. This assay was modified from studies previously described [191]. Overnight cultures were grown at 30°C for 16 h. Following incubation, bacteria were mixed with top agar made from LB broth and poured onto LB agar plates. Sterile discs were placed onto the plates and loaded with one of each of the compounds included in our screening panel. The plates were incubated at 30°C for 18 h and then imaged. The diameter of the zone of inhibition was then measured. Experiments were performed twice.

Envelope permeability assay. Overnight cultures were grown at 30°C in RPMI plus 1% casamino acids with chloramphenicol. Cultures were normalized to an OD_{600} of 0.3 in fresh media using a black wall, 96-well plate. The indicated treatments were added to the cultures and allowed to incubate at 37°C for 30 min. Ethidium bromide was added rapidly at 1 μg/mL and the fluorescence (Ex: 530nm, Em: 600nm) was immediately read kinetically using a BioTek Cytation 5 plate reader.

Cardiolipin relative quantification. Lipids were extracted from cell pellets (normalized by OD) using the Bligh-Dyer method [192]. Extracts were dried under nitrogen and reconstituted in 100 μL of 65% acetonitrile, 30% isopropyl alcohol, and 5% water. All samples contained 5 μg/mL of a cardiolipin standard (CL(16:0/18:1) (Avanti Polar Lipids, Inc., Alabaster, AL, USA). Fifteen μL of each sample was injected into an Acquity Arc UPLC (Waters Corporation, Milford, MA, USA). Lipids were separated using an Acquity UPLC HSS C18 column (Waters Corporation, Milford, MA, USA) with 1.8 μm particle size and dimensions of 2.1 mm by 150 mm. The aqueous solvent system (A) consisted of 60% acetonitrile, 40% water, 0.1% formic acid, and 10 mM of ammonium acetate. The organic solvent system (B) consisted of 90% isopropyl alcohol, 10% acetonitrile, 10 mM ammonium acetate, and 0.1% formic acid [193]. The following gradient was used: 0 min 70%

A; 0-5 min, 70% - 57% A; 5 – 5.1 min, 57% - 50% A; 5.1- 14 min, 50% - 30% A; 14- 21 min, 30% - 1% A; 21- 30 min, 1% A; 30-30.1 min, 1%- 70% A. The column was allowed to equilibrate at 70% A for 9.9 min prior to the next injection. The column heater was set at 40°C, and the flow rate was 0.22 mL/min. Post separation, samples were introduced by electrospray ionization (2.5 kV capillary; 100°C source temperature; 40 V sampling cone) to a quadrupole-time-of-flight mass spectrometer (Waters Synapt G2-Si, Waters Corporation, Milford, MA, USA) for analysis in negative ionization mode (trap and transfer collision energies: 15 V; resolution mode; ion mobility not enabled). Samples were analyzed in data dependent mode with a survey window from mass-to-charge (*m/z*) 500- 1750 with a scan time of 0.2 sec. Fragmentation data were acquired using a collision energy ramp from 6 - 147 eV depending on the *m/z* value selected with a 30 sec exclusion window. The instrument was calibrated using sodium formate prior to analysis, and a lock spray containing a tuned mix of known *m/z* values (Agilent Technologies, Inc., Santa Clara, CA, USA) was infused (flow rate 5 µL/min; scan time 1 sec; 10 sec intervals; 3 scans averaged) during analysis for internal calibration of data post-acquisition. Cardiolipin lipids eluted between 24-26 min. Data were analyzed by separately extracting ion chromatograms for all annotated cardiolipins within spectra obtained from parent strain samples. Peaks from extracted ion chromatograms were integrated manually and normalized to the area of the internal cardiolipin standard. Normalized areas were then summed for all annotated species. Data are comprised of biological triplicates with two technical replicates each.

Data Availability. RNA sequencing data deposited in the Gene Expression Omnibus (GSE142363).

Table 2-1: Bacterial strains utilized in Chapter II

Species	Genotype	Description	Reference
B. anthracis strain Sterne	Wildtype/Parental	Wildtype/Parental laboratory stock	[24]
B. anthracis strain Sterne	Δ*edsRS*	In frame deletion of *BAS5200 and BAS5201*	This study
B. anthracis strain Sterne	Δ*edsRS BAS5207::edsRS*	In frame deletion of *BAS5200 and BAS5201* and genomic complementation of *BAS5200 and BAS5201* within *BAS5207*	This study
B. anthracis strain Sterne	Δ*BAS1661-BAS1663ΔclsT*	In frame deletion of *BAS1661, BAS1662, BAS1663, and clsT*	This study
E. coli strain K1077	Wildtype	Wildtype laboratory stock for cloning	[185]
S. aureus strain RN4220	Wildtype	Wildtype laboratory stock for cloning	[194, 195]

Table 2-2: Plasmids utilized in Chapter II

Plasmid	Description	Reference
pLM4	Allelic exchange vector for *B. anthracis*	[84]
pLM4-*edsRS*	Vector to delete *edsRS*	This study
pLM4-*5207*	Vector to integrate genes within *BAS5207*	This study
pLM4.*edsRScomp*	Vector to integrate *edsRS* within *BAS5207*	This study
pLM4-*BAS1661-BAS1663clsT*	Vector to delete *BAS1661-BAS1663clsT*	This study
pOS1 P_{lgt}	Empty vector	[84]
pOS1 P_{eds}*xylE*	*xylE* reporter vector	This study
pOS1 P_{lgt}*edsRS*	*edsRS* complementation vector	This study
pOS1 P_{lgt}*clsT*	*clsT* complementation vector	This study

Table 2-3: Primers utilized in Chapter II

Primer	Sequence	Use
edsRS KO XmaI fwd	GCATGACCCGGGATAGAAGTTTTACG TACATTTCG	Mutagenesis
edsRS KO SOE-L	CTTCCTTGGTACCTTATACCGCTTCCT GTCTTTTTC	Mutagenesis
edsRS KO SOE-R	CGGTATAAGGTACCAAGGAAGTTTAC CTATGAATGG	Mutagenesis
edsRS KO SacI rev	GCATGAGAGCTCGTGCATACTTACTC ACCATCC	Mutagenesis
5207 XmaI fwd	GCATGACCCGGGCTATGTAATTAGCT GGG	Chromosomal insertion
5207 SOE-L	GCTAGCGCATGCGGTACCGTTACTTTA CCATCCGCACC	Chromosomal insertion
5207 SOE-R	GGTACCGCATGCGCTAGCGTTAAAGA CTTGGAGCCTGG	Chromosomal insertion
5207 KO SacI rev	GCATGAGAGCTCCTTCATTCGTATCTC TATTAACG	Chromosomal insertion
edsRScomp KpnI fwd	GCATGAGGTACCTCGAATATATATCTT ACCCG	Chromosomal complementation
edsRScomp SOE-L	CTTCTCTATCATCTCTCCACCCCCGCT	Chromosomal complementation
edsRScomp SOE-R	GGTGGAGAGATGATAGAGAAGAAGA GGATTG	Chromosomal complementation
edsRScomp NheI rev	GCATGAGAATTCGCTAGCGGACTATG TAACTAAGACGG	Chromosomal complementation
BAS1661-BAS1663clsT KO XmaI fwd	GCATGACCCGGGAAAGATATGCAGCG ACTTACG	Mutagenesis
BAS1661-BAS1663clsT KO SOE-L	CAACCTTTATACCCCTATTTCGGTTTC TCTGC	Mutagenesis
BAS1661-BAS1663clsT KO SOE-R	CGAAATAGGGGTATAAAGGTTGATGG GAAAAGG	Mutagenesis
BAS1661-BAS1663clsT KO SacI rev	GCATGAGAGCTCATGAGGCCATATAA ACGTGTC	Mutagenesis
P_{eds}*xylE* EcoRI fwd	GCATGAGAATTCTATCTTACCCGATTG TATCATG	Reporter
P_{eds}*xylE* SOE-L	CTTTGTTCATCTCTCCACCCCCGCTG	Reporter
P_{eds}*xylE* SOE-R	GGGTGGAGAGATGAACAAAGGTGTA ATGCGAC	Reporter
P_{eds}*xylE* BamHI rev	GCATGAGGATCCTCAGGTCAGCACGG TCATG	Reporter

P_{lgt}*edsRS* fwd	CAATTGAGGTGAACATATGCTCGAGATGATAGAGAAGAAGAGGATTGAGATTTTTC	Complementation
P_{lgt}*edsRS* rev	AAACACTACCCCCTTGTTTGGATCCTATCCATCCCTTTTCTTCC	Complementation
P_{lgt}*clsT* fwd	CAATTGAGGTGAACATATGCTCGAGATGAACATGATTAAAAAAATATTGC	Complementation
P_{lgt}*clsT* rev	AAACACTACCCCCTTGTTTGGATCCTTATAAATAAAAATCCACCATCC	Complementation
edsR fwd	TTTTGCTCCTGCCATAAGCC	qRT-PCR
edsR rev	CGCCCTGGATACTTTGAACG	qRT-PCR
edsS fwd	CCCTCACCCCATCTTTTCCT	qRT-PCR
edsS rev	ATGGAAATGGCATTCGTGGT	qRT-PCR
BAS1661 fwd	GCAAGAGTGGAGGAAGCACT	qRT-PCR
BAS1661 rev	CCAACTGTCGGCTCATCCAT	qRT-PCR
BAS1662 fwd	CAATGTAGCGGCCGAAGTTG	qRT-PCR
BAS1662 rev	TCGTCGTCATTACAACCGCA	qRT-PCR
BAS1663 fwd	GTAAAGTGGCAGGGACGGAT	qRT-PCR
BAS1663 rev	TCCTGATAAGTTCGCTGCTGA	qRT-PCR
clsT fwd	GAAGCGGCGTATCCATACAT	qRT-PCR
clsT rev	GCCCTACAATAGGACCACCA	qRT-PCR

Results

Bacillus anthracis transcriptional responses to the antibacterial compound targocil.

The recently identified antibiotic targocil inhibits WTA biosynthesis in *S. aureus*. To identify the mechanism of action of targocil in *B. anthracis*, which lacks WTA, we defined the transcriptional response of *B. anthracis* to targocil by RNA sequencing. Alterations in the gene expression profile of parent *B. anthracis* after a brief exposure to targocil were measured during mid-exponential phase growth in rich media. The attenuated *B. anthracis* Sterne strain will serve as the parent strain in all experiments in this study [24]. There were 28 total transcripts significantly altered in targocil-treated samples, the majority of which were upregulated (Fig. 2-1A). The primary pathways affected by targocil included transport and gene regulation, though transcriptional changes were also observed in genes involved in metabolism, electron transport and phage genes (Fig. 2-1B). One set of genes, *BAS5200-BAS5203*, displayed the highest fold change over untreated cells. Alignment of the sequencing reads to the genome suggests that *BAS5200-BAS5203* are in an operon and expressed as a monocistronic transcript. This operon encodes for a putative response regulator (*BAS5200*), histidine kinase (BAS5201), ABC transporter permease (*BAS5202*), and an ABC transporter ATP-binding protein (*BAS5203*). BAS5200 and BAS5201 contain domains associated with known two-component systems. BAS5201 is predicted to contain a HisKA3 phosphoacceptor domain and a HATPase domain for ATP hydrolysis [196, 197]. BAS5200 contains a phosphoacceptor domain for activation by the histidine kinase and a GerE helix-turn-helix domain for DNA binding [198]. *BAS5202-5203* codes for a putative ABC-transporter. This family of proteins is associated with the transport of a wide range of substrates, including antimicrobials [199]. Due to the described role of targocil in disrupting barrier function, and for reasons described below, we named this operon the *e*nvelope

*d*isruption *s*ensor (*eds*) system (*edsRSAB*) (Fig. 2-1C). Quantitative reverse transcription PCR (q-RT PCR) was performed on transcripts isolated from targocil-treated samples to confirm RNA sequencing results. Treatment of the parent strain with targocil showed higher relative expression of both *edsR* and *edsS* compared to untreated samples (Fig. 2-1D). Collectively, this suggests that targocil treatment induces expression of a putative TCS (*edsRS*) and an ABC transporter (*edsAB*).

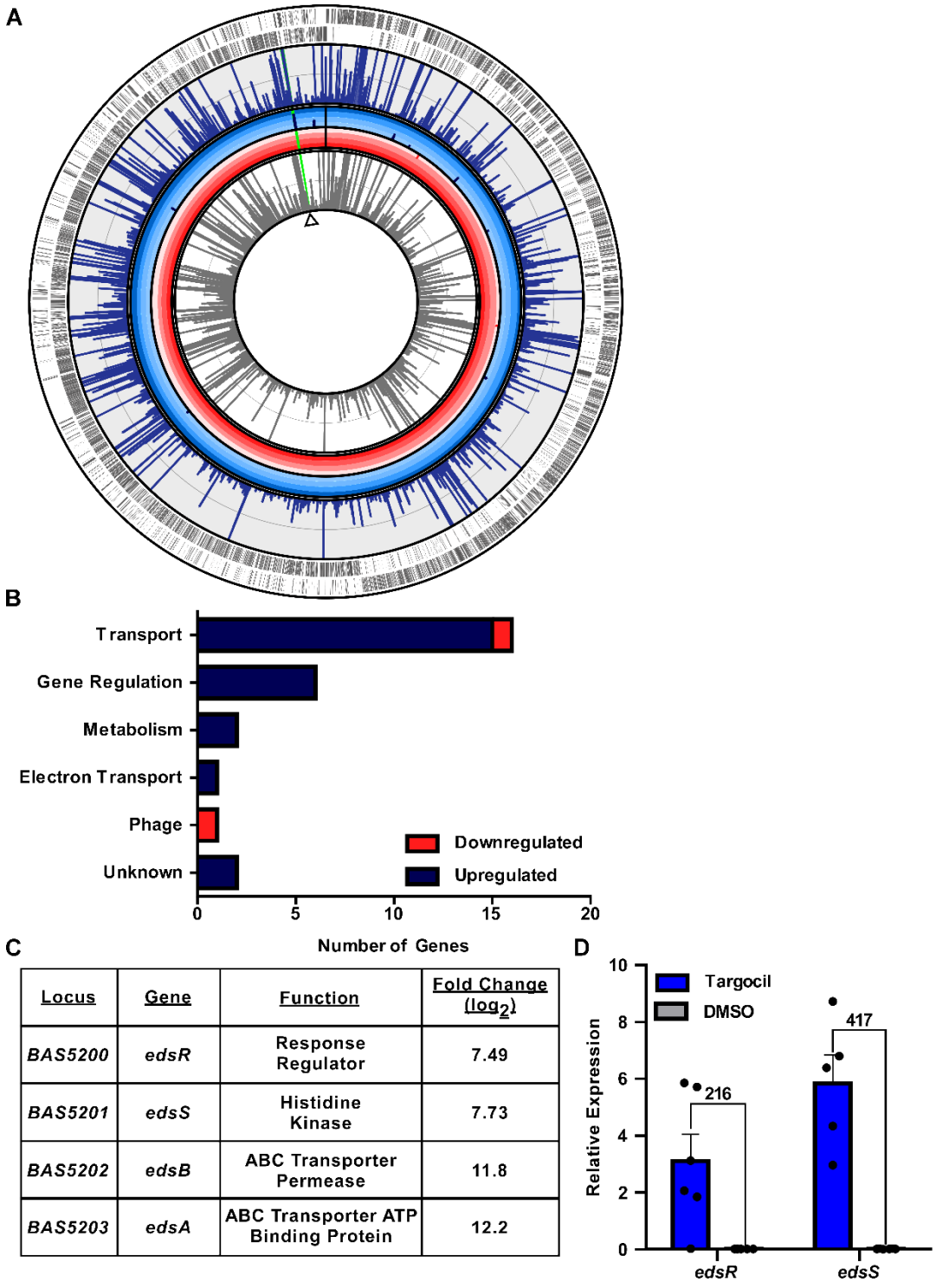

Locus	Gene	Function	Fold Change (log_2)
BAS5200	*edsR*	Response Regulator	7.49
BAS5201	*edsS*	Histidine Kinase	7.73
BAS5202	*edsB*	ABC Transporter Permease	11.8
BAS5203	*edsA*	ABC Transporter ATP Binding Protein	12.2

Figure 2-1. Targocil induces gene expression changes in *B. anthracis*. A. Genomic map of *B. anthracis* Sterne. Indicated are the open reading frames (outer ring in grey) and on which strand the gene is encoded. The degree of expression for each transcript is shown for cultures grown in targocil (blue bars in outer ring) and DMSO control (grey bars). Those transcripts which were significantly altered with a log_2fold change of at least two, and the degree of fold change in

increments of three (concentric gradient) are shown for transcripts that were upregulated (navy bars) and downregulated (red bars). The most significantly upregulated operon is indicated (green bar). **B.** The number of transcripts that fall into unique KEGG pathways are displayed, as well as whether they were upregulated or downregulated. **C.** Fold change values for those transcripts that were most significantly increased in abundance after targocil treatment. Included is the locus, gene name, predicted protein function, and $\log_2$ fold change. **D.** qRT-PCR validation of RNASeq results for the *edsRS* operon represented by targocil-induced expression relative to expression in DMSO normalized to *gyrA* expression. Fold changes between targocil and DMSO treated samples are shown above the relative expression bars. Data presented are averages of three independent experiments performed in biological triplicate ± SEM.

EdsRS signaling is activated in response to targocil.

Targocil is toxic to *B. anthracis* at high concentrations when grown in rich media (Fig. 2-2A). However, when compared to the previously determined toxicity observed in *S. aureus, B. anthracis* is over 100-fold more resistant to targocil [94]. We hypothesized that the EdsRS two-component system is activated in *B. anthracis* to resist targocil-dependent killing. This hypothesis was quantified using a vector that contained the *eds* promoter driving expression of a catechol oxidase, XylE. Activation of the promoter can be measured by quantifying the rate of conversion of catechol to a colorimetric product using a spectrophotometer [200]. In the parent strain, targocil treatment increases P_{eds} activation compared to a vehicle control (Fig 2-2B). The Δ*edsRS* mutant lacks this activation, and this phenotype can be complemented by expressing *edsRS* in *trans* (Δ*edsRS BAS5207*::*edsRS*) (Fig. 2-2B). These results demonstrate that targocil exposure activates *edsRSAB* expression and that this is dependent on EdsRS. However, when the parent strain and Δ*edsRS* were grown in rich medium containing increasing concentrations of targocil, increased susceptibility of Δ*edsRS* to targocil was not observed (Fig 2-2A-C). These data suggest that targocil-dependent activation of EdsRS signaling induces expression of its own operon, but that this TCS-activation is not required for resistance to toxicity. We propose that this could be due to the presence of additional mechanisms that can defend against targocil-induced damage and are active in mid-log cultures. EdsRS is activated under these conditions, but alternative systems could compensate in maintenance of cellular stability

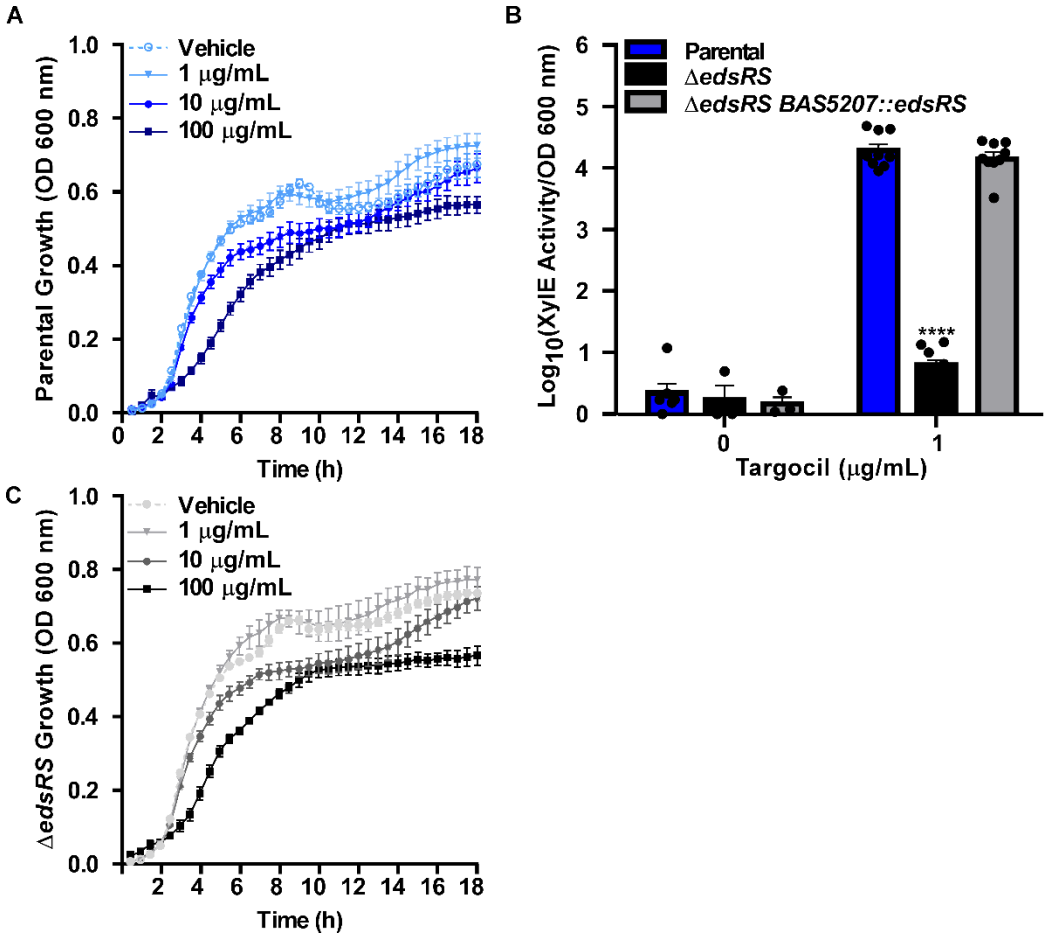

Figure 2-2. Targocil induces expression of *edsRSAB* in an EdsRS-dependent manner. A. Growth of *B. anthracis* Sterne (Parental) measured by optical density at 600 nm (OD600) in LB containing 0, 1, 10, or 100 μg/mL targocil. Data presented are averages of two independent experiments performed in biological triplicate ± SEM. **B.** Activity of *eds* promoter in response to targocil was quantified using Parental, Δ*edsRS,* and Δ*edsRS BAS5207*::*edsRS* carrying the *xylE* reporter plasmid. Strains were grown in triplicate in the presence of vehicle or 1 μg/mL of targocil for 6 h. XylE activity was quantified and normalized to bacterial density at the time of assay termination. Data presented are averages of three independent experiments performed in biological triplicate ± SEM. Statistical significance compared to parental was determined using a two-way ANOVA with a Tukey's test adjustment for multiple comparisons (****$p \leq 0.0001$). **C.** Growth of Δ*edsRS* measured by OD600 in LB containing 0, 1, 10, or 100 μg/mL targocil. Data presented are averages of two independent experiments performed in biological triplicate ± SEM.

Targocil activates EdsRS-dependent expression of *BAS1661-1663clsT*.

To define the regulon of EdsRS, we performed RNA sequencing on the parent strain and Δ*edsRS* that were treated with or without targocil. Targocil and EdsRS are required for expression changes of *edsRSAB* and an uncharacterized, *BAS1661-BAS1664.* Both operons were upregulated in the presence of targocil, in an EdsRS-dependent manner (Fig. 2-3A). Alignment of the RNA sequencing reads to the region of *BAS1661-1664* suggests these genes are expressed as an operon. This operon contains a putative ABC transporter (*BAS1661-1663*) and a putative cardiolipin synthase (*BAS1664*) (Fig. 2-3B). BAS1661-1663 are predicted to contain domains from the ABC-2 subfamily of transporters associated with the export of drugs and carbohydrates [201]. In addition to *BAS1664*, the genome of *B. anthracis* Sterne codes for four other putative cardiolipin synthase genes (Fig. 2-4A). BAS1664 contains the HKD motif associated with this superfamily of proteins that is required for the synthesis of cardiolipin [202, 203]. There is significant protein identity shared between the previously described ClsA and ClsB of *B. subtilis* and BAS1112 and BAS5195, respectively, but BAS1664 shares less identity with the previously characterized proteins (Fig. 2-4B). Based on the activation in response to targocil, we have named *BAS1664* *c*ardio*l*ipin *s*ynthase *t*argocil (*clsT*). To confirm that EdsRS activation results in upregulation of *BAS1661-1663clsT* we performed qRT-PCR on RNA extracted from the parent strain and Δ*edsRS*, either treated with targocil or untreated (Fig. 2-3C). These results indicate that targocil activates EdsRS to increase expression of *BAS1661-1663clsT*. Therefore, ClsT is a previously unstudied cardiolipin synthase that is expressed when EdsRS is activated by targocil.

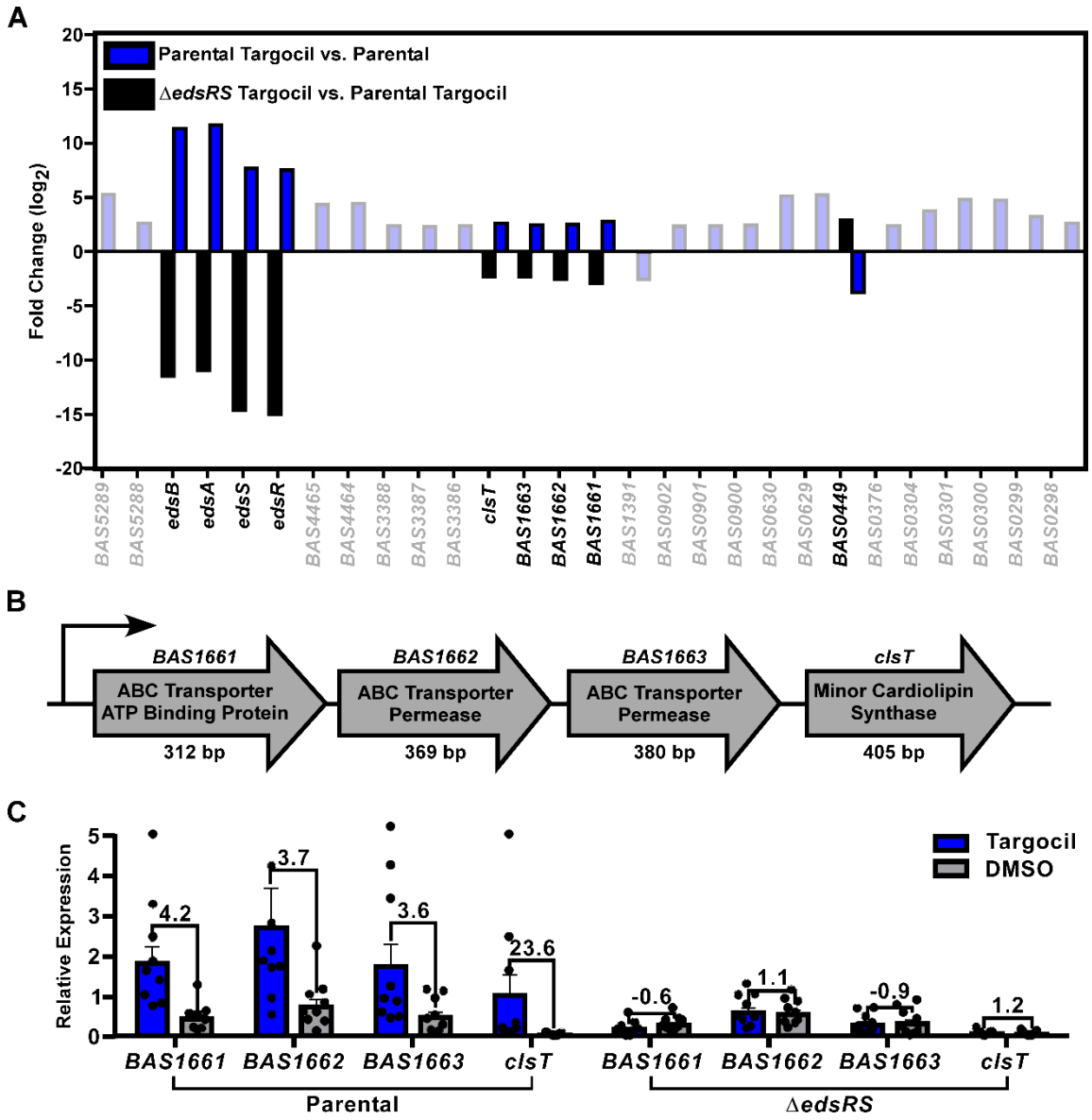

Figure 2-3. Targocil activation of EdsRS leads to induction of *BAS1661-1664* expression. A. Depiction of the significant fold changes for two distinct RNA sequencing comparisons. Shown are those genes altered in *B. anthracis* Sterne (Parental) treated with targocil as compared to Parental untreated (blue) and Δ*edsRS* treated with targocil compared to Parental treated with targocil (black). Transcripts altered in these conditions, but in opposite direction indicate genes altered by targocil that require *edsRS* (dark bars). **B.** *BAS1661-1663clsT* encodes an ABC transporter ATP binding protein (*BAS1661*), an ABC transporter permease (*BAS1662*), an ABC transporter permease (*BAS1663*), and a cardiolipin synthase (*clsT*)**. C**. qRT-PCR validation represented by relative expression of the *BAS1661-1663clsT* operon in Parental and a Δ*edsRS* mutant when grown in DMSO and targocil normalized to *gyrA* expression. Data presented are averages of three independent experiments performed in biological triplicate ± SEM. Fold changes between targocil and DMSO treated samples are shown above the relative expression bars.

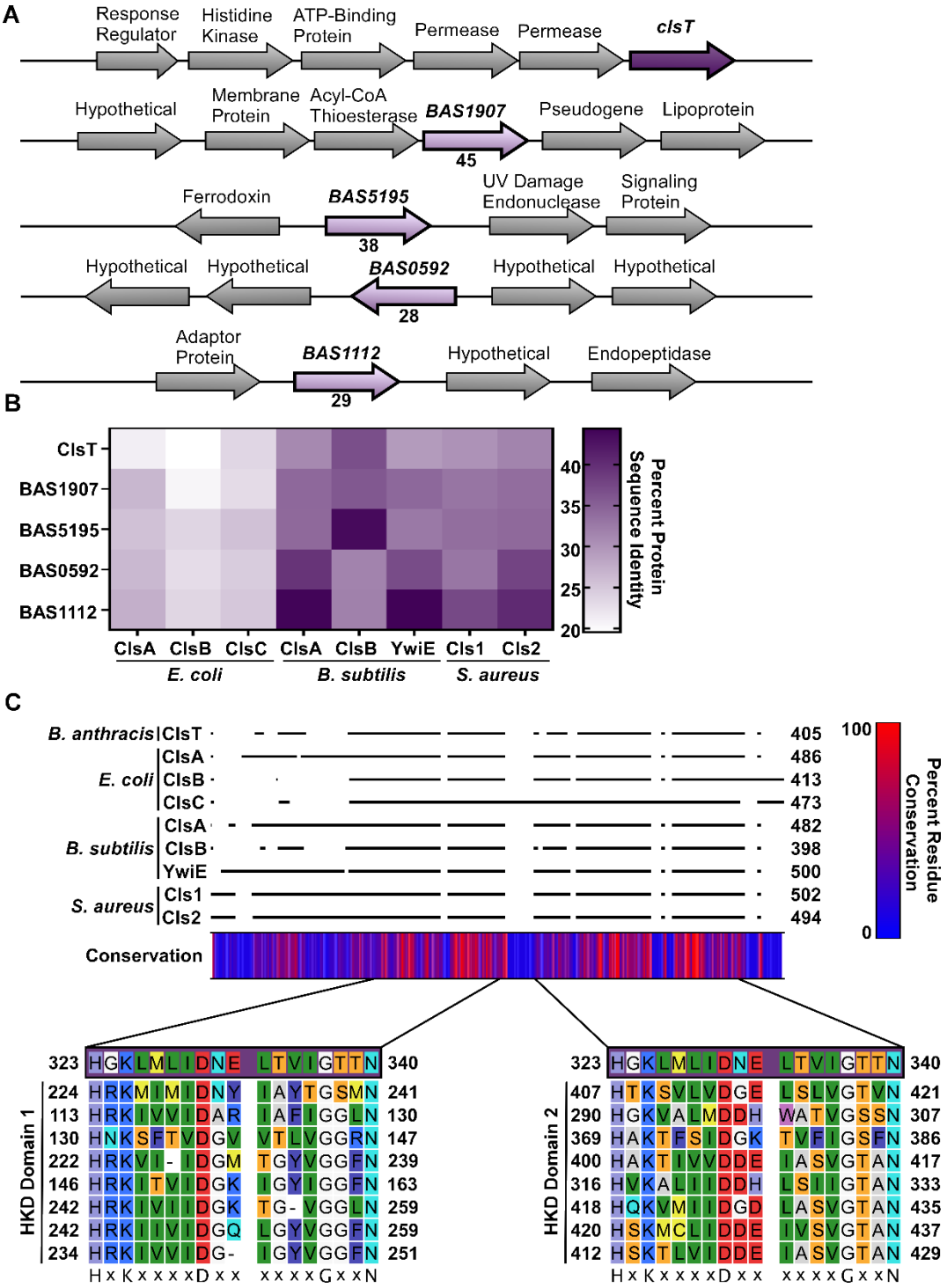

Figure 2-4. *B. anthracis* encodes five putative cardiolipin synthases. A. Genetic map of cardiolipin synthase genes in *B. anthracis*. Shown in purple are the cardiolipin synthase genes, with *clsT* shown in dark purple. Clustal Omega was used to calculate the percent protein sequence identity of each cardiolipin synthase as compared to ClsT. This value is represented below each gene. The genetic context of each synthase gene is shown in grey arrows. **B.** Heat map representing the percent protein sequence identity of the *B. anthracis* predicted cardiolipin synthase genes as compared to the cardiolipin synthase genes referenced in this study. Percent identity was obtained

through the comparison of sequences using the Clustal Omega Multiple Sequence Alignment tool [204]. **C.** The protein sequences of *B. anthracis* ClsT and other cardiolipin synthases proteins discussed in this study are fully aligned. Regions of continuous homology are represented by a line with the overall conservation at each residue represented via heat map. The ClsT catalytic HKD domain is aligned with those of the described cardiolipin synthases proteins and conservation is shown. *B. anthracis* encodes for one HKD domain while all other sequences analyzed contain two of the characteristic H-x-K-x(4)-D-x(6)-G-x-x-N motif.

EdsRS signaling is required for spore outgrowth in the presence of targocil.

Targocil exposure inhibits growth of *B. anthracis*. Based on the EdsRS-dependent activation of ClsT, we hypothesized that EdsRS senses targocil to coordinate an increase in barrier stability required for growth during treatment. To test this hypothesis under defined conditions, growth experiments were performed in RPMI with casamino acids [205-208]. Growth of the parent strain during targocil treatment in RPMI was assessed by measuring optical density at 600 nm over time. Cultures grown in 100 μg/mL targocil did not reach the same maximum optical density as those grown in the presence of vehicle control, indicating targocil is toxic in this semi-defined media (Fig. 2-5A).

The infectious particle of *B. anthracis* is the endospore, which germinates during infection of a mammalian host [8, 10, 22, 23, 52, 209]. As a spore germinates, the cell must elongate into a full-length vegetative cell. This process involves the elaboration of cellular barriers including phospholipid bilayer, S-layer, and peptidoglycan wall. We hypothesized that targocil would be more toxic to newly germinating *B. anthracis* spores than actively growing vegetative cells. To test this, complete growth kinetics after spores were inoculated into RPMI containing targocil were assessed. Outgrowth of spores lacking *BAS1661-1663clsT* (Δ*BAS1661-1663*Δ*clsT*) showed a slight growth delay compared to parental spores in the presence of targocil (Fig. 2-5B). Additionally, both the Δ*BAS1661-1663*Δ*clsT* and Δ*edsRS* spores exhibited altered growth kinetics at later time points in stationary phase upon targocil exposure. These phenotypes were not observed when exponential phase cultures were used to inoculate growth curves under the same conditions (Fig. 2-5C). The mutant strains did not display altered growth compared to parental in semi-defined media containing a vehicle control (Fig. 2-5D). This result indicates that Δ*BAS1661-1663*Δ*clsT* and Δ*edsRS* spores are not less fit overall and the altered growth is due to the activity

of targocil. We hypothesized that the defect in outgrowth observed in Δ*BAS1661-1663*Δ*clsT* and Δ*edsRS* spores (Fig. 2-5B) is due to delayed spore germination in the presence of targocil. An indicator of spore germination is the loss of heat resistance. The degree of heat resistance that remained in samples exposed to rich media in the presence of vehicle or targocil was enumerated. Germination of Δ*BAS1661-1663*Δ*clsT* was significantly reduced in samples treated with targocil compared to all other conditions (Fig. 2-5E). Disc diffusion assays were performed using the parent strain, Δ*edsRS,* and Δ*BAS1661-1663*Δ*clsT* challenged with a panel of toxic compounds. Of those tested, no additional compounds were found to have differential toxicity in the mutant strains compared to the parent strain (Fig. 2-6). Therefore, EdsRS, BAS1661-1663, and ClsT are important for protecting against targocil during spore germination,

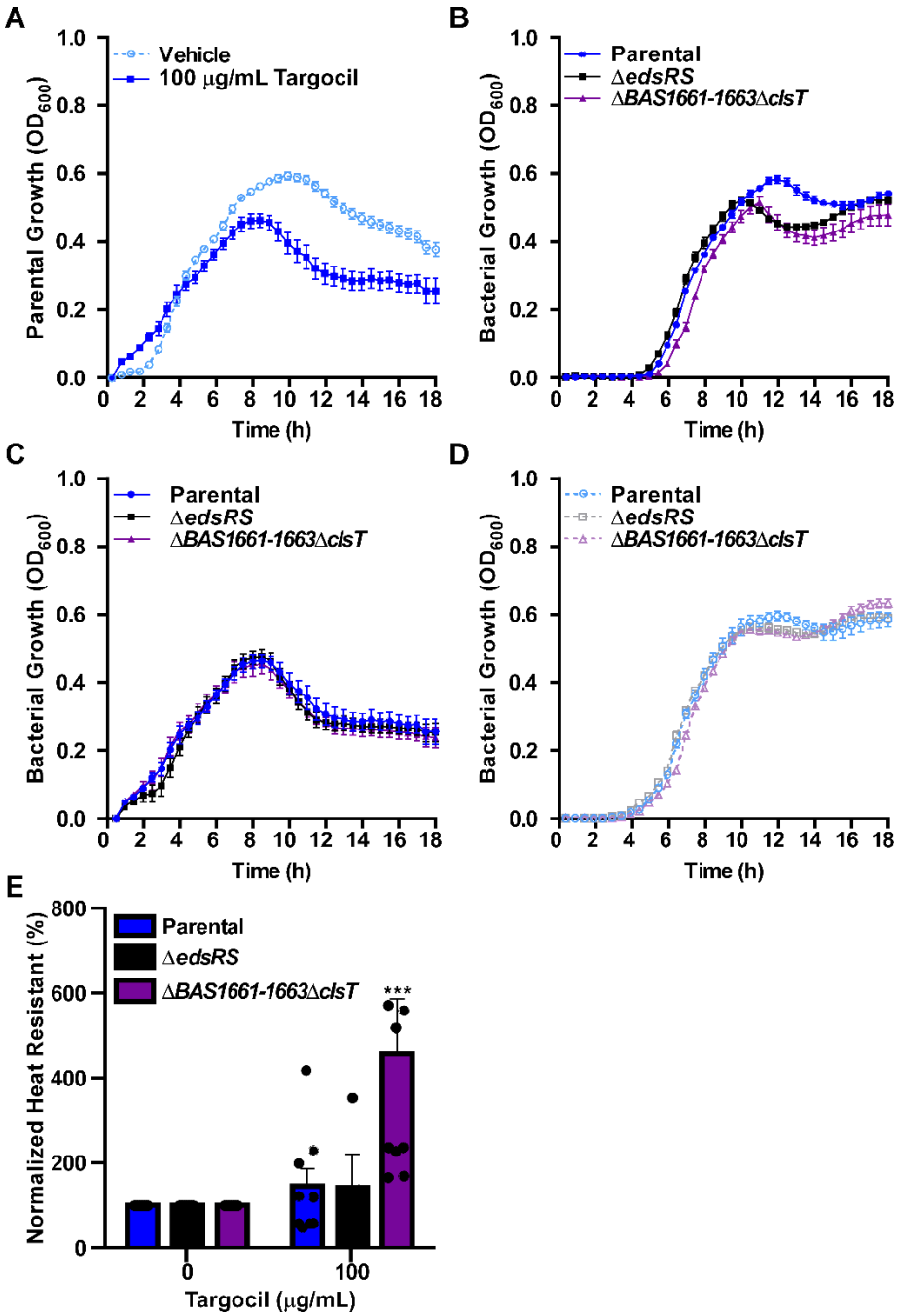

Figure 2-5. Activation of EdsRS signaling is required for spore germination during targocil treatment in defined media. A. Growth of *B. anthracis* Sterne (Parental) measured by OD600 in RPMI plus 1% casamino acids containing 0 or 100 µg/mL targocil. Data presented are averages of three independent experiments performed in biological quadruplicate ± SEM. **B.** Germination and subsequent growth of Parental, Δ*edsRS*, and Δ*BAS1661-BAS1663*Δ*clsT* spores in RPMI plus 1% casamino acids containing 25 µg/mL targocil. Data presented are averages of three independent experiments performed in biological triplicate ± SEM. **C.** Growth of Parental, Δ*edsRS*, and Δ*BAS1661-BAS1663*Δ*clsT* measured by OD600 in RPMI plus 1% casamino acids containing 100 µg/mL targocil. Data presented are averages of three independent experiments performed in biological quadruplicate ± SEM. **D.** Germination and subsequent growth of Parental, Δ*edsRS*, and

Δ*BAS1661-BAS1663*Δ*clsT* spores in RPMI plus 1% casamino acids containing a vehicle control. Data presented are averages of three independent experiments performed in biological triplicate ± SEM. **E.** After 5 min of incubation of Parental, Δ*edsRS*, and Δ*BAS1661-BAS1663*Δ*clsT* spores with rich media with and without 100 μg/mL targocil, samples were analyzed for total bacterial counts and heat resistance. The percent heat resistant bacteria is normalized to the control treated sample. Data presented are the averages of three independent experiments performed in biological triplicate ± SEM. Statistical significance compared to other treated samples was determined using a two-way ANOVA with a Tukey's test adjustment for multiple comparisons (**$p \leq 0.01$).

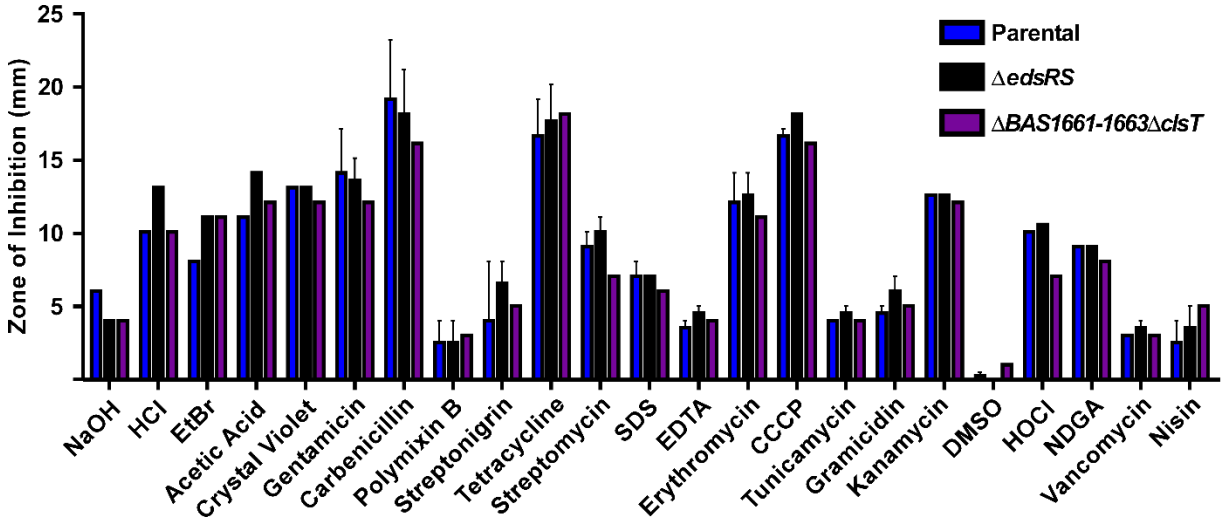

Figure 2-6. Screening of potential EdsRS activators. Zone of inhibition on LB agar plates surrounding discs loaded with the indicated compounds before *B. anthracis* Sterne (Parental), Δ*edsRS*, and Δ*BAS1661-BAS1663*Δ*clsT* growth was observed. Data presented are averages of two independent experiments performed ± SD

EdsRS activation of *clsT* expression is required to combat targocil-induced envelope permeability.

ClsT is predicted to be a cardiolipin synthase. Cardiolipin is a component of phospholipid bilayers and is primarily associated with bacterial and mitochondrial membranes. Cardiolipin makes up roughly 17% of total phospholipid in pathogenic bacilli species, and is mobilized as a component of the membrane damage response [210, 211]. Due to the increased targocil sensitivity of the Δ*BAS1661-1663*Δ*clsT* mutant during spore germination and outgrowth, upregulation of *clsT* in targocil treatment, and the role of cardiolipin in membrane maintenance, we hypothesized that targocil induces barrier damage in *B. anthracis*. Permeability of the cellular envelope can be quantified using an ethidium bromide (EtBr) uptake assay to measure the rate at which EtBr crosses the cell wall and lipid bilayer [212-214]. Targocil-induced permeability in the parent strain *B. anthracis* in both LB and RPMI plus casamino acids (Fig. 2-7A). However, the rate of EtBr uptake after targocil treatment was significantly higher in the cultures grown in semi-defined media compared to rich media (Fig. 2-7B). From these results, we conclude that targocil increases cellular permeability.

Next, we hypothesized that activation of *BAS1661-1663clsT* expression by EdsRS is required for the response to targocil-induced envelope damage. In the EtBr uptake assay, Δ*BAS1661-1663*Δ*clsT* and Δ*edsRS* exhibited increased barrier permeability relative to the parent strain after 30 min of exposure to 100 μg/mL targocil in RPMI (Fig. 2-7C). Constitutive expression of *edsRS* in the Δ*edsRS* background resulted in a significant decrease in permeability of this mutant, making it comparable to levels in the parent strain (Fig. 2-7D). This finding indicates that EdsRS activation is important to protect against targocil-induced envelope permeability, but does not exclude the possibility that activation occurs via direct interaction of targocil with EdsS in the

membrane. Interestingly, the increased permeability of Δ*BAS1661-1663*Δ*clsT* can be complemented by in *trans* expression of the cardiolipin synthase gene *clsT*. In fact, overexpression of *clsT* leads to a 35% reduction in envelope permeability compared to Δ*BAS1661-1663*Δ*clsT* in targocil (Fig. 2-7D). These results indicate that *edsRS* and *clsT* are required for preserving envelope integrity following targocil exposure.

The addition of exogenous cardiolipin to bacteria can alter phenotypes observed with envelope targeting antimicrobials [215-217]. Therefore, cardiolipin was added to targocil-exposed Δ*BAS1661-1663*Δ*clsT* cultures, which resulted in significantly reduced envelope permeability (Fig. 2-7E). The rates of EtBr uptake in the vehicle and cardiolipin-only control samples were comparable (Fig. 2-7F), suggesting that the effect of exogenous cardiolipin is only realized upon membrane damage. Overall, these data indicate that EdsRS and ClsT respond to targocil-mediated envelope damage in *B. anthracis*.

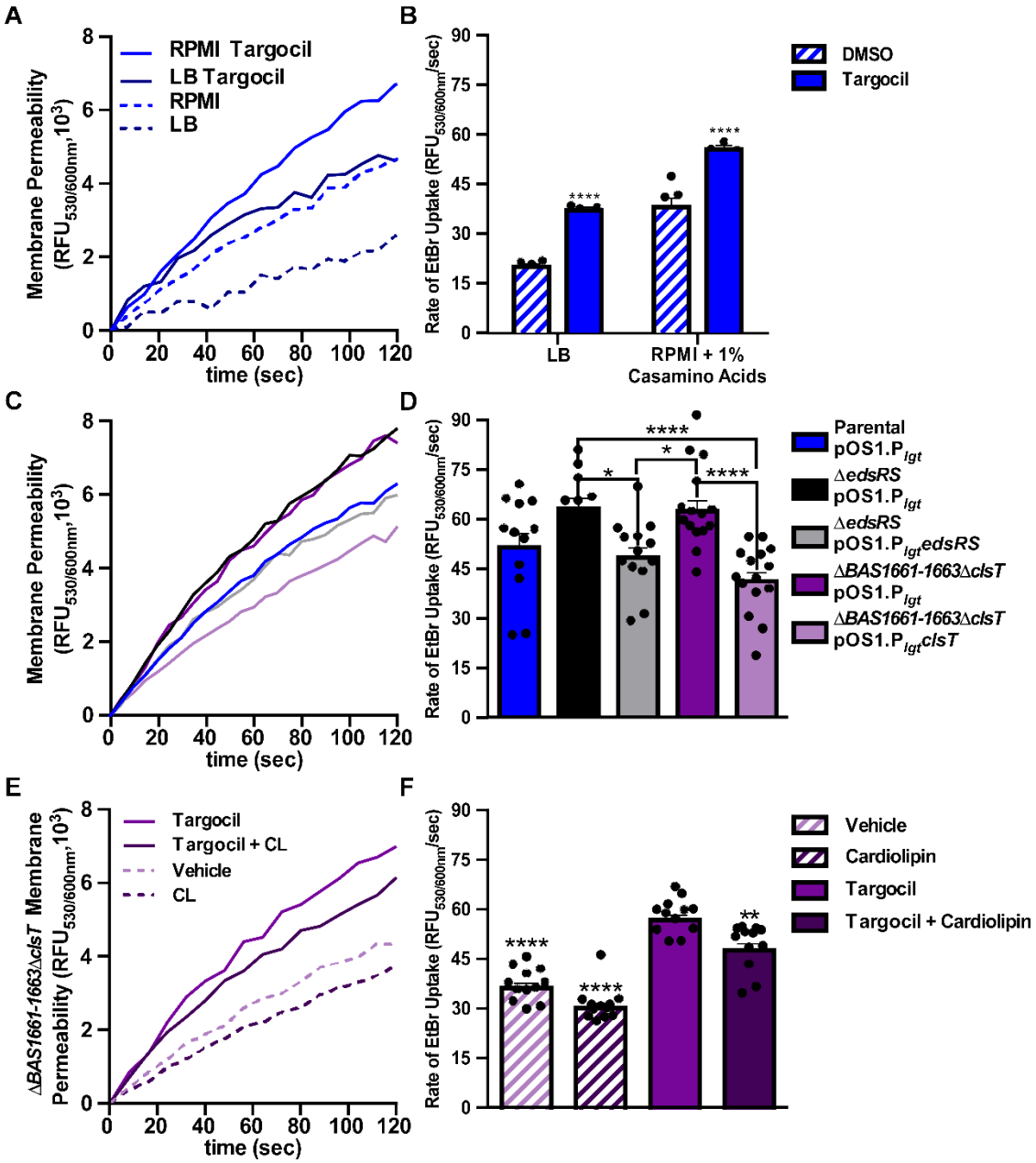

Figure 2-7. Cardiolipin synthesis is required for an intact cellular barrier during targocil treatment. A. Ethidium bromide uptake over time after growth of *B. anthracis* Sterne (Parental) in RPMI plus 1% casamino acids or LB with or without 100 µg/mL targocil**.** Data presented are averages of three independent experiments performed in biological triplicate ± SEM. **B.** The rate of ethidium bromide uptake shown in **A**. Data presented are averages of three independent experiments performed in biological triplicate ± SEM. Statistical significance compared to Parental was determined using a two-way ANOVA with a Tukey's test adjustment for multiple comparisons (****$p \leq 0.0001$). **C.** Ethidium bromide uptake over time after growth of Parental, Δ*edsRS*, Δ*BAS1661-BAS1663*Δ*clsT* containing either empty vector (pOS1 P_{lgt}) or vectors for phenotypic complementation in RPMI plus 1% casamino acids with 100 µg/mL targocil**.** Data presented are averages of three independent experiments performed in biological triplicate ± SEM. **B.** The rate of ethidium bromide uptake shown in **C.** Data presented are averages of three

independent experiments performed in biological triplicate ± SEM. Statistical significance compared to Parental was determined using a one-way ANOVA with a Tukey's test adjustment for multiple comparisons (*$p \leq 0.05$, ****$p \leq 0.0001$). **E.** Ethidium bromide uptake over time after growth of Δ*BAS1661-BAS1663*Δ*clsT in* RPMI plus 1% casamino acids with or without 100 µg/mL targocil, in the presence and absence of 100 µg/mL cardiolipin (CL)**.** Data presented are averages of three independent experiments performed in biological quadruplicate ± SEM. **F.** The rate of ethidium bromide uptake shown in **E.** Data presented are averages of three independent experiments performed in biological quadruplicate ± SEM. Statistical significance compared to targocil treated samples was determined using a one-way ANOVA with a Dunnett's test adjustment for multiple comparisons (**$p \leq 0.01$, ****$p \leq 0.0001$).

EdsRS responds to targocil-induced envelope permeability via synthesis of cardiolipin.

EdsRS responds to targocil and increases expression of *clsT,* and this activation maintains the cell barrier in *B. anthracis*. Therefore, we hypothesized that cardiolipin levels within the bacterial membrane increase in the presence of targocil, and that this is dependent on expression of both *edsRS* and *clsT*. To test this, liquid chromatography with tandem mass spectrometry (LC-MS/MS) was used to quantify relative levels of cardiolipin species in *B. anthracis*. Whole cell lysates were collected after a 30 min exposure to 100 μg/mL targocil in RPMI plus casamino acids prior to lipid extraction and LC-MS/MS analysis (Fig. 2-8). Comparisons of cardiolipin levels in the parent strain with and without targocil exposure indicate that there was a significant increase in cardiolipin after treatment (Fig. 2-9A). In support of this hypothesis, Δ*edsRS,* and Δ*BAS1661-1663*Δ*clsT* do not show a significant increase in cardiolipin upon targocil treatment (Fig. 2-9A). In accordance with the importance of ClsT, Δ*BAS1661-1663*Δ*clsT* has lower cardiolipin than the parent strain even in the absence of targocil. The phenotypes observed for the mutant strains were complemented above the parent strain levels when *edsRS* or *clsT* were constitutively expressed in *trans* (Fig. 2-9B). Consistent with earlier experiments (Fig 2-7C-D), complementation of cardiolipin levels in Δ*BAS1661-1663*Δ*clsT* only required expression of the cardiolipin synthase (*clsT*). Therefore, the cellular response to targocil involves the synthesis of cardiolipin by ClsT. The expression of *clsT* under these conditions is driven by signaling through EdsRS, establishing this TCS as being required for sensing and responding to targocil-mediated envelope damage in *B. anthracis*.

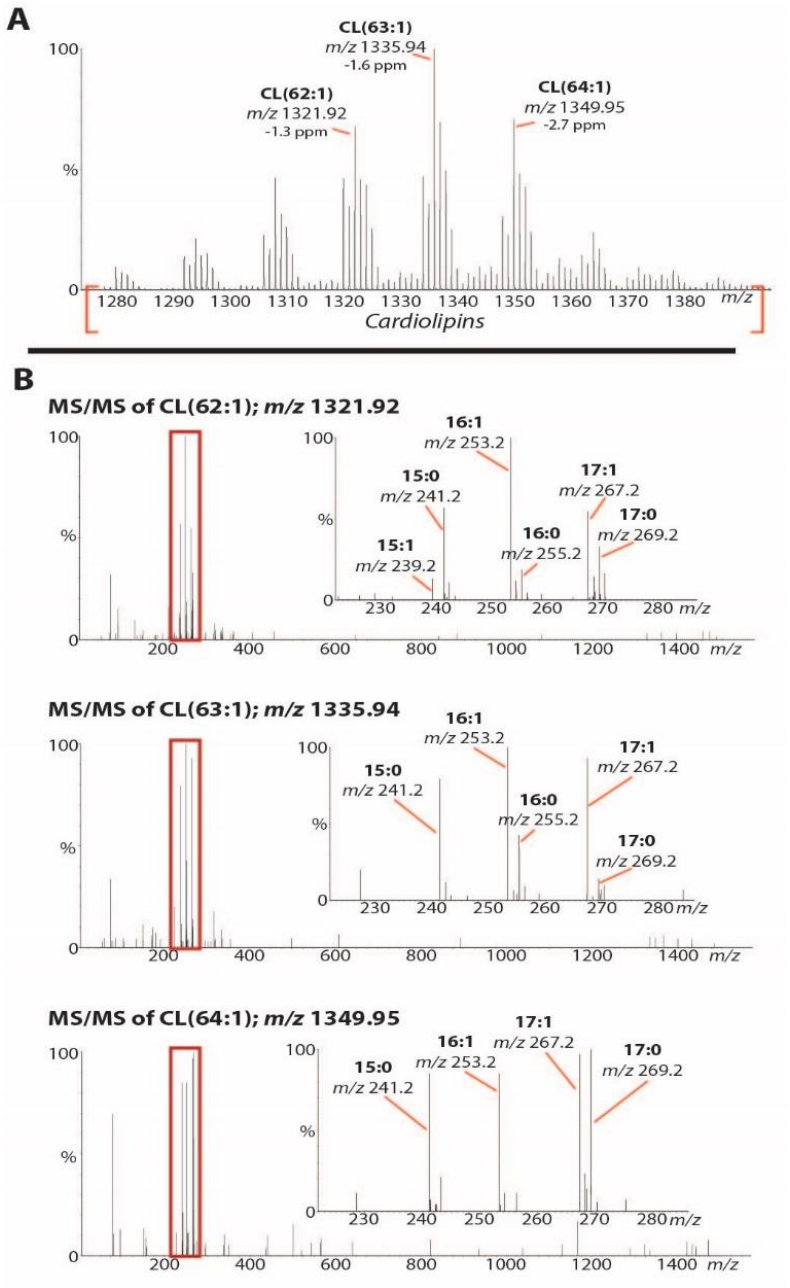

Figure 2-8. Mass spectrometry data for quantification of *B. anthracis* cardiolipin. A. A mass spectrum from LC-MS/MS analysis of a parental *B. anthracis* lipid extract shows cardiolipin (CL) species varying in alkyl chain length and number of unsaturations from *m/z* 1280 -1380. Three cardiolipin lipids are annotated with low mass error in parts per million (ppm) when compared to the theoretical *m/z* value for the cardiolipin lipid. **B.** MS/MS spectra for annotated cardiolipin lipids in **A** show multiple fatty acid fragments that combined form the total chain lengths and unsaturations for the cardiolipin species. Due to the presence of many cardiolipin isomers, various fatty acid fragments can be combined to construct the precursor cardiolipin.

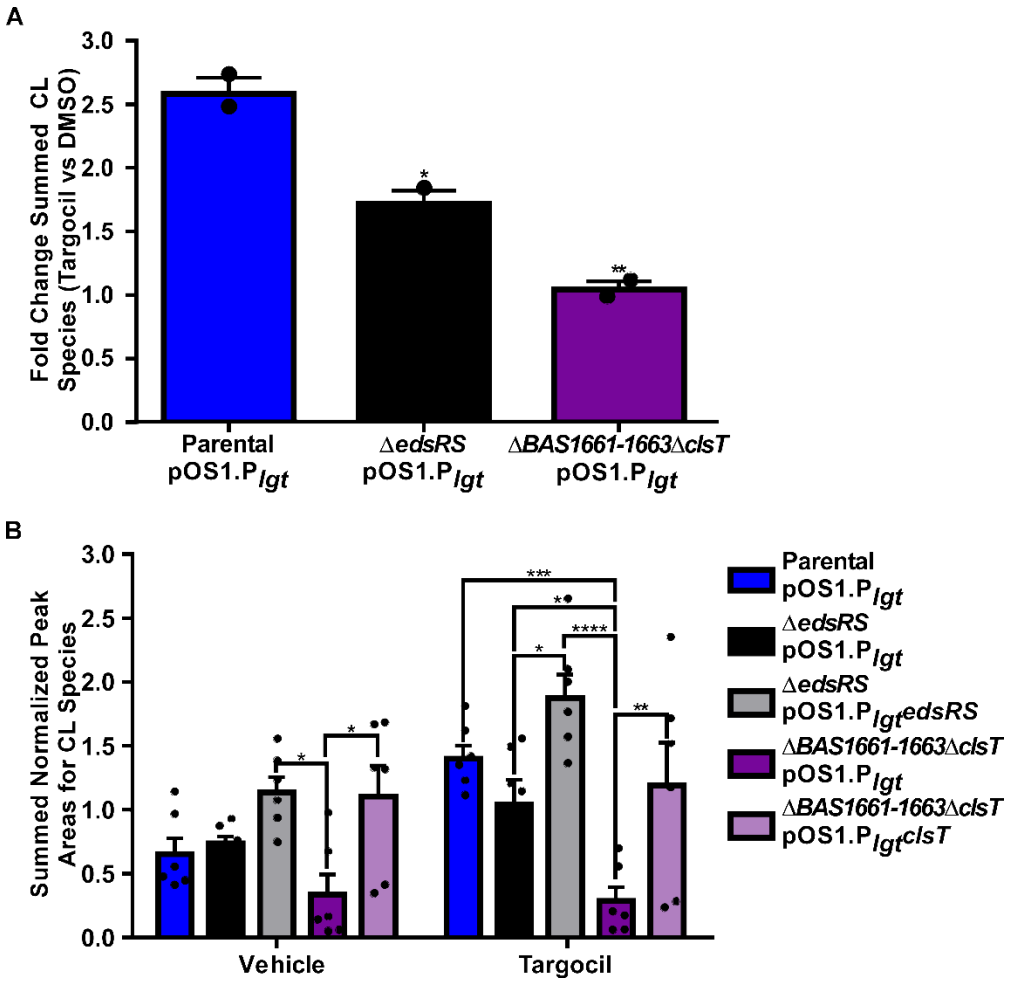

Figure 2-9. Targocil activation of EdsRS is required for ClsT-dependent increases in cardiolipin. A. Whole cell cardiolipin relative quantification using liquid chromatography coupled to tandem mass spectrometry (LC-MS/MS). Fold change of *B. anthracis* Sterne (Parental), Δ*edsRS*, and Δ*BAS1661-BAS1663*Δ*clsT* grown in RPMI plus 1% casamino acids and then exposed to 100 µg/mL targocil relative to vehicle-treated samples. Data presented are averages of two technical runs performed in biological triplicate ± SEM. Statistical significance compared within treatment groups samples was determined using a two-way ANOVA with a Tukey's test adjustment for multiple comparisons (***$p \leq 0.001$, ****$p \leq 0.0001$). **B.** Cardiolipin relative quantification of complementation strains for Parental, Δ*edsRS* and Δ*BAS1661-BAS1663*Δ*clsT* using LC-MS/MS. Cultures were also grown in RPMI plus 1% casamino acids and then exposed to 100 µg/mL targocil for 30 min. Data presented are averages of two technical runs performed in biological triplicate ± SEM. Statistical significance compared to targocil-treated samples was determined using a two-way ANOVA with a Tukey's test adjustment for multiple comparisons (**$p \leq 0.05$, **$p \leq 0.01$, ****$p \leq 0.0001$).

Discussion

In this study, the *B. anthracis* response to the antimicrobial compound targocil was analyzed. Targocil induces damage to the cellular envelope (Fig. 2-7A-B) and activates the TCS EdsRS (Fig. 2-2B). Upon activation, EdsRS increases expression of a cardiolipin synthase (ClsT) (Fig. 2-3D). EdsRS and ClsT are required for the production of cardiolipin in response to targocil (Fig 9) to protect *B. anthracis* from damage caused by targocil (Fig. 2-7C-E). Collectively, these data uncover a TCS that is activated to alter membrane composition in response to cell envelope damage.

Due to the synthetic nature of targocil, it is unlikely that EdsRS evolved to respond to this antimicrobial. However, the ability of *B. anthracis* to activate a TCS in response to envelope damage highlights the adaptability of this pathogen. The presence of over forty TCSs equips *B. anthracis* to respond to a wide range of environments [218]. Thus far, studies have assigned activating stimuli to eleven of these systems, but not all of them have defined downstream functions within the cell [72, 91, 122-124, 128, 219]. Despite the importance of TCSs, there are still over thirty histidine kinase-response regulator pairs in *B. anthracis* that are not well understood. Our work exemplifies the importance of studying TCSs in this pathogen to uncover the contribution of signaling responses to anthrax pathogenesis.

The data presented here suggest that cardiolipin abundance in the membrane affects the efficacy of antimicrobials targeted to the cell envelope, and that alterations in the regulation of cardiolipin synthesis is a bacterial strategy for adaptation. *B. anthracis* encodes five cardiolipin synthase genes. This genetic redundancy in the biogenesis of cardiolipin has been reported for other bacterial species. Bacterial cardiolipin synthases (Cls) classically synthesize cardiolipin through the condensation of two molecules of phosphatidylglycerol to produce cardiolipin and glycerol [216, 220]. *cls* genes have been studied in *Escherichia coli*, which encodes for three of

these enzymes (ClsA, ClsB, and ClsC). Each of the Cls enzymes in this bacterium uses unique precursors and contributes to cardiolipin abundance under distinct conditions including stationary or hyperosmotic growth [203, 221]. This specificity enables tight control of membrane phospholipid composition and preservation of resources. Similar to *E. coli*, *B. subtilis* encodes three cardiolipin synthases (ClsA, YwjE, and YwiE) with differentially ascribed functions [222]. ClsA is the primary cardiolipin synthase in this species during vegetative growth and osmotic stress, but works together with YwjE to produce the phospholipid during the process of sporulation [222-224]. Although it has not been empirically tested, transcription data suggest that the third synthase gene, *ywiE*, is involved in the response to heat shock [225].The use of multiple Cls variants is important in gram-positive pathogens. The human pathogen *S. aureus* expresses two cardiolipin synthases (Cls1 and Cls2) [226, 227]. Cls2 is the primary producer of cardiolipin, which accumulates in *S. aureus* during stationary phase growth. However, after phagocytosis and during growth in high salt, both Cls1 and Cls2 contribute to cardiolipin synthesis [227]. These examples highlight the versatility of bacterial phospholipid synthesis. Synthesis of cardiolipin depends on the growth phase and specific stress encountered and results in unique routes of biogenesis depending on available lipid resources. The extreme adaptability of *B. anthracis* to survive in the environment and during infection of mammalian hosts is likely supported not only by the presence of TCSs, but also by flexibility in pathways used for generation of key cellular molecules, like cardiolipin.

Cardiolipin has been associated with the efficacy of antimicrobials, specifically daptomycin. Daptomycin forms pores in the membranes of bacteria resulting in barrier permeabilization and has been linked to disruption of cell division [228-230]. Daptomycin was first used clinically in 2003 and since then resistance to this drug has been reported in *Enterococcus*

and *Staphylococcus* species [231]. Sequencing of daptomycin resistant *Enterococcus* strains identified mutations within a cardiolipin synthase [232, 233]. Although the mechanism by which cardiolipin protects against daptomycin remains unclear, a follow up study found that addition of exogenous cardiolipin to liposomes diminished the pore-forming activity of daptomycin [216]. However, a TnSeq study in *S. aureus* found that mutation of a cardiolipin synthase confers resistance to daptomycin [234]. These results suggest that bacterial cells can increase the abundance of cardiolipin within their outer membranes to repair damage by antimicrobials that breach this barrier, similar to the findings presented here in *B. anthracis*, but that the consequence of these modifications can be species specific.

While cardiolipin synthesis can enable bacteria to resist some antimicrobial compounds, the role of cardiolipin in the response to antimicrobials is context dependent. Cardiolipins can also increase the efficacy of other antimicrobials. For instance, the toxicity of an amphiphilic aminoglycoside derivative against *Pseudomonas aeruginosa* was enhanced with addition of cardiolipin to the culture conditions [217]. The derivative altered the biophysical structure of lipid bilayers to cause increased permeability in a cardiolipin-dependent manner [235]. In another example, the activity of plantazolicin was interrogated in *B. anthracis* [215]. Plantazolicin inserts into the cellular envelope of bacilli and disrupts membrane potential, indicating damage to the bilayer. Of the species tested, *B. anthracis* was the only gram-positive organism sensitive to this compound [236]. This study observed that EdsRS (then referred to as *BAS5200-BAS520*) was upregulated upon plantazolicin exposure, providing an additional link between EdsRS and damage to the envelope of *B. anthracis* [215]. In an effort to understand the mechanism of plantazolicin toxicity, selection studies were performed looking for resistant mutants. Molohon et al. identified isolates that showed resistance phenotypes containing mutations within *BAS1662, BAS1663,* and

the promoter region of the *BAS1661-1663clsT* operon. As a follow up to this finding, they showed that exogenous cardiolipin increases the efficacy and membrane insertion of plantazolicin. Therefore, EdsRS is activated by treatment with plantazolicin however subsequent induction of *BAS1661-1663clsT* and increase in cardiolipin levels is detrimental due to the mechanism of drug insertion. Using two small molecules that are similar in function but divergent in mechanism, the work of Molohon et al. combined with results reported here support a link between envelope disruption, EdsRS two-component system signaling, and cardiolipin synthesis.

The intracellular environment of host immune cells is a site for germination of *B. anthracis* spores during infection [27, 43, 237-240]. The importance of EdsRS signaling to the germination and viability of *B. anthracis* during outgrowth in the presence of envelope damaging agents indicates that this system could be used during dissemination in vertebrate hosts. TCSs are important for intracellular survival where they enable a response to metal limitation or acidic environments [241, 242]. Future studies are needed to test the role of EdsRS signaling in resistance to barrier attack and germination within phagocytes. The subsequent EdsRS-dependent induction of ClsT synthesis of cardiolipin may reverse barrier permeability to promote bacilli survival (Fig. 2-3C, 2-5B, 2-7C-F, 2-9). Cardiolipin synthesis is induced after phagocytosis occurs in *S. aureus* [227]. The kinetics of this induction in *S. aureus* suggest that increased membrane cardiolipin is important for defense against later stages of immune attack following escape from the host phagocyte [227]. Therefore, the bacteria may respond to recognition of the host environment to prepare for survival during infection. The precise role of cardiolipin synthesis in *B. anthracis* immune evasion should be elucidated in future studies as this suggests a role for EdsRS in defense against host attack. Reacting to host effectors in this manner may promote *B. anthracis* pathogenesis, providing significant insight into how this organism causes severe infections

CHAPTER III

DNAJ AND CLPX ARE REQUIRED FOR HITRS AND HSSRS TWO-COMPONENT SYSTEM SIGNALING IN *BACILLUS ANTHRACIS*

Introduction

Bacillus anthracis is a spore-forming pathogen and the causative agent of the infectious disease anthrax. Due to the severe threat posed by this pathogen, *B. anthracis* is included on the Select Agents and Toxins List as managed by the United States Department of Agriculture Administration, Centers for Disease Control and Prevention, and Health and Human Services [243]. Anthrax can result from exposure to *B. anthracis* spores via cutaneous contact, inhalation, or ingestion [8, 10, 15]. Mortality rates for inhalation anthrax approach 90% [18]. Regardless of the site of infection, spores are phagocytosed as a part of the host innate immune response. Upon internalization, spores germinate into vegetative bacilli that initiate virulence factor production [91, 190, 244]. The most well-studied virulence factors produced by *B. anthracis* include protective antigen, lethal factor, edema factor, and the poly γ-D-glutamic acid capsule. The toxins are expressed early and are used for dissemination, tissue destruction, and disruption of central host immune signaling pathways [8, 10]. The poly γ-D-glutamic acid capsule coats the surface of the bacterium to evade phagocyte mediated killing [10, 22, 23]. The bacilli escape into the bloodstream, where growth can reach densities as high as 10^9 bacterial cells per milliliter of blood [8]. This rapid bacterial multiplication results in intoxication and death of the host. Though the precise mechanisms of bacterial dissemination remain obscure within the host, it is clear that *B. anthracis* encounters many environmental stresses within the host during the progression of anthrax.

Pathogen proliferation during infection requires the ability to adapt to the diverse environments encountered within the host. Two-component system (TCS) signaling is the most highly conserved multi-component model for signal transduction in bacteria. Bacteria use these systems to sense and respond to alterations in their environment. A TCS is activated upon detecting a specific signal by a histidine kinase (HK) that is typically localized to the membrane. After HK activation through autophosphorylation, the phosphate group is transferred to the cognate partner response regulator (RR). The RR dimerizes and undergoes conformational changes that enable binding to the DNA resulting in expression changes of target genes. TCS activation often leads to alterations in gene expression relating to the sensed stimuli and can also result in upregulation of the HK and RR to amplify the response.

Though TCSs are classically thought to signal as a single pair, with one HK activating one RR, there are increasing examples of TCS cross-regulation. Cross-regulation refers to instances of TCS interaction that provide benefit to the bacterium [87]. Beyond the complexity of TCS signal integration is the importance of a coordinated response that has beneficial implications for bacterial pathogenesis. Reacting to host factors in this cooperative manner may provide *B. anthracis* with the foundation for successful pathogenesis, enabling this organism to cause severe infections. Examples of TCS cross-regulation exist in a number of bacterial pathogens, including *Escherichia coli*, where PmrAB cross-regulates QseBC to integrate detection of ferric iron with quorum sensing for pathogenesis and biofilm formation [103, 245]. Cross-regulation between PmrAB and PhoPQ, a phosphate-sensing TCS, occurs in *Salmonella enterica*, *Yersinia pestis*, and *Klebsiella pneumoniae* via the connector protein PmrD [246]. During phosphate limitation in *Bacillus subtilis*, PhoPQ activates the YycF response regulator, and YycFG feeds back to cross-regulate PhoPQ [247]. *B. anthracis* harbors two TCSs, HssRS (*H*eme *s*ensor *s*ystem) and HitRS (*H*ssRS

*i*nterfacing *T*CS), that exhibit cross-regulation [91]. HssRS responds to toxic levels of heme, the iron-binding component of hemoglobin. Heme is a key iron source for pathogens, but it can be toxic at high concentrations. To alleviate heme toxicity, activated HssRS facilitates expression of the predicted heme efflux pump, HrtAB [70, 72, 90]. HssRS also interacts with the components of HitRS, a TCS activated by cell envelope stress and a synthetic compound identified in a high throughput screen for HitRS activators, ‘205 [248, 249]. We previously demonstrated that the HKs, RRs, and promoter regions of HssRS and HitRS cross-signal with each other [248]. However, the response of HitRS and HssRS to the range of identified activators has not been defined. To maintain efficient use of energy and resources, signaling pathways such as these must themselves be tightly controlled.

In addition to controlling responses to various stimuli through transcriptional changes, additional mechanisms exist to regulate the translation, stability, degradation, and quality of proteins in bacteria. A balance of protein stabilization and degradation has evolved within cells to post-translationally control key functional networks. Heat shock proteins represent a select set of proteins that are activated in hostile environments [142, 144]. These proteins support the refolding of damaged peptides, stabilization of aggregated proteins, and folding of newly translated peptides [132]. These activities impact subcellular localization and indirectly control regulatory protein activity. The DnaJK chaperone complex is a highly conserved piece of this stress response, and protein chaperones DnaJK/GrpE are responsible for maintaining the stability of DNA replication, protein expression, and cellular division machinery [142]. DnaJK stabilizes proteins during periods of stress to prevent aggregation, as the accumulation of aggregated peptides can be toxic to cells [141]. DnaJ transiently binds to protein substrates via a conserved zinc finger domain and passes protein substrates to DnaK via interaction at the J domain of DnaJ [143, 144, 250]. DnaK then

hydrolyzes ATP to provide energy for peptide refolding before GrpE facilitates protein release and ADP recycling [142, 144]. Though DnaJK/GrpE are highly effective chaperones, there exist stress conditions where protein degradation is the preferred mechanism of protein regulation.

ATP-dependent proteases also function in the maintenance of protein homeostasis during stress, though in contrast to chaperones, this family of proteins is largely responsible for the degradation of its substrates [132, 149, 150]. Caseinolytic protease (Clp) proteases are bipartite complexes associated with cellular development and transcriptional regulation encoded in the genomes of Gram-positive and Gram-negative bacterial species [149, 251, 252]. This complex starts with one of many nucleotide-binding proteins (ClpA, ClpX, ClpC, or ClpB), which are responsible for the recognition of protein substrates bearing specific conserved motifs [132, 149]. Targeted peptides are recognized, bound, and unfolded in a hexameric ring comprised of one of the nucleotide binding proteins [253]. The unfolded substrate is transported to the protease subunit, ClpP, where it is degraded, and the components are released [254]. A vital quality control role is played by Clp proteases to regulate damaged proteins in both stressed and non-stressed cells. In *B. anthracis*, a *clpX* mutant is attenuated in mammalian infection models due to an inability to degrade host antimicrobial effectors [154]. The necessity of Clp complexes is highlighted by their requirement in bacterial pathogens [150, 153, 164, 255, 256].

Here we define new targets for the protein homeostasis regulators, DnaJ and ClpX, in the maintenance of the *B. anthracis* TCSs HssRS and HitRS. DnaJ and ClpX were identified using a genetic selection to detect contributors to TCS signaling. These post-translational regulators are required for the activation of HitRS-dependent expression of the *hit* operon and cross-regulation of HssRS-dependent gene expression. DnaJ and ClpX are dispensable for HitS membrane localization. Instead, DnaJ keeps HitR levels low while both DnaJ and ClpX stabilizing HitS

protein. This work describes how an unbiased selection led to the elucidation of new roles for key protein homeostasis modulators in the regulation of *B. anthracis* TCS function.

Materials and methods

Bacterial strains and growth conditions. *B. anthracis* strain Sterne was used was used as wildtype in all experiments under BSL2 conditions [24, 98]. Cultures were streaked from 25% glycerol freezer stocks on lysogeny broth agar (LBA) plates and grown at 30 °C for 16 h. Lysogeny broth (LB) in an aerated tube was inoculated using a single colony from these plates. Cultures were grown at 30 °C shaking at 180 rpm for all overnight growth or any incubation over 8 h. For growth assays performed for 8 h or less, growth was monitored at 37°C. Plasmids used in this study were constructed using *E. coli* DH5α or TOP10 strains. Plasmids were then moved from *E. coli* to *B. anthracis* after first transforming them into *E. coli* K1077 or *S. aureus* RN4220. Antibiotic concentrations used were 50 μg mL^{-1} carbenicillin for *E. coli* (reporter and protein expression vectors), 10 μg mL^{-1} chloramphenicol for *S. aureus* and *B. anthracis* (reporter vectors), 100 μg mL^{-1} spectinomycin (protein expression vectors), and kanamycin at 20 μg mL^{-1} in *B. anthracis* and 40 μg mL^{-1} in *E. coli* (genetic manipulation vectors). The bacterial strains (Table 3-1), plasmids (Table 3-2), and primers (Table 3-3) used in this study are listed in their indicated tables below.

Preparation of compound stocks. All chemicals were purchased from Sigma Aldrich unless otherwise noted. Fifty mM stocks of ‘205 were made in DMSO and stored at -20 °C [91]. Ten mM stocks of hemin (Frontier Scientific) were made fresh for each use in 0.1 M NaOH. Fifty mg mL^{-1} carbenicillin stocks were prepared in diH_2O and stored at -20 °C. Ten mg mL^{-1} chloramphenicol stocks were made in 70% EtOH and stored at -20 °C.

Genetic manipulation of *B. anthracis.* Genetic manipulation was performed as previously described [72, 91, 98, 249]. Plasmids were introduced into the strain of interest via electroporation

according to previously described protocols [72, 91, 98, 185]. The generation of knockout strains was performed by inserting the flanking sequences for mutations of interest into the mutagenesis plasmid pLM4. Plasmid construction and mutagenesis was performed using this vector as described previously [84, 98] and confirmed by PCR and Sanger sequencing.

TCS-RelE strain selection and sequence analysis. The selection strain, as outlined in Table 1, was used to select for mutations in genes required for HitRS or HssRS function. TCS-RelE strain selection using the HitRS and HssRS selection strains were performed as described previously [249]. Briefly, the selection strain was grown overnight in LB prior to dilution (1:1, 1:3, 1:10, and 1:30) and plated onto LBA containing low concentrations of activator (2 and 4 μM ’205, 4 and 8 μM heme) before incubation at 30 °C for up to 5 days. For both selections, spontaneous mutations were streaked for single colony isolation on fresh LBA and then saved for further confirmation of resistance to ‘205/heme. Genomic DNA was isolated from mutants of interest using the DNeasy Blood and Tissue Kit (Qiagen) and sent for whole genome sequencing and analysis through the Microbial Genome Sequencing Center (University of Pittsburgh).

Growth Curves. Strains of interest were streaked on LBA and grown at 30 °C for 16-18 h. Single colonies were used to start liquid cultures containing the same media used for the assay as annotated and were grown for 16 h at 30 °C with shaking. Cultures were diluted 1:100 into fresh media and grown with shaking for 6 h at 37 °C. One μL of each culture was added to 99 μl of LB containing the annotated compounds or a vehicle control in a 96-well flat-bottomed plate. Growth was monitored over time at 37 °C by measuring the optical density at 600 nm in a BioTek Epoch2 spectrophotometer and analyzed with BioTek Gen5 software.

Temperature sensitivity. Strains of interest were streaked on LBA and grown at 30°C for 16-18 h. Single colonies were used to start liquid cultures containing LB used for the assay as annotated and were grown for 16 h at 30°C with shaking. Cultures were diluted 1:100 into fresh media and grown with shaking for 6 h at either 37°C or 42°C. Samples were serially diluted and plated onto LB agar to enumerate the total bacterial density.

Sporulation assay. *B. anthracis* strains of interest were streaked on LBA and grown at 30 °C for 16-18 h. Single colonies of the indicated strains were used to start liquid cultures in LB and were grown for 16 h at 30 °C with shaking. Cultures were diluted 1:100 into Modified G Medium (MGM) sporulation media [190] and grown with shaking for 24 h at 37 °C. Samples were serially diluted and plated on LB agar to enumerate the total bacterial density. The same samples were then incubated at 65 °C for 30 min to lyse vegetative cells. The boiled suspension was serially diluted and plated to enumerate spore counts.

XylE assay. XylE reporter plasmids were generated previously [72, 248] and used in this study to monitor TCS promoter activity. Single colonies of strains containing the XylE reporter plasmids were used to start liquid cultures LB containing chloramphenicol and were grown for 16 h at 30 °C with shaking. Overnight cultures were diluted 1:100 into in LB containing chloramphenicol and the indicated concentration of activator or an equal volume of the appropriate vehicle. After 6 h of growth at 37 °C, the abundance of the XylE enzyme present in *B. anthracis* cellular lysates was assessed by measuring the rate at which exogenously catechol was converted to 2-hydroxymuconic acid using a spectrophotometer as described previously [72, 98].

Gene expression studies. Overnight cultures of *B. anthracis* were back-diluted 1:100 in fresh LB and grown at 37 °C with shaking for 6 h (mid-log phase). Cultures were divided in half and then dosed with either control or activator. Cultures were returned to 37 °C for 15 min. Cultures were mixed at a ratio of 1:1 (V/V) with a 1:1 (V/V) mixture of cold acetone and EtOH and stored at -80 °C until RNA isolation. RNA was isolated using the RNeasy kit as per manufacturer's instructions (Qiagen) and DNA was removed using the Turbo DNA-free kit (Invitrogen, Thermo Scientific). Quantification of RNA was performed using a Thermo Scientific Spectrophotometer NanoDrop before cDNA was synthesized using the iScript cDNA Synthesis kit (Bio-Rad). qRT-PCR was performed as previously described using *gyrA* as a housekeeping gene, iQ SYBR Green Supermix (Bio-Rad), and the $\Delta\Delta^{CT}$ method [98, 188].

Protein detection and Western Blotting. *B. anthracis* strains of interest were grown overnight and then diluted 1:100 into 5 mL of LB with spectinomycin. Cultures were grown at 37 °C for 2 h prior to induction. Isopropyl β-d-1-thiogalactopyranoside (IPTG, Roche) was added to the cultures (100 μM for HitR, 250 μM for HitS) with or without 50 μM '205. Growth was continued for 6 h before samples were subjected to the following protocol for whole cell lysis. Cells were treated with 6 mg/mL lysozyme in 10 mM $MgCl_2$ in phosphate buffered saline (PBS) at 37°C for 30 min. 2% IGEPAL CA-630 and 20 mM Phenylmethylsulfonyl fluoride (PMSF) were added at 4 °C for 10 min. Cells were lysed using the Lysing Matrix B tubes on the FastPrep Bead Beater instrument (MP Biomedical) and then treated with 20 μg DNase I (Roche) for 30 min at 37 °C. Protein concentration for loading into SDS-PAGE (Bio-Rad) was normalized using the Pierce Coomassie (Bradford) Protein Assay Kit (Thermo Fisher Scientific). Loading controls were stained using

Simply Blue (Thermo Fisher Scientific) and gels for Western Blot were transferred using the Trans-Blot Turbo Transfer System (Bio-Rad). Blots were rocked overnight at 4 °C in the primary Ab diluted 1:2,500 in Odyssey Blocking Buffer, washing in 0.1% Triton-X in PBS (PBST) three times, rocked 1 h at room temperature in the secondary Ab (Thermo Fisher Scientific) diluted 1:3,000 in PBST, and then washed prior to imaging on a ChemiDoc Imaging System (Bio-Rad). The primary Ab included ab9132 α-myc (Abcam) and α-SrtA rabbit serum [257]. The blots shown are representative images of three independent experiments performed in technical triplicate. Densitometry analysis of band intensity, minus background signal, for the proteins of interest and loading control was performed using ImageJ.

Structured Illumination Microscopy. *B. anthracis* mutants harboring the HitS protein fusion vector were grown overnight. Cultures were collected and washed in PBS. The genomes were stained with 1 μg/mL Hoechst 33342 (ThermoFisher) for 10 min at RT prior to fixation in 4% paraformaldehyde (Invitrogen) for 20 min at RT. Cells were washed with PBS and then with diH_20 prior to drying bacteria onto a coverslip. Prepared coverslips were adhered to slides using Prolong Gold (ThermoFisher). Super-resolution imaging was performed on a Nikon Structured Illumination Microscopy (SIM) using 3D-SIM mode and a 100X objective. Images were collected using an Andor DU-897 EMCCD camera using settings determined with wildtype control samples. The brightness and contrast were adjusted to allow for the visualization of both the genomes and membrane localization of the tagged HitS. Analysis was performed using Nikon Elements General Analysis 3 (GA3) capabilities. Signal thresholds were determined for each channel. For each signal the sum intensity, total volume, overlapping volume, and overlapping signal intensity was calculated using the GA3.

Table 1: Bacterial strains utilized in this study

Species	Genotype	Description	Reference
B. anthracis strain Sterne	WT	Wildtype laboratory stock	[184]
B. anthracis strain Sterne	HitRS-RelE strain	Genomic insertion of P_{hit}*relE*, P_{hit}*relE*, and P_{hit}*hitRS* within *BAS3009*, *BAS4599*, and *BAS4927*, respectively	[249]
B. anthracis strain Sterne	HssRS-RelE strain	Genomic insertion of P_{hrt}*relE*, P_{hrt}*relE*, and P_{hrt}*hssRS* within *BAS3009*, *BAS4599*, and *BAS4927*, respectively	This study
B. anthracis strain Sterne	Δ*hitRS*	In-frame deletion of *hitRS*	[248]
B. anthracis strain Sterne	Δ*hssRS*	In-frame deletion of *hssRS*	[72]
B. anthracis strain Sterne	$DnaJ^{Q171*}$	Recreation of HitRS mutant 1, in-frame truncation of DnaJ after glutamaine 171	This study
B. anthracis strain Sterne	$ClpX^{A88X,V89X}$	Recreation of HitRS mutant 3 and HssRS mutants 1-3, in-frame deletion of ClpX alanine 88 and valine 89	This study
B. anthracis strain Sterne	Δ*dnaJ*	In-frame deletion of *dnaJ*	This study
B. anthracis strain Sterne	*clpX::tet*	In-frame substitution of *clpX* with a tetracycline resistance cassette	This study
B. anthracis strain Sterne	$HitR^{M58I}$	In-frame substitution of HitR methionine 58 to isoleucine	[249]
B. anthracis strain Sterne	$HitS^{S141L}$	In-frame substitution of HitS serine 141 to lysine	[249]
B. anthracis strain Sterne	Δ*dnaJ* $HitR^{M58I}$	In-frame deletion of *dnaJ* and in-frame substitution of HitR methionine 58 to isoleucine	This study
B. anthracis strain Sterne	Δ*dnaJ* $HitS^{S141L}$	In-frame deletion of *dnaJ* and in-frame substitution of HitS serine 141 to lysine	This study
B. anthracis strain Sterne	*clpX::tet* $HitR^{M58I}$	In-frame substitution of *clpX* with a tetracycline resistance cassette and in-frame substitution of HitR methionine 58 to isoleucine	This study
B. anthracis strain Sterne	*clpX::tet* $HitS^{S141L}$	In-frame substitution of *clpX* with a tetracycline resistance cassette and in-frame substitution of HitS serine 141 to lysine	This study

S. aureus strain RN4220	WT	Wildtype laboratory stock for cloning	[194, 195]
E. coli strain K1077	WT	Wildtype laboratory stock for cloning	[185].

Table 2: Plasmids utilized in this study

Plasmid	Description	Reference
pLM4	Allelic exchange vector for *B. anthracis*	[84]
pLM4-*3009*	Vector to integrate genes within *BAS3009*	[249]
pLM4-*4599*	Vector to integrate genes within *BAS4599*	[249]
pLM4-*4927*	Vector to integrate genes within *BAS4927*	[249]
pLM4-*3009::P_{hit}relE*	Vector to integrate *hit-relE* fusion within *BAS3009*	[249]
pLM4-*4599::P_{hit}relE*	Vector to integrate *hit-relE* fusion within *BAS4599*	[249]
pLM4-*4927::hitRS*	Vector to integrate *hitRS* within *BAS4927*	[249]
pLM4-*3009::P_{hrt}relE*	Vector to integrate *hrt-relE* fusion within *BAS3009*	This study
pLM4-*4599::P_{hrt}relE*	Vector to integrate *hrt-relE* fusion within *BAS4599*	This study
pLM4-*4927::hssRS*	Vector to integrate *hssRS* within *BAS4927*	This study
pLM4.DnaJ^{Q171*}	Vector to recreate DnaJ^{Q171*}mutation	This study
pLM4.ClpX^{A88X,V89X}	Vector to recreate ClpX^{A88X,V89X} mutation	This study
pLM4.*dnaJ*	Vector to delete *dnaJ*	This study
pLM4.*clpXtet*	Vector to replace *clpX* with *tet*	This study
pLM4.HitR^{M58I}	Vector to create in frame HitR^{M58I}	(19)
pLM4.HitS^{S141L}	Vector to create in frame HitS^{S141L}	(19)
pUTE657.P_{hspank}	Empty vector with IPTG inducible hyper-spank promoter	[258]
pUTE657. P_{hspank}*hitR*.myc	IPTG inducible, myc-tagged HitR vector	This study
pUTE657. P_{hspank}*hitS*.myc	IPTG inducible, myc-tagged HitS vector	This study
pOS1	Empty vector	[84]
pOS1.P_{hit}xylE	HitRS XylE reporter vector	[91]
pOS1.P_{hrt}*xylE*	HssRS XylE reporter vector	[72, 91]
pOS1.P_{lgt}*hitS.mcherry*	HitS-mCherry protein-fluorophore fusion vector	This study
pOS1. P_{lgt}*mcherry*	mCherry vector	This study

Table 3: Primers utilized in this study

Primer	Sequence	Use
P_{hrt}*relE*_NheI_fwd	GCATGAGCTAGCACTCCTTGAATAAATTTACTCG	Chromosomal insertion
P_{hrt}*relE*_SOE_L	GAAAATACGCCATTTCGCTCGCTCCTTCCTC	Chromosomal insertion
P_{hrt}*relE*_SOE_R	CGAGCGAAATGGCGTATTTTCTGGATTTTG	Chromosomal insertion
P_{hrt}*relE*_KpnI_rev	GCATGAGGTACCTCAGAGAATGCGTTTGACCG	Chromosomal insertion
*hssRS*_KpnI_fwd	GCATGAGGTACCGGTATTGGAACTATATTAACCG	Chromosomal insertion
*hssRS*_KpnI_rev	GCATGAGGTACCGGCGATTTTCACAATATATCGG	Chromosomal insertion
*dnaJ*_XmaI_fwd	GCATGACCCGGGATTTTGCATACTGTAAGTGAGG	Mutagenesis
*dnaJ*_SacI_fwd	GCATGAGAGCTCATCAATAGATGACTTTACACC	Mutagenesis
*clpX*_XmaI_fwd	CCATGACCCGGGCTAACGCTGAAATCGACATTC	Mutagenesis
*clpX*_SacI_fwd	CCATGAGAGCTCATCAACAAGAGCATCTTCATC	Mutagenesis
*dnaJ*_XmaI_fwd	CCATGACCCGGGATTCGATATTGATGCGAACGG	Mutagenesis
*dnaJ*_SOE-L	CCATTTTTTATTTCCAAATTTTACAACCCCCGAATCTTTC	Mutagenesis
*dnaJ*_SOE-R	GTTGTAAAATTTGGAAATAAAAAATGGAGTTGG	Mutagenesis
*dnaJ*_SacI_rev	CCATGAGAGCTCTTTAAACGTACATTCATTTCTGC	Mutagenesis
*clpX*_XmaI_fwd	CCATGACCCGGGCTAACGCTGAAATCGACATTC	Mutagenesis
*clpX*_SOE-L	CGCATTATGATTTTCACACCCCTTACAAAGTG	Mutagenesis
*clpX*_SOE-R	GGGTGTGAAAATCATAATGCGAAGGAGAAACAG	Mutagenesis
*clpX*_SacI_rev	CCATGAGAGCTCCCGTGTGCATCTGTTACCG	Mutagenesis
*clpX*_StuI_fwd	AGGCCTCATAATGCGAAGGAGAAAC	Mutagenesis
*clpX*_StuI_rev	ATTTTCACACCCCTTACAAAG	Mutagenesis
*hitRmyc*_fwd	CGGATAACAATTAAGCTTAGTCGACAGGAGGTTGAAAATCGTTTATATGAATAATCAGTGGGGATTG	Vector construction

*hitRmyc*_rev	CCACCGAATTAGCTTGCATGCTCAGAGGTCCTCCTCGCTGATGAGCTTCTGCTCTTTACTTACCTCTAAGCGATATCC	Vector construction
*hitSmyc*_fwd	CGGATAACAATTAAGCTTAGTCGACAGGAGGTTGAAAATCGTTTATATGAGTAAATTCAAGATGCTGAAAG	Vector construction
*hitSmyc*_rev	CCACCGAATTAGCTTGCATGCTCAGAGGTCCTCCTCGCTGATGAGCTTCTGCTCTTTCTCTTCATAATTTGGAATACAAAC	Vector construction
*hitSmcherry*_Nde1 fwd	GCATGACATATGATGAGTAAATTCAAGATGC	Vector construction
*hitSmcherry*_BamH1 rev	GCATGAGGATCCACCTTTCTCTTCATAATTTGGAATAC	Vector construction
*hitSmCherry*_BamH1_fwd	GCATGAGGATCCGGTGGTGTTTCTAAAGGAGAAGAAGATAAC	Vector construction
*hitSmCherry*__Pst1_rev	GCATGACTGCAGTTATTTATATAATTCATCCATTCC	Vector construction
mCherry fwd	CAATTGAGGTGAACATATGCTCGAGATGGTTTCTAAAGGAGAAGAAG	Vector construction
mCherry rev	AAACACTACCCCCTTGTTTGGATCCTTATTTATATAATTCATCCATTCCG	Vector construction
hitP fwd	TGCTTTCTACGGGAGCAAGTT	qRT-PCR
hitP rev	ACGTTCTCTCAGTCCAGCTAC	qRT-PCR
hitR fwd	CTAGTAGTGAGGGTTAAGGCGT	qRT-PCR
hitR rev	CGAACAAGTTCTCCCCGCTT	qRT-PCR
hits fwd	AATGAGACCGAAGCGAGAGG	qRT-PCR
hitS rev	ACGCATCTTCTCCATCGCAT	qRT-PCR
gyrA fwd	TCTATGGGACGTAATGCGGC	qRT-PCR
gyrA rev	CTTTACCACCACGGCTTTGC	qRT-PCR

Results

Targeted genetic selection identifies regulatory factors that contribute to TCS signaling in *B. anthracis.*

TCSs are conserved within bacteria and are vital for bacterial detection, response, and adaptation to changes in the environment. Each TCS may have distinctive stimuli that trigger HK autophosphorylation and subsequent TCS activation, but signaling can be modulated to maintain the appropriate specificity and magnitude of activation [155]. In *Bacillus* species, regulatory proteins modulate TCS activity to tightly control their activity [167, 259-265]. *B. anthracis* encounters innumerable chemical and physical changes during growth in the soil or in a mammalian host, which can include conditions that compromise TCS protein integrity. We hypothesized that *B. anthracis* TCS require accessory factors, particularly in the context of HitRS- and HssRS-activating conditions, to maintain signaling protein integrity. To identify proteins that function upstream of TCS activation in *B. anthracis*, we developed a genetic strategy that enables the selection of mutations required for TCS signaling [249, 266]. In brief, strains that allow for TCS-induced bacterial death were constructed. Each strain contains a genomic insertion of the toxin-encoding *relE* gene that is expressed under the control of the TCS-regulated promoter of interest, at a neutral site in the genome. RelE is a toxin that degrades bacterial mRNA, resulting in arrest of cellular function [267]. Treatment of each strain with its corresponding TCS-activating molecule results in lethality unless there is a mutation in the genome which inhibits signaling such that the promoter is not induced [91]. Based on our experience with promoter-based genetic selection, the most commonly isolated inactivating mutations are in the TCS, the TCS-regulated promoter, or the *relE* toxin [249]. Therefore, we inserted an additional copy of the genes encoding both the TCS and TCS-controlled *relE* into a pseudogene locus in the genome to increase the rate

of selecting mutants that inactivate TCS signaling outside of these loci. We have termed this collection of strains TCS-RelE, where TCS is replaced by either HitRS or HssRS depending on the system being investigated (Fig. 3-1A).

Using the TCS-RelE strains described above, we performed genetic selections by plating these strains in the presence of activator for the TCS of interest. We generated TCS-RelE strains to identify factors required for HitRS and HssRS-dependent activation of gene expression. The HitRS-RelE selection was performed using a small molecule activator of the system, ‘205, and the HssRS-RelE selection was performed in the presence of heme.The induction of *relE* expression killed the majority of the bacterial population but a few resistant isolates appeared as colonies on the plate. Using these genetic tools, three suppressor mutants were independently identified in both the HitRS selection and the HssRS selection. Suppression phenotypes were validated by assessing growth of wildtype (WT) *B. anthracis*, the TCS-RelE parental strains, and the suppressor mutants in rich media containing TCS activator. The concentrations of ‘205 and heme used in these growth experiments were not lethal to WT *B. anthracis* (Fig. 3-1B-C). All of the selected mutants grew after a decreased lag phase in the presence of the relevant activator as compared to the 14-16 hour lag phase observed in the TCS-RelE strains (Fig. 3-1B-C). These results indicate that HitRS mutants 1-3 and HssRS mutants 1-3 harbor mutations that prevent TCS-dependent, RelE-mediated toxicity (Fig. 1B-C), indicating that the extended lag phase in the TCS-RelE strains was dependent on decreased TCS activation.

To determine the genotypes responsible for conferring the resistance phenotype, whole genome sequencing was performed. Sequencing revealed that all six independently isolated strains did not have mutations within the TCS, and instead harbored mutations in genes known to be involved in protein stabilization and degradation, specifically within *dnaJ* or *clpX* (Fig. 3-1D).

DnaJ is the substrate-binding subunit of the DnaJK protein chaperone and ClpX is the protein substrate recognition and ATP-binding subunit of the Clp protease complex [144]. A single mutation was mapped in each strain: a nonsense mutation resulting in truncation of DnaJ at glutamine 171 (HitRS strain mutant 1), a point mutation of C16Y in ClpX, (HitRS strain mutant 2), a deletion of two residues Ala88 and Val89 in ClpX (HitRS strain mutant 3), and a deletion of the same two residues in ClpX (HssRS strain mutant 1-3) (Fig. 3-1D). The resistance phenotypes of the strains harboring mutations in DnaJ and ClpX indicated that wildtype forms of these proteins are required for activation of the *hit* (P_{hit}) and *hrt* (P_{hrt}) promoters.

To determine if the identified mutations in *dnaJ* and *clpX* result in inactivation of their respective gene products, two of the mutations were recreated in a wildtype background. A nonsense mutation was introduced in the coding sequence for DnaJ to truncate the protein after residue 171 ($DnaJ^{Q171*}$). Six nucleotides were deleted in the coding region of ClpX to delete Ala88 and Val89 ($ClpX^{A88X,V89X}$). We then generated full genetic deletions of *dnaJ* and *clpX* (Δ*dnaJ*, *clpX::tet*) to determine if the identified mutations are inactivating mutations. We compared growth of the selection mutants to Δ*dnaJ* or *clpX::tet* under conditions where either DnaJ or ClpX are known to be necessary for optimal growth. As part of the heat stress response, DnaJ is required for the growth of many bacterial species at high temperatures [132, 141, 143, 144]. When grown at 42°C, both $DnaJ^{Q171*}$ and Δ*dnaJ* mutants were significantly inhibited for growth relative to WT, whereas there were no significant growth differences between the strains at 37°C (Fig. 3-2A). ClpX promotes sporulation through the degradation of a sporulation inhibitor in *B. subtilis* [151]. Both $ClpX^{A88X,V89X}$ and *clpX::tet* mutants exhibited a 50% reduction in sporulation efficiency compared to wildtype (Fig. 3-2B). The strains harboring the mutations isolated from the selection behaved comparably to those lacking the entire coding sequence indicating that the selected

mutations led to inactivation of DnaJ and ClpX. These results indicate that DnaJ and ClpX are required for activation of the P_{hit} and P_{hrt} promoters.

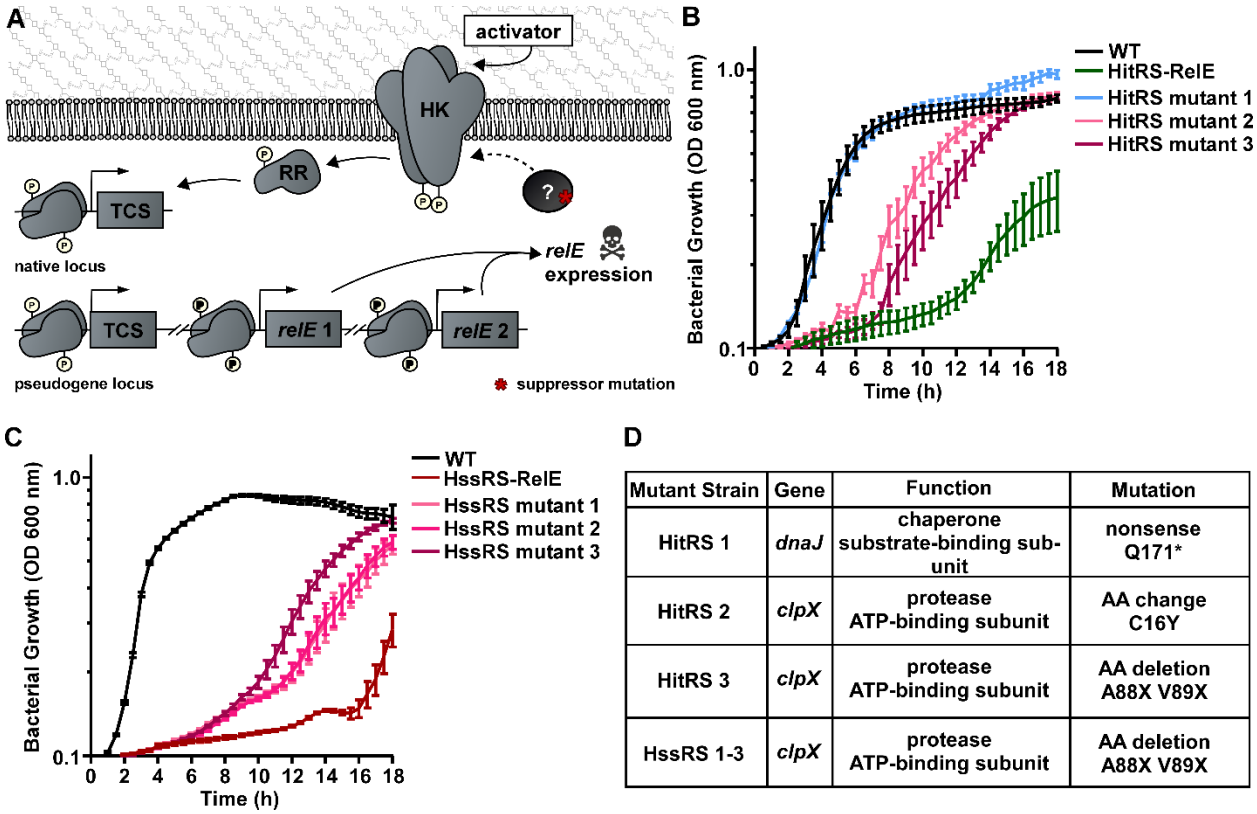

Mutant Strain	Gene	Function	Mutation
HitRS 1	*dnaJ*	chaperone substrate-binding sub-unit	nonsense Q171*
HitRS 2	*clpX*	protease ATP-binding subunit	AA change C16Y
HitRS 3	*clpX*	protease ATP-binding subunit	AA deletion A88X V89X
HssRS 1-3	*clpX*	protease ATP-binding subunit	AA deletion A88X V89X

Figure 3-1. An unbiased genetic selection revealed critical roles of two protein stability regulators in TCS activation. A. Schematic representing the genetic modifications that result in death of the TCS-RelE strain upon TCS activation. Activation of the TCS of interest leads to RelE toxin production. Mutation in any protein upstream of *relE* expression can rescue *B. anthracis*. Genetic redundancy of the TCS and RelE toxin prevent selection of mutations in these gene products, resulting in identification of novel gene products involved in signaling. **B.** Growth of the HitRS-RelE strain compared to WT and isolated mutant strains in the presence of 4 μM ‘205 measured by optical density at 600 nm (OD600). Data are averages of three independent experiments performed in biological triplicate ± SEM. **C.** Growth of the HssRS-RelE strain compared to WT and isolated mutant strains measured by OD600 in the presence of 2 μM heme. Data are averages of three independent experiments performed in biological triplicate ± SEM. **D.** Gene product mutations independently selected for using HitRS- and HssRS-RelE selection strains.

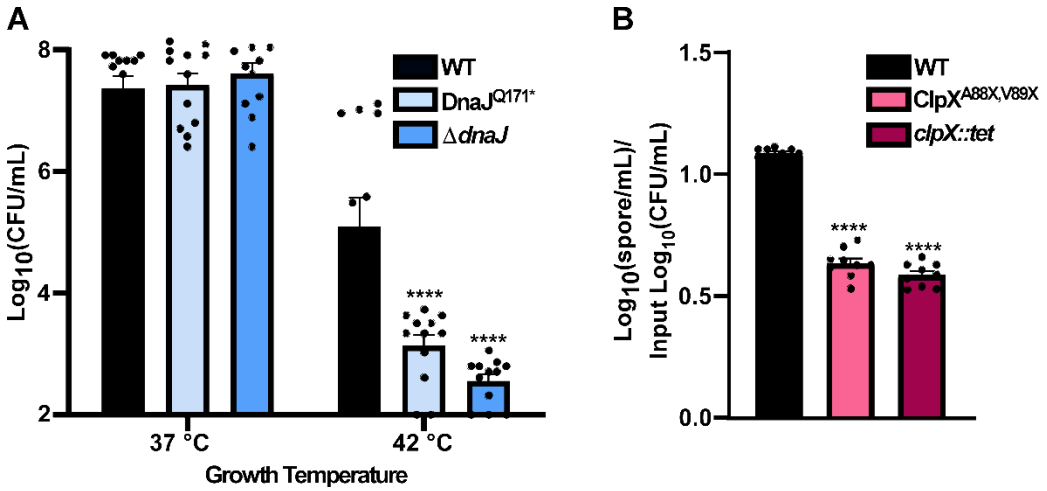

Figure 3-2. Mutations identified in genetic selections are inactivating. A. Growth of WT, DnaJ^{Q171*}, and Δ*dnaJ* after 6 h of growth at 37 °C and 42 °C measured through enumeration of colony forming units (CFU) per mL of culture. Data are averages of three independent experiments performed in biological triplicate ± SEM. Statistical significance compared to WT was determined using a two-way ANOVA with a Sidak's test adjustment for multiple comparisons (****$p \leq$ 0.0001). **B.** After 24 h growth of WT, ClpX^{A88X,V89X}, and *clpX::tet* in MGM sporulation media, samples were analyzed for heat-resistant spores. Spore counts were normalized to the number of bacteria in the initial inoculum. Data presented are the averages of three independent experiments performed in biological triplicate ± SEM. Statistical significance compared to WT was determined using a one-way ANOVA with Tukey's test for multiple comparisons (****$p \leq 0.0001$).

DnaJ and ClpX are required for target gene expression by HitRS and HssRS.

To determine if DnaJ and ClpX are required for HitRS- or HssRS-dependent changes in gene expression, activation of TCS signaling was tested. Expression was quantified using a plasmid-based XylE reporter system driven by either the P_{hit} or P_{hrt} promoter in conjunction with the corresponding activating compound for HitRS and HssRS, respectively. In the case of P_{hit} activation, cultures were grown in the presence of '205 and then cell lysates were exposed to catechol, the substrate of XylE. The rate at which catechol is processed is indicative of the amount of XylE expressed, which therefore indicates the degree to which HitRS signaling is activated by '205. In wildtype, 50 μM '205 resulted in P_{hit} promoter activation (Fig. 3-3A). As a control, a strain lacking HitRS (Δ*hitRS*) lacked activation of the promoter (Fig. 3-3A). Strains containing the recreated *dnaJ and clpX* mutations ($DnaJ^{Q171*}$ and $ClpX^{A88X,V8X}$) showed a significant reduction in P_{hit} activation in the presence of '205 as compared to wildtype (Fig. 3-3A). The requirement of DnaJ and ClpX for HitRS activation was even more evident in the deletion mutant of either *dnaJ* or *clpX*, in which the activation of P_{hit} was decreased by ten-fold (Fig. 3-3B). These results indicate that DnaJ and ClpX are required for optimal HitRS promoter activation by '205.

Similar experiments to those described above were performed to test the contribution of DnaJ and ClpX to HssRS promoter activation. The *hit* promoter was replaced with the *hrt* promoter (P_{hrt}) and XylE expression in the presence of the HssRS activator, heme, was tested. Again, growth in the presence of 1 μM heme increased XylE activity in wildtype as compared to a vehicle treated control (Fig. 3-3C). A lower concentration of heme was used to allow for growth of a strain lacking HssRS (Δ*hssRS*) that abolished XylE activity, indicating that this TCS is responsible for the XylE signal observed in wildtype cells (Fig. 3-3C). Mutation of *dnaJ* and *clpX* resulted in significantly

less P_{hrt} activation than wildtype both in vehicle and heme treated samples (Fig. 3-3C). Similar to what was observed with P_{hit} activation, full genetic inactivation of *dnaJ* or *clpX* resulted in a greater reduction in P_{hrt} activation (Fig. 3-3D). Collectively, this suggests that DnaJ and ClpX contribute to HitRS- and HssRS-dependent promoter activation.

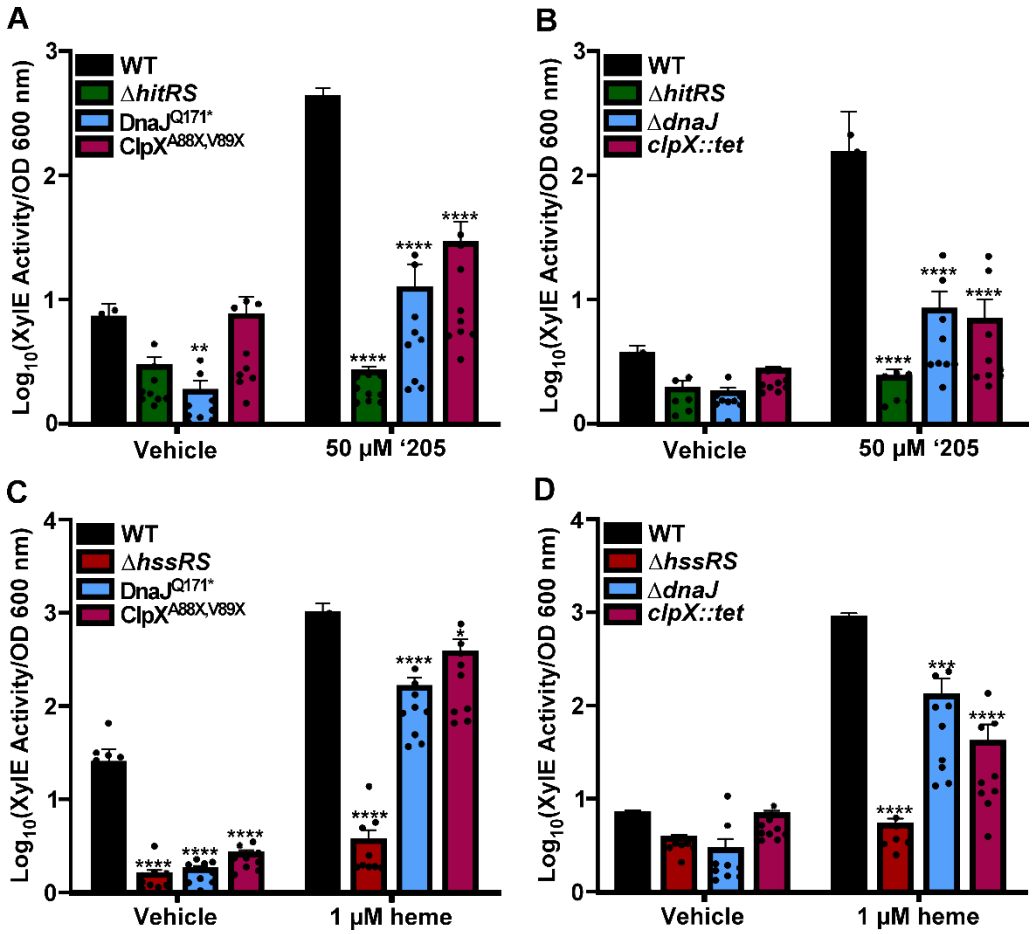

Figure 3-3. DnaJ and ClpX are required for HitRS- and HssRS-dependent gene activation in *B. anthracis*. **A.** Activity of the *hit* promoter in response to vehicle or 50 μM '205 was quantified using WT, Δ*hitRS*, DnaJ^{Q171*}, and ClpX^{A88X,V89X} carrying the *xylE* reporter plasmid. **B.** Activity of *hit* promoter in response to vehicle or 50 μM '205 was quantified using WT, Δ*hitRS*, Δ*dnaJ*, and *clpX::tet* carrying the *xylE* reporter plasmid. **C.** Activity of *hrt* promoter in response to vehicle or 1 μM heme was quantified using WT, Δ*hssRS*, DnaJ^{Q171*}, and ClpX^{A88X,V89X} carrying the *xylE* reporter plasmid. **D.** Activity of *hrt* promoter in response to vehicle or 1 μM heme was quantified using WT, Δ*hitRS*, Δ*dnaJ*, and *clpX::tet* carrying the *xylE* reporter plasmid. XylE activity was quantified and normalized to bacterial density after six hours of growth. Data are averages of three independent experiments performed in biological triplicate ± SEM. Statistical significance compared to WT was determined using a two-way ANOVA with a Sidak's test adjustment for multiple comparisons (*$p \leq 0.05$,**$p \leq 0.01$,***$p \leq 0.001$,****$p \leq 0.0001$).

DnaJ and ClpX are required for activation of HitRS signaling.

DnaJ and ClpX play important roles in both HitRS- and HssRS-induced gene activation, but we focused our studies specifically on the regulation of the less studied HitRS system (Fig. 3-3). It is unclear at which step in TCS signaling these two proteins are involved. We posited three possible mechanisms by which DnaJ and ClpX are required for HitRS signaling including (i) TCS activation, (ii) HK membrane localization, or (iii) TCS protein levels. To first investigate if the fundamental step in HitRS signaling, HK activation, is dependent on DnaJ and ClpX, constitutively active HitR or HitS mutations were made in the background of *dnaJ* or *clpX* deletions [249]. Mutation of specific single amino acids in HitR ($HitR^{M58I}$) or HitS ($HitS^{S141L}$) results in their constitutive phosphorylation via stabilization of their phospho-residues, which allowed us to investigate the requirement of DnaJ and ClpX for protein level activation in the autoregulation of the *hit* operon [249]. If DnaJ or ClpX facilitate HK activation or phosphorylation, then these constitutively active mutations would bypass both the need for activator and DnaJ or ClpX. Constitutive signaling as a result of genetically activated HitR or HitS overwhelmed the XylE reporter and resulted in toxicity in these mutant backgrounds (data not shown). Therefore, the integrity of TCS signal transduction was assessed in the constitutively active mutants using qRT-PCR to measure expression of *hitP* in the presence or absence of 50 μM ‘205 (Fig. 3-4A). Constitutive activation of either HitR or HitS results in expression of *hitPRS* regardless of the presence of stimuli (Fig. 3-4A-C). Δ*dnaJ* did not show induction of *hitPRS* expression in the presence of activator, confirming the results of the XylE reporter assay (Fig. 3-4A-C). If DnaJ were required for HK or RR protein activation, then constitutive activation of HitRS in the Δ*dnaJ* background would likely compensate for the defect in *hitPRS* expression. Both Δ*dnaJ* $HitR^{M58I}$ and Δ*dnaJ* $HitS^{S141L}$ showed constitutive expression of the *hit* operon when treated with either

vehicle or ‘205 (Fig. 3-4A-C). Constitutive activation of HitR and HitS in Δ*dnaJ* had nearly identical results, indicating that the requirement for DnaJ is upstream of HitRS signal transduction.

The same experiments described above for DnaJ were also performed using the constitutively active HitR and HitS mutants to assay the requirement of ClpX for HitRS protein activation. As compared to wildtype, *clpX::tet* exhibited decreased expression of *hitPRS* when treated with ‘205 (Fig. 3-4D-F). Similar to what was observed in Δ*dnaJ*, constitutively active strains lacking *clpX* (*clpX::tet* $HitR^{M58I}$ and *clpX::tet* $HitS^{S141L}$) also showed high levels of *hitP* expression, regardless of the presence of ‘205 (Fig. 3-4D-F). HitRS and HssRS engage in cross-regulation whereby phosphorylated HitR can activate the expression of *hrtAB* [72, 91]. Constitutive HitS or HitR activation led to increased P_{hrt} promoter activation in the vehicle-treated samples (Fig. 3-5). Deletion of either *dnaJ* or *clpX* in the $HitR^{M58I}$ and $HitS^{S141L}$ backgrounds had no effect on expression from the *hrt* promoter indicating that constitutive HitRS signaling eliminates the need for these proteins in cross-regulation of P_{hrt} (Fig. 3-5). Thus, it is possible to bypass the requirement of *dnaJ* and *clpX* via constitutive activation of the TCS.

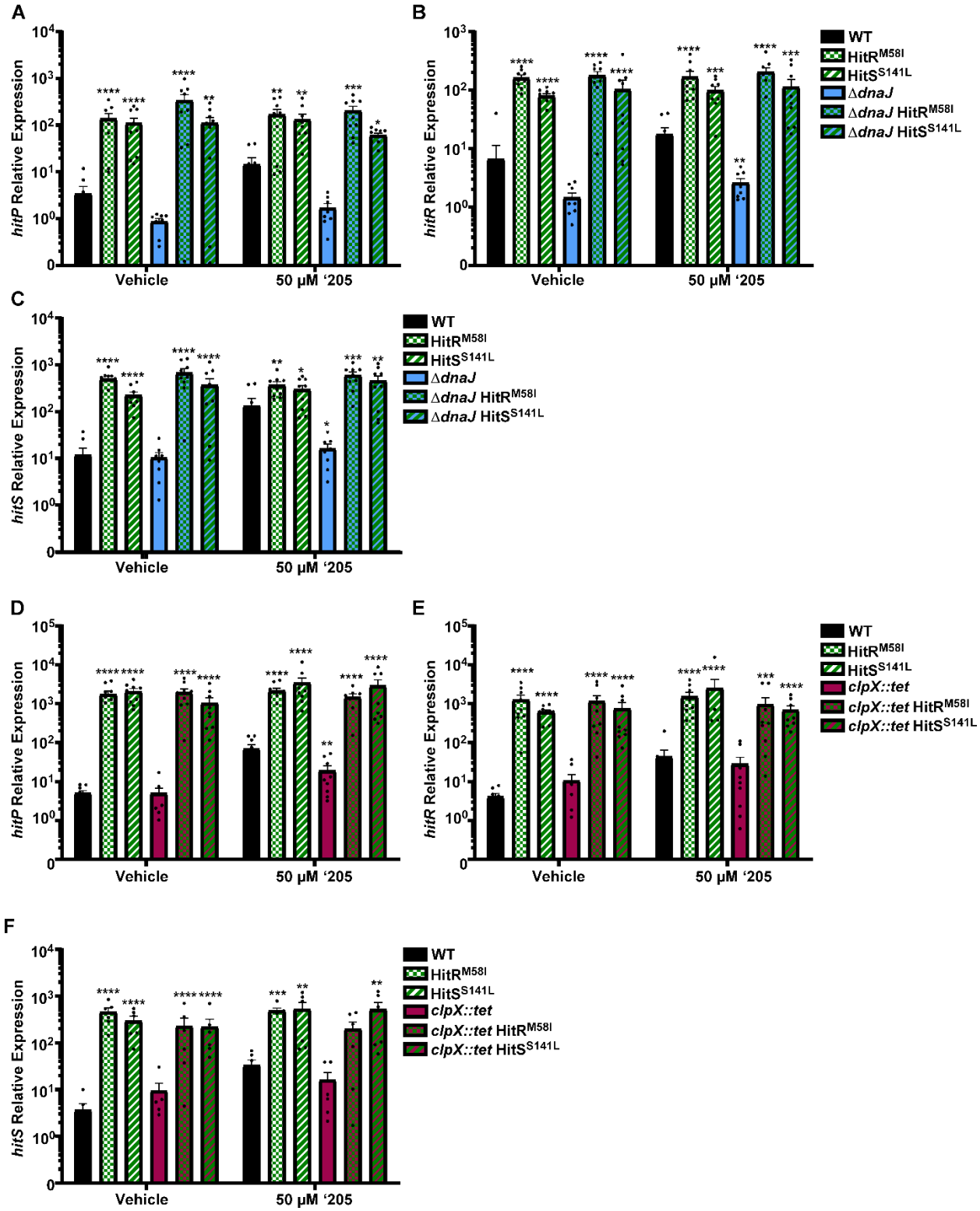

Figure 3-4. Constitutive activation of HitS bypasses requirement of DnaJ and ClpX for expression of *hit* operon. A-C. qRT-PCR analysis of *hitP* (**A**), *hitR*(**B**), and *hitS* (**C**) expression was performed on WT, Δ*dnaJ*, HitR^{M58I}, HitS^{S141L}, Δ*dnaJ* HitR^{M58I}, and Δ*dnaJ* HitS^{S141L} after treatment with vehicle or 50 μM '205. **D-F.** qRT-PCR analysis of *hitP* (**D**), *hitR*(**E**), and *hitS* (**F**)

expression was performed on WT, *clpX::tet*, HitR^{M58I}, HitS^{S141L}, *clpX::tet* HitR^{M58I}, and *clpX::tet* HitS^{S141L} after treatment with vehicle or 50 μM ‘205. Data are averages of three independent experiments performed in biological triplicate ± SEM. Statistical significance compared to WT was determined using a two-way ANOVA with a Sidak’s test adjustment for multiple comparisons (*$p \leq 0.05$,**$p \leq 0.01$,***$p \leq 0.001$,****$p \leq 0.0001$).

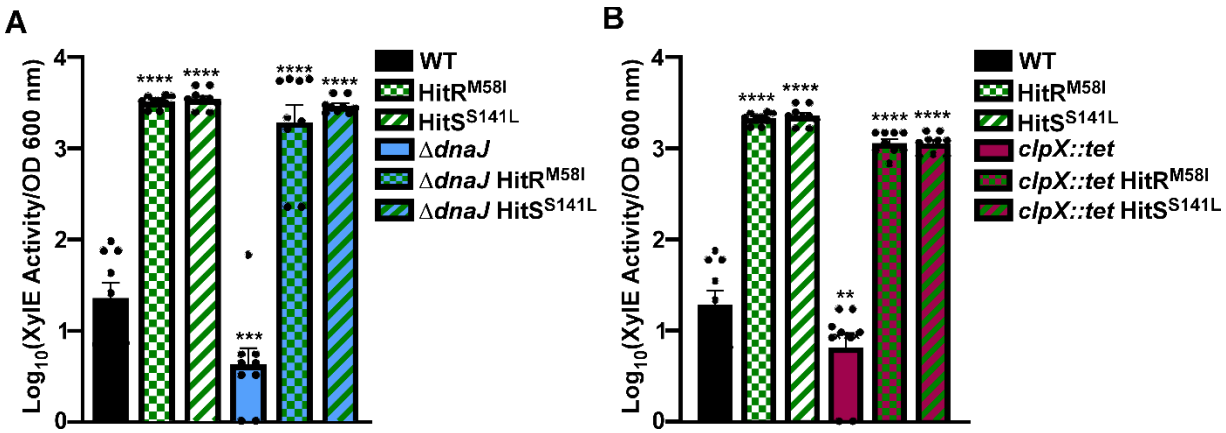

Figure 3-5. Cross-regulation of the *hrt* promoter by HitRS involves DnaJ and ClpX. A. Activity of the *hrt* promoter in response to vehicle was quantified using WT, Δ*dnaJ*, HitR^{M58I}, HitS^{S141L}, Δ*dnaJ* HitR^{M58I}, and Δ*dnaJ* HitS^{S141L} carrying the *xylE* reporter plasmid. **B.** Activity of *hrt* promoter in response to vehicle was quantified using WT, *clpX::tet*, HitR^{M58I}, HitS^{S141L}, *clpX::tet* HitR^{M58I}, and *clpX::tet* HitS^{S141L} carrying the *xylE* reporter plasmid. XylE activity was quantified and normalized to bacterial density at the time of assay termination. Data are averages of three independent experiments performed in biological triplicate ± SEM. Statistical significance compared to WT was determined using a two-way ANOVA with a Dunnett's test adjustment for multiple comparisons (*$p \leq 0.05$,**$p \leq 0.01$,****$p \leq 0.0001$).

Membrane localization of HitS is independent of DnaJ or ClpX.

Activation of a TCS begins with HK detection of a specific stimulus. For HitRS activation and signal transduction to occur, HitS must be appropriately localized to the membrane to sense its activating stress signal. Membrane loading of HitS was tested using a protein-fluorophore fusion and visualized with super-resolution microscopy. Constitutively expressed mCherry-tagged HitS was observed in the periphery of wildtype bacilli when imaged using structured illumination microscopy (Fig. 3-6A). When *dnaJ* (DnaJ^{Q171*} and Δ*dnaJ*) and *clpX* mutants (ClpX^{A88X,V89X} and *clpX::tet*) harboring this reporter were imaged using this method, HitS localization to the membrane was maintained (Fig. 3-6A). When either the sum intensity or total volume of HitS signal is quantified across strains and normalized to the amount of DNA in each image, the abundance of HitS becomes significantly less in mutants of ClpX as compared to wildtype (Fig. 3-6B-C). Though not significant, the abundance of HitS in mutants of DnaJ also trended lower (Fig. 3-6B-C). To analyze differences in surface localization of HitS, the overlapping signal of HitS and DNA was quantified across strains. The intensity of HitS overlap was normalized to the abundance of HitS in each image to adjust for the bacilli not expressing mCherry-labeled HitS. The localization of HitS is therefore measured as the ratio of cytoplasmic localized HK to total HK. The normalized signal intensity of HitS in the cytoplasm of the bacilli is not significantly different in mutants lacking DnaJ or ClpX (Fig. 3-6D). The use of this approach to quantify protein localization to the membrane was validated using an untagged mCherry expressed under the same promoter and imaged and quantified using the same analysis (Fig. 3-7). Therefore, DnaJ and ClpX are not required for HitS membrane insertion or localization.

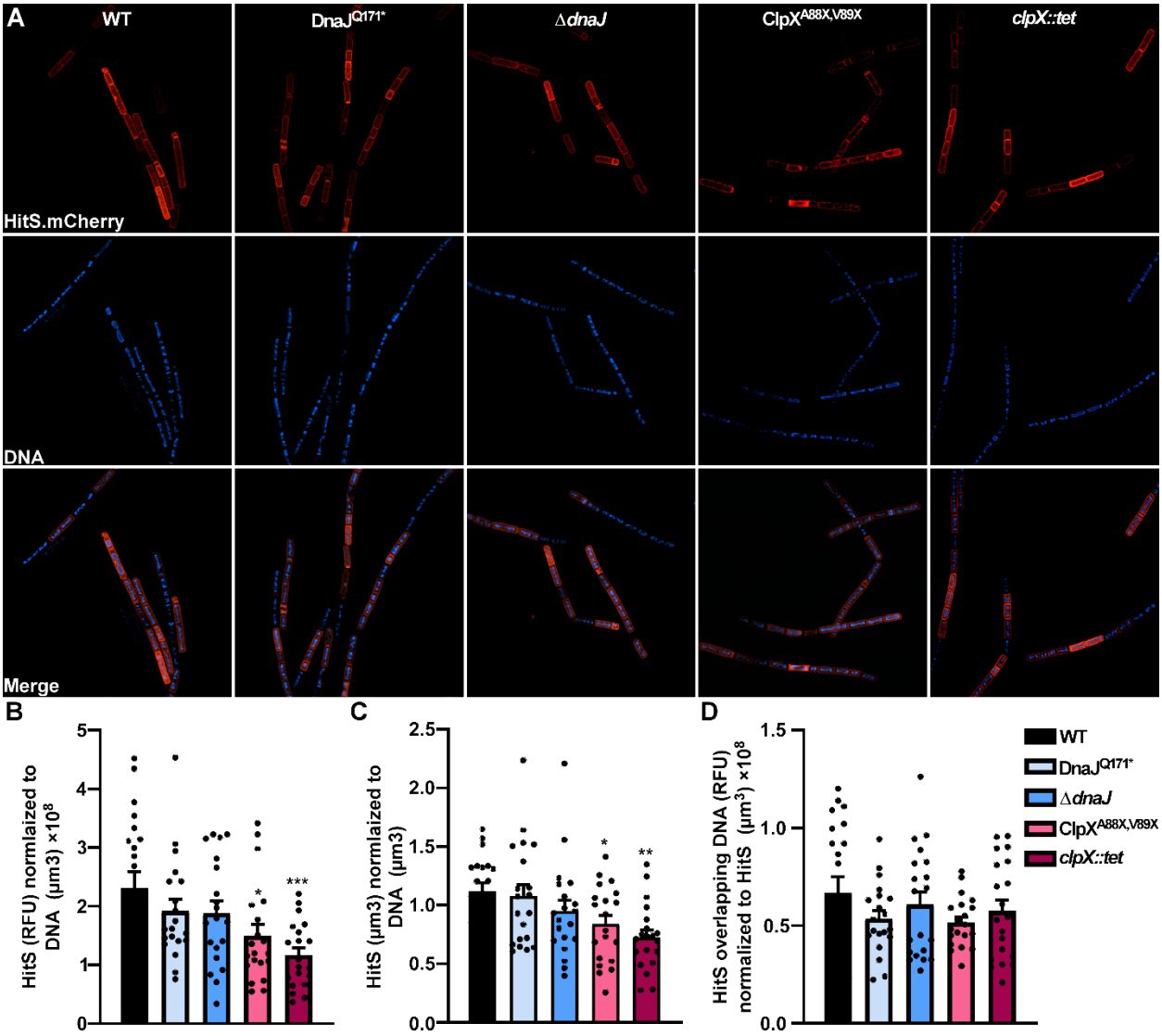

Figure 3-6. HitS localizes to the membrane independently of DnaJ and ClpX. A. Super-resolution images depicting HitS barrier localization. Wildtype, DnaJ^{Q171*}, Δ*dnaJ*, ClpX^{A88X,V89X}, and *clpX::tet* were grown overnight prior to staining with Hoescht. Samples were fixed for imaging via Nikon Structured Illumination Microscopy at 100X. Images shown represent 20 individual fields of view were collected per sample as part of two individual experiments. **B.** Sum HitS signal intensity normalized to DNA volume. **C.** Total HitS signal volume normalized to DNA volume. **D.** Ratio of cytoplasmic HitS signal intensity normalized to total HitS volume. Data presented are averages of 20 individual fields of view; collected as two independent experiments ± SEM. Statistical significance was determined using a two-way ANOVA with a Dunnett's test adjustment for multiple comparisons. (*$p \leq 0.05$,**$p \leq 0.01$,***$p \leq 0.001$).

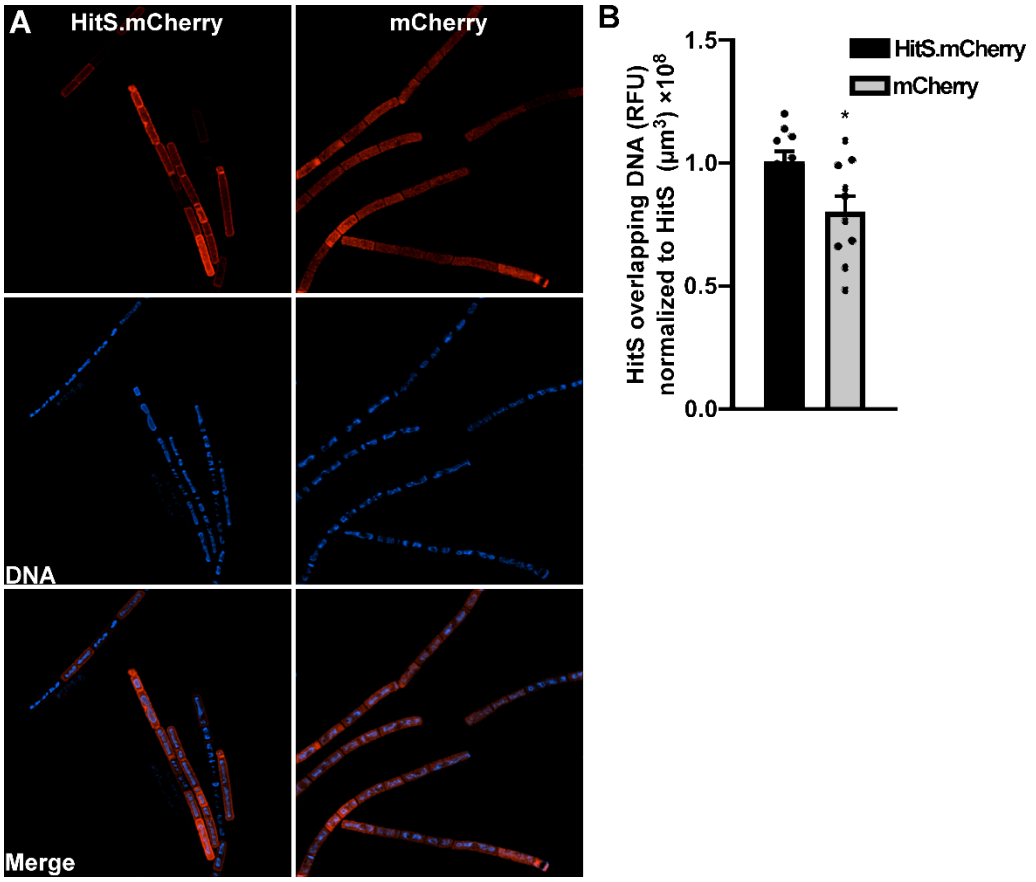

Figure 3-7. Validation of membrane localization quantification for HitS. A. Super-resolution images depicting mCherry signal fused or unfused to HitS. Wildtype expressing either of these fluorophores was grown overnight prior to staining with Hoescht. Samples were fixed for imaging via Nikon Structured Illumination Microscopy. Images shown represent 10 individual fields of view were collected per sample as part of two individual experiments. **B.** Ratio of cytoplasmic HitS signal intensity normalized to total HitS volume. Data presented are averages of 10 individual fields of view ± SD. Statistical significance was determined using Student's t-test. (*$p \leq 0.05$).

DnaJ and ClpX are required for HitRS protein stability.

Based on the previous results as well as known functions of DnaJ and ClpX, we propose a model in which DnaJ and ClpX are required for stability of HitRS in *B. anthracis* during HitRS activation. Both DnaJ and ClpX are associated with abundance control for their target proteins [132, 133]. We hypothesized that DnaJ and ClpX are required for TCS signaling because they maintain the requisite abundance of the HK and RR. To determine if HitR and HitS protein levels are affected by the absence of DnaJ and ClpX, myc-tagged constructs were generated whereby the expression of the HK or RR was controlled by an inducible promoter. This approach ensures that any effects of DnaJ and ClpX are a result of altered post-translational regulation rather than changes in gene expression profiles, which is especially important considering that the *hit* promoter, P_{hit}, is regulated by HitRS [248]. Vectors containing either a tagged HitR or HitS were transformed into wildtype, Δ*dnaJ*, and *clpX::tet*. Strains were grown to mid-log phase prior to induction of tagged protein expression. To determine if HitRS activating conditions contributed to the effects of DnaJ and ClpX on TCS protein regulation, ‘205 was added to cultures during the induction phase of the experiment. After reaching stationary phase, cultures were collected for assessment of protein levels via immunoblot.

HitS proteins levels were significantly decreased in both Δ*dnaJ* and *clpX::tet* compared to wildtype (Fig. 3-8A-B, Fig. 3-9). HitS was observed at the lowest levels in the mutant lacking *clpX*, at nearly undetectable levels, providing a mechanism for the reduction of HitRS activation observed in the ClpX mutants (Fig. 3-8A-B). Addition of ‘205 to the culture media had no effect on the trends observed. HitS abundance remained highest in wildtype and was significantly reduced in both Δ*dnaJ* and *clpX::tet* (Fig. 3-8A, C). Therefore, DnaJ and ClpX appear to function, at least in part, to maintain the abundance of the HitS protein at an optimal level for TCS signaling.

Despite mutants in DnaJ being defective at HitRS signal activation (Fig. 3-2), low but appreciable amounts of the HitS protein were still observed in the Δ*dnaJ* mutant. Conversely, investigation into HitR revealed significantly more HitR protein in Δ*dnaJ* as compared to wildtype regardless of the presence of ‘205 (Fig. 3-10, Fig. 3-11). ClpX showed no significant change in HitR levels in vehicle- or ‘205-treated samples suggesting ClpX is not involved in the regulation of HitR abundance. These results indicate that while ClpX is primarily involved in the regulation of HitS, DnaJ is required for the reduction of HitR abundance and for the maintenance of HitS. In the absence of DnaJ and ClpX, the ratio between HK and RR is disrupted. These results establish DnaJ and ClpX as key modulators of HitR and HitS protein levels that are required for HitRS signal transduction to occur in response to activating conditions.

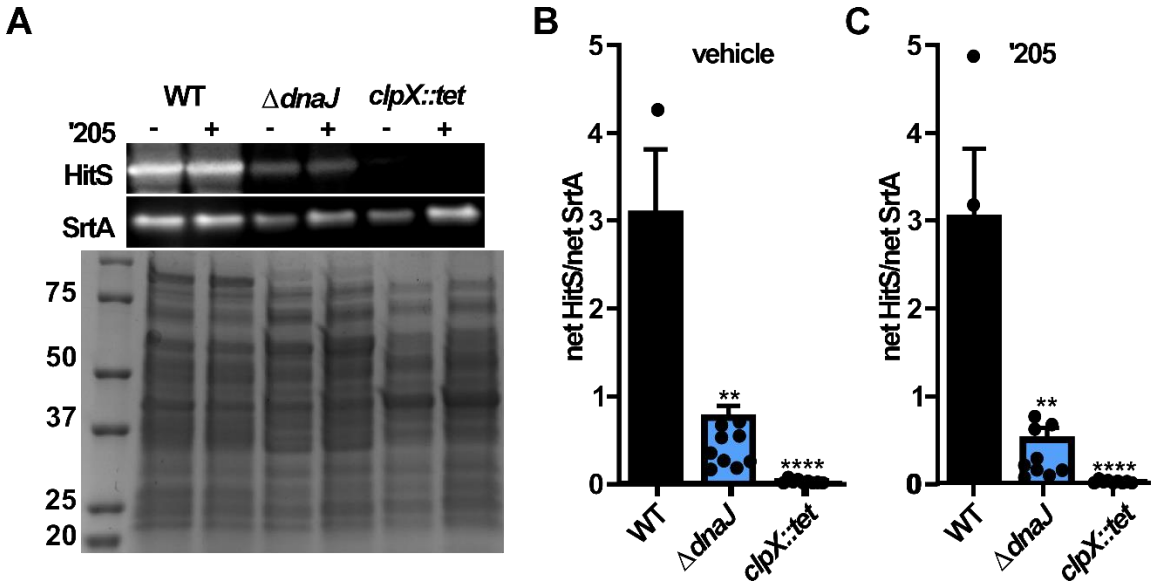

Figure 3-8. DnaJ and ClpX determine cellular HitS abundance. A. HitS abundance in WT, Δ*dnaJ*, and *clpX::tet* grown in vehicle or 50 μM '205. Immunoblot performed on lysates containing pUTE657.P$_{hspank}$*hitS*.myc treated with 250 μM IPTG. Anti-SrtA serum was used as a normalization control and SDS PAGE is shown to visualize loading consistency. Quantification of immunoblots was performed using densitometry analysis of HitS abundance in WT, Δ*dnaJ*, and *clpX::tet* grown in vehicle (**B**) or 50 μM '205 (**C**). Data are averages of three independent experiments performed in biological triplicate ± SEM. Statistical significance compared to WT was determined using a one-way ANOVA with a Dunnett's test adjustment for multiple comparisons (**$p \leq 0.01$,****$p \leq 0.0001$).

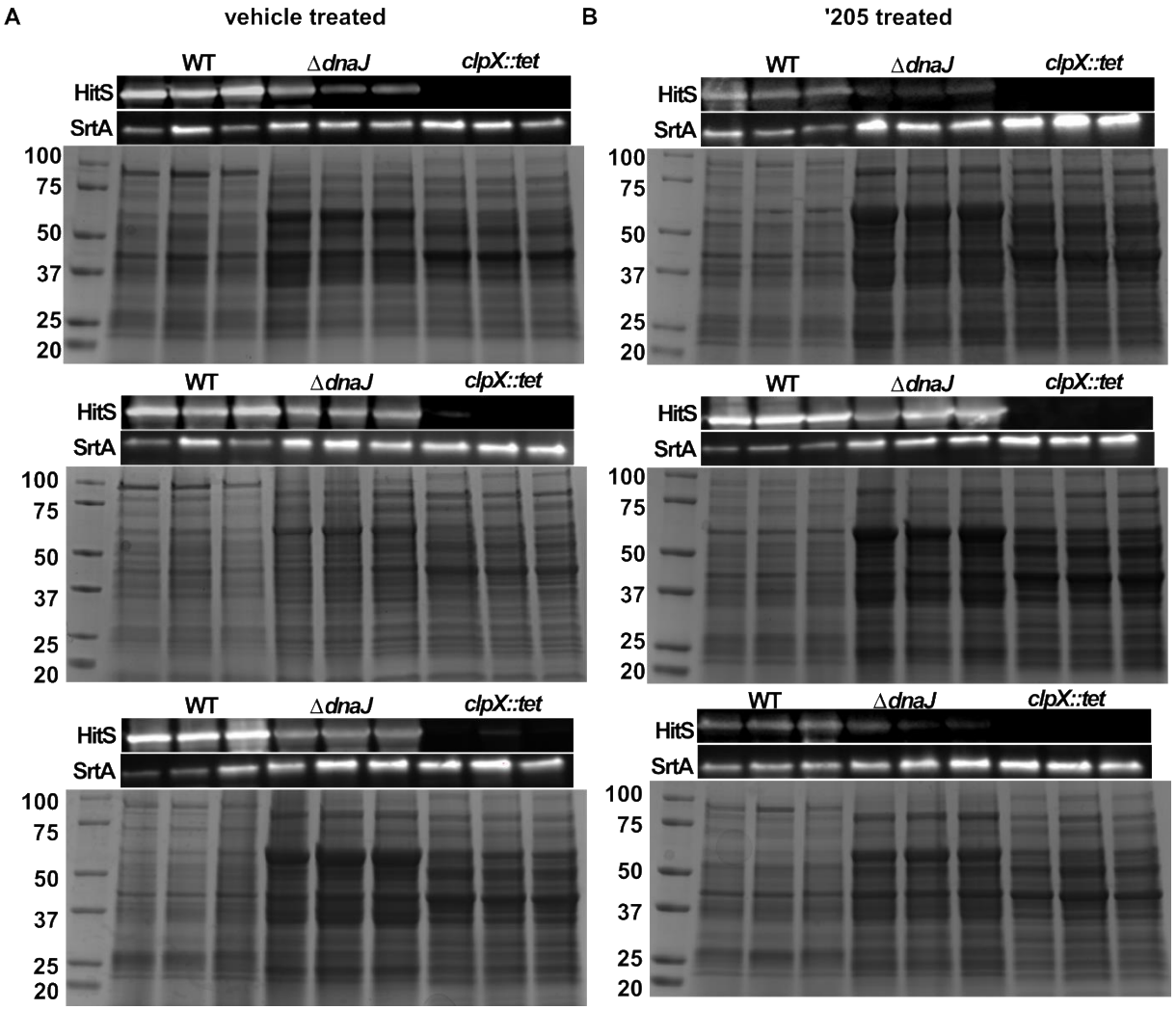

Figure 3-9. HitS abundance is reduced in the absence of DnaJ and ClpX. HitS abundance in WT, Δ*dnaJ*, and *clpX::tet* grown in triplicate in vehicle (**A**) or 50 μM ‘205 (**B**). Immunoblot used for quantification were performed on lysates containing pUTE657.P$_{hspank}$*hitS*.myc treated with 250 μM IPTG. Anti-SrtA serum was utilized as a normalization control and SDS-PAGE is shown to demonstrate loading consistency.

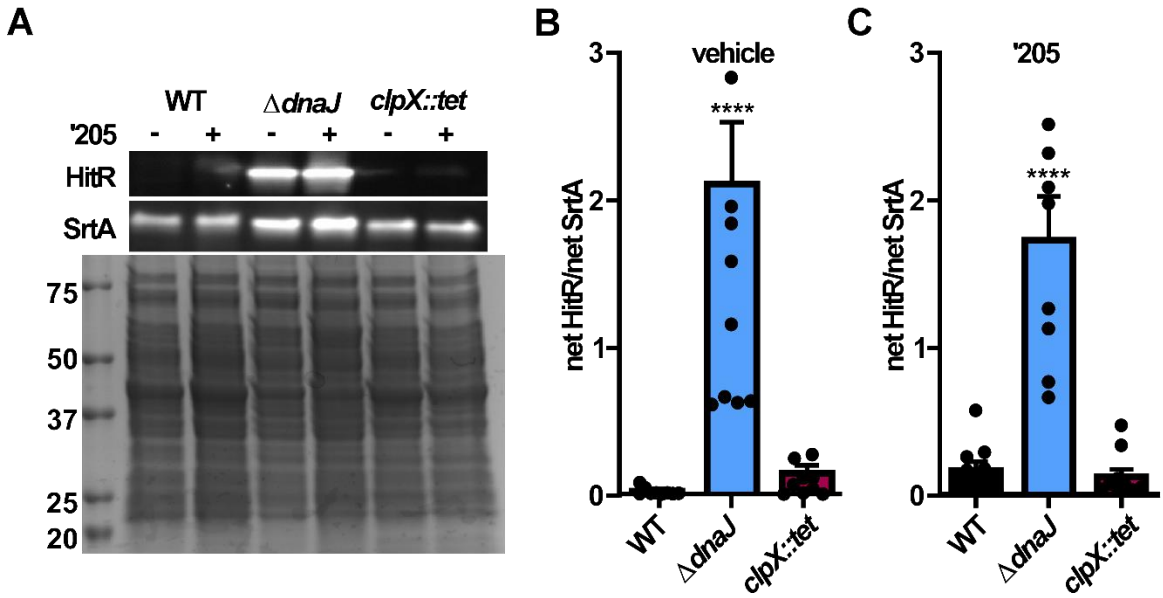

Figure 3-10. HitR abundance is modulated by DnaJ. A. HitR abundance in WT, Δ*dnaJ*, and *clpX::tet* grown in vehicle or 50 μM '205. Immunoblot performed on lysates containing pUTE657.P$_{hspank}$*hitR*.myc treated with 100 μM IPTG. Anti-SrtA serum was utilized as a normalization control and an SDS page gel is shown to demonstrate loading consistency. **B.** Quantification of immunoblots using densitometry analysis of HitR abundance in WT, Δ*dnaJ*, and *clpX::tet* grown in vehicle or 50 μM '205. Data are averages of three independent experiments performed in biological triplicate ± SEM. Statistical significance compared to WT was determined using a one-way ANOVA with a Dunnett's test adjustment for multiple comparisons (****$p \leq$ 0.0001).

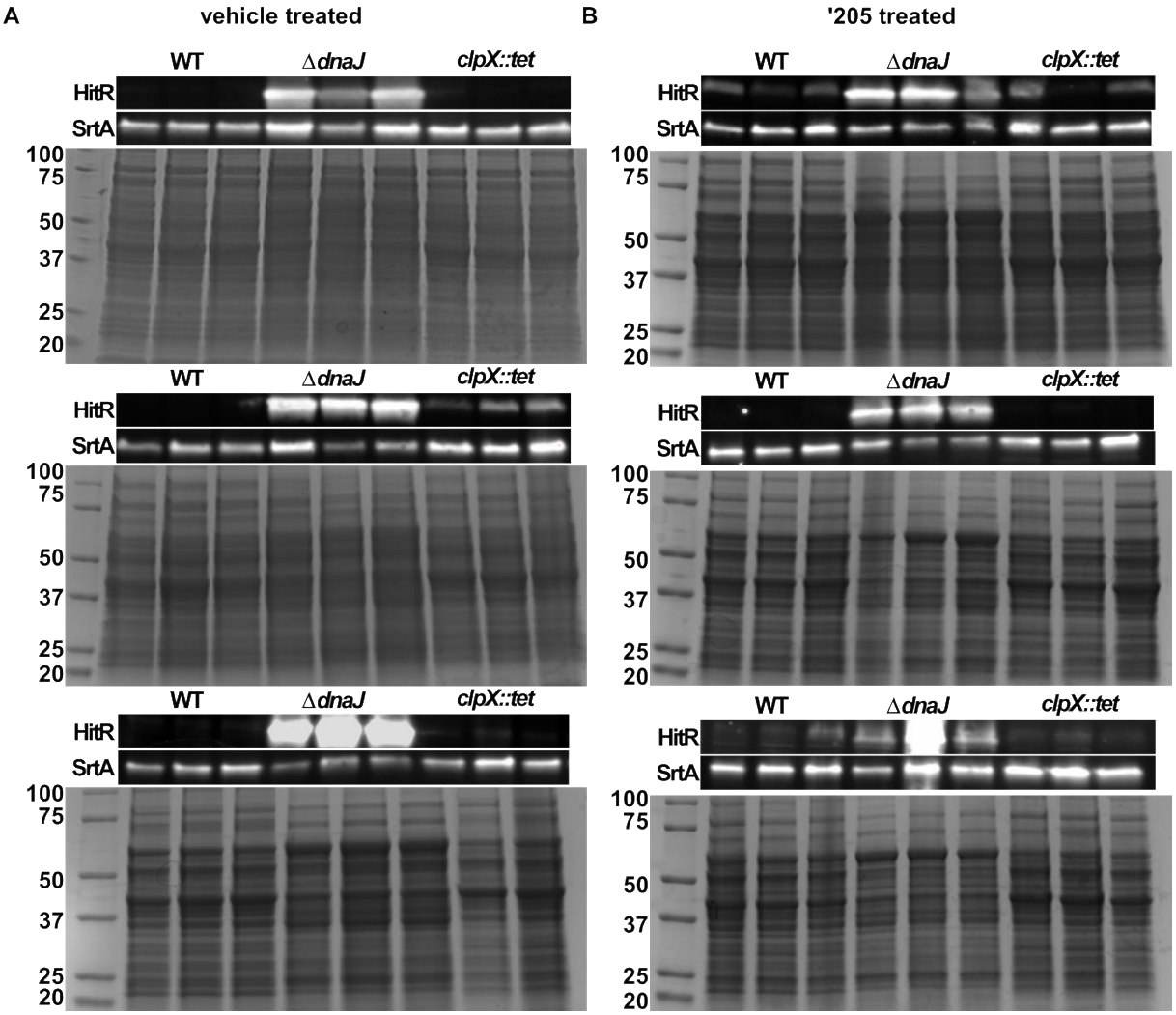

Figure 3-11. HitR abundance increases in the absence of DnaJ, but not ClpX. HitR abundance in WT, Δ*dnaJ*, and *clpX::tet* grown in triplicate in vehicle (**A**) or 50 μM '205 (**B**). Immunoblots used for quantification were performed on lysates containing pUTE657.P$_{hspank}$*hitR*.myc treated with 100 μM IPTG. Anti-SrtA serum was used as a normalization control and SDS-PAGE is shown for loading consistency.

Discussion

Two component systems (TCSs) are signaling networks that trigger a cellular response to a direct stimulus. *B. anthracis* uses TCSs to respond to various stressors that can compromise cellular functions, including envelope damage and heme-induced toxicity [88, 268]. It is therefore vital that the integrity of the signaling proteins is maintained in these circumstances. To identify proteins required for HitRS and HssRS function in *B. anthracis*, a genetic selection was designed to find accessory proteins involved in TCS signaling. Stimulation of HitRS- and HssRS-driven toxicity led to the repeated identification of resistance-conferring mutations in DnaJ and ClpX. The identified mutations resulted in inactivation of the respective protein products, revealing that both DnaJ and ClpX are required for HitRS- and HssRS-dependent gene expression changes. Further investigation revealed that activation of HitRS signaling, including cross-regulation of the HssRS-activated promoter, is contingent on DnaJ and ClpX. Super-resolution imaging visualized consistent HitS localization in the absence of DnaJ and ClpX, but immunoblotting experiments revealed that both DnaJ and ClpX are required to maintain wildtype levels of the HK. Only DnaJ regulates HitR abundance and is required for reduction in levels of the RR. The post-translational regulation of both HitR and HitS by DnaJ and ClpX is independent of TCS-activating conditions. Collectively, these data uncover a role for DnaJ and ClpX in the maintenance of HitRS protein stability.

Anthrax begins with phagocytosis of spores at the site of infection, which then germinate into the metabolically active vegetative bacilli. Despite initial antibacterial action of the host, *B. anthracis* expands into an overwhelming bacterial population. The ability of *B. anthracis* to replicate to such high numbers within the host indicates that it harbors the gene products that sense and respond to immune system attacks. TCSs are important for *in vivo* survival by enabling a bacterial response to antimicrobial attacks including host cell metal limitation or creation of an

acidic environment [241, 242, 269, 270]. Therefore, *B. anthracis* TCSs likely assist in survival by adapting to eukaryotic effector exposure [218]. The activating stimuli for HitRS and HssRS, envelope targeting agents and high levels of heme, respectively, are encountered within the dynamic host environment during infection [64, 70-72, 90, 91, 271-275]. Results presented in this study suggest that HitRS and HssRS require the activity of the protein chaperone DnaJ and the protease ClpX, which are key contributors to bacterial pathogenesis [276]. It was previously shown that *Campylobacter jejuni* is unable to colonize chickens when lacking DnaJ [277]. DnaJK in *Salmonella enterica* serovar Typhimurium is required for macrophage survival and mouse colonization [278]. The Clp proteases commonly emerge as key drivers of virulence in human pathogens such as *S. enterica* serovar Typhimurium, *Staphylococcus aureus, Francisella novicida,* and *Streptococcus pneumoniae* [279-283]. For example, Clp complexes are required for *Listeria monocytogenes* target cell invasion and escape from the phagolysosome [284-286]. *In vivo* virulence of *Streptococcus mutants* requires Clp protease activity for posttranscriptional regulation of the pneumolysin toxin [287]. The role of posttranscriptional regulation in anthrax infection may involve TCS support. Action of DnaJ or ClpX on HitRS and HssRS may restore signaling capability, which could be compromised in the host environment. The accumulation of heme inside the cell not only activates HssRS, but also leads to redox cycling, increasing the intracellular levels of reactive oxygen species (ROS) [64]. The subsequent ROS can damage macromolecules, including proteins, which could result in impairment of TCS proteins, preventing signaling [288]. Both HitRS- and HssRS-activating conditions have the potential to damage the TCSs in the absence of stabilization and, accordingly, these TCSs are integrated with central cellular systems for protein stability management. The appropriate stoichiometric ratio of HK to RR must be maintained for TCS function, particularly in activating conditions [289-291]. Therefore, we

hypothesize that synchronization of the response to envelope damage and heme stress must be tightly regulated at the protein level because it is required for TCS signal transduction as *B. anthracis* transitions throughout various host niches.

The DnaJK complex is broadly utilized to protect proteins from irreversible aggregation during stress, which would include host-derived conditions that may activate TCSs [132, 292]. Here, DnaJ contributes to HitR degradation and HitS preservation. Protein chaperones have been associated with the central cellular pathways listed above, but there exists literature linking DnaJK and its accessory protein, GrpE, to bacterial signaling. In an example of self-regulation, DnaJK/GrpE interact with the stationary phase sigma factor, RpoS, to downregulate the heat shock response via negative feedback [144, 293-296]. However, protein chaperones have a role beyond their own stress signaling response. RcsBC is a desiccation and osmotic shock-sensing TCS in *Escherichia coli* that is supported by a DnaJ homolog, DjlA, in a manner dependent on DnaK [159, 160]. In *Pseudomonas putida*, the GacAS TCS regulates putisolvin biosynthesis which is key for biofilm cycling [161]. GacAS is positively regulated by DnaJK/GrpE chaperone activity. Though the mechanisms of TCS regulation were not elucidated in these examples, they mirror the observations presented here whereby DnaJ is required for HitRS signaling.

Bacterial proteases play vital roles in cell viability, adaptation, and pathogenesis by degrading misfolded and defective proteins [132, 133, 297]. Results indicate that ClpX is required for HitS protein preservation. Precedence exists for Clp proteases being involved in bacterial TCS signaling. The *S. aureus* Clp protease binds to the active form of SaeR, an RR involved in host-effector sensing, as indicated by proteomics analysis [163]. Additionally, the expression of AgrAC-regulated genes is dependent on ClpX specifically [164]. VgrS, a *Xanthomonas campestrism* HK, is stimulated by osmotic stress and is degraded via protease activity to temper

the strength of activation [162]. The activated form of the *Bacillus subtilis* RR DegU is specifically degraded by ClpCP also to dampen TCS signaling [165]. These examples support the role for *B. anthracis* ClpX in HitS regulation and provide a notable contrast in that direct degradation by the protease is not dependent on activation of the TCS protein in this case. While the work here may provide an example of regulation of HitS by ClpX, it is counterintuitive that the HK is observed at lower abundance in the absence of a protease typically responsible for degradation. In addition to direct interaction of ClpX with peptide sequence motifs, adaptor proteins are sometimes required to link degradation targets with the Clp protease. This mechanism has been described for TCS proteins and may provide a model for the reversed relationship observed for ClpX and HitS. In these cases, the adaptor protein provides the substrate specificity and can act either as an inhibitor or promoter of TCS degradation [298]. Within *Caulobacter crescentus*, CtrA is a RR of a TCS linked to control of cell maturation and division [299]. CtrA is controlled by ClpXP proteolysis to ensure accurate regulation of cell cycle checkpoints [300]. Degradation is dependent on the accessory protein RcdA for subcellular localization near the Clp protease to expand on the temporal regulation of CtrA via phosphorylation [301]. To exemplify negative TCS regulation, *B. subtilis* Sda is an inhibitor of two sporulation HKs and is degraded by ClpXP [167-169]. Therefore, ClpX maybe be responsible for the maintenance of HitS protein abundance via indirect action through a similar adapator protein.

DnaJ and ClpX are well-known regulators of protein homeostasis, despite having conflicting roles as components of a chaperone and protease complex, respectively. Here we present evidence that protein chaperone and protease components affect HK protein abundance in a similar manner. HitS levels are reduced in mutants of both *dnaJ* and *clpX*. Though indirect effects of DnaJ and ClpX on HitS cannot be discounted, it is tempting to speculate that both DnaJ and

ClpX act independent of their associated protein complexes to stabilize HitS levels. DnaJ can function autonomously of DnaK and interact with peptide substrates [292, 294]. This interaction occurs through the zinc-finger like domain which is required to bind denatured protein substrates for stabilization [143, 302]. ClpX contains a similar zinc-finger motif for target peptide binding within the Clp protease [298, 303]. When ClpX is associated with ClpP it facilitates protein unfolding and translocates the peptide to the protease, but this is not always the case. ClpX can also prevent protein aggregation or disaggregate already formed protein aggregates [255]. DnaJ and ClpX might both act as chaperones for HitS to maintain abundance of the HK, thereby enabling constant sensing of the environment.

Systems for the maintenance of protein homeostasis are thoroughly described throughout biology. Though bacterial chaperone and protease networks are often thought of as key modulators of replication, translation, and transcription, there is a role for these systems in the modulation of signaling responses. The conserved nature of proteins such as DnaJ and ClpX, combined with their broad impact on pathogen homeostasis, make them appealing targets for therapeutic development [276]. Pyrrhocoricin is an antibacterial peptide that binds and inhibits the peptide chaperone activity of DnaJK [304]. Analogs of pyrrhocoricin are effective antibiotics for *E. coli, Salmonella typhimurium, Klebsiella pneumoniae, Haemophilus influenzae, Pseudomonas aeruginosa,* and *Moraxella catarrhalis* [305]. Burdens of *H. influenzae* were significantly reduced in a murine inhalation model of infection when the mice received pyrrhocoricin analogs [305]. Clp proteases in bacteria have been successfully targeted previously, but a specific ClpXP inhibitor was identified using a screen in *E. coli* that is highly inhibitory against the *B. anthracis* and *S. aureus* protease complexes as well [306-309]. Not only did inhibition of ClpXP in these pathogens enhance the activity of cathelicidin antimicrobial peptides, but it also boosted the activity of cell

envelope-targeting antimicrobials [306]. This result exemplifies the potential for pharmacological inhibition of Clp proteases and highlights the key role played by ClpXP in barrier maintenance to support TCSs. The findings of this study suggest that use of chaperone or protease inhibitors would work to prevent HitRS and HssRS TCS signaling in *B. anthracis.* Though the role of these TCSs in anthrax infection has yet to be directly studied, therapeutic targeting of TCSs has been an appealing strategy to limit pathogens' ability to respond to environmental changes [310-312].

TCSs make up the largest family of multi-step signal transduction pathways with tens of thousands of TCS sequences being deposited into databases [268]. However, the identification of accessory proteins for TCS signaling has proven challenging. We have devised a genetic selection strategy to overcome this limitation and have used it to refine TCS stress-sensing and signaling mechanisms. The genetic selection tools and methodology utilized in this study could be broadly applicable to identifying accessory components of TCSs in many microorganisms. This approach takes advantage of synthetic biology to specifically detect molecular changes in the cell that are linked to TCS function. Modifications are made to the genome such that in addition to the native gene expression changes, TCS activation drives expression of an *E. coli* toxin, RelE, which degrades mRNA [267]. Exposure of this strain to the TCS stimulus results in death of the majority of the population, apart from isolates where a mutation has occurred that halts TCS signal transduction. Sequencing reveals mutations throughout the TCS that can be investigated to define the molecular determinants of signaling [249]. Alternatively, mutations can be identified in gene products previously unrelated to the TCS, as was observed here. In principle, this approach can be applied to any TCS, in any bacterium, that has an identified condition that activates a tightly controlled promoter. This selection is a powerful tool for the identification of previously unknown TCS signal sensing and transduction contributors.

Appropriate activation of HitRS and HssRS requires regulators of protein abundance and stability. DnaJ and ClpX are identified using an unbiased genetic selection as being required for *B. anthracis* TCS-dependent promoter activation. Further investigation indicated that activation of the HitRS signal transduction pathway is dependent on both proteins. DnaJ chaperones both HitR and HitS, while ClpX is required only for the maintenance of HitS abundance. We propose a model whereby (i) HitRS is required for resistance to barrier attack [91], (ii) HssRS is required for survival in the blood [70, 72, 248], (iii) cross-regulation between HitRS and HssRS prepares for survival in changing stress conditions [248], and (iv) DnaJ and ClpX work to maintain the integrity of the response. The accurate modulation of TCS proteins to stabilize the cellular stress response via TCS sigaling is critical to ensure that *B. anthracis* can readily respond to environmental changes.

CHAPTER IV

MACROPHAGES ACTIVATE *BACILLUS ANTHRACIS* HITRS TWO-COMPONENT SYSTEM SIGNALING

Introduction

The bacterial pathogen, *Bacillus anthracis,* is the causative agent of anthrax. Anthrax infections are primarily zoonotic and occur within livestock that are environmentally exposed [8, 10, 15, 170]. *B. anthracis* is a Gram-positive bacterium that naturally resides within the soil in the form of infectious spores, which are resistant to desiccation, UV radiation, chemical treatment, pressure, extreme temperatures, and reduced nutrients [313, 314]. Through incidental exposure or bioterror weapon use humans can become infected.

Due to the severe threat to both the agricultural industry and public health, the Centers for Disease Control and Prevention and United States Department of Agriculture partnered together to list *B. anthracis* as a Tier 1 Select Agent through the Federal Select Agent Program [243]. This regulated list of biologics and toxins have the potential to threaten the public health and national security of the United States of America. *B. anthracis* infection can manifest in one of three ways depending on the route of spore exposure; cutaneous, inhalation, or gastrointestinal anthrax [8, 10, 22]. Cutaneous anthrax encompasses the majority of infections at 90% worldwide [18, 315, 316]. Exposure of open wounds in the skin to spores results in ulceration of the tissue around the site of infection within a week of exposure. When treated with antibiotics, 80% of cutaneous anthrax infections are non-lethal [317]. In contrast, when the spores are exposed to the internal cavities of the body via inhalation or ingestion, disease is far more severe. Case fatality ratios for inhalation

anthrax approach 90% unless treated early with antimicrobials, at which point mortality drops to 45% as was observed in the 2001 Amerithrax bioterror attack [11, 18, 318-321].

Because it is nonmotile, spread of the bacteria between body sites must be facilitated by the host [322]. The exact cell type and molecular determinants for *B. anthracis* dissemination are not yet clear [323]. Systemic anthrax begins with phagocytosis of spores by immune cells, followed by spore germination and pathogen dissemination throughout the body. The spore coat protein, BclA, activates the classical complement pathway, which results in the rapid phagocytosis of spores at the site of infection by resident and migratory innate immune cells [324, 325]. As the internalized spores detect germinant factors, the process of vegetative bacilli growth initiates. Throughout this process, *B. anthracis* begins producing the anthrax toxins, anti-phagocytic poly-γ-D-glutamate capsule, and other virulence factors [23, 326-328]. The anthrax toxins are three proteins that polymerize in distinct combinations to produce bipartite complexes that disrupt host cell signaling pathways. Edema factor (EF) is an adenylate cyclase that increases the intracellular levels of the host signaling molecule cAMP after binding to calmodulin, resulting in cellular junction disruption and increased anti-inflammatory cytokines [21, 329-331]. Lethal factor (LF) is a zinc metalloprotease that cleaves mitogen-activated protein-kinase-kinase (MAPKK) to prevent ERK1/2, JNK/SAPK and p38 signaling [19, 330, 332]; thereby disrupting cell cycle regulation, immunity, and proliferation. EF and LF independently combine with protective antigen (PA). PA then delivers the toxin across membrane barriers through oligomerization that leads to pore formation [333]. Interruption of cellular function via the activity of LF and EF facilitates *B. anthracis* escape from the carrier cell releasing the highly toxigenic bacilli into the bloodstream. The subsequent stage of anthrax is characterized by uncontrolled bacterial growth in the blood, where burdens will reach levels as high as 10^9 cells per milliliter of blood [8].

Previous work suggests that bacilli spread can be facilitated via one of the following mechanisms; (i) hijacking migrating phagocytic cells, (ii) phagocytosis by resident cells, (iii) extracellular germination and traversing the epithelial barrier, or (iv) a combination of these [54, 57, 323, 334]. As studies continue to expand upon early observations of macrophages containing *B. anthracis* spores, it is clear that phagocytic cells play a role in anthrax infection [335]. Much work has been done to investigate the role of phagocytic cells in the progression of anthrax from the site of infection to the bloodstream, largely in the context of inhalation models. Studies depleting macrophages and neutrophils highlight the requirement of these cells in the defense against *B. anthracis* [27]. The spores are capable of germination within phagocytes prior to replication and escape, a process that is dependent on the anthrax toxins [42]. During the process of vegetation, *B. anthracis* must cope with the toxic onslaught of antimicrobial effectors employed by innate immune cells.

The initial stages of phagocytosis are not inherently toxic to *B. anthracis* until the macrophage triggers phagosome maturation [273]. The pathogen-containing vesicle will transition into a mature phagolysosome via sequential protein recruitment and gradual acidification [336, 337]. The vacuolar ATPase pumps hydrogen ions into the phagosome to reduce the pH to five or less [337]. Microbial macromolecules are damaged by the well-characterized reactive burst. Myeloperoxidase, NADPH oxidase, and iNOS catalyze the production of reactive oxygen and nitrogen species [338, 339]. Phagocytic cells employ nutritional immunity strategies within the phagolysosome where the bacteria are physically contained [241, 340]. Metal specific transporters in the phagolysosome facilitate starvation or intoxication of the microbe. Because pathogens require iron, manganese, and magnesium, limitation of these nutrient metals from the phagolysosome limits bacterial viability [341, 342]. The mismetallation of bacterial

metalloproteins can also threaten pathogen physiology. During phagocytosis, the pathogen is inundated with high levels of zinc and copper to poison the pathogen [343, 344]. Bacterial barriers are compromised through the action of antimicrobial peptides, such as LL-37, or through the activity of lysozymes that cleave peptidoglycan [271, 275]. Antimicrobial proteins in the phagolysosome also include proteases, lipases, and glycanases that enzymatically degrade the bacterial components [272, 273]. Collectively, this arsenal of effectors eliminates the pathogen unless it is well equipped to respond to these stresses accordingly [273, 274].

One strategy used by bacterial pathogens to respond to dynamic environments is via two-component systems (TCSs). TCSs are key mediators of signal transduction in response to condition changes surrounding the cell. Distinct stimuli result in cellular reprogramming via specific TCSs. Signaling begins with activation of a histidine kinase (HK), which is transferred via phosphorylation to a partner response regulator (RR). In most cases, the RR acts as a transcriptional regulator to change gene expression patterns. TCSs provide an efficient response to distinct stimuli with limited opportunity for error due to the simplicity of two primary signaling components.

To cope with the onslaught of toxic molecules during colonization of the host, bacterial pathogens alter gene expression in response to stress via TCSs [87, 345, 346]. To date, there are no known *B. anthracis* TCSs associated with survival in innate immune cells despite this being necessary for anthrax disease progression. Our lab has previously identified that HitRS responds to envelope stress, but no biologically relevant stressor is known [91, 249]. The phagolysosomal compartment elicits a complex array of stressors; therefore, we hypothesized that HitRS might be necessary for intracellular survival of *B. anthracis* in macrophages. Here, HitRS, a TCS known to be activated by envelope damaging agents *in vitro*, was investigated for activation in host

environments [91]. Using an *ex vivo* model of inhalational anthrax, HitRS signaling was observed in slices of intact murine lung tissue. As phagocytic cells serve a central role in the distribution and proliferation of *B. anthracis* during anthrax infection, the contribution of HitRS signaling to *B. anthracis* survival in phagocytes was examined using high-resolution imaging. HitRS signaling occurred following intracellular germination of phagocytosed *B. anthracis* spores and was required for viability when co-cultured with primary murine macrophages. Using the same fluorescent reporter systems to detect HitRS signaling within cells, a CRISPR/Cas9 library screen is in development to identify the host factors responsible for HitRS activation. Cas9-expressing RAW 264.7 phagocytes will be used in an arrayed CRISPR/Cas9 screen using robotics systems. CRISPR RAW 264.7 mutants that do not activate the HitRS reporter will be identified as clones of interest. Genes found to be hits in the CRISPR/Cas9 screen will indicate the host effector pathways responsible for *B. anthracis* TCS activation. Determination of screening conditions for the *B. anthracis* confirmed HitRS activation in screen-relevant circumstances. A screen of this design will provide an innovative technique for the characterization of microbial-host interactions. These results indicate that HitRS signaling is activated in conditions relevant to *B. anthracis* pathogenesis and contributes to survival within macrophages. Long-term, the strategic expansion of this technology will continue to uncover the signals in the host that are sensed by *B. anthracis*.

Materials and methods

Bacterial growth conditions. Bacterial strains (Table 1), plasmids (Table 2), and primers (Table 3) used in this manuscript are indicated below. BSL2 conditions were used in all experiments when handling *Bacillus anthracis* strain Sterne [24]. *B. anthracis* was streaked from freezer stocks on LB agar (LBA) and grown for 16 h at 30°C. LB broth was inoculated with a single colony and grown at 30°C shaking at 180 rpm with aeration for overnight growth. Reporter plasmids were constructed using *E. coli* DH5α or TOP10 cloning strains. Constructed reporters were moved into *B. anthracis* after transforming them into *E. coli* K1077 or *S. aureus* RN4220. Antibiotic concentrations used were 50 μg/mL carbenicillin for *E. coli* (reporter and complementation vectors), 10 μg/mL chloramphenicol for *S. aureus* and *B. anthracis* (reporter and complementation vectors), and kanamycin at 20 μg/mL in *B. anthracis* and 40 μg/mL in *E. coli* (genetic manipulation vector).

***B. anthracis* plasmid and strain construction.** Genetic manipulations were performed as previously described [72, 91, 98]. Plasmids for genome alterations were constructed and utilized as described previously [98]. To assemble the reporter plasmid used in this study, the previously defined *hit* promoter (P_{hit}) [91] was amplified from the genome and fused to the codon optimized sequence for *mcherry,* and inserted within the multicopy plasmid pOS1 (Schneewind, Model et al. 1992). The completed construct was moved into *B. anthracis* through the transitional strains as described above.

Spore preparation. Spores were prepared as described previously [98]. Briefly, *B. anthracis* strains of interest were grown for 72 h in Modified G Medium (MGM) sporulation media at 37°C

with shaking [190]. The bacteria were collected via centrifugation and repeatedly washed using sterile diH_2O. After washing, the spore preparations were boiled at 65°C for 30 min. Samples were washed again with sterile diH_2O again before being enumerated via serial dilution plating.

Scanning oblique plane illumination (SOPi) imaging of *B. anthracis* infected precision-cut lung slices (PCLS). Precision-cut lung slices (PCLSs) that were 300 mm in thickness were made from the lungs of one-week-old mouse pups using previously described methods [347-349]. Briefly, euthanized mice were dissected, and the lungs were filled with 2% low gelling temperature agarose (Sigma) in sterile DMEM/F-12 (Gibco). After sealing the trachea to limit agarose leakage, the lungs were removed, and the individual lobes were separated. Each lobe was then cut with a Hyrax V50 vibratome (Zeiss) into 300 µm thick slices (frequency: 80 Hz, amplitude of the knife: 1 mm, forward speed of the knife: 10 µm/s). Slices were cultured in DMEM/F-12 (Gibco) for 24 h in standard cell culture conditions (37 °C, 5% CO_2) prior to experimentation.

On the day of the experiment, a lung slice was moved into fresh media containing 1 µM JF646–Hoechst (JF_{646}, [350]) and incubated for 30 min (37 °C, 5% CO_2). After this incubation, $6x10^5$ *B. anthracis* spores were added to the media above the lung. Interactions between *B. anthracis* and the lung were imaged using a (SOPi) single objective lightsheet microscope built by members of the Vanderbilt Keck Free Electron Laser Center. Images were collected every five minutes for 18 hours. Each imaging dataset was deconvolved and denoised using NIS-Elements Artificial Intelligence algorithms.

Bone marrow derived macrophage (Mφ) cultures. To differentiate bone marrow derived Mφs (BMMφs), we generated L929 cell (European Collection of Cell Cultures) supernatant by plating

$2.5x10^5$ cells into a T150 flask with 50 mL of D10 media (DMEM + 10% (vol/vol) FBS) (Gibco) and incubating for 12 days (37 °C, 5% CO_2). After 12 days, supernatant was collected and filtered.

Single-cell suspensions of bone marrow were prepared from the tibias and femurs of C57BL/6 mice. Mononuclear cells were isolated by using Lympholyte Separation Medium (CEDARLANE Laboratories), plated in a 60-mm Petri dish with 6 mL of BMMφ differentiation media (D10 media with 10% (vol/vol) L-cell supernatant), and cultured overnight (37 °C, 5% CO_2). Nonadherent cells were plated into non-tissue culture-treated 100-mm Petri dishes (1 mL cells per Petri dish) with 7 mL of fresh BMMφ differentiation media. To promote BMMφ differentiation, cells were incubated for 6 days (37 °C, 5% CO_2) with an additional 5 mL of BMMφ differentiation media being added on day 4. The resulting BMMφs were removed from the dish by washing with ice cold PBS. BMMφ cultures were 98% $CD11b^+$, $I\text{-}A^{lo}$ and $B7.2^{lo}$.

Confocal imaging of *B. anthracis* infected BMMφs. BMMφs were cultured for 2 h in D10 media to allow cells to attach to sterilized coverslips. BMMφs were cultured with bacteria at a MOI of 10/1 (10,000,000 spores per 100,000 immune cells) in D10 media (37 °C, 5% CO_2). After 1, 2, 4, and 6 h, samples were prepared for microscopy. 4% paraformaldehyde (Invitrogen) was used for 15 min of fixation (37 °C, 5% CO_2). Following 5 min permeabilitzation with 0.1% Triton-X in Phosphate Buffered Saline (PBS), BMMφs were stained with 1 μg/mL Hoechst 33342 (ThermoFisher) and 5 μM Alexa Fluor 647 phalloidin (Invitrogen) for 30 min at room temperature. Dried coverslips were adhered to slides using Prolong Gold (ThermoFisher). Confocal imaging was performed using 63X oil objective on the Zeiss LSM 880 with AiryScan. Super-resolution imaging was collected using Nikon Structured Illumination Microscopy (SIM) using 3D-SIM mode and a 100X objective. Images were collected using an Andor DU-897 EMCCD camera using

settings determined with positive and negative control samples. The brightness and contrast were adjusted consistently to allow for the visualization based on control images. Signal thresholds were determined for each channel. The intensity of mCherry that overlapped with GFP, indicating it was bacterial in origin, and overlapped with Alexa Flour 647 signal, indicating association with a macrophage, calculated. This value was normalized to the area of the Alexa Flour 647 signal per image as an indicator of the number of macrophages. Analysis was performed using Nikon Elements General Analysis 3 (GA3) capabilities.

Bacterial killing assay. BMMφs were cultured for 2 h in D10 media to allow cells to attach to the bottom of a 96 well plate. Spores were diluted 1:10 into non-heat inactivated FBS for 1 h on ice prior to culturing with BMMφs. BMMφs were cultured with bacteria at a MOI of 1/5 (20,000 spore per 100,000 immune cells) in D10 media (37 °C, 5% CO_2). After 0, 1, 2, 4, and 6 h, the entire contents of the well were serially diluted and spot-plated onto LB agar.

Generation of Cas9-expressing RAW 267.4 macrophages. RAW 267.4 phagocytes (ATCC) were engineered to express Cas9 under a doxycycline inducible promoter using pCW-Cas9-Blast. pCW-Cas9-Blast was a gift from Mohan Babu (Addgene plasmid #83481; http://n2t.net/addgene:83481; RRID:Addgene_83481). pMD2.G was a gift from Didier Trono (Addgene plasmid #12259 ; http://n2t.net/addgene:12259 ; RRID:Addgene_12259). psPAX2 was a gift from Didier Trono (Addgene plasmid # 12260; http://n2t.net/addgene:12260 ; RRID:Addgene_12260).

293T (ATCC® CRL-3216™) were obtained from ATCC and cultured in DMEM and 10% heat inactivated FBS. 293T cells were then transfected with pCW-Cas9-Blast, pMD2.G, and

psPAX2 using Lipofectamine-3000. Lentiviral containing media was purified and used to infect RAW 264.7 cells. After lentiviral transduction, cells were treated with blasticidin (2μg/mL) for selection. Single cell clones were then plated, expanded, and validated for the presence of Cas9 using a monoclonal anti-FLAG antibody (Sigma). Cas9-expressing RAW 264.7 cells were maintained in cell culture dishes using D10 media (DMEM + 10% (vol/vol) FBS, 37 °C, 5% CO_2) (Gibco) supplemented with 2μg/mL of blasticidin. Upon reaching desired confluence, cells were passaged by gently scraping the cells off the dish, counting cell density, and replating at a density of 1×10^5 cells/mL in fresh media.

CRISPR/Cas9 library screen optimization studies. RAW 264.7 were plated into black wall, clear bottom 96-well plates (Costar) at 20,000 cells per well. *B. anthracis* WT gGFP pOS1.P$_{hit}$*mCherry* and Δ*hitRS* gGFP pOS1.P$_{hit}$*mCherry* spores were inoculated onto the cells at multiplicity of infections 1, 2, 5 and 10 using the Agilent Bravo liquid handler. At this time CellMask Deep Red plasma membrane stain was added at 1.25 μg/mL (Thermo Fisher Scientific). Following brief centrifugation at 277 × g for 2 min, co-cultures were incubated 30 minutes in the Cytomat automated incubator (37 °C, 5% CO_2) to allow for phagocytosis. Wells were subsequently washed using the BioTek plate washer to remove extracellular bacteria and then fresh D10 media was added. Plates were imaged using the High-content imaging ImageXpress Micro XL System over a period of 6 h.

Table 4-1: Bacterial strains utilized in Chapter IV

Species	Genotype	Description	Reference
B. anthracis strain Sterne	Wildtype/Parental	Wildtype laboratory strain	[24]
B. anthracis strain Sterne	Δ*hitRS*	In frame deletion of *hitRS*	[248]
B. anthracis strain Sterne	Δ*bla1*::p0253-*gfp*	Chromosomal insertion of GFP, gGFP	[351]
B. anthracis strain Sterne	Δ*hitRS* Δ*bla1*::p0253-*gfp*	In frame deletion of *hitRS,* Chromosomal insertion of GFP, Δ*hitRS* gGFP	This study
E. coli strain K1077	Wildtype	Wildtype laboratory stock for cloning	[185]
S. aureus strain RN4220	Wildtype	Wildtype laboratory stock for cloning	[194, 195]

Table 4-2: Plasmids utilized in Chapter IV

Plasmid	Description	Reference
pLM4	Allelic exchange vector for *B. anthracis*	[84]
pLM4-*hitRS*	Vector to delete *hitRS*	[91]
pOS1.P$_{hit}$*mCherry*	mCherry reporter vector	This study

Table 4-3: Primers utilized in Chapter IV

Primer	Sequence	Use
P_{hit} fwd	GCCTTAAAGACGATCCGGGGAATTCCTCTTTTTTGAAGGCACG	vector construction
P_{hit} rev	TAGAAACCATTCATGTTCATCTCCTCGTG	vector construction
mCherry fwd	ATGAACATGAATGGTTTCTAAAGGAGAAG	vector construction
mCherry rev	AAACACTACCCCCTTGTTTGGATCCTTATTTATATAATTCATCCATTCCG	vector construction

Results

HitRS is activated following spore germination in murine lung tissue *ex vivo*.

Inhalation anthrax is the deadliest form of *B. anthracis* infection [352]. Despite the highly effective host defense system in the lung environment, this pathogen is capable of surviving the immune response and progressing into a septic infection. We hypothesized that HitRS is activated in the lung environment to promote viability during early interactions with innate immune effectors. To visualize the spatio-temporal activation of HitRS signaling in living lung tissue, imaging experiments were performed following inoculation of *B. anthracis* spores harboring a fluorescent HitRS reporter onto *ex vivo* cultures of precision-cut lung slices (PCLS) [349, 353]. Murine lung slices were sectioned into PCLSs and maintained in cell culture media according to established methods to serve as a validated 3D model of the lung epithelium [347, 349, 354, 355]. This tissue processing technique was combined with state-of-the-art Scanning Oblique Plane Illumination (SOPi) single objective lightsheet imaging to observe *B. anthracis* infection of living lung tissue. Lightsheet technologies allow for 4D imaging of tissue with larger fields of view, reduced signal scattering, and rapid imaging speeds. Sample integrity is prioritized to reduce fluorophore bleaching and exposure toxicity [356]. We engineered strains of *B. anthracis* to constitutively express GFP and express mCherry upon activation of HitRS (gGFP P_{hit}*mcherry*). Therefore, these cells constitutively fluoresce green and only fluoresce red upon HitRS activation. Wildtype, reporter *B. anthracis* spores were inoculated onto PCLSs. Spores were detected on the lung tissue at the start of the experiment and after two to four hours, spores germinated into vegetative bacilli (Fig. 4-1A). Following germination, subsequent growth of the population occurred rapidly that was visible after six hours (Fig. 4-1A). Upon germination of spores, reporter activity was observed after four hours (Fig. 4-1B). Viewing the lung slice from the side confirmed HitRS reporter activation in the bacilli growing in the tissue (Fig. 4-1C). To

confirm that the HitRS signal observed in Fig. 4-1A-C was not due to signal bleed through from the JF dye used to label the DNA of both the PCLS and bacteria, an experiment was performed where no tissue label was used. Results from this experiment confirmed that the promoter for the *hit* operon was activated within the lung environment as the mCherry reporter signal was still observed at multiple foci during imaging (Fig. 4-1D). Using reporter spores lacking *hitRS*, the dependence of reporter activity on the TCS was confirmed. In a PCLS infected with Δ*hitRS* gGFP P_{hit}*mcherry* spores, germination occurred as in wildtype, but no reporter activity was observed (Fig. 4-1E). These results suggest that there is a host-derived activator(s) of *B. anthracis* HitRS signaling within murine lung tissue.

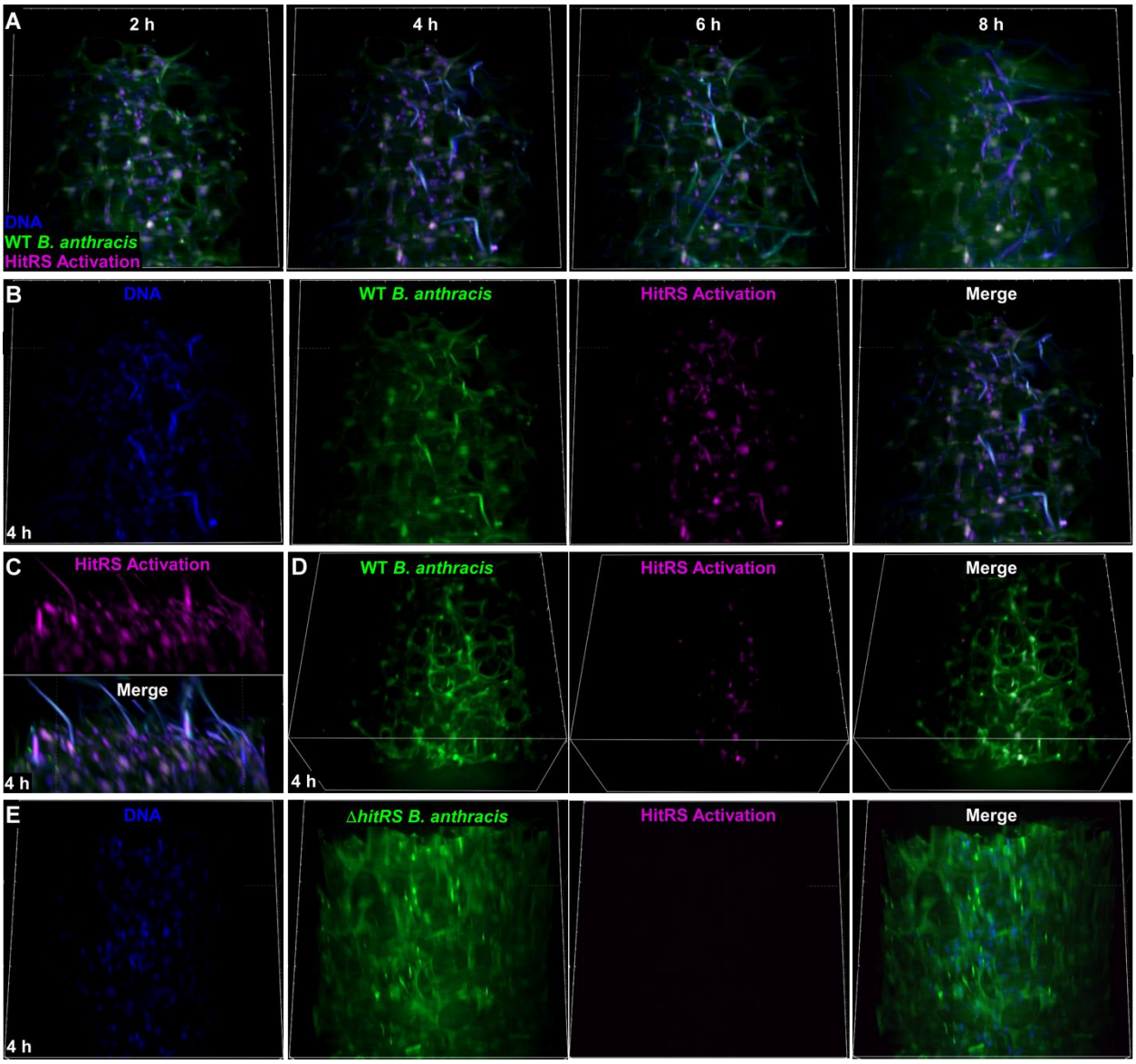

Figure 4-1. HitRS activation in an *ex vivo* lung model. A. E*x-vivo* murine lung sections infected with wildtype *B. anthracis* that express GFP constitutively and a HitRS-inducible mCherry, labeled with JF dye, and then imaged using SOPi over an eight-hour period. The four-hour time point was expanded into individual channels (**B**) and turned 90 degrees to observe HitRS activation (**C**). **D.** E*x-vivo* murine lung sections infected with wildtype *B. anthracis* that express GFP constitutively and a HitRS-inducible mCherry and then imaged after four hours using SOPi. **E.** E*x-vivo* murine lung sections infected with Δ*hitRS B. anthracis* that express GFP constitutively and a HitRS-inducible mCherry, labeled with JF dye, and then imaged using SOPi for four hours.

HitRS is activated within bone marrow-derived macrophages.

The *ex vivo* lung model of anthrax infection allowed for the visualization of HitRS signaling in a complex tissue environment. Activation was only observed in a subpopulation of the vegetative cells, indicating that HitRS functions following exposure to specific host stimuli. Ample literature has described the relationship between *B. anthracis* and innate immune cells, which represent a population of resident cells in the lungs [357, 358]. Macrophages are linked to both *B. anthracis* defense and dissemination [26, 27, 32, 43, 44, 46]. Due to the importance of phagocytic cells in the pathogenesis of *B. anthracis* and the multitude of stressors produced by these cells, we hypothesized HitRS would be activated in the phagolysosomal compartment. To test this hypothesis, primary bone marrow-derived macrophages (BMMφs) were inoculated with wildtype gGFP P_{hit}*mcherry* spores and fixed for imaging at the indicated time points (Fig. 4-2). Starting at one hour, the constitutive signal associated with the spores was detected in association with the BMMφs, suggesting phagocytosis had occurred (Fig. 4-2). Germination of the spores into bacilli began at two hours, with presence of vegetative bacilli increasing over the course of the experiment (Fig. 4-2). In instances where vegetative cells were associated with BMMφs, mCherry fluorescence was observed, indicating that HitRS signaling was activated (Fig.4-2). Bacilli not associated with the BMMφs also displayed limited instances of HitRS reporter activation indicating a secreted factor can activate P_{hit} or these bacilli escaped the macrophages. Reporter activation persisted through the course of the experiment, until the six-hour time point when *B. anthracis* overtook the BMMφs with significantly increased numbers of bacilli. Super-resolution imaging performed on WT-infected samples from the four-hour time point revealed that the bacilli with HitRS reporter activity were located inside of the BMMφs (Fig. 4-3). Imaging through three-

dimensional space allowed for the visualization of the bacilli expressing the HitRS reporter encapsulated by the phalloidin labeled actin (Fig. 4-3B).

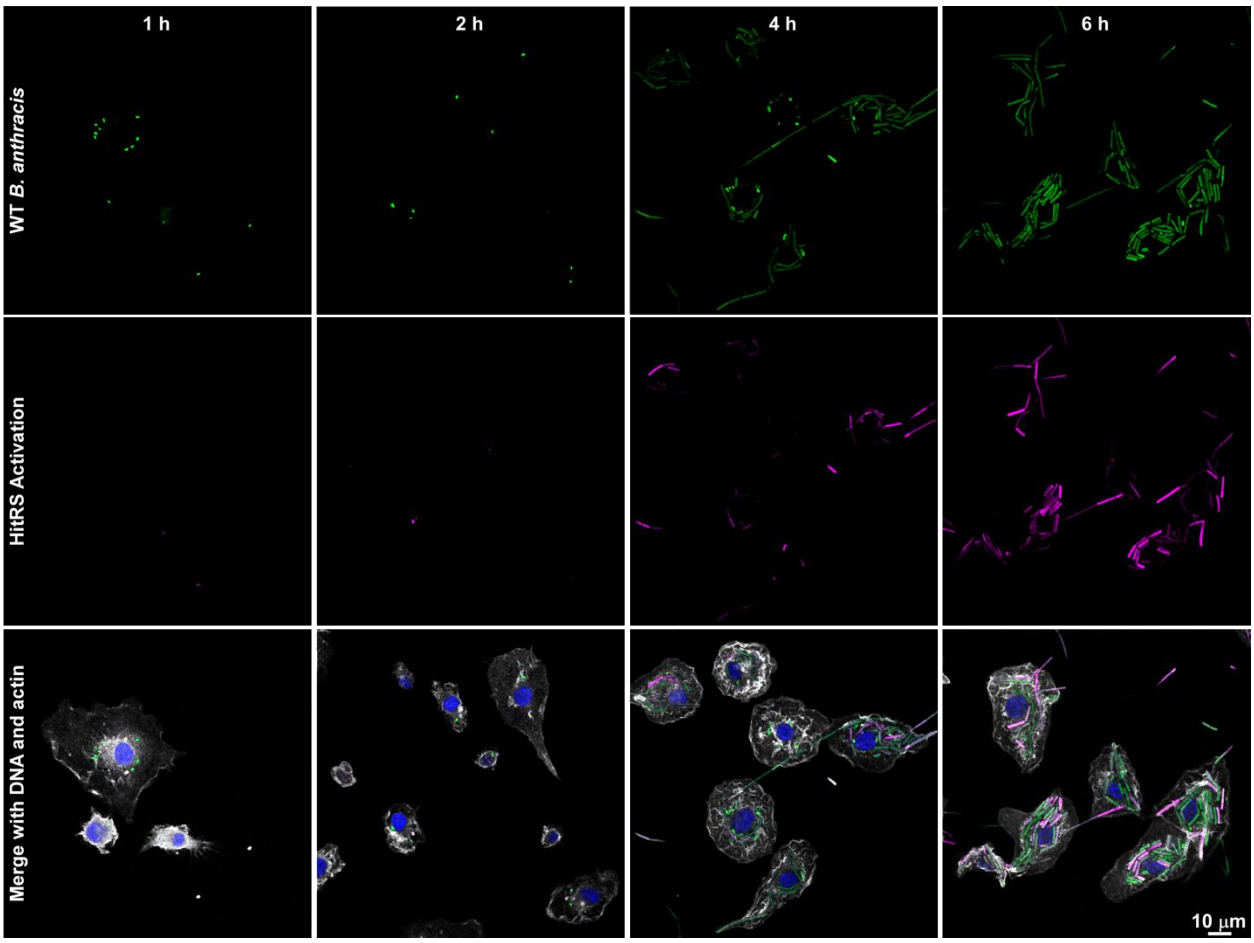

Figure 4-2. *B. anthraics* P_{hit} activation following inoculation of primary bone marrow derived macrophages. A. Macrophages were inoculated with wildtype *B. anthracis* spores that express GFP constitutively and a HitRS-inducible mCherry. Cells were fixed and stained one, two, four, and six hours post inoculation using anti-CD11b allophycocyanin (APC)-conjugated antibodies and Hoechst 33342. Samples were imaged on a confocal microscope with Airyscan.

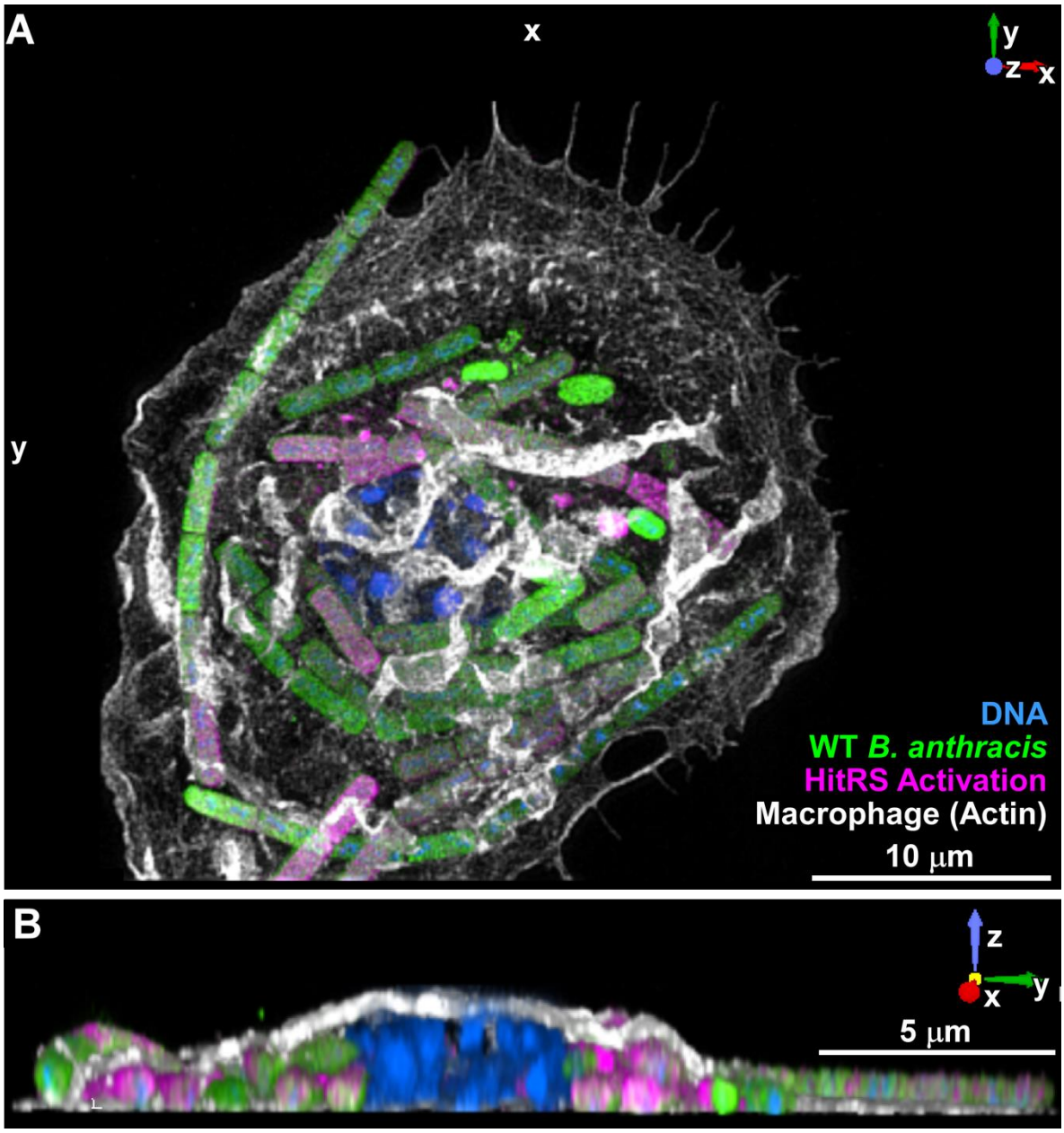

Figure 4-3. P_{hit} activation occurs within primary bone marrow macrophages. A. Macrophages were inoculated with wildtype *B. anthracis* spores that express GFP constitutively and a HitRS-inducible mCherry. Cells were fixed and stained four hours after inoculation using Alexa Fluor 647 phalloidin and Hoechst 33342. Samples were imaged on a structured illumination microscope (SIM). Shown here is a 3D rendering. **B.** 3D rendering of the merge image from 4-3A tilted and fractioned to display the actin surrounded-bacilli.

To test whether the activation of the P_{hit}*mcherry* reporter was dependent on the HitRS TCS, Δ*hitRS* gGFP P_{hit}*mcherry* spores were inoculated onto BMMφs. Spores were observed associated with macrophages at one hour as was observed in wildtype (Fig. 4-4). Vegetative bacilli were minimally detected at two hours post-inoculation and increased over the course of the experiment starting at the four-hour time point (Fig. 4-4). However, P_{hit}*mcherry* reporter signal was not detected in any of the fields of view at the time points tested. HitRS reporter activation was quantified over time from this imaging data set (Fig. 4-5A). Wildtype bacilli displayed P_{hit} activation starting at two hours, which correlated with the start of spore germination. The signal in wildtype samples intensified with time, as bacterial growth increased. As observed, quantification revealed that in the absence of HitRS, P_{hit} is not activated when co-cultured with BMMφs. Reporter activity in this mutant was significantly less than wildtype at two, four, and six hours post inoculation. This result suggests that HitRS is required for the activation of P_{hit}*mcherry* observed in wildtype *B. anthracis* co-cultured with primary macrophages. Therefore, HitRS TCS signaling is activated in BMMφs.

The detection of HitRS promoter activation in cultured phagocytes suggested that HitRS signaling is important in the host immune cell environment. This observation raised the question as to whether the HitRS mutant strain may have germination or survival defects in the presence of primary macrophages. We hypothesized that HitRS is required for viability of *B. anthracis* in macrophages. To investigate the observations made during imaging, BMMφs were inoculated with wildtype or Δ*hitRS* spores and total bacterial burdens were monitored over time. As expected, the bacterial burden of wildtype *B. anthracis* increased over time starting at four hours post inoculation (Fig. 4-5B). Δ*hitRS* showed reduced viability at each time point compared to wildtype

at all timepoints, a trend that became significant at two and six hours post inoculation (Fig. 4-5B). These results suggested that HitRS activation in BMMφs is required for maximal viability.

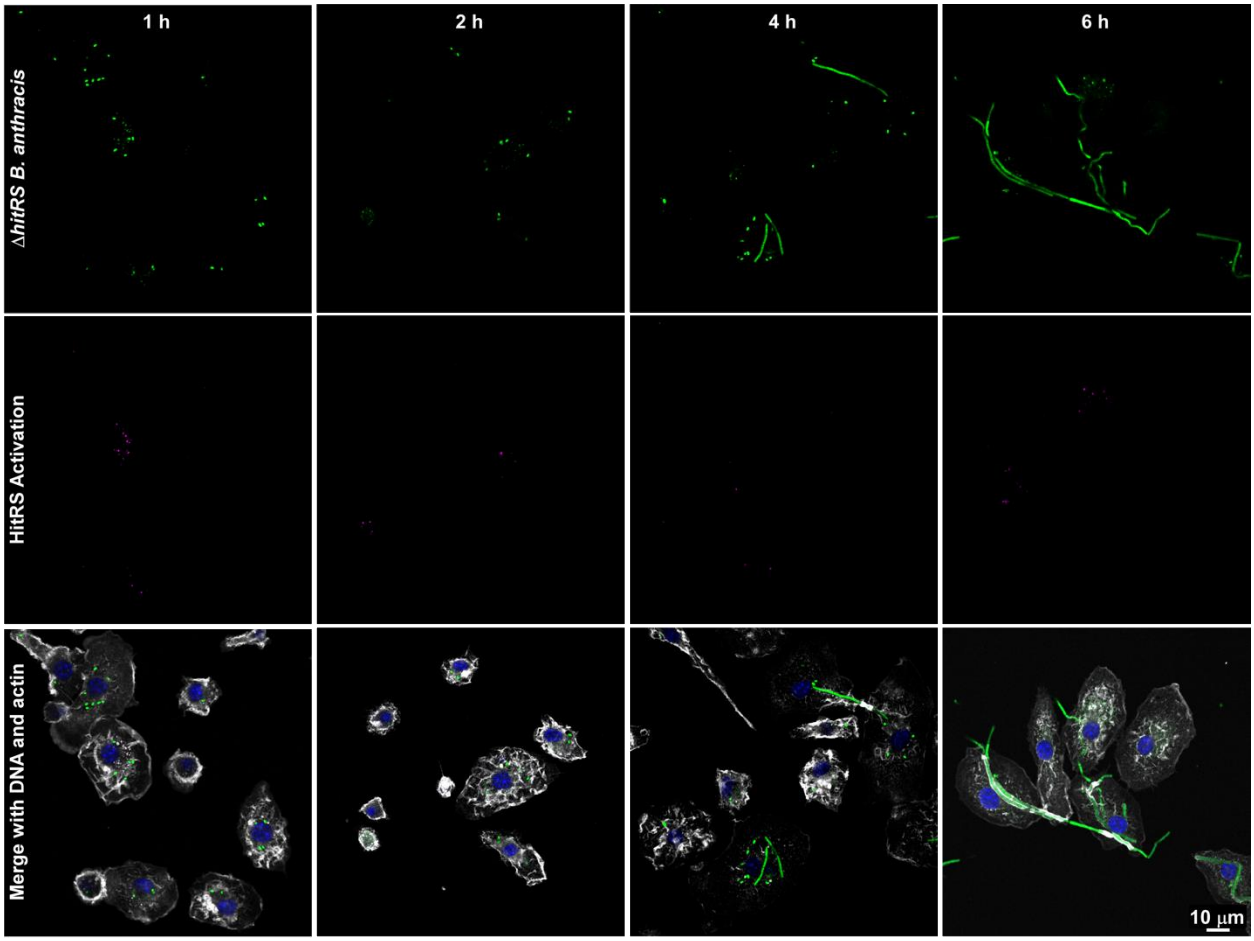

Figure 4-4. HitRS is activated by primary bone marrow derived macrophages. Macrophages were infected with Δ*hitRS B. anthracis* spores that express GFP constitutively and a HitRS-inducible mCherry. Cells were fixed and stained at one, two, four, and six hours post inoculation using Alexa Fluor 647 phalloidin and Hoechst 33342. Samples were imaged on a confocal microscope with Airyscan. Images shown are representative of 12 images per sample, repeated over three experiments.

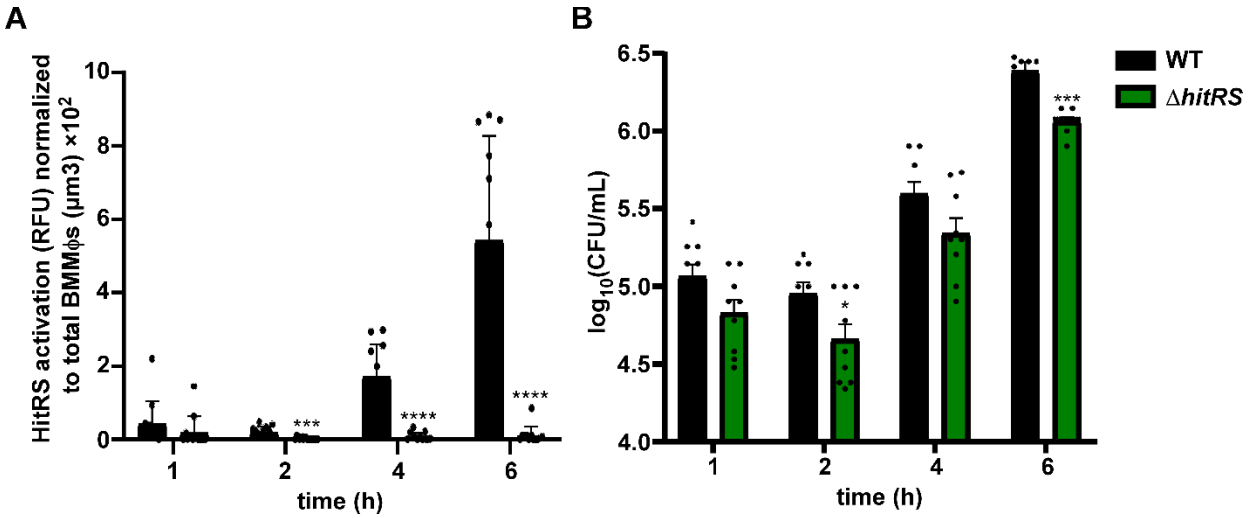

Figure 4-5. HitRS is required for P_{hit} activation and viability when co-cultured with primary macrophages. A. Images presented in Fig. 4-2 and Fig. 4-4 were used to quantify HitRS reporter activation that coincided with constitutive GFP bacilli-derived signal that occurred within macrophages. Data are averages of quantification 12 individual images ± SD. **B.** Bone marrow derived macrophages were inoculated with WT or Δ*hitRS* spores (MOI = 1:5). At the indicated time points, the contents of each well were assessed for bacterial burden using serial plating for colony forming units (CFU). Data are averages of three independent experiments performed in biological triplicate ± SEM. Statistical significance compared to WT was determined using a Student's t-test (*$p \leq 0.05$, ***$p \leq 0.001$, ****$p \leq 0.0001$).

Identification of host derived activators of HitRS signaling.

Results of the above imaging studies revealed that HitRS signaling occurs intracellularly within macrophages and contributes to bacterial viability (Fig. 4-3, 5). We hypothesized that specific host factors drive HitRS signaling. Identification of these effectors presented a unique challenge, as the intracellular environment of activated macrophages is highly complex. The advent of CRISPR/Cas9 libraries has provided opportunities to identify novel functions of host genes in a variety of well-described cellular processes [359-361]. To test our hypothesis, we will utilize an arrayed CRISPR/Cas9 library obtained from Sigma-Aldrich, in combination with robotic liquid handling and high-throughput robotic imaging technology, to identify host factors required to stimulate bacterial TCS signaling. Screening of single cell clones in an arrayed library will allow for identification of hits with less repetition of the screen and reduced library coverage, therefore providing a more efficient approach than pooled screening methods [362]. Additionally, this approach will reduce the risk of false positives and allow for temporal monitoring of the reporter. RAW 264.7 murine macrophage-like cells were engineered to express Cas9 upon induction with doxycycline for use in the screen (data not shown). RAW 264.7 cells are immortal monocyte/macrophage-like cells capable of phagocytosis that provide a technical advantage over primary cells in the generation of the CRISPR/Cas9 library due to stability in culture conditions. RAW 264.7 cells have been used previously in a pooled CRISPR/Cas9 screen, but we plan to expand on this approach by using an arrayed lentivirus library that contains two guide RNAs (gRNA) targeting each protein-coding gene [363, 364]. Collectively, there are 118 384-well plates whereby each well targets a distinct gene in the murine genome using a gRNA that has been validated experimentally by the library manufacturer. The screen will proceed as follows: (i) Cas9 expressing RAW 264.7 cells will be plated into 384 well plates, (ii) cells will be transfected with

the arrayed lentiviral library, (iii) CRISPR mutants will be identified using blue fluorescent protein signal and puromycin resistance encoded on library vector, (iv) B. *anthracis* HitRS reporter spores will be inoculated, and (v) outcomes will be observed using high throughput imaging of each well at 6 hours (Fig. 4-6).

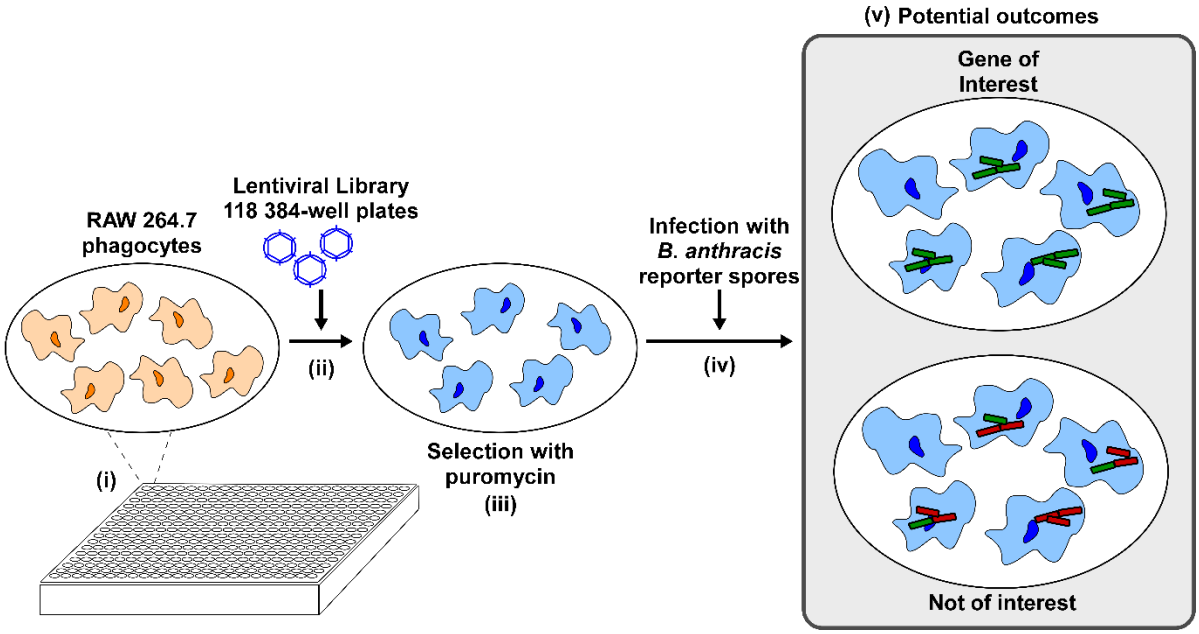

Figure 4-6. Screening of arrayed phagocyte CRISPR/Cas9 library for host-derived activators of HitRS. RAW 264.7 phagocytes have been transfected with an inducible Cas9 and used to create an arrayed CRISPR library (i-iii). These cells will be infected with *B. anthracis* spores that express GFP constitutively and a HitRS-inducible mCherry (iv). The infected library will be imaged using the high-throughput ImageXpress system to identify CRISPR clones that do not activate HitRS.

Wildtype gGFP P_{hit}*mcherry* will be used in the screen and therefore, consistent with the BMMφs, RAW264.7 macrophages infected with *B. anthracis* will fluoresce both red and green, indicating HitRS activation (Fig. 4-1,2). In contrast, RAW264.7 macrophages with CRISPR mutations in genes responsible for HitRS activation will contain *B. anthracis* that only fluoresces green. In each plate, we will use non-target lentiviral negative controls to visualize HitRS activation in non-mutated RAW 264.7 cells and Δ*hitRS* spores harboring the reporters as a control for TCS signaling. These controls are important for the normalization of the data, and determining if each CRISPR mutant activates HitRS within experiments and across all of the 384 well plates.

To determine screening conditions, optimization experiments were performed whereby wildtype gGFP P_{hit}*mcherry* and Δ*hitRS* gGFP P_{hit}*mcherry* spores were inoculated onto wildtype RAW 264.7 cells at a multiplicity of infection (MOI) of five and allowed to incubate for 30 min. Extracellular bacteria were washed prior to addition of fresh media. All liquid handling was performed using robotic liquid handling and imaging. Cells were imaged once an hour, over a period of five hours. As observed in the BMMφs, spore phagocytosis and early instances of germination occurred by one-hour post inoculation, regardless of bacterial genotype (Fig. 4-7A-B). Early after germination, wildtype bacilli associated with macrophages expressed the HitRS activator. Reporter activity was detected in wildtype bacilli associated with RAW 264.7 cells throughout the duration of the experiment (Fig. 4-7A). Reporter activity was never observed in Δ*hitRS* gGFP P_{hit}*mcherry* spores at any time point (Fig. 4-7B).

Because *B. anthracis* is highly toxic to eukaryotic cells, we sought to define the appropriate ratio of bacilli to phagocytes considering the goal of maximum possible reporter signal from bacteria and minimal RAW 264.7 cell death. To determine the ideal MOI of *B. anthracis* reporter spores to RAW 264.7 cells for the library screen, we assayed viability of bacilli and host

phagocytes in co-culture overtime. Bacteria were added in excess to phagocytes at ratios of one, two, five, or ten to one and then imaged after four hours (Fig. 4-7C-D). Constitutive reporter signal was maximally observed in both wildtype and Δ*hitRS* inoculated at an MOI of ten. At this dose, RAW 264.7 cells were still detectable by CellMask staining. Taken together, results from these experiments confirmed HitRS activation in RAW 264.7 phagocytes and determined that imaging an inoculation of ten spores per phagocyte five hours into the experiment is ideal for CRISPR/Cas9 library screening.

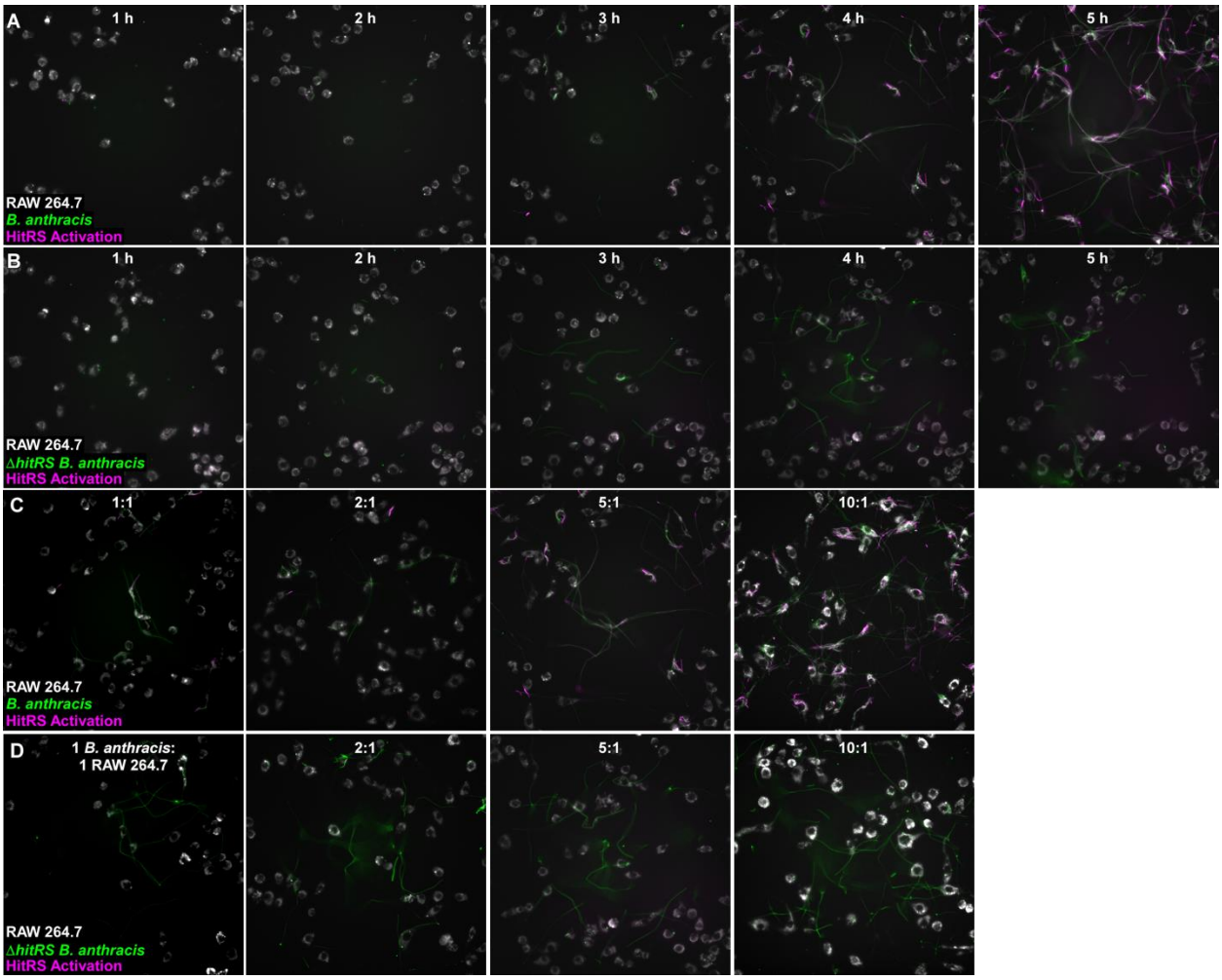

Figure 4-7. P_{hit} is activated by RAW 264.7 phagocytes. ImageXpress high-throughput imaging of a five-hour time course of CellMask Deep Red-labeled RAW 264.7 phagocytes that were inoculated at an MOI of 5 with wildtype **(A)** or Δ*hitRS* **(B)** *B. anthracis* that express GFP constitutively and a HitRS-inducible mCherry. ImageXpress high-throughput imaging at five hours post inoculation of CellMask Deep Red-labeled RAW 264.7 phagocytes were inoculated at the indicated multiplicities of infection with wildtype **(C)** or Δ*hitRS* **(D)** *B. anthracis* that express GFP constitutively and a HitRS-inducible mCherry.

Upon completion of two runs of screening, image analysis will be performed using high-throughput imaging computational methods to identify wells that are associated with a lack of mCherry signal. Wells that are deemed "hits" will be linked to their target genes using the arrayed plate maps for the lentiviral library. Those genes that are confirmed as hits for both gRNAs in the library will be re-screened using WT and Δ*hitRS* gGFP P_{hit}*mcherry* spores over a time course of imaging. Due to the known function of HitRS in response to envelope damage, prioritization will be given to genes that have been associated with cell membrane damage, such as antimicrobial peptides, degradative enzymes and mediators of the reactive species burst. Additional future directions include generation of clonal mutant populations in the phagocytes and the use of commercially available inhibitors/activators of identified pathways to investigate HitRS activation, or the expansion of our results into mutant murine models.

The use of CRISPR/Cas9, imaging, and robotics technologies represents a combinatorial approach to address the hypothesis that there are host effectors present in phagocytes that activate *B. anthracis* HitRS signaling. While research has been done to identify eukaryotic factors conferring susceptibility to bacteria effectors, developing a method to find host pathways involved in activation of pathogen stress sensing presents a unique opportunity for the identification of eukaryotic genes responsible for triggering TCS signaling within the bacterial cell [359, 360, 365]. A screen of this design will provide an innovative platform for the characterization of microbial-host interactions.

Discussion

Bacillus anthracis causes a potentially lethal infection and has been successfully used as a bioterror weapon in the United States. During anthrax infection, the bacterium must contend with the host innate immune response, which includes antimicrobial effectors in macrophages. Here, we identified a *B. anthracis* TCS, HitRS, that is triggered when the pathogen is internalized by phagocytes (Fig. 4-3). While HitRS was previously shown to be activated by envelope damage [91], we further determine it is required for full viability when co-cultured with primary macrophages (Fig. 4-5). To identify the host factor(s) that target the HitRS system, an arrayed CRISPR/Cas9 library screen has been designed that will be performed using high throughput robotics and imaging (Fig. 4-6).

Lethality of anthrax infections can approach 90% in patients that fail to receive antibiotic treatment [8, 10, 366]. Although this pathogen can be visualized using standard microscopic diagnostics, the rare occurrence of systemic *B. anthracis* infection, coupled with early symptoms that resemble a flu-like disease, often results in delayed diagnosis. Much like untreated patients, in cases where disease is not caught early, the patient often succumbs to infection [367]. Therefore, the research community has increased efforts to define the early stages of anthrax infection to better diagnose and treat patients. Imaging provides a powerful tool to understand early host-pathogen interactions. Real-time imaging revealed that 10% of phagocytosed spores will germinate into bacilli that are capable of intracellular replication [368]. Vegetative *B. anthracis* then escapes from cultured macrophages four to six hours following phagocytosis as was visualized using fluorescent and electron imaging [40]. Similar observations were made throughout the imaging presented here. Though variation in time to spore germination was observed, the bacilli were consistently proliferating and escaping from the macrophages starting

at four hours post-inoculation (Fig. 4-2, 4). However, here, bacilli germination coincided with activation of bacterial signaling.

Published intravital imaging of inhalational anthrax revealed close interactions between macrophages and dendritic cells harboring *B. anthracis* intracellularly [369]. These results are corroborated by histological and immunofluorescence analysis indicating that macrophages are the first cell type to come in contact with the *B. anthracis* spores [239]. Following this line of observation, we hypothesized that the HitRS activation observed within the PCLSs occurred in a phagocytic cell (Fig. 4-1). Super-resolution SIM imaging permitted the observation of macrophage-pathogen interactions at the subcellular level with a resolution that has previously not been attainable for *B. anthracis* in fluorescence imaging (Fig. 4-3). We applied this technology to investigate signaling in *B. anthracis* using host-dependent *in vitro* activation of a fluorescent reporter (Fig. 4-2, 4). Using this approach, we observed the activation of HitRS two-component system signaling within the intracellular environment. Signaling was observed in bacilli frequently associated with macrophages, but not in all bacterial cells. This finding may indicate loss of the reporter plasmid or that there is some heterogeneity in the host antimicrobial response against *B. anthracis.* Here, the use of *ex vivo* and super-resolution imaging expanded the ability to dissect these interactions that occur between host cells and *B. anthracis* to better understand the survival mechanisms employed by this professional pathogen.

Pathogen survival in the host is challenged by the activity of the immune response. Both innate and adaptive immune cells will target the bacteria with antimicrobial effectors to compromise the cell barrier, deprive nutrients, or damage macromolecules [32, 56, 274, 339, 370-374]. TCSs that are stimulated during these attacks therefore become required for infection of vertebrate hosts. HK to RR signal transduction under these conditions results in vital

transcriptomic changes that facilitate the adaptation of the pathogen to the host-derived assault as represented in the following examples [107, 108, 155, 311]. In *Legionella pneumophila,* PmrAB is activated during intracellular growth in macrophages, for which it is required [270]. GraXRS is required for *Staphylococcus aureus* adaptation to the acidification of host immune cells [269]. The burst of reactive species activates ScnRK in *Streptotoccus mutans* and AirSR in *S. aureus* to promote viability in the presence of destructive oxidants [375, 376]. Examples of TCSs responding to the many of the antimicrobial conditions found in phagocytes exist in the literature. Based on these examples, we hypothesize that HitRS activation by phagocytic immune cells facilitates *B. anthracis* survival in the host, representing the first description of a TCS linked to defense against macrophages. If this is true, then this system could be important for the initial stages of anthrax infection during phagocytosis of spores. However, the exact host factors responsible for the activation of bacterial signal transduction have yet to be elucidated.

The intracellular environment of an activated innate immune cell is complex and dynamic [34]. Previous work revealed that HitRS is activated by compounds that damage the envelope of cells including vancomycin, nordihydroguaiaretic acid (NDGA), chlorpromazine, and targocil [91]. These compounds share little structural similarity, but each is implicated in cell envelope stress suggesting that HitRS senses specific perturbations in the cell envelope and not the molecules directly. Data presented here indicate that HitRS signals in the intracellular macrophage environment. To identify the host effectors that activate HitRS, we will perform a phagocyte CRISPR/Cas9 library screen. CRISPR/Cas9 library screening is a tool that can be used to study the effects of loss of function mutations across the eukaryotic genome [360, 361]. Efficient gene editing and the adaptability of this approach provide the necessary framework for a novel screen design to investigate the host pathogen interface. This technology has been previously employed

to investigate the phagocytic function of innate immune cells. For example, human myeloid cell CRISPR mutants that were defective at phagocytosis were identified in a pooled library using magnetic beads that were provided as an uptake substrate [364]. Sequencing of mutants of interest identified known drivers of phagocytosis, but also uncovered novel regulators of actin and filopodia dynamics [364]. To interrogate factors required for the molecular specificity that drives the host antimicrobial response, CRISPR/Cas9 technology is highly valuable. A large proportion of pathogens are capable of inducing damage to host cells that results in their death and is a clear phenotype that can be screened for in large scales. Therefore, whole genome libraries can be screened for host mutants that remain viable in the presence of a particular pathogen, indicating that the factor enabling virulence factor susceptibility has been disrupted. This strategy has been employed with increasing frequency to study viral and bacterial interactions with the host and have revealed novel roles for eukaryotic pathways not previously associated with infection [359, 377-380]. For example, in *Vibrio parahaemolyticus*, sulfation is now known to be required for sensitivity to the first type three secretion system (T3SS), but fucosylation is required for killing of host cells by a distinct T3SS [359]. In Enterohemorrhagic *Escherichia coli* (EHEC) infection, TP9SF2 and LAPTM4A were identified through CRISPR/Cas9 library screen to be required for infection of intestinal epithelial cells [380]. These host genes were required for epithelial cell sensitivity to EHEC T3SS and toxins during the early stages of host-pathogen interactions [380]. In both of these examples, novel therapeutic targets within the host were identified that, when targeted by pharmacological interventions, may reduce the pathogenicity of these bacteria. This finding reveals an alternative treatment strategy to classic antibiotics, something that help to combat issues of drug resistance. Upon identification of biological activators of HitRS using the

CRISPR/Cas9 library, we will be able to interrogate, and potentially exploit, the stress response systems used by *B. anthracis* during infection.

Presented here is the description of a *B. anthracis* stress-sensing system that functions during the intracellular phase of anthrax infection. HitRS is activated by host effectors present within phagocytes and therefore is crucial for the survival of *B. anthracis*. Innovative imaging approaches allowed for the investigation of this host-pathogen interface in real time at high resolution. Precision cut lung slices provided a unique platform for the investigation of the *B. anthracis* host-pathogen interface. The effectors driving the activation of HitRS signaling in host tissues will be identified and confirmed using an imaging-based CRISPR/Cas9 library screen. Results from this innovative screen can be combined with the observations made during the imaging of HitRS activation to fully elucidate the contribution of TCS signaling to the defense of *B. anthracis* against the innate immune response.

CHAPTER V

SUMMARY AND FUTURE DIRECTIONS

Summary

Bacillus anthracis is a Gram-positive, spore-forming bacterial pathogen that is the causative agent of anthrax [8, 10]. Spores, the infectious form of the bacterium, are phagocytosed at the site of infection by innate immune cells [42, 52, 324, 381]. Following phagocytosis intracellular *B. anthracis* spores germinate into vegetative bacilli and eventually escape the host cell. Extracellular bacilli proliferate to extreme bacterial densities in the blood [8]. Such high bacterial burdens lead to septicemia, intoxication and death of the host [22, 382]. The complete mechanisms for *B. anthracis* dissemination to the blood and viability during infection remain unclear, but it is evident that this bacterium encounters numerous dynamic conditions within the host. As a highly evolved pathogen, the factors that provide the basis for *B. anthracis* pathogenesis such as the key virulence regulators, anthrax toxins, anti-phagocytic capsule, primary antigens, and others have been thoroughly investigated [8, 10, 19, 21-23, 84, 327, 328, 383, 384]. However, a major gap exists in the knowledge regarding the mechanisms of *B. anthracis* survival used by this pathogen to defend against the toxic and antimicrobial conditions found in mammalian hosts such as livestock and humans. To expand our understanding of how *B. anthracis* detects environmental changes, we hypothesized that this pathogen specifically evolved a comprehensive collection of systems for survival within the stresses encountered during anthrax. Our results suggest that *B. anthracis* can survive hostile environments through the signaling activity of two-component systems (TCSs), which couple environmental sensing and transcriptional activation to

initiate a coordinated response to stress. This work identifies activating conditions associated with infection and antibacterial compounds, in addition to protein regulators that modulate the activity of three key TCSs. Results presented here not only expand the field's understanding of the *B. anthracis* response to toxic conditions, but also provide potential therapeutic targets that can be inhibited to hinder pathogen stress adaptation.

EdsRS responds to targocil-induced barrier damage.

Compromising the integrity of the bacterial cell barrier is a common action of antimicrobials including beta lactam antibiotics, CAMPs, biocides, etc. Targocil is an antimicrobial initially discovered for its toxicity against *Staphylococcus aureus* that is mediated through inhibiting bacterial envelope elaboration [94, 97, 98]. We hypothesized that *B. anthracis*, a potential weapon of bioterror, senses and responds to targocil to alleviate targocil-dependent cell damage. In Chapter II, we show that targocil treatment increased the permeability of the cellular envelope, which was particularly toxic to *B. anthracis* spores during growth early after germination. In vegetative cells, a newly identified TCS, EdsRS, mediated the *B. anthracis* response to targocil. EdsRS activation resulted in an increase in the production of cardiolipin via a cardiolipin synthase, ClsT, which restored the loss of barrier function, thereby reducing the effectiveness of targocil. These experiments uncovered a mechanism *B. anthracis* employs to resist the toxic effects of membrane-targeting antimicrobials. Further, these findings revealed possible therapeutic targets that are important for the bacterial defense against membrane damage [98].

ClpX and DnaJ regulate HitRS protein levels.

Survival of *B. anthracis* within the vertebrate host is dependent on sensing of stress within the host. TCS signaling facilitates this survival, which enables a response to alterations in the environment through changes in expression of target genes [107, 108, 311, 385]. HitRS and HssRS are cross-regulating TCSs in *B. anthracis* that respond to cell envelope disruptions and toxic heme levels, respectively [248]. In this dissertation, an unbiased and targeted genetic selection was designed to identify gene products that are involved in HitRS and HssRS signaling. This selection led to the identification of inactivating mutations within *dnaJ* and *clpX* that disrupt HitRS- and HssRS-dependent gene expression. DnaJ and ClpX are the substrate binding subunits of the DnaJK protein chaperone and ClpXP protease [132, 143, 255, 302, 303]. DnaJ functions in HitRS activation by balancing the levels of HitR and HitS to facilitate signal transduction. ClpX, however, was specifically required for the maintenance of HitS levels. Together these results revealed that the well-described protein homeostasis modulators, DnaJ and ClpX, play a role in *B. anthracis* TCS protein maintenance. This finding adds to the growing list of TCS accessory proteins that have a role in the modulation of TCS signaling function. In fact, the requirement of DnaJ and ClpX for *B. anthracis* TCS activity represents a potentially conserved strategy to maintain bacterial signaling integrity in fluctuating environments, such as those encountered during infection.

HitRS is activated in macrophages.

Early in anthrax *B. anthracis* spores are phagocytosed by host cells where they germinate into vegetative bacilli while defending against antimicrobial attacks mounted by the host immune response. [42, 45, 52, 324, 368, 371]. In Chapter III, the activation of HitRS was investigated in

conditions relevant to *B. anthracis* infection using microscopy-based approaches in combination with fluorescent bacterial reporters. HitRS TCS signaling was observed during a model of inhalation anthrax infection using the attenuated Sterne strain. Further investigation revealed that HitRS was activated in the intracellular environment of macrophages. Signaling occurred as the bacilli germinated from spores into vegetative bacilli and was required for bacterial viability in the presence of macrophages. At this time, the host factor(s) responsible for HitRS activation are unknown. Therefore, a strategy has been devised to discover these factors. Identification of the host effector functions that drive HitRS signaling will occur through the use of an arrayed CRISPR/Cas9 library screen based in high throughput liquid handling and imaging. The results presented confirm a biological role for HitRS TCS signaling in the *B. anthracis* defense against innate immunity.

Conclusions

Bacillus anthracis is a threat to human health and national security [8, 10, 13, 22, 367]. While much work has been done to uncover the contribution of spores, toxins, and the capsule to the pathogenesis of *B. anthracis*, this dissertation aims to define the specific bacterial stress detection signaling that is triggered during infection of mammalian hosts. This pathogen encodes 45 TCSs to mediate signal transduction in response to chemical and physical changes in the environment. Previous studies have specifically investigated the role of only eight TCSs in *B. anthracis* [72, 91, 98, 122-124, 127, 128]. While many of the other TCSs share homology to systems functionally characterized in other species, a large proportion of the *B. anthracis* stress response remains opaque [218]. Work presented here addresses the function of three TCSs, including one newly described system, that all are key contributors to *B. anthracis* survival under

the stress conditions associated with infection (Fig. 5-1). During infection, *B. anthracis* is actively targeted by host antimicrobial effectors and therapeutics that may compromise the integrity of the TCS signaling pathway. In Chapter II, EdsRS is identified as a TCS that responds to barrier damage caused by the antibiotic targocil through an increase in cardiolipin synthesis to restore envelope integrity [98]. HitRS is known to alleviate envelope damage whereas, the extraordinary resistance of *B. anthracis* to heme toxicity can be attributed to the activity of HssRS signaling that occurs *in vivo* [70, 72, 91]. Cross-regulation between these systems suggests a synchronized response to heme toxicity and cell envelope stress in *B. anthracis.* Results of genetic screening performed in Chapter III revealed that HitRS and HssRS systems require the activity of the protein chaperone, DnaJ, and protease component, ClpX. Appropriate activation of HitRS and HssRS requires these regulators for protein abundance. In Chapter IV, HitRS signaling was observed in *B. anthracis* following phagocytosis by macrophages providing a biologically relevant context for this TCS. We propose a model whereby the coordination of the response to antibiotic compounds, phagocytic membrane damage, and heme stress must be tightly regulated at the protein level to maintain HK to RR stoichiometry because TCS signaling is required as *B. anthracis* transitions throughout various host niches and phases of anthrax infection.

Model systems considerations.

Bacillus anthracis is categorized as a biosafety level three (BSL3) pathogen due to the potential to cause serious or lethal disease via inhalational exposure [386, 387]. Due to the safety precautions that are essential when performing biomedical research in BSL3 conditions, bacteriological studies involving the fully virulent strain of *B. anthracis* have reduced feasibility. In the 1930s, an attenuated live vaccine was developed that lacks the major virulence plasmid that encodes for the poly γ-D-glutamic acid capsule [8, 24]. Though this strain, Sterne, expresses the

anthrax toxins and the master regulator encoded on the counterpart virulence plasmid, it is unable to cause disease in non-immunocompromised mammals [8, 388, 389]. As a result, the Sterne strain can be worked with in Biosafety Level 2 (BSL2) conditions and was used for all experiments presented here [386]. This increases the accessibility of studying *B. anthracis*, but considerations need to be made for the lack of capsule. In Chapter II, targocil was found to damage the barrier integrity of *B. anthracis* Sterne. While it is possible that targocil has more direct access to its target in Sterne than in a capsulated strain, it is known that the target is still present in the attenuated cells as EdsRS signaling is activated. HitRS is similarly activated by envelope disruptions and is investigated in Chapters III and IV. Previously described functions of ClpX in *B. anthracis* physiology are conserved between Sterne and the fully virulent strain, suggesting that the studies performed in Chapter III for the role of DnaJ and ClpX in TCS signaling are not impacted [154]. In contrast, the HitRS work presented in Chapter IV more directly involves the capsule. The transcriptional activator of capsule production is activated early after intracellular spore germination and the magnitude of the pro-inflammatory response in macrophages is altered after infection with Sterne compared to a capsulated *B. anthracis* strain [190, 381, 390]. Therefore, the activation of HitRS within the precision cut lung slices (PCLSs) or macrophages might be altered in a fully virulent strain due to alterations in the macrophage response to the bacillus or due to the capsule inclusion in the cell envelope that alters HitRS stimuli sensing. Ultimately, the activation of HitRS TCS signaling in macrophages should be repeated in a fully virulent strain to determine the full implication of the findings to the progression of anthrax infection.

Additional model systems were presented in Chapter IV including the PCLSs and phagocytic cell lines (RAW 264.7 cells). These eukaryotic model systems were used due to increased assay feasibility, reduced loss of life, reduced cost, and strong literature support for their

reliability. The PCLS model of the lung epithelium was developed in 1994 and has since been used extensively as a 3D model of the lung architecture due to a maintenance of lung structure, cellular diversity and maintained viability [391]. Since their development, PCLSs have been validated for use in studying infectious diseases, toxicology, and respiratory illnesses [391-394]. Advantages of using PCLSs include the preserved macroarchitecture, ease of visualization and manipulation, reproducibility in multiple slices from the same organism, and potential to use human tissues [391]. Limitations do exist for the PCLS model including a lack of accurate oxygen tension, presence of damage response induced during slice generation, lack of blood flow and lack of cell recruitment [393]. Here, PCLSs were used to investigate the activation of a *B. anthracis* signaling system by a host factor present in the lung epithelium. PCLSs are sufficient to address this question and provided a tool for the visualization of HitRS reporter activation. Further studies to describe the details of HitRS activation during *B. anthracis* interaction with the lung epithelium would require a more complete model or special considerations for key components missing from the experiments. The complexity of the cell populations present in the PCLSs is advantageous, but focusing investigation on a single cell type is ideal when defining detailed host-pathogen interactions. Studies presented here used murine bone marrow derived primary macrophages and RAW 264.7 phagocytes to describe host-derived HitRS activation. Primary cells are the preferred method for studying physiological events within single cell populations and were utilized for the primary investigation of TCS activation [395]. In contrast, due to the complex technical nature of performing an arrayed CRISPR/Cas9 library screen, the RAW 264.7 cell line provides numerable advantages over the primary cells. Not only are the surface markers on the RAW 264.7 cells similar to bone marrow derived macrophages indicating that phagocytic function is largely maintained [396], but also cell lines are less nutritionally restriction, cost effective, and provide an unlimited

supply [397]. The limitations of the RAW 264.7 cells have the potential to be genetically unstable in the long term and have acquired phenotypic differences from their primary counterparts [395, 398]. Future work will involve the validation of observations made using RAW 264.7 cells within primary macrophages to confirm the results. Broadly, extrapolation of the observations surrounding HitRS activation made using the PCLSs and cell lines into more complex models or across species would increase the impact of the results shown here.

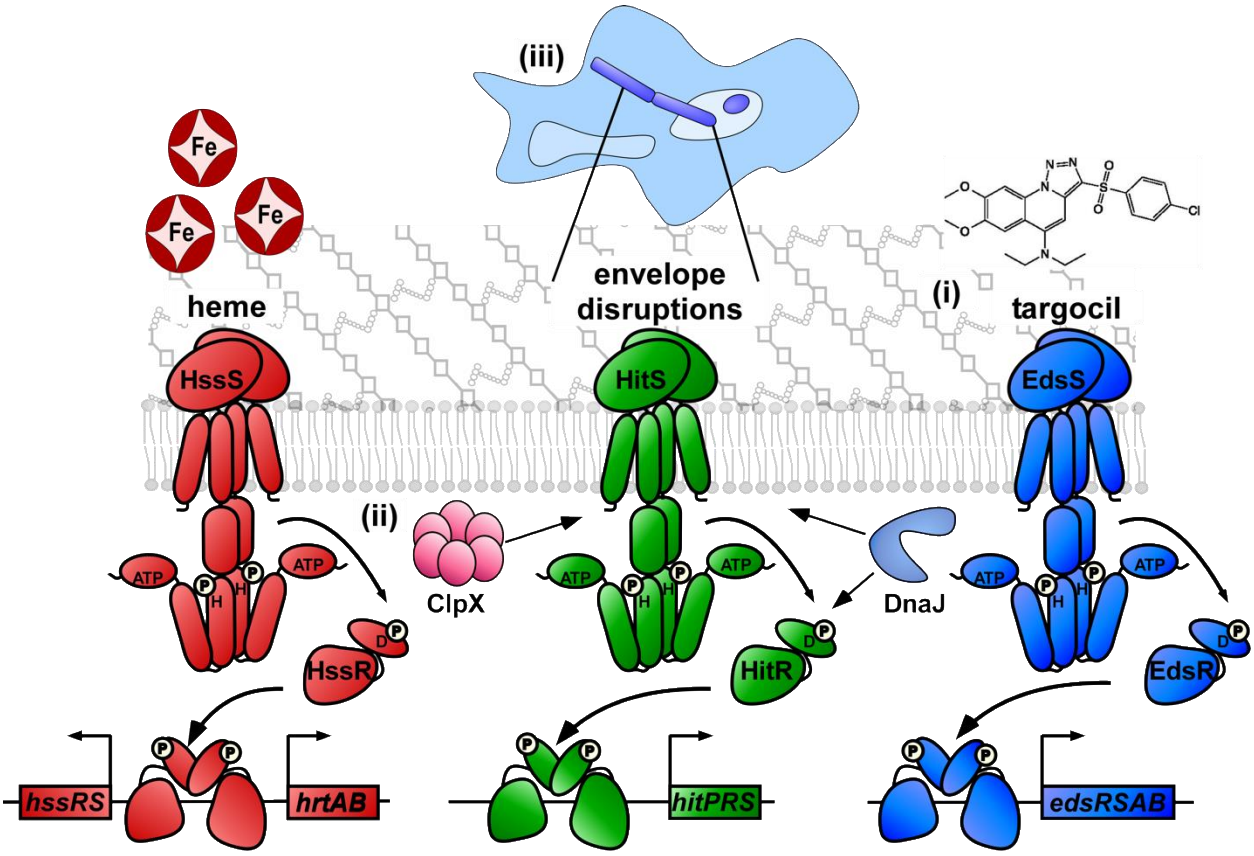

Figure 5-1. Conclusion model. *B. anthracis* TCSs, HssRS HitRS, and EdsRS respond to high levels of heme, envelope disruptions and targocil, respectively. EdsRS is activated by targocil to induce production of cardiolipin to restore barrier integrity (i). DnaJ and ClpX are required for HitRS and HssRS activation through the maintenance of TCS protein abundance (ii). HitRS is activated with host macrophages (iii).

Future Directions

Contribution of cardiolipin synthesis during targocil treatment.

Work presented in Chapter II revealed that targocil treatment of *B. anthracis* not only activated the EdsRS TCS, but also damaged the cell barrier and increased membrane permeability [98]. We hypothesized that the damage induced by targocil to the envelope provides the activation signal for EdsS. Screening of a TCS-RelE strain directed at identification of EdsRS accessory proteins as described in Chapter III has been unsuccessful. Suppressor mutants from this screen repeatedly occur in the HK within the sensor domain, even in the presence of two genetic copies of the TCS. This observation suggests that this histidine kinase (HK) is responding directly to changes in the barrier architecture as has been described in the literature for other *Bacillus* sp. TCSs [115, 116, 118, 120, 121, 178, 399, 400]. Therefore, characterization of the targocil-induced changes that occur to the surface of *B. anthracis* may provide specific insights into the mechanism(s) of EdsRS signal activation. The *B. anthracis* envelope consists of the poly γ-D-glutamic acid capsule, proteinaceous S layer, short chain wall polysaccharides, peptidoglycan cell wall and phospholipid bilayer [78, 80]. Any one of these components could be the target of targocil. For these studies, the attenuated Sterne strain that lacks capsule has been used, thus eliminating the need for studies investigating this component [24]. S layer integrity can be observed using transmission electron microscopy whereby the S layer proteins are clearly visible as high density objects surrounding the cell [81]. Relative changes in abundance of the cell wall and membrane components can be quantified using liquid chromatography with tandem mass spectrometry (LC-MS/MS) [98, 213]. A collective characterization of the *B. anthracis* cell barrier in the presence and absence of subtoxic concentrations of targocil will provide insight about the effects this compound has on the bacilli and the mechanism of EdsRS activation.

Treatment of wildtype *B. anthracis* with targocil increases the relative amount of the membrane phospholipid cardiolipin (CL). This change is hypothesized to be dependent on EdsRS upregulation of a CL synthases, ClsT. As discussed in Chapter II, ClsT is one of five predicated CL synthases encoded by *B. anthracis.* The impact of this work could be expanded by confirming that ClsT is a functional CL synthase and that the residual CL observed in the *clsT* mutant is present due to functional redundancy. This line of investigation could be addressed by performing the following experiments in a strain that expresses *clsT* but is genetically inactivated for the additional predicated CL synthases; *BAS1907, BAS5195, BAS0592,* and *BAS1112.* Using this quadruple mutant CL levels can be quantified with and without targocil treatment via LC-MS/MS. We would also hypothesize that this strain would display increased sensitivity to targocil treatment and therefore growth assessments such as kinetic growth curves and spore germination assays could be performed. A strain lacking four out of five CL synthases will be more sensitive to targocil treatment, highlighting the role of this phospholipid in defense against this compound. Results of these experiments would solidify the role of ClsT in *B. anthracis* CL synthesis for defense against targocil.

In addition to the induction of *clsT* expression, targocil treatment activated EdsRS-dependent expression of *edsAB* and *BAS1661-1663.* EdsAB and BAS1661-1663 are both predicted ABC transporters. Thus far our work has focused on the effects of targocil on the bacilli and the implicated TCS, but a functional understanding of these transport systems may provide key insight into their function and the function of TCSs more broadly. Potential hypotheses for the role of an ABC transporter based on the current model for EdsRS signaling would include (i) import or export of targocil, (ii) import of CL precursors, (ii) export of newly synthesized CL, (iv) export of damaged envelope components, or (v) another unknown function. Mutants of *edsAB* and

BAS1661-1663 have been generated that could be used to test these hypotheses. Experiments could include quantification of targocil, CL, and other membrane molecules in the cytoplasmic, membrane and supernatant fractions of treated cells. Tracking of these molecules in wildtype and the mutants could identify a role for them in the response to targocil. However, full validation of EdsAB or BAS1661-1663 as transporters would require thorough structure-function studies.

Thus far, EdsRS has only been shown to be responsive to the synthetic compound, targocil, that damages the bacilli envelope. Though targocil has no biological function during anthrax infection, *B. anthracis* does face an onslaught of barrier damaging effectors from the innate immune system. Therefore, we hypothesize that EdsRS is activated during the early stages of mammalian infection at peak interaction with the innate immune response. TCS signaling can be detected in mice using an *in vivo* imaging system (IVIS) (Fig. 5-2A) [72]. Signal can be detected on the scale of the whole organism over time or to investigate signal coming from individual organs after dissection at endpoints. A P_{eds} luciferase reporter that is responsive to EdsRS signaling has been created and used to generate spores (Fig. 5-2B). These spores can be injected into mice and used to define the location and timing of EdsRS activation during a model of anthrax infection. Further investigation of targocil-dependent activation of EdsRS and the resultant expression of *BAS1661-1663clsT* using these proposed studies will build a model of the contribution of TCS to the stress response of *B. anthracis* and other pathogens. This model includes an understanding of the mechanism of action for an antimicrobial, the signaling in response to envelope damage, the synthesis of a phospholipid to repair barrier function, and the coordination of this reaction. From these studies, combined with the results presented in Chapter II, we highlight the potential biology that remains to be discovered regarding the description of a TCS network from initial stimulation to final output.

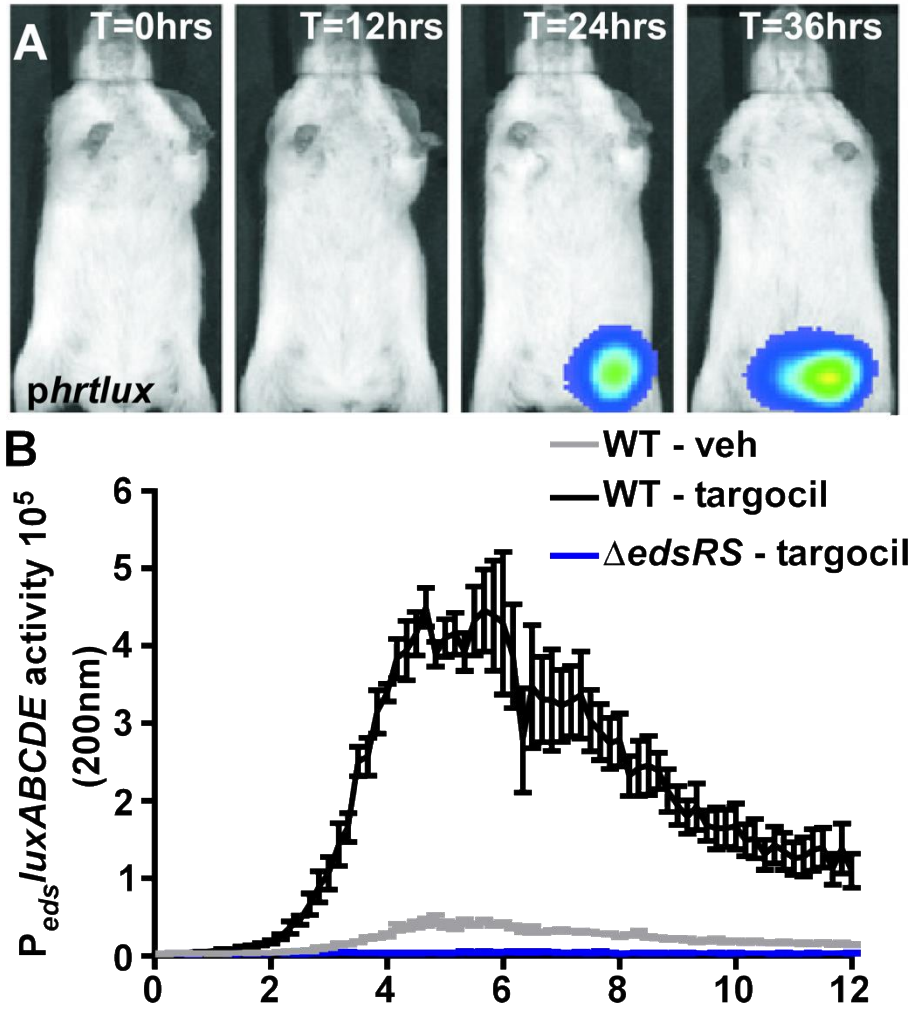

Figure 5-2. *In vivo* imaging system can be used to detect EdsRS activation during infection. **A.** *B. anthracis* spores harboring a P*hrtAB*l*uxABCDE* reporter driven by the *Staphylococcus aureus* promoter or an empty vector were used to infect A/J mice sub-dermally in the inguinal region. Luminescence was imaged every 12 hours using IVIS [72]. **B.** WT and Δ*edsRS* harboring Peds*luxABCDE* reporter plasmid were growth with and without 5 μg/mL targocil and luminescence was monitored over a period of 12 hours.

The regulation of TCS activity by DnaJ and ClpX.

Chapter III studies identified DnaJ and ClpX as regulators of HitRS protein levels that are required for HitRS and HssRS signaling. However, the directness of the interaction between the HK and response regulator (RR) and DnaJ or ClpX has not been fully elucidated. DnaJ and ClpX are both the substrate-binding subunits of their respective complexes [132, 143, 255, 302, 303]. The next set of experiments for this project should set out to test the hypothesis that the TCS proteins are binding partners of DnaJ and ClpX. The protein-protein interactions between HitR/HitS and DnaJ/ClpX could be investigated using co-immunoprecipitation experiments or biomolecular fluorescence complementation [401, 402]. Both of these approaches take advantage of tagged protein constructs that can be used to detect an interaction with another target protein. Due to the adaptability of this approach, it could easily be expanded to investigate other TCS both in *B. anthracis* and other species as discussed later.

Genetic mutation of HitR or HitS that results in constitutive activation overrides the requirement for DnaJ or ClpX in HitRS activation. Activation of HitS signal transduction following stimuli detection therefore depends on DnaJ and ClpX. The requirement for these proteins is due to the fact that both proteins contribute to the maintenance of HitS abundance. In data presented in Chapter III, this effect is not changed by ‘205 treatment. However, as mentioned above, genetic activation of HitS overcomes the need for DnaJ and ClpX. This result suggests that the activation state of the HK, not the effect of activator on the cell, contributes to the regulation. To test this hypothesis, tagged versions of the constitutively active mutants could be generated to track protein levels when they are so highly expressed. Performing this experiment with and without ‘205 activator would delineate if DnaJ and ClpX are required for HitR and HitS protein regulation in a manner dependent on protein activation or if it is a result of ‘205 effects on the cell.

DnaJ and ClpX are both a part of complexes required for the maintenance of protein homeostasis [132]. These proteins are required for the appropriate abundance of HitR and HitS within the cell. An outstanding set of experiments that may provide significant insight into the mechanism of this regulation involves investigating DnaK and ClpP for their role in TCS modulation. To begin this line of investigation, genetic deletions of *dnaK* and *clpP* could be generated. These strains could then be used in XylE reporter experiments to test HitRS and HssRS activation of the P_{hit} and P_{hrt} promoters as was done in Chapter III. These studies would reveal if these systems not only require DnaJ and ClpX, but also their partner proteins, for TCS activity. Follow up experiments would involve the replication of the same localization and protein abundance experiments to determine the extent to which DnaK and ClpP are required.

Protein homeostasis has been studied throughout biology using a wide range of approaches. The ability of protein chaperones, such as DnaJK, to protect substrates from degradation can be tested directly. Results from Chapter III indicate that both HitR and HitS are targets of DnaJ regulation. Therefore, purified HitR and HitS can be placed into stress conditions in the presence and absence of purified DnaJK complex. Following exposure to stress, the level of HitR or HitS protein degradation over time can be monitored [403, 404]. Though, ClpX was only found to affect levels of HitS, similar experiments can be performed whereby proteolysis of HitS by ClpXP can be tested in the presence of ATP [405, 406]. Results from these experiments would indicate if HitR and HitRS are regulated by the chaperone or protease activity of DnaJK and ClpXP, respectively.

Each step in signaling of a TCS, such as HitRS, can be studied using well-established biochemical approaches [103, 104, 249]. Purified forms of these proteins can be used to investigate HK autophosphorylation, HK to RR phosphate transfer, RR-DNA binding and HK phosphatase activity. Our group has extensive experience with these methods and could quickly adapt them to

investigate the contribution of DnaJ and ClpX on protein function. Specifically, based on the regulation of HitR by DnaJ presented in Chapter III, we hypothesize that DnaJ facilitates dephosphorylation of HitR. To test this, purified DnaJ would be mixed with phosphorylated HitR. HitR could be monitored for stability in this state or HitS could be added to track dephosphorylation of the RR in the presence of DnaJ. Results would provide a mechanism for DnaJ regulation of HitR levels based on known TCS biology. The role of DnaJK and ClpXP in the maintenance of protein homeostasis have been mechanistically described using structure function studies [250, 293, 302, 303]. The regulation of TCSs by these complexes could be defined to the same degree using the experiments presented and add to the field's appreciation for the preservation of the cellular proteome.

Conservation of DnaJ and ClpX regulation of TCSs.

B. anthracis harbors 45 TCSs to mediate transcriptional regulation in response to chemical or physical changes in the environment. Data presented in Chapter III describe the requirement of DnaJ and ClpX for both HitRS and HssRS TCS signaling. While these TCSs do cross-regulate and share higher protein identity with each other than other HK/RR pairs, the general roles of DnaJ and ClpX in protein homeostasis suggest they may affect other TCSs. We hypothesize that DnaJ and ClpX are also required for the activation of the remaining *B. anthracis* TCS through maintenance of protein abundance. The EdsRS TCS was characterized in Chapter I and was used to preliminarily test this hypothesis. Using the XylE reporter assay, P_{eds} promoter activation was significantly reduced in point mutants of *dnaJ* and *clpX* (Fig. 5-3). The investigation of DnaJ and ClpX for TCS activity using this approach requires the knowledge of both the promoter and activating condition. Based on previously published studies the activator is known for nine TCSs

for which XylE reporter assays could be generated [122-124, 127, 407-411]. However, this leaves some systems unaddressed. DnaJ and ClpX support HitRS signaling through the maintenance of accurate HK and RR levels. This result was described in Chapter III using biochemical quantification of protein abundance. Generation of IPTG inducible, tagged versions of the remaining HK and RR in *B. anthracis* would reveal if DnaJ and ClpX are broadly required for TCS protein abundance, independent of activating conditions. Results from these studies would expand the findings of Chapter III from the regulation of just two systems to TCS signaling broadly in *B. anthracis.*

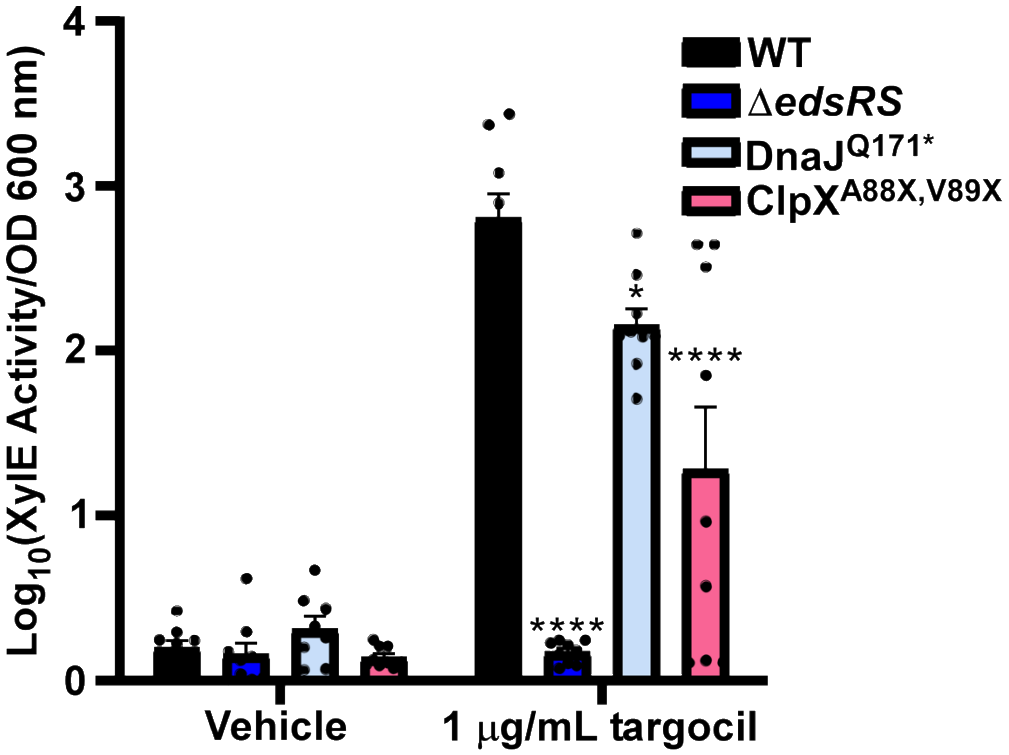

Figure 5-3. Activation of EdsRS requires wildtype DnaJ and ClpX. XylE reporter assay tested ‘205 activation of *edsRSAB* expression in WT, Δ*edsRS*, DnaJ^{Q171*}, and ClpX^{A88X,V89X}. Statistical significance was determined using a two-way ANOVA with a Tukey’s test adjustment for multiple comparisons (*, $p < 0.05$ ***, $p < 0.001$****).

A future direction not addressed in Chapter III is whether or not mutation of DnaJ and ClpX disrupted protein homeostasis in a manner that impacted central processes, significantly compromising cellular physiology. The mutant strains showed no defect in growth in rich media and the proteomes showed no overt differences, compared to wildtype (Fig. 5-4). This phenotype could be investigated further in *B. anthracis* using growth-based assays, but what is especially relevant to this work would be studies to determine the requirement of DnaJ and ClpX for signaling pathway integrity. Signaling, including non-TCS-mediated, is often used during stress. Though the literature suggests that DnaJ and ClpX are central to cellular function, we hypothesize that this is specific to stress conditions and could contribute to non-TCS signaling pathways [132]. The integrity of non-TCS pathways in response to stimuli could be studied using transcriptomic or proteomic analysis of other signaling networks. For example, in *B. anthracis* iron-starvation triggers the Fur-dependent induction of the iron-regulated surface determinant system for the acquisition of iron [66, 412, 413]. Increases in Fur-regulated genes in response to iron chelation in the absence of DnaJ or ClpX would test this hypothesis. Alternatively, the quorum sensing signaling pathway could be tested using the addition of autoinducer-2 in Δ*dnaJ* and *clpX::tet* [414-416]. These studies would build on the observations that DnaJ and ClpX are required for TCS signaling and instead add signaling to the list of cellular functions for which the regulation of proteins by chaperones and proteases is directly necessary.

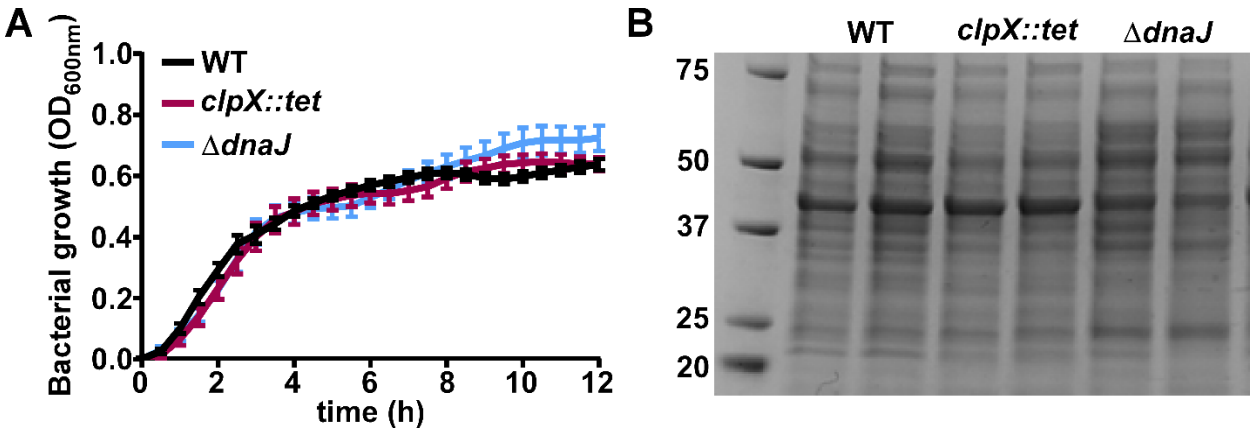

Figure 5-4. DnaJ and ClpX are not required for growth or maintenance of the proteome in a nutrient rich environment. A. Growth of WT, *clpX::tet*, and Δ*dnaJ* in rich media. **B.** Whole cell lysates of WT, *clpX::tet*, and Δ*dnaJ* were prepared, samples were analyzed by SDS-PAGE gel, and stained using Simply Blue general protein stain.

Beyond the TCSs in *B. anthracis*, DnaJ and ClpX could be a conserved system for the stabilization of TCS proteins in other pathogenic bacteria. DnaJ and Clp proteases have been previously linked to TCS function in species such as *S. aureus* and *Escherichia coli*, though the mechanisms have not been consistently elucidated [160, 164]. Using the transcriptional and biochemical approaches presented in Chapter III or described above would provide a direct method for the determination of the conservation of this relationship. TCSs make up the largest family of multi-component signaling systems in bacteria. These studies would reveal if the contribution of DnaJ and ClpX to TCS protein abundance is a conserved strategy to maintain the integrity of signaling pathways during stress conditions such as those encountered during infection.

If DnaJ and ClpX are not found to be required for general TCSs, other chaperone and protease complexes could be investigated. The work presented in this dissertation does not acknowledge the possibility that other systems for protein regulation may also play a role in TCS signaling. DnaJK and ClpXP are representatives of a family of proteins used for the maintenance of protein homeostasis. GroEL/GroES chaperones and Lon proteases are conserved systems used to regulate protein levels in bacteria [132, 138, 139, 145, 292, 417]. The contribution of these proteins could be investigated to determine the degree to which the TCS signaling is integrated with post-translational regulation. The findings presented in Chapter III illustrating that proteases function in TCS signaling may indicate a previously unappreciated aspect of the regulation of TCS function. Efficient and effective use of TCSs is vital for their role in bacterial physiology. While the contribution of GroEL/GroES and Lon could be investigated using genetic mutants that are employed in TCS reporter assays, it may be prudent to also take an approach that directly investigates the therapeutic potential interlaced in this project. Inhibitors have been described for DnaK, GroEL/GroES, Clp, and Lon [304, 306, 418, 419]. Use of these compounds to test the

inhibition of TCS signaling in key bacterial pathogens, such as *B. anthracis,* could describe the effects these proteins on TCS signaling and provide a useful reagent. TCSs are appealing targets for therapeutic development in their own right and a combination of TCS-specific drugs with those that target a protein homeostasis complex could provide an effective strategy to treat infection through the inhibition of pathogen stress sensing [311].

Accessory proteins for the DnaJ and ClpX modulation of TCS signaling.

If results from the studies proposed above prove that neither DnaJ nor ClpX are direct binding partners for HitR or HitS, experiments can be performed to identify adaptor proteins that function in between DnaJ or ClpX and the TCS. Studies have described accessory proteins for specific TCS regulation and adaptor proteins for protein homeostasis complexes [155, 420, 421]. Additionally, a consensus peptide sequence has been defined for ClpX substrate binding [422]. Though this sequence has been shown to not be required for degradation by ClpXP in all cases, it is of note that neither HitR nor HitS contain this sequence. This finding suggests that the interaction of the TCS proteins with the regulators may be indirect. Identification of possible accessory proteins could be carried out through the use of a modified version of the TCS-RelE selections as described in Chapter III. We have devised a genetic selection that uncovers mutations that lead to activation of TCS signaling rather than interruption (Fig. 5-5) [249]. TCS-driven *relE* is replaced with *ermC,* which provides resistance to erythromycin [423]. *B. anthracis* is sensitive to erythromycin and therefore growth of this strain in the presence of the antibiotic will result in growth arrest. However, if a mutation arises that leads to activation of the TCS, *ermC* will be expressed and a suppressor mutant will grow during selection. An additional copy of the TCS is inserted at a pseudogene locus to prevent mutation of the HK or RR. A positive control for this

experiment includes the treatment of the TCS-ErmC strain with inducer. This condition triggers promoter activation of erythromycin resistance and growth is detected. Previous work has demonstrated that in the absence of *dnaJ* or *clpX* HitRS, HssRS, and EdsRS do not exhibit TCS signaling. To identify gene products that are acting between these TCS of interest and DnaJ/ClpX, these genes could be deleted in the background of the TCS-ErmC strain. In these strains, treatment of TCS-ErmC does not induce growth as deletion of these genes hinders promoter activation. Therefore, growth will only occur in Δ*dnaJ* TCS-ErmC and *clpX::tet* TCS-ErmC if a mutation arises that activates the TCS through specific complementation of the protein homeostasis mutation. Gene products involved in signal transduction to HitRS, HssRS, or EdsRS will be interrogated to define the mechanism by which these factors support TCS protein abundance. Follow up experiments will determine the accessory proteins' mechanism starting with confirmation of the effects on signaling followed by direct binding to DnaJ/ClpX and the TCS of interest. Identification of these gene products through sequencing will provide insight into the mechanism of ClpX and DnaJ regulation of TCSs.

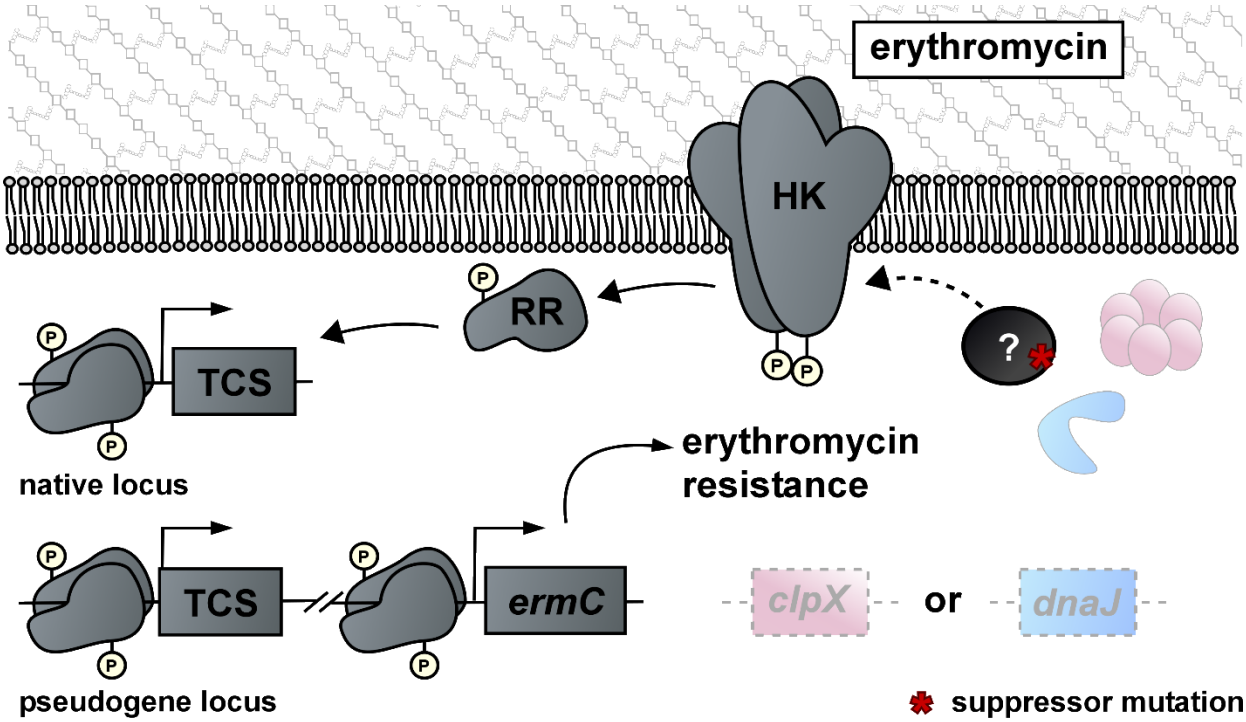

Figure 5-5. Genetic selection to reveal mutations required for activation of TCS activity. This strain is unable to grow in the presence of erythromycin unless a mutation arises that results in activation of the TCS of interest. This treatment triggers activation of *ermC* expression being controlled by the TCS-dependent promoter. The requirement of ClpX and DnaJ for TCS activation in *B. anthracis* suggests that deletion of either *clpX* or *dnaJ* in the TCS-ErmC strain background could identify mutations in gene products specifically linked to the regulation of TCSs by these proteins.

***In vivo* live imaging of HitRS activation in murine model of cutaneous anthrax.**

B. anthracis HitRS signaling occurs upon disturbance to the envelope barrier and is activated during the intracellular survival within macrophages as presented in Chapter IV [248]. During the course of anthrax infection, the pathogen encounters numerous conditions that challenge the envelope integrity due to the immune response and toxin-induced cell death. Published intravital imaging of inhalational anthrax revealed close interactions between macrophages and dendritic cells [369]. Therefore, we hypothesize that HitRS is activated during infection of mammalian hosts and upon encounter with these phagocytic cells. To test this hypothesis an innovative intravital imaging approach is being developed. The Nikon A1R MP+ multiphoton confocal microscope allows for higher depth imaging of living mice with greater speed and sharper resolution [424]. For preliminary imaging experiments, cutaneous wounds were introduced to the ears of mice. The wounds were subsequently inoculated with wildtype strains of *B. anthracis* that constitutively express GFP and express mCherry upon activation of HitRS (gGFP P_{hit}*mcherry*). Signal from both the constitutive and HitRS activation reporters was detected *in vivo* (Fig. 5-6). This observation suggests that not only are the bacteria detected during cutaneous infection using this innovative imaging technique, but also that the TCS is activated. These promising results could be expanded upon using larger scale experiments and the addition of Δ*hitRS* spores to confirm that the reporter signal is dependent on the TCS. Should these experiments prove successful, this would represent the first successful imaging of *B. anthracis* signaling using multiphoton, intravital imaging and would also confirm that HitRS is utilized during models of anthrax infection.

The advent of this imaging technology represents a monumental advancement for imaging biology. Bacterial signaling *in vivo* is largely limited to population level investigation. The use of

multi-photon confocal microscopy of living and infected animals could be expanded to answer pressing questions using other bacterial reporters and within other pathogens. This tool is going to be instrumental in future studies of the host-pathogen interface.

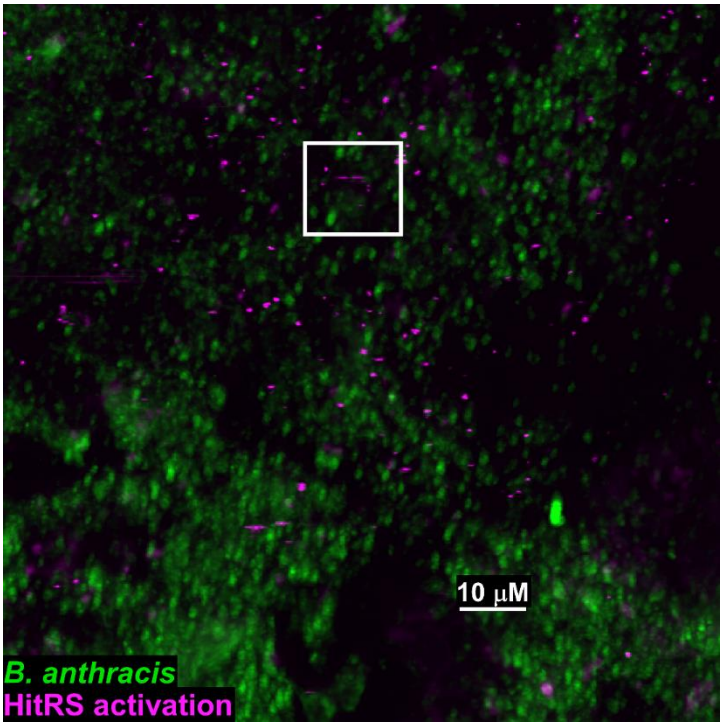

Figure 5-6. *In vivo* imaging of HitRS activation. Multiphoton imaging of cutaneous murine infection of the ear using *B. anthracis* that express GFP constitutively and a HitRS-inducible mCherry.

In Chapter 4, HitRS signaling is investigated following spore inoculation of macrophages. This cell type plays a central role in *B. anthracis* infection progression, but is not the only cell type that could induce bacterial cell envelope damage that would trigger HitRS signaling. Ears from mice infected for the above experiments could be collected for multiplexed immunohistological analysis. Using an extensive immune cell-staining panel could reveal other cell types associated with *B. anthracis* with an active P_{hit} promoter [425-427]. Alternatively, the reporter-infected tissue samples could be homogenized and prepared for population analysis via flow cytometry to determine which cell types are associated with the bacterial-derived signals. Results from this analysis could be used to design targeted studies to confirm the role of additional cell types in the activation of HitRS signaling.

Cross-regulating signaling response to heme and cell envelope stress during the pathogenesis of anthrax.

B. anthracis HssRS and HitRS exhibit an integrated cross-regulatory response to heme toxicity and cell envelope stress [248]. Although these signal transduction systems have been identified, the coordination of the proteins in these systems during infection is not well understood. In this dissertation, these systems have been studied as separate pathways, but not fully investigated as part of a signaling network. We hypothesize that there is an integrated signaling response to these stressors involving post-translational modulation that *B. anthracis* requires for infection. An integrated signaling network can improve the efficiency and effectiveness of *B. anthracis* adaptation during infection. Previous work in our laboratory biochemically defined the interactions between HssRS and HitRS signaling components [248]. This work was done using purified proteins, a full panel of mutant strains, and a transcriptional reporter. Genetic inactivation of one or more of the proteins in the two-component systems

revealed cross-regulation that occurs at the HK to RR level, as well as between the response regulators and target promoters [248]. HssRS is activated during murine infection [72]. Data presented in Chapter IV revealed that HitRS is also activated in murine tissue using microscopy. To expand the observations of activation in host-derived conditions, effective HssRS and HitRS fluorescent reporters have been generated that can be used to investigate cross-regulation *in vivo*. These reporters can be translated to *in vivo* imaging approach used in Chapter IV in mutants that are indicative of cross-regulation (Δ*hssS*Δ*hitR*, Δ*hitS*Δ*hssR*). This approach will be translated to *in vivo* analysis using two-photon imaging to confirm the activation and localization of HssRS and HitRS cross-signaling during the course of infection. Using this approach, which is adaptable to tissue localization due to expanded imaging depth capability, allows for the tracking of the location of the bacteria within the mouse. Use of a constitutive fluorophore expressed in bacterial cells will reveal the progression of disease in different genotypes. The use of the promoter reports will indicate the location and temporal occurrence of HitRS and HssRS signaling. The requirement for the coordination of HssRS and HitRS signaling upon exposure to the host environment during infection has not been studied. Additionally, the magnitude of heme and cell envelope stress *B. anthracis* experiences during infection is unknown. We hypothesize that the innate immune response will provide a source of membrane stress early in infection and that after dissemination to the bloodstream the bacilli experience heme stress. We would expect HitRS signaling to occur immediately following spore germination near the site of infection, but HssRS signaling will occur following bacterial dissemination to the bloodstream. The use of TCS mutants to investigate cross-regulation would reveal if the system interaction contributes to the patterns of signaling observed. We would define the temporal activation of each system in addition to the cross-regulation. These experiments would confirm the activation of TCS signal integration in the

infectivity of *B. anthracis*, which would help to outline potential points of pathogen vulnerability during anthrax infection.

In vitro experiments have confirmed that HitRS is required for viability in macrophages and HssRS is required for growth in high heme conditions. To test this hypothesis, we could take advantage of these models and design an experiment to test the requirement of cross-regulation in these conditions individually or for a transition between them. For example, a panel of *B. anthracis* TCS mutants that cannot engage in cross-regulation could be exposed to macrophages or to heme and their growth assessed. Separate experiments could be designed whereby these same mutants are exposed to macrophages for a short period of time, then the bacteria collected and directly exposed to high heme, or the reverse. This *in vitro* study would represent the step in *B. anthracis* dissemination where the bacilli transition from the intracellular state to the bloodstream and would reveal if HitRS/HssRS cross-regulation is utilized in this transition. Results of this experiment will determine the function of cross-regulation in stress-sensing of heme and phagocytes during a model of anthrax infection.

Identification of HitRS and EdsRS activators using CRISPR/Cas9 library screen

HitRS is activated within phagocytes. A CRISPR screen to identify the host factor that triggers TCS signaling was presented in Chapter IV. Briefly, an arrayed library of CRISPR/Cas9 phagocyte mutants covering the entire murine genome will be inoculated with spores of *B. anthracis* TCS reporter strains using high-throughput liquid handling. The screen will progress with robotics-mediated data collection via the ImageXpress system.

EdsRS is a TCS identified in Chapter I that is activated by disruption of barrier integrity. We hypothesize that EdsRS is also activated within phagocytes and would be an additional

candidate for screening in the CRISPR/Cas9 library platform. To test this hypothesis, an EdsRS fluorescent reporter could be used in combination with imaging to determine if this TCS is activated during intracellular survival. Follow up experiments would include the determination of timing and infection doses that would be useful in the CRISPR/Cas9 screen. Upon confirmation of optimal conditions for phagocyte factors of EdsRS signaling, the whole genome library could be screened using the same technologies proposed for the HitRS screen.

When screening for macrophage activators of TCS, we expect to identify genes that are related to the successful maturation and functionality of the phagolysosome. This result is particularly expected for genes associated with damage to the barrier of the bacteria due to the activation of HitRS and EdsRS by envelope disruptions. Results could include genes involved in the reactive burst, lipidases, glycanases, peptidases, or antimicrobial peptides. We expect to not only identify the effector enzymes themselves, but also regulators of phagolysosome maturation or activity. Repeated identification of CRISPR mutants in a specific antimicrobial pathway will focus follow up investigations and act as increased validation of the results. Additionally, using changes in the constitutively active signal coming from the *B. anthracis*, we may identify macrophage gene products involved in phagocytosis, phagosome-lysosome fusion, and bacterial killing that could be investigated independently of the TCS-focused studies. Selected hits will be validated by testing clean knockout cell lines for their ability to activate the TCS and to kill a *B. anthracis* strain lacking the *hit* or *eds* operon relative to the WT strain. This experiment will identify the host effectors that activate the HitRS and EdsRS-mediated cell envelope damage response during phagocyte infection and define host-induced stressors that *B. anthracis* must contend with intracellularly. Results will define a subset of the stressors that *B. anthracis* counteracts through two-component system signaling.

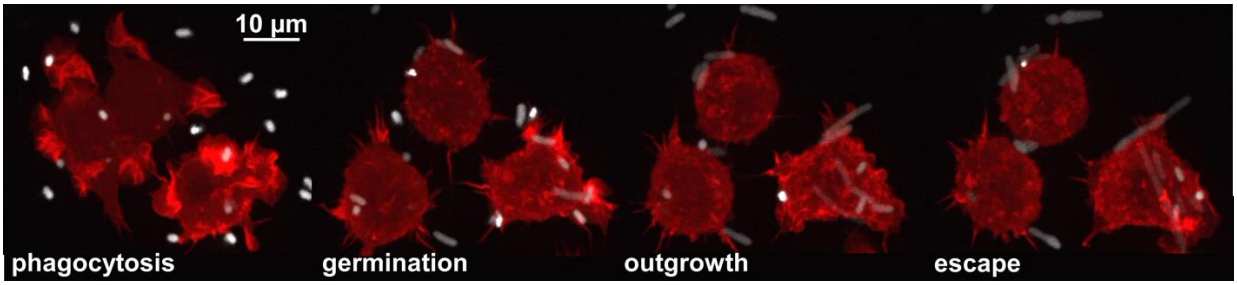

Figure 5-7. Super-resolution, live imaging of *B. anthracis* spore interactions with phagocytes. GFP expressing *B. anthracis* infected RAW macrophages expressing HALOLifeAct labeled Actin imaged over the course of 6 hours using a Nikon Spinning Disk microscope

We propose the use of a newly developed live cell super-resolution imaging method to determine the kinetics of TCS activation by the host stimuli identified using this screening approach. The short frame temporal occurrence of this activation and the relationship to phagocyte maturation are unknown. Preliminary optimization of this technique has been performed using a Nikon spinning disk microscope (Fig. 5-7). Cultured phagocytes that represent the hits from the CRISPR screen can be inoculated with TCS reporter spores and subsequently imaged rapidly using the Nikon spinning disk microscope. Imaging at this resolution and speed will relate the kinetics of TCS activation to phagocyte function in the CRISPR mutants. These experiments could be expanded to test the importance of phagocyte maturation using inhibitors of key antibacterial functions. Compounds such as cytochalasin and latrunculin to inhibit actin-mediated phagocytosis, concanamycin to inhibit phagosome acidification, and brefeldin to inhibit intracellular transport [428-431]. These studies will provide a thorough follow up to the CRISPR screens and specifically investigate possible connections between TCS signaling and the targeted host stressors.

The experiments proposed will expand on the studies presented in this dissertation and will identify regulatory mechanisms of bacterial two-component system signaling and the contribution of resulting cross-regulation to the pathogenesis of *B. anthracis.*

BIBLIOGRAPHY

1. Carlson, C.J., et al., *The global distribution of Bacillus anthracis and associated anthrax risk to humans, livestock and wildlife.* Nat Microbiol, 2019. **4**(8): p. 1337-1343.
2. Nakanwagi, M., et al., *Outbreak of gastrointestinal anthrax following eating beef of suspicious origin: Isingiro District, Uganda, 2017.* PLoS Negl Trop Dis, 2020. **14**(2): p. e0008026.
3. Kisaakye, E., et al., *Outbreak of Anthrax Associated with Handling and Eating Meat from a Cow, Uganda, 2018.* Emerg Infect Dis, 2020. **26**(12): p. 2799-2806.
4. Mwenye, K.S., S. Siziya, and D. Peterson, *Factors associated with human anthrax outbreak in the Chikupo and Ngandu villages of Murewa district in Mashonaland East Province, Zimbabwe.* Cent Afr J Med, 1996. **42**(11): p. 312-5.
5. Chakraborty, A., et al., *Anthrax outbreaks in Bangladesh, 2009-2010.* Am J Trop Med Hyg, 2012. **86**(4): p. 703-10.
6. Sekamatte, M., et al., *Multisectoral prioritization of zoonotic diseases in Uganda, 2017: A One Health perspective.* PLoS One, 2018. **13**(5): p. e0196799.
7. Munyua, P., et al., *Prioritization of Zoonotic Diseases in Kenya, 2015.* PLoS One, 2016. **11**(8): p. e0161576.
8. Dixon, T.C., et al., *Anthrax.* N Engl J Med, 1999. **341**(11): p. 815-26.
9. Moran, G.J., *Bioterrorism alleging use of anthrax and interim guidelines for management - United States, 1998 - Commentary.* Annals of Emergency Medicine, 1999. **34**(2): p. 231-232.
10. Mock, M. and A. Fouet, *Anthrax.* Annu Rev Microbiol, 2001. **55**: p. 647-71.
11. Jernigan, J.A., et al., *Bioterrorism-related inhalational anthrax: The first 10 cases reported in the United States.* Emerging Infectious Diseases, 2001. **7**(6): p. 933-944.
12. Rasko, D.A., et al., *Bacillus anthracis comparative genome analysis in support of the Amerithrax investigation.* Proc Natl Acad Sci U S A, 2011. **108**(12): p. 5027-32.
13. Inglesby, T.V., et al., *Anthrax as a biological weapon, 2002: updated recommendations for management.* JAMA, 2002. **287**(17): p. 2236-52.
14. Burke, L.K., C.P. Brown, and T.M. Johnson, *Historical Data Analysis of Hospital Discharges Related to the Amerithrax Attack in Florida.* Perspect Health Inf Manag, 2016. **13**(Fall): p. 1c.
15. Weir, E., *Anthrax: of bison and bioterrorism.* Canadian Medical Association Journal, 2000. **163**(5): p. 608-608.
16. Shafazand, S., et al., *Inhalational anthrax: epidemiology, diagnosis, and management.* Chest, 1999. **116**(5): p. 1369-76.
17. Gold, H., *Anthrax; a report of one hundred seventeen cases.* AMA Arch Intern Med, 1955. **96**(3): p. 387-96.
18. Kamal, S.M., et al., *Anthrax: an update.* Asian Pac J Trop Biomed, 2011. **1**(6): p. 496-501.

19. Klimpel, K.R., N. Arora, and S.H. Leppla, *Anthrax toxin lethal factor contains a zinc metalloprotease consensus sequence which is required for lethal toxin activity.* Mol Microbiol, 1994. **13**(6): p. 1093-100.

20. Wu, A.G., et al., *Anthrax toxin induces hemolysis: An indirect effect through polymorphonuclear cells.* Journal of Infectious Diseases, 2003. **188**(8): p. 1138-1141.

21. Leppla, S.H., *Anthrax toxin edema factor: a bacterial adenylate cyclase that increases cyclic AMP concentrations of eukaryotic cells.* Proc Natl Acad Sci U S A, 1982. **79**(10): p. 3162-6.

22. Moayeri, M., et al., *Anthrax Pathogenesis.* Annu Rev Microbiol, 2015. **69**: p. 185-208.

23. Drysdale, M., et al., *Capsule synthesis by Bacillus anthracis is required for dissemination in murine inhalation anthrax.* EMBO J, 2005. **24**(1): p. 221-7.

24. Sterne, M., *Avirulent anthrax vaccine.* Onderstepoort J Vet Sci Anim Ind, 1946. **21**: p. 41-3.

25. Ivins, B.E., et al., *Immunization studies with attenuated strains of Bacillus anthracis.* Infect Immun, 1986. **52**(2): p. 454-8.

26. Cote, C.K., et al., *The use of a model of in vivo macrophage depletion to study the role of macrophages during infection with Bacillus anthracis spores.* Microb Pathog, 2004. **37**(4): p. 169-75.

27. Cote, C.K., N. Van Rooijen, and S.L. Welkos, *Roles of macrophages and neutrophils in the early host response to Bacillus anthracis spores in a mouse model of infection.* Infect Immun, 2006. **74**(1): p. 469-80.

28. Barua, S., et al., *Toxin inhibition of antimicrobial factors induced by Bacillus anthracis peptidoglycan in human blood.* Infect Immun, 2013. **81**(10): p. 3693-702.

29. Popescu, N.I., et al., *Monocyte procoagulant responses to anthrax peptidoglycan are reinforced by proinflammatory cytokine signaling.* Blood Adv, 2019. **3**(16): p. 2436-2447.

30. Yang, J., et al., *Bacillus anthracis lethal toxin attenuates lipoteichoic acid-induced maturation and activation of dendritic cells through a unique mechanism.* Mol Immunol, 2009. **46**(16): p. 3261-8.

31. Chakrabarty, K., et al., *Bacillus anthracis spores stimulate cytokine and chemokine innate immune responses in human alveolar macrophages through multiple mitogen-activated protein kinase pathways.* Infect Immun, 2006. **74**(8): p. 4430-8.

32. Chakrabarty, K., et al., *Human lung innate immune response to Bacillus anthracis spore infection.* Infect Immun, 2007. **75**(8): p. 3729-38.

33. Sternbach, G., *The history of anthrax.* J Emerg Med, 2003. **24**(4): p. 463-7.

34. Weiss, G. and U.E. Schaible, *Macrophage defense mechanisms against intracellular bacteria.* Immunol Rev, 2015. **264**(1): p. 182-203.

35. Marshansky, V. and M. Futai, *The V-type H+-ATPase in vesicular trafficking: targeting, regulation and function.* Curr Opin Cell Biol, 2008. **20**(4): p. 415-26.

36. Kinchen, J.M. and K.S. Ravichandran, *Phagosome maturation: going through the acid test.* Nat Rev Mol Cell Biol, 2008. **9**(10): p. 781-95.

37. Babior, B.M., *NADPH oxidase.* Curr Opin Immunol, 2004. **16**(1): p. 42-7.

38. Minakami, R. and H. Sumimotoa, *Phagocytosis-coupled activation of the superoxide-producing phagocyte oxidase, a member of the NADPH oxidase (nox) family.* Int J Hematol, 2006. **84**(3): p. 193-8.

39. Nauseef, W.M., *Myeloperoxidase in human neutrophil host defence.* Cell Microbiol, 2014. **16**(8): p. 1146-55.

40. Ruthel, G., et al., *Time-lapse confocal imaging of development of Bacillus anthracis in macrophages.* Journal of Infectious Diseases, 2004. **189**(7): p. 1313-1316.

41. Kang, T.J., et al., *Murine macrophages kill the vegetative form of Bacillus anthracis.* Infect Immun, 2005. **73**(11): p. 7495-501.

42. Dixon, T.C., et al., *Early Bacillus anthracis-macrophage interactions: intracellular survival survival and escape.* Cell Microbiol, 2000. **2**(6): p. 453-63.

43. Guidi-Rontani, C., et al., *Fate of germinated Bacillus anthracis spores in primary murine macrophages (vol 42, pg 931, 2000).* Molecular Microbiology, 2002. **44**(1): p. 297-297.

44. Guidi-Rontani, C., et al., *Germination of Bacillus anthracis spores within alveolar macrophages.* Mol Microbiol, 1999. **31**(1): p. 9-17.

45. Welkos, S., et al., *In-vitro characterisation of the phagocytosis and fate of anthrax spores in macrophages and the effects of anti-PA antibody.* J Med Microbiol, 2002. **51**(10): p. 821-831.

46. Guidi-Rontani, C., *The alveolar macrophage: the Trojan horse of Bacillus anthracis.* Trends Microbiol, 2002. **10**(9): p. 405-9.

47. Tournier, J.N., et al., *Anthrax edema toxin cooperates with lethal toxin to impair cytokine secretion during infection of dendritic cells.* J Immunol, 2005. **174**(8): p. 4934-41.

48. Maldonado-Arocho, F.J. and K.A. Bradley, *Anthrax edema toxin induces maturation of dendritic cells and enhances chemotaxis towards macrophage inflammatory protein 3beta.* Infect Immun, 2009. **77**(5): p. 2036-42.

49. Hansen, K.C., et al., *Lymph formation, composition and circulation: a proteomics perspective.* Int Immunol, 2015. **27**(5): p. 219-27.

50. Lowe, D.E., et al., *Bacillus anthracis has two independent bottlenecks that are dependent on the portal of entry in an intranasal model of inhalational infection.* Infect Immun, 2013. **81**(12): p. 4408-20.

51. Tournier, J.N., et al., *Contribution of toxins to the pathogenesis of inhalational anthrax.* Cell Microbiol, 2007. **9**(3): p. 555-65.

52. Brittingham, K.C., et al., *Dendritic cells endocytose Bacillus anthracis spores: implications for anthrax pathogenesis.* J Immunol, 2005. **174**(9): p. 5545-52.

53. Plaut, R.D., et al., *Dissemination bottleneck in a murine model of inhalational anthrax.* Infect Immun, 2012. **80**(9): p. 3189-93.

54. Lincoln, R.E., et al., *Role of the lymphatics in the pathogenesis of anthrax.* J Infect Dis, 1965. **115**(5): p. 481-94.

55. Kim, C., et al., *Antiinflammatory cAMP signaling and cell migration genes co-opted by the anthrax bacillus.* Proc Natl Acad Sci U S A, 2008. **105**(16): p. 6150-5.

56. Thompson, I.J., et al., *Specific activation of dendritic cells enhances clearance of Bacillus anthracis following infection.* PLoS One, 2014. **9**(11): p. e109720.

57. Glomski, I.J., et al., *Primary involvement of pharynx and peyer's patch in inhalational and intestinal anthrax.* PLoS Pathog, 2007. **3**(6): p. e76.

58. Dumetz, F., et al., *Noninvasive imaging technologies reveal edema toxin as a key virulence factor in anthrax.* Am J Pathol, 2011. **178**(6): p. 2523-35.

59. Loving, C.L., et al., *Role of anthrax toxins in dissemination, disease progression, and induction of protective adaptive immunity in the mouse aerosol challenge model.* Infect Immun, 2009. **77**(1): p. 255-65.

60. Popov, S.G., et al., *Effective antiprotease-antibiotic treatment of experimental anthrax.* BMC Infect Dis, 2005. **5**: p. 25.

61. Braun, V., *Iron uptake mechanisms and their regulation in pathogenic bacteria.* Int J Med Microbiol, 2001. **291**(2): p. 67-79.

62. Wandersman, C. and I. Stojiljkovic, *Bacterial heme sources: the role of heme, hemoprotein receptors and hemophores.* Current Opinion in Microbiology, 2000. **3**(2): p. 215-220.

63. Gutteridge, J.M.C. and B. Halliwell, *Mini-Review: Oxidative stress, redox stress or redox success?* Biochem Biophys Res Commun, 2018. **502**(2): p. 183-186.

64. Choby, J.E. and E.P. Skaar, *Heme Synthesis and Acquisition in Bacterial Pathogens.* J Mol Biol, 2016. **428**(17): p. 3408-28.

65. Crichton, R.R., *Iron Metabolism: From Molecular Mechanisms to Clinical Consequences, 4th Edition*

4ed. **2016**, United Kingdom: John Wiley & Sons, Ltd.

66. Skaar, E.P., A.H. Gaspar, and O. Schneewind, *Bacillus anthracis IsdG, a heme-degrading monooxygenase.* Journal of Bacteriology, 2006. **188**(3): p. 1071-1080.

67. Maresso, A.W., T.J. Chapa, and O. Schneewind, *Surface protein IsdC and sortase B are required for heme-iron scavenging of Bacillus anthracis.* Journal of Bacteriology, 2006. **188**(23): p. 8145-8152.

68. Maresso, A.W., G. Garufi, and O. Schneewind, *Bacillus anthracis secretes proteins that mediate heme acquisition from hemoglobin.* Plos Pathogens, 2008. **4**(8).

69. Skaar, E.P., et al., *Iron-source preference of Staphylococcus aureus infections.* Science, 2004. **305**(5690): p. 1626-1628.

70. Torres, V.J., et al., *A Staphylococcus aureus regulatory system that responds to host heme and modulates virulence.* Cell Host & Microbe, 2007. **1**(2): p. 109-119.

71. Mike, L.A., et al., *Activation of heme biosynthesis by a small molecule that is toxic to fermenting Staphylococcus aureus.* Proc Natl Acad Sci U S A, 2013. **110**(20): p. 8206-11.

72. Stauff, D.L. and E.P. Skaar, *Bacillus anthracis HssRS signalling to HrtAB regulates haem resistance during infection.* Molecular Microbiology, 2009. **72**(3): p. 763-778.

73. Lechardeur, D., et al., *Discovery of intracellular heme-binding protein HrtR, which controls heme efflux by the conserved HrtB-HrtA transporter in Lactococcus lactis.* J Biol Chem, 2012. **287**(7): p. 4752-8.

74. Rieske, J.S., *Composition, structure, and function of complex III of the respiratory chain.* Biochim Biophys Acta, 1976. **456**(2): p. 195-247.

75. Skaar, E.P., A.H. Gaspar, and O. Schneewind, *Bacillus anthracis IsdG, a heme-degrading monooxygenase.* J Bacteriol, 2006. **188**(3): p. 1071-80.

76. Clark, J., et al., *Heme catabolism in the causative agent of anthrax.* Mol Microbiol, 2019. **112**(2): p. 515-531.

77. Cybulski, R.J., Jr., et al., *Four superoxide dismutases contribute to Bacillus anthracis virulence and provide spores with redundant protection from oxidative stress.* Infect Immun, 2009. **77**(1): p. 274-85.

78. Navarre, W.W. and O. Schneewind, *Surface proteins of gram-positive bacteria and mechanisms of their targeting to the cell wall envelope.* Microbiol Mol Biol Rev, 1999. **63**(1): p. 174-229.

79. Giesbrecht, P., J. Wecke, and B. Reinicke, *On the morphogenesis of the cell wall of staphylococci.* Int Rev Cytol, 1976. **44**: p. 225-318.

80. Leoff, C., et al., *Secondary cell wall polysaccharides of Bacillus anthracis are antigens that contain specific epitopes which cross-react with three pathogenic Bacillus cereus strains that caused severe disease, and other epitopes common to all the Bacillus cereus strains tested.* Glycobiology, 2009. **19**(6): p. 665-73.

81. Missiakas, D. and O. Schneewind, *Assembly and Function of the Bacillus anthracis S-Layer.* Annu Rev Microbiol, 2017. **71**: p. 79-98.

82. Bruckner, V., J. Kovacs, and G. Denes, *Structure of poly-D-glutamic acid isolated from capsulated strains of B. anthracis.* Nature, 1953. **172**(4376): p. 508.

83. Fouet, A., *The surface of Bacillus anthracis.* Mol Aspects Med, 2009. **30**(6): p. 374-85.

84. Kern, J.W. and O. Schneewind, *BslA, a pXO1-encoded adhesin of Bacillus anthracis.* Mol Microbiol, 2008. **68**(2): p. 504-15.

85. Ebrahimi, C.M., et al., *Penetration of the blood-brain barrier by Bacillus anthracis requires the pXO1-encoded BslA protein.* J Bacteriol, 2009. **191**(23): p. 7165-73.

86. Skerker, J.M., et al., *Rewiring the specificity of two-component signal transduction systems.* Cell, 2008. **133**(6): p. 1043-1054.

87. Laub, M.T. and M. Goulian, *Specificity in two-component signal transduction pathways.* Annual Review of Genetics, 2007. **41**: p. 121-145.

88. Capra, E.J. and M.T. Laub, *Evolution of two-component signal transduction systems.* Annu Rev Microbiol, 2012. **66**: p. 325-47.

89. Torres, V.J., et al., *A Staphylococcus aureus regulatory system that responds to host heme and modulates virulence.* Cell Host Microbe, 2007. **1**(2): p. 109-19.

90. Stauff, D.L. and E.P. Skaar, *The Heme Sensor System of Staphylococcus aureus.* Bacterial Sensing and Signaling, 2009. **16**: p. 120-135.

91. Mike, L.A., et al., *Two-Component System Cross-Regulation Integrates Bacillus anthracis Response to Heme and Cell Envelope Stress.* Plos Pathogens, 2014. **10**(3).

92. Ordal, G.W., *Recognition sites for chemotactic repellents of Bacillus subtilis.* J Bacteriol, 1976. **126**(1): p. 72-9.

93. Watanakunakorn, C., *Mode of action and in-vitro activity of vancomycin.* J Antimicrob Chemother, 1984. **14 Suppl D**: p. 7-18.

94. Campbell, J., et al., *An antibiotic that inhibits a late step in wall teichoic acid biosynthesis induces the cell wall stress stimulon in Staphylococcus aureus.* Antimicrob Agents Chemother, 2012. **56**(4): p. 1810-20.

95. Lee, K., et al., *Development of improved inhibitors of wall teichoic acid biosynthesis with potent activity against Staphylococcus aureus.* Bioorg Med Chem Lett, 2010. **20**(5): p. 1767-70.

96. Suzuki, T., et al., *In vitro antimicrobial activity of wall teichoic acid biosynthesis inhibitors against Staphylococcus aureus isolates.* Antimicrob Agents Chemother, 2011. **55**(2): p. 767-74.

97. Tiwari, K.B., et al., *Exposure of Staphylococcus aureus to Targocil Blocks Translocation of the Major Autolysin Atl across the Membrane, Resulting in a Significant Decrease in Autolysis.* Antimicrob Agents Chemother, 2018. **62**(7).

98. Laut, C.L., et al., *Bacillus anthracis Responds to Targocil-Induced Envelope Damage through EdsRS Activation of Cardiolipin Synthesis.* mBio, 2020. **11**(2).

99. Klubes, P., P.J. Fay, and I. Cerna, *Effect of chlorpromazine on cell wall biosynthesis and incorporation of orotic acid into nucleic acids in Bacillus megaterium.* Biochem Pharmacol, 1971. **20**(2): p. 265-77.

100. Howell, A., et al., *Interactions between the YycFG and PhoPR two-component systems in Bacillus subtilis: the PhoR kinase phosphorylates the non-cognate YycF response regulator upon phosphate limitation (vol 59, pg 1199, 2006).* Molecular Microbiology, 2006. **60**(2): p. 535-535.

101. Rietkotter, E., D. Hoyer, and T. Mascher, *Bacitracin sensing in Bacillus subtilis.* Molecular Microbiology, 2008. **68**(3): p. 768-785.

102. Matsubara, M., et al., *Tuning of the porin expression under anaerobic growth conditions by His-to-Asp cross-phosphorelay through both the EnvZ-osmosensor and ArcB-anaerosensor in Escherichia coli.* Genes to Cells, 2000. **5**(7): p. 555-569.

103. Guckes, K.R., et al., *Strong cross-system interactions drive the activation of the QseB response regulator in the absence of its cognate sensor.* Proc Natl Acad Sci U S A, 2013. **110**(41): p. 16592-7.

104. Guckes, K.R., et al., *Signaling by two-component system noncognate partners promotes intrinsic tolerance to polymyxin B in uropathogenic Escherichia coli.* Science Signaling, 2017. **10**(461).

105. Sivaneson, M., et al., *Two-component regulatory systems in Pseudomonas aeruginosa: an intricate network mediating fimbrial and efflux pump gene expression.* Mol Microbiol, 2011. **79**(5): p. 1353-66.

106. Bone, M.A., et al., *Bordetella PlrSR regulatory system controls BvgAS activity and virulence in the lower respiratory tract.* Proc Natl Acad Sci U S A, 2017. **114**(8): p. E1519-E1527.

107. Bhagirath, A.Y., et al., *Two Component Regulatory Systems and Antibiotic Resistance in Gram-Negative Pathogens.* Int J Mol Sci, 2019. **20**(7).

108. Tierney, A.R. and P.N. Rather, *Roles of two-component regulatory systems in antibiotic resistance.* Future Microbiol, 2019. **14**: p. 533-552.

109. Li, L., et al., *Sensor histidine kinase is a beta-lactam receptor and induces resistance to beta-lactam antibiotics.* Proc Natl Acad Sci U S A, 2016. **113**(6): p. 1648-53.

110. Hu, W.S., et al., *The expression levels of outer membrane proteins STM1530 and OmpD, which are influenced by the CpxAR and BaeSR two-component systems, play important roles in the ceftriaxone resistance of Salmonella enterica serovar Typhimurium.* Antimicrob Agents Chemother, 2011. **55**(8): p. 3829-37.

111. Kurabayashi, K., et al., *Role of the CpxAR two-component signal transduction system in control of fosfomycin resistance and carbon substrate uptake.* J Bacteriol, 2014. **196**(2): p. 248-56.

112. Mileykovskaya, E. and W. Dowhan, *The Cpx two-component signal transduction pathway is activated in Escherichia coli mutant strains lacking phosphatidylethanolamine.* J Bacteriol, 1997. **179**(4): p. 1029-34.

113. Srinivasan, V.B., et al., *Role of the two component signal transduction system CpxAR in conferring cefepime and chloramphenicol resistance in Klebsiella pneumoniae NTUH-K2044.* PLoS One, 2012. **7**(4): p. e33777.

114. Weatherspoon-Griffin, N., et al., *The CpxR/CpxA two-component regulatory system up-regulates the multidrug resistance cascade to facilitate Escherichia coli resistance to a model antimicrobial peptide.* J Biol Chem, 2014. **289**(47): p. 32571-82.

115. Aguilar, P.S., et al., *Molecular basis of thermosensing: a two-component signal transduction thermometer in Bacillus subtilis.* EMBO J, 2001. **20**(7): p. 1681-91.

116. Beranova, J., et al., *Differences in cold adaptation of Bacillus subtilis under anaerobic and aerobic conditions.* J Bacteriol, 2010. **192**(16): p. 4164-71.

117. Bredeston, L.M., et al., *Thermal regulation of membrane lipid fluidity by a two-component system in Bacillus subtilis.* Biochem Mol Biol Educ, 2011. **39**(5): p. 362-6.

118. Cybulski, L.E., et al., *Bacillus subtilis DesR functions as a phosphorylation-activated switch to control membrane lipid fluidity.* J Biol Chem, 2004. **279**(38): p. 39340-7.

119. Inda, M.E., et al., *A lipid-mediated conformational switch modulates the thermosensing activity of DesK.* Proc Natl Acad Sci U S A, 2014. **111**(9): p. 3579-84.

120. Martin, M. and D. de Mendoza, *Regulation of Bacillus subtilis DesK thermosensor by lipids.* Biochem J, 2013. **451**(2): p. 269-75.

121. Najle, S.R., et al., *Oligomerization of Bacillus subtilis DesR is required for fine tuning regulation of membrane fluidity.* Biochim Biophys Acta, 2009. **1790**(10): p. 1238-43.

122. Gupta, V., et al., *Characterization of a two component system, Bas1213-1214, important for oxidative stress in Bacillus anthracis.* J Cell Biochem, 2018. **119**(7): p. 5761-5774.

123. Aggarwal, S., et al., *Functional characterization of PhoPR two component system and its implication in regulating phosphate homeostasis in Bacillus anthracis.* Biochim Biophys Acta Gen Subj, 2017. **1861**(1 Pt A): p. 2956-2970.

124. Dhiman, A., et al., *Functional characterization of WalRK: A two-component signal transduction system from Bacillus anthracis.* FEBS Open Bio, 2014. **4**: p. 65-76.

125. Dhiman, A., et al., *Role of the recognition helix of response regulator WalR from Bacillus anthracis in DNA binding and specificity.* Int J Biol Macromol, 2017. **96**: p. 257-264.

126. Dhiman, A., M. Gopalani, and R. Bhatnagar, *WalRK two component system of Bacillus anthracis responds to temperature and antibiotic stress.* Biochem Biophys Res Commun, 2015. **459**(4): p. 623-8.

127. Vetter, S.M. and P.M. Schlievert, *The two-component system Bacillus respiratory response A and B (BrrA-BrrB) is a virulence factor regulator in Bacillus anthracis.* Biochemistry, 2007. **46**(25): p. 7343-52.

128. Gupta, V., et al., *Functional analysis of BAS2108-2109 two component system: Evidence for protease regulation in Bacillus anthracis.* Int J Biochem Cell Biol, 2017. **89**: p. 71-84.

129. Wagner, C., et al., *Genetic analysis and functional characterization of the Streptococcus pneumoniae vic operon.* Infect Immun, 2002. **70**(11): p. 6121-8.

130. Delaune, A., et al., *The WalKR system controls major staphylococcal virulence genes and is involved in triggering the host inflammatory response.* Infect Immun, 2012. **80**(10): p. 3438-53.

131. Senadheera, M.D., et al., *A VicRK signal transduction system in Streptococcus mutans affects gtfBCD, gbpB, and ftf expression, biofilm formation, and genetic competence development.* J Bacteriol, 2005. **187**(12): p. 4064-76.

132. Wong, P. and W.A. Houry, *Chaperone networks in bacteria: analysis of protein homeostasis in minimal cells.* J Struct Biol, 2004. **146**(1-2): p. 79-89.

133. Mogk, A., D. Huber, and B. Bukau, *Integrating protein homeostasis strategies in prokaryotes.* Cold Spring Harb Perspect Biol, 2011. **3**(4).

134. Hartl, F.U., *Molecular chaperones in cellular protein folding.* Nature, 1996. **381**(6583): p. 571-9.

135. Kramer, G., et al., *The ribosome as a platform for co-translational processing, folding and targeting of newly synthesized proteins.* Nat Struct Mol Biol, 2009. **16**(6): p. 589-97.

136. Hesterkamp, T., et al., *Escherichia coli trigger factor is a prolyl isomerase that associates with nascent polypeptide chains.* Proc Natl Acad Sci U S A, 1996. **93**(9): p. 4437-41.

137. Chapman, E., et al., *Global aggregation of newly translated proteins in an Escherichia coli strain deficient of the chaperonin GroEL.* Proc Natl Acad Sci U S A, 2006. **103**(43): p. 15800-5.

138. Fayet, O., T. Ziegelhoffer, and C. Georgopoulos, *The groES and groEL heat shock gene products of Escherichia coli are essential for bacterial growth at all temperatures.* J Bacteriol, 1989. **171**(3): p. 1379-85.

139. Horwich, A.L., A.C. Apetri, and W.A. Fenton, *The GroEL/GroES cis cavity as a passive anti-aggregation device.* FEBS Lett, 2009. **583**(16): p. 2654-62.

140. Keskin, O., et al., *Molecular mechanisms of chaperonin GroEL-GroES function.* Biochemistry, 2002. **41**(2): p. 491-501.

141. Rungeling, E., T. Laufen, and H. Bahl, *Functional characterisation of the chaperones DnaK, DnaJ, and GrpE from Clostridium acetobutylicum.* FEMS Microbiol Lett, 1999. **170**(1): p. 119-23.

142. Mayer, M.P. and B. Bukau, *Hsp70 chaperone systems: diversity of cellular functions and mechanism of action.* Biol Chem, 1998. **379**(3): p. 261-8.

143. Szabo, A., et al., *A zinc finger-like domain of the molecular chaperone DnaJ is involved in binding to denatured protein substrates.* EMBO J, 1996. **15**(2): p. 408-17.

144. Gamer, J., et al., *A cycle of binding and release of the DnaK, DnaJ and GrpE chaperones regulates activity of the Escherichia coli heat shock transcription factor sigma32.* EMBO J, 1996. **15**(3): p. 607-17.

145. Riethdorf, S., et al., *Cloning, nucleotide sequence, and expression of the Bacillus subtilis lon gene.* J Bacteriol, 1994. **176**(21): p. 6518-27.

146. Downs, D., et al., *Isolation and characterization of lon mutants in Salmonella typhimurium.* J Bacteriol, 1986. **165**(1): p. 193-7.

147. Bukhari, A.I. and D. Zipser, *Mutants of Escherichia coli with a defect in the degradation of nonsense fragments.* Nat New Biol, 1973. **243**(129): p. 238-41.

148. Wang, N., et al., *A human mitochondrial ATP-dependent protease that is highly homologous to bacterial Lon protease.* Proc Natl Acad Sci U S A, 1993. **90**(23): p. 11247-51.

149. Baker, T.A. and R.T. Sauer, *ClpXP, an ATP-powered unfolding and protein-degradation machine.* Biochim Biophys Acta, 2012. **1823**(1): p. 15-28.

150. Gerth, U., et al., *Clp-dependent proteolysis down-regulates central metabolic pathways in glucose-starved Bacillus subtilis.* J Bacteriol, 2008. **190**(1): p. 321-31.

151. Pan, Q., D.A. Garsin, and R. Losick, *Self-reinforcing activation of a cell-specific transcription factor by proteolysis of an anti-sigma factor in B. subtilis.* Mol Cell, 2001. **8**(4): p. 873-83.

152. Yamamoto, T., et al., *Disruption of the genes for ClpXP protease in Salmonella enterica serovar Typhimurium results in persistent infection in mice, and development of*

persistence requires endogenous gamma interferon and tumor necrosis factor alpha. Infect Immun, 2001. **69**(5): p. 3164-74.

153. Tomoyasu, T., et al., *The ClpXP ATP-dependent protease regulates flagellum synthesis in Salmonella enterica serovar typhimurium.* J Bacteriol, 2002. **184**(3): p. 645-53.

154. McGillivray, S.M., et al., *ClpX contributes to innate defense peptide resistance and virulence phenotypes of Bacillus anthracis.* J Innate Immun, 2009. **1**(5): p. 494-506.

155. Mitrophanov, A.Y. and E.A. Groisman, *Signal integration in bacterial two-component regulatory systems.* Genes Dev, 2008. **22**(19): p. 2601-11.

156. Firon, A., et al., *The Abi-domain protein Abx1 interacts with the CovS histidine kinase to control virulence gene expression in group B Streptococcus.* PLoS Pathog, 2013. **9**(2): p. e1003179.

157. Kato, A. and E.A. Groisman, *Connecting two-component regulatory systems by a protein that protects a response regulator from dephosphorylation by its cognate sensor.* Genes Dev, 2004. **18**(18): p. 2302-13.

158. Kato, A., A.Y. Mitrophanov, and E.A. Groisman, *A connector of two-component regulatory systems promotes signal amplification and persistence of expression.* Proc Natl Acad Sci U S A, 2007. **104**(29): p. 12063-8.

159. Chen, M.H., et al., *Characterization of the RcsC-->YojN-->RcsB phosphorelay signaling pathway involved in capsular synthesis in Escherichia coli.* Biosci Biotechnol Biochem, 2001. **65**(10): p. 2364-7.

160. Kelley, W.L. and C. Georgopoulos, *Positive control of the two-component RcsC/B signal transduction network by DjlA: a member of the DnaJ family of molecular chaperones in Escherichia coli.* Mol Microbiol, 1997. **25**(5): p. 913-31.

161. Dubern, J.F., et al., *The heat shock genes dnaK, dnaJ, and grpE are involved in regulation of putisolvin biosynthesis in Pseudomonas putida PCL1445.* J Bacteriol, 2005. **187**(17): p. 5967-76.

162. Deng, C.-Y., et al., *Proteolysis of histidine kinase VgrS inhibits its autophosphorylation and promotes osmostress resistance in Xanthomonas campestris.* Nature Communications, 2018. **9**(1): p. 4791.

163. Feng, J., et al., *Trapping and proteomic identification of cellular substrates of the ClpP protease in Staphylococcus aureus.* J Proteome Res, 2013. **12**(2): p. 547-58.

164. Frees, D., et al., *Alternative roles of ClpX and ClpP in Staphylococcus aureus stress tolerance and virulence.* Mol Microbiol, 2003. **48**(6): p. 1565-78.

165. Ogura, M. and K. Tsukahara, *Autoregulation of the Bacillus subtilis response regulator gene degU is coupled with the proteolysis of DegU-P by ClpCP.* Mol Microbiol, 2010. **75**(5): p. 1244-59.

166. Hengge-Aronis, R., *Signal transduction and regulatory mechanisms involved in control of the sigma(S) (RpoS) subunit of RNA polymerase.* Microbiol Mol Biol Rev, 2002. **66**(3): p. 373-95, table of contents.

167. Burkholder, W.F., I. Kurtser, and A.D. Grossman, *Replication initiation proteins regulate a developmental checkpoint in Bacillus subtilis.* Cell, 2001. **104**(2): p. 269-79.

168. Rowland, S.L., et al., *Structure and mechanism of action of Sda, an inhibitor of the histidine kinases that regulate initiation of sporulation in Bacillus subtilis.* Mol Cell, 2004. **13**(5): p. 689-701.

169. Francis, V.I. and S.L. Porter, *Multikinase Networks: Two-Component Signaling Networks Integrating Multiple Stimuli.* Annu Rev Microbiol, 2019. **73**: p. 199-223.

170. Mwakapeje, E.R., et al., *Anthrax outbreaks in the humans - livestock and wildlife interface areas of Northern Tanzania: a retrospective record review 2006-2016.* BMC Public Health, 2018. **18**(1): p. 106.

171. Hanczaruk, M., et al., *Injectional anthrax in heroin users, Europe, 2000-2012.* Emerg Infect Dis, 2014. **20**(2): p. 322-3.

172. Alpuche Aranda, C.M., et al., *Salmonella typhimurium activates virulence gene transcription within acidified macrophage phagosomes.* Proc Natl Acad Sci U S A, 1992. **89**(21): p. 10079-83.

173. Fields, P.I., E.A. Groisman, and F. Heffron, *A Salmonella locus that controls resistance to microbicidal proteins from phagocytic cells.* Science, 1989. **243**(4894 Pt 1): p. 1059-62.

174. Garcia Vescovi, E., F.C. Soncini, and E.A. Groisman, *Mg2+ as an extracellular signal: environmental regulation of Salmonella virulence.* Cell, 1996. **84**(1): p. 165-74.

175. Wosten, M.M., et al., *A signal transduction system that responds to extracellular iron.* Cell, 2000. **103**(1): p. 113-25.

176. Lina, G., et al., *Transmembrane topology and histidine protein kinase activity of AgrC, the agr signal receptor in Staphylococcus aureus.* Mol Microbiol, 1998. **28**(3): p. 655-62.

177. Mansilla, M.C., et al., *Regulation of fatty acid desaturation in Bacillus subtilis.* Prostaglandins Leukot Essent Fatty Acids, 2003. **68**(2): p. 187-90.

178. Albanesi, D., M.C. Mansilla, and D. de Mendoza, *The membrane fluidity sensor DesK of Bacillus subtilis controls the signal decay of its cognate response regulator.* J Bacteriol, 2004. **186**(9): p. 2655-63.

179. de Mendoza, D., *Temperature sensing by membranes.* Annu Rev Microbiol, 2014. **68**: p. 101-16.

180. Beveridge, T.J., et al., *Functions of S-layers.* FEMS Microbiol Rev, 1997. **20**(1-2): p. 99-149.

181. Mesnage, S., et al., *The capsule and S-layer: two independent and yet compatible macromolecular structures in Bacillus anthracis.* J Bacteriol, 1998. **180**(1): p. 52-8.

182. Wessels, M.R., et al., *Definition of a bacterial virulence factor: sialylation of the group B streptococcal capsule.* Proc Natl Acad Sci U S A, 1989. **86**(22): p. 8983-7.

183. Molnar, J. and B. Pragai, *Attempts to detect the presence of teichoic acid in Bacillus anthracis.* Acta Microbiol Acad Sci Hung, 1971. **18**(2): p. 105-8.

184. Garufi, G., et al., *Synthesis of lipoteichoic acids in Bacillus anthracis.* J Bacteriol, 2012. **194**(16): p. 4312-21.

185. Kim, H.S., et al., *Characterization of a major Bacillus anthracis spore coat protein and its role in spore inactivation.* J Bacteriol, 2004. **186**(8): p. 2413-7.

186. Horton, R.M., et al., *Gene splicing by overlap extension: tailor-made genes using the polymerase chain reaction.* Biotechniques, 1990. **8**(5): p. 528-35.

187. Juttukonda, L.J., et al., *Acinetobacter baumannii OxyR Regulates the Transcriptional Response to Hydrogen Peroxide.* Infect Immun, 2019. **87**(1).

188. Choby, J.E., et al., *Staphylococcus aureus HemX Modulates Glutamyl-tRNA Reductase Abundance To Regulate Heme Biosynthesis.* MBio, 2018. **9**(1).

189. Schneewind, O., P. Model, and V.A. Fischetti, *Sorting of protein A to the staphylococcal cell wall.* Cell, 1992. **70**(2): p. 267-81.

190. Bergman, N.H., et al., *Transcriptional profiling of Bacillus anthracis during infection of host macrophages.* Infect Immun, 2007. **75**(7): p. 3434-44.

191. Juttukonda, L.J., et al., *Dietary Manganese Promotes Staphylococcal Infection of the Heart.* Cell Host Microbe, 2017. **22**(4): p. 531-542 e8.

192. Bligh, E.G. and W.J. Dyer, *A RAPID METHOD OF TOTAL LIPID EXTRACTION AND PURIFICATION.* Canadian Journal of Biochemistry and Physiology, 1959. **37**(8): p. 911-917.

193. Narváez-Rivas, M. and Q. Zhang, *Comprehensive untargeted lipidomic analysis using core–shell C30 particle column and high field orbitrap mass spectrometer.* Journal of Chromatography A, 2016. **1440**: p. 123-134.

194. Kreiswirth, B.N., et al., *The toxic shock syndrome exotoxin structural gene is not detectably transmitted by a prophage.* Nature, 1983. **305**(5936): p. 709-12.

195. Novick, R.P., *Genetic systems in staphylococci.* Methods Enzymol, 1991. **204**: p. 587-636.

196. Alex, L.A. and M.I. Simon, *Protein histidine kinases and signal transduction in prokaryotes and eukaryotes.* Trends Genet, 1994. **10**(4): p. 133-8.

197. Swanson, R.V., L.A. Alex, and M.I. Simon, *Histidine and aspartate phosphorylation: two-component systems and the limits of homology.* Trends Biochem Sci, 1994. **19**(11): p. 485-90.

198. Ducros, V.M., et al., *Crystal structure of GerE, the ultimate transcriptional regulator of spore formation in Bacillus subtilis.* J Mol Biol, 2001. **306**(4): p. 759-71.

199. Theodoulou, F.L. and I.D. Kerr, *ABC transporter research: going strong 40 years on.* Biochem Soc Trans, 2015. **43**(5): p. 1033-40.

200. Chien, Y., et al., *SarA, a global regulator of virulence determinants in Staphylococcus aureus, binds to a conserved motif essential for sar-dependent gene regulation.* J Biol Chem, 1999. **274**(52): p. 37169-76.

201. Reizer, J., A. Reizer, and M.H. Saier, Jr., *A new subfamily of bacterial ABC-type transport systems catalyzing export of drugs and carbohydrates.* Protein Sci, 1992. **1**(10): p. 1326-32.

202. Koonin, E.V., *A duplicated catalytic motif in a new superfamily of phosphohydrolases and phospholipid synthases that includes poxvirus envelope proteins.* Trends Biochem Sci, 1996. **21**(7): p. 242-3.

203. Tan, B.K., et al., *Discovery of a cardiolipin synthase utilizing phosphatidylethanolamine and phosphatidylglycerol as substrates.* Proc Natl Acad Sci U S A, 2012. **109**(41): p. 16504-9.

204. Madeira, F., et al., *The EMBL-EBI search and sequence analysis tools APIs in 2019.* Nucleic Acids Res, 2019. **47**(W1): p. W636-W641.

205. Terwilliger, A., et al., *Bacillus anthracis Overcomes an Amino Acid Auxotrophy by Cleaving Host Serum Proteins.* J Bacteriol, 2015. **197**(14): p. 2400-11.

206. Buyck, J.M., et al., *Increased susceptibility of Pseudomonas aeruginosa to macrolides and ketolides in eukaryotic cell culture media and biological fluids due to decreased expression of oprM and increased outer-membrane permeability.* Clin Infect Dis, 2012. **55**(4): p. 534-42.

207. Kumaraswamy, M., et al., *Standard susceptibility testing overlooks potent azithromycin activity and cationic peptide synergy against MDR Stenotrophomonas maltophilia.* J Antimicrob Chemother, 2016. **71**(5): p. 1264-9.

208. Lin, L., et al., *Azithromycin Synergizes with Cationic Antimicrobial Peptides to Exert Bactericidal and Therapeutic Activity Against Highly Multidrug-Resistant Gram-Negative Bacterial Pathogens.* EBioMedicine, 2015. **2**(7): p. 690-8.

209. Cleret, A., et al., *Lung dendritic cells rapidly mediate anthrax spore entry through the pulmonary route.* J Immunol, 2007. **178**(12): p. 7994-8001.

210. Haque, M.A. and N.J. Russell, *Strains of Bacillus cereus vary in the phenotypic adaptation of their membrane lipid composition in response to low water activity, reduced temperature and growth in rice starch.* Microbiology, 2004. **150**(Pt 5): p. 1397-404.

211. Epand, R.F., P.B. Savage, and R.M. Epand, *Bacterial lipid composition and the antimicrobial efficacy of cationic steroid compounds (Ceragenins).* Biochim Biophys Acta, 2007. **1768**(10): p. 2500-9.

212. Dalebroux, Z.D., et al., *Delivery of cardiolipins to the Salmonella outer membrane is necessary for survival within host tissues and virulence.* Cell Host Microbe, 2015. **17**(4): p. 441-51.

213. Lonergan, Z.R., et al., *An Acinetobacter baumannii, Zinc-Regulated Peptidase Maintains Cell Wall Integrity during Immune-Mediated Nutrient Sequestration.* Cell Rep, 2019. **26**(8): p. 2009-2018 e6.

214. Kamischke, C., et al., *The Acinetobacter baumannii Mla system and glycerophospholipid transport to the outer membrane.* Elife, 2019. **8**.

215. Molohon, K.J., et al., *Plantazolicin is an ultra-narrow spectrum antibiotic that targets the Bacillus anthracis membrane.* ACS Infect Dis, 2016. **2**(3): p. 207-220.

216. Zhang, T., et al., *Cardiolipin prevents membrane translocation and permeabilization by daptomycin.* J Biol Chem, 2014. **289**(17): p. 11584-91.

217. El Khoury, M., et al., *Targeting Bacterial Cardiolipin Enriched Microdomains: An Antimicrobial Strategy Used by Amphiphilic Aminoglycoside Antibiotics.* Sci Rep, 2017. **7**(1): p. 10697.

218. de Been, M., et al., *Comparative analysis of two-component signal transduction systems of Bacillus cereus, Bacillus thuringiensis and Bacillus anthracis.* Microbiology-Sgm, 2006. **152**: p. 3035-3048.

219. Chandramohan, L., et al., *An overlap between the control of programmed cell death in Bacillus anthracis and sporulation.* J Bacteriol, 2009. **191**(13): p. 4103-10.

220. Tropp, B.E., *Cardiolipin synthase from Escherichia coli.* Biochim Biophys Acta, 1997. **1348**(1-2): p. 192-200.

221. Ohta, A., et al., *Molecular cloning of the cls gene responsible for cardiolipin synthesis in Escherichia coli and phenotypic consequences of its amplification.* J Bacteriol, 1985. **163**(2): p. 506-14.

222. Kawai, F., et al., *Cardiolipin domains in Bacillus subtilis marburg membranes.* J Bacteriol, 2004. **186**(5): p. 1475-83.

223. Eichenberger, P., et al., *The sigmaE regulon and the identification of additional sporulation genes in Bacillus subtilis.* J Mol Biol, 2003. **327**(5): p. 945-72.

224. Lopez, C.S., et al., *Role of anionic phospholipids in the adaptation of Bacillus subtilis to high salinity.* Microbiology, 2006. **152**(Pt 3): p. 605-16.

225. Helmann, J.D., et al., *Global transcriptional response of Bacillus subtilis to heat shock.* J Bacteriol, 2001. **183**(24): p. 7318-28.

226. Tsai, M., et al., *Staphylococcus aureus requires cardiolipin for survival under conditions of high salinity.* BMC Microbiol, 2011. **11**: p. 13.

227. Koprivnjak, T., et al., *Characterization of Staphylococcus aureus cardiolipin synthases 1 and 2 and their contribution to accumulation of cardiolipin in stationary phase and within phagocytes.* J Bacteriol, 2011. **193**(16): p. 4134-42.

228. Laganas, V., J. Alder, and J.A. Silverman, *In vitro bactericidal activities of daptomycin against Staphylococcus aureus and Enterococcus faecalis are not mediated by inhibition of lipoteichoic acid biosynthesis.* Antimicrob Agents Chemother, 2003. **47**(8): p. 2682-4.

229. Alborn, W.E., Jr., N.E. Allen, and D.A. Preston, *Daptomycin disrupts membrane potential in growing Staphylococcus aureus.* Antimicrob Agents Chemother, 1991. **35**(11): p. 2282-7.

230. Silverman, J.A., N.G. Perlmutter, and H.M. Shapiro, *Correlation of daptomycin bactericidal activity and membrane depolarization in Staphylococcus aureus.* Antimicrob Agents Chemother, 2003. **47**(8): p. 2538-44.

231. Kelesidis, T., et al., *Daptomycin nonsusceptible enterococci: an emerging challenge for clinicians.* Clin Infect Dis, 2011. **52**(2): p. 228-34.

232. Davlieva, M., et al., *Biochemical characterization of cardiolipin synthase mutations associated with daptomycin resistance in enterococci.* Antimicrob Agents Chemother, 2013. **57**(1): p. 289-96.

233. Palmer, K.L., et al., *Genetic basis for daptomycin resistance in enterococci.* Antimicrob Agents Chemother, 2011. **55**(7): p. 3345-56.

234. Coe, K.A., et al., *Multi-strain Tn-Seq reveals common daptomycin resistance determinants in Staphylococcus aureus.* PLoS Pathog, 2019. **15**(11): p. e1007862.

235. Swain, J., et al., *Effect of cardiolipin on the antimicrobial activity of a new amphiphilic aminoglycoside derivative on Pseudomonas aeruginosa.* PLoS One, 2018. **13**(8): p. e0201752.

236. Molohon, K.J., et al., *Structure determination and interception of biosynthetic intermediates for the plantazolicin class of highly discriminating antibiotics.* ACS Chem Biol, 2011. **6**(12): p. 1307-13.

237. Hu, H., J. Emerson, and A.I. Aronson, *Factors involved in the germination and inactivation of Bacillus anthracis spores in murine primary macrophages.* FEMS Microbiol Lett, 2007. **272**(2): p. 245-50.

238. Russell, B.H., et al., *Bacillus anthracis internalization by human fibroblasts and epithelial cells.* Cell Microbiol, 2007. **9**(5): p. 1262-74.

239. Sanz, P., et al., *Detection of Bacillus anthracis spore germination in vivo by bioluminescence imaging.* Infect Immun, 2008. **76**(3): p. 1036-47.

240. Barua, S., et al., *The mechanism of Bacillus anthracis intracellular germination requires multiple and highly diverse genetic loci.* Infect Immun, 2009. **77**(1): p. 23-31.

241. Hood, M.I. and E.P. Skaar, *Nutritional immunity: transition metals at the pathogen-host interface.* Nat Rev Microbiol, 2012. **10**(8): p. 525-37.

242. Mellman, I., R. Fuchs, and A. Helenius, *Acidification of the endocytic and exocytic pathways.* Annu Rev Biochem, 1986. **55**: p. 663-700.

243. Program, F.S.A., *Select agents and toxins list.* CDC website, 2014.

244. Guidi-Rontani, C., et al., *Identification and characterization of a germination operon on the virulence plasmid pXO1 of Bacillus anthracis.* Mol Microbiol, 1999. **33**(2): p. 407-14.

245. Hadjifrangiskou, M., et al., *A central metabolic circuit controlled by QseC in pathogenic Escherichia coli.* Mol Microbiol, 2011. **80**(6): p. 1516-29.

246. Mitrophanov, A.Y., et al., *Evolution and dynamics of regulatory architectures controlling polymyxin B resistance in enteric bacteria.* PLoS Genet, 2008. **4**(10): p. e1000233.

247. Howell, A., et al., *Interactions between the YycFG and PhoPR two-component systems in Bacillus subtilis: the PhoR kinase phosphorylates the non-cognate YycF response regulator upon phosphate limitation.* Mol Microbiol, 2006. **59**(4): p. 1199-215.

248. Mike, L.A., et al., *Two-component system cross-regulation integrates Bacillus anthracis response to heme and cell envelope stress.* PLoS Pathog, 2014. **10**(3): p. e1004044.

249. Pi, H., et al., *Directed evolution reveals the mechanism of HitRS signaling transduction in Bacillus anthracis.* PLoS Pathog, 2020. **16**(12): p. e1009148.

250. Pellecchia, M., et al., *NMR structure of the J-domain and the Gly/Phe-rich region of the Escherichia coli DnaJ chaperone.* J Mol Biol, 1996. **260**(2): p. 236-50.

251. Frees, D., et al., *Clp ATPases and ClpP proteolytic complexes regulate vital biological processes in low GC, Gram-positive bacteria.* Mol Microbiol, 2007. **63**(5): p. 1285-95.

252. Chandu, D. and D. Nandi, *Comparative genomics and functional roles of the ATP-dependent proteases Lon and Clp during cytosolic protein degradation.* Res Microbiol, 2004. **155**(9): p. 710-9.

253. Grimaud, R., et al., *Enzymatic and structural similarities between the Escherichia coli ATP-dependent proteases, ClpXP and ClpAP.* J Biol Chem, 1998. **273**(20): p. 12476-81.

254. Wang, J., J.A. Hartling, and J.M. Flanagan, *The structure of ClpP at 2.3 A resolution suggests a model for ATP-dependent proteolysis.* Cell, 1997. **91**(4): p. 447-56.

255. Wawrzynow, A., et al., *The ClpX heat-shock protein of Escherichia coli, the ATP-dependent substrate specificity component of the ClpP-ClpX protease, is a novel molecular chaperone.* EMBO J, 1995. **14**(9): p. 1867-77.

256. Gora, K.G., et al., *Regulated proteolysis of a transcription factor complex is critical to cell cycle progression in Caulobacter crescentus.* Mol Microbiol, 2013. **87**(6): p. 1277-89.

257. Gaspar, A.H., et al., *Bacillus anthracis sortase A (SrtA) anchors LPXTG motif-containing surface proteins to the cell wall envelope.* J Bacteriol, 2005. **187**(13): p. 4646-55.

258. Britton, R.A., et al., *Genome-wide analysis of the stationary-phase sigma factor (sigma-H) regulon of Bacillus subtilis.* J Bacteriol, 2002. **184**(17): p. 4881-90.

259. Wang, L., et al., *A novel histidine kinase inhibitor regulating development in Bacillus subtilis.* Genes Dev, 1997. **11**(19): p. 2569-79.

260. Perego, M., *A new family of aspartyl phosphate phosphatases targeting the sporulation transcription factor Spo0A of Bacillus subtilis.* Mol Microbiol, 2001. **42**(1): p. 133-43.

261. Smits, W.K., et al., *Temporal separation of distinct differentiation pathways by a dual specificity Rap-Phr system in Bacillus subtilis.* Mol Microbiol, 2007. **65**(1): p. 103-20.

262. Ng, B., J.W. Hekkelman, and J.N. Heersche, *The effect of cortisol on the adenosine 3',5'-monophosphate response to parathyroid hormone of bone in vitro.* Endocrinology, 1979. **104**(4): p. 1130-5.

263. Jiang, M., R. Grau, and M. Perego, *Differential processing of propeptide inhibitors of Rap phosphatases in Bacillus subtilis.* J Bacteriol, 2000. **182**(2): p. 303-10.

264. Lazazzera, B.A., et al., *An autoregulatory circuit affecting peptide signaling in Bacillus subtilis.* J Bacteriol, 1999. **181**(17): p. 5193-200.

265. Nakano, S., et al., *A regulatory protein that interferes with activator-stimulated transcription in bacteria.* Proc Natl Acad Sci U S A, 2003. **100**(7): p. 4233-8.

266. Surdel, M.C., et al., *Antibacterial photosensitization through activation of coproporphyrinogen oxidase.* Proc Natl Acad Sci U S A, 2017. **114**(32): p. E6652-E6659.

267. Gotfredsen, M. and K. Gerdes, *The Escherichia coli relBE genes belong to a new toxin-antitoxin gene family.* Mol Microbiol, 1998. **29**(4): p. 1065-76.

268. Bourret, R.B. and R.E. Silversmith, *Two-component signal transduction.* Curr Opin Microbiol, 2010. **13**(2): p. 113-5.

269. Flannagan, R.S., et al., *Staphylococcus aureus Uses the GraXRS Regulatory System To Sense and Adapt to the Acidified Phagolysosome in Macrophages.* mBio, 2018. **9**(4).

270. Al-Khodor, S., et al., *The PmrA/PmrB two-component system of Legionella pneumophila is a global regulator required for intracellular replication within macrophages and protozoa.* Infect Immun, 2009. **77**(1): p. 374-86.

271. Schroder, B.A., et al., *The proteome of lysosomes.* Proteomics, 2010. **10**(22): p. 4053-76.

272. Wu, Y., et al., *Type-IIA secreted phospholipase A2 is an endogenous antibiotic-like protein of the host.* Biochimie, 2010. **92**(6): p. 583-7.

273. Flannagan, R.S., G. Cosio, and S. Grinstein, *Antimicrobial mechanisms of phagocytes and bacterial evasion strategies.* Nat Rev Microbiol, 2009. **7**(5): p. 355-66.

274. Flannagan, R.S., B. Heit, and D.E. Heinrichs, *Antimicrobial Mechanisms of Macrophages and the Immune Evasion Strategies of Staphylococcus aureus.* Pathogens, 2015. **4**(4): p. 826-68.

275. Tang, X., et al., *P2X7 Receptor Regulates Internalization of Antimicrobial Peptide LL-37 by Human Macrophages That Promotes Intracellular Pathogen Clearance.* J Immunol, 2015. **195**(3): p. 1191-201.

276. Henderson, B., E. Allan, and A.R. Coates, *Stress wars: the direct role of host and bacterial molecular chaperones in bacterial infection.* Infect Immun, 2006. **74**(7): p. 3693-706.

277. Konkel, M.E., et al., *Characterization of the thermal stress response of Campylobacter jejuni.* Infect Immun, 1998. **66**(8): p. 3666-72.

278. Takaya, A., et al., *The DnaK/DnaJ chaperone machinery of Salmonella enterica serovar Typhimurium is essential for invasion of epithelial cells and survival within macrophages, leading to systemic infection.* Infect Immun, 2004. **72**(3): p. 1364-73.

279. Hensel, M., et al., *Simultaneous identification of bacterial virulence genes by negative selection.* Science, 1995. **269**(5222): p. 400-3.

280. Mei, J.M., et al., *Identification of Staphylococcus aureus virulence genes in a murine model of bacteraemia using signature-tagged mutagenesis.* Mol Microbiol, 1997. **26**(2): p. 399-407.

281. Turner, A.K., et al., *Identification of Salmonella typhimurium genes required for colonization of the chicken alimentary tract and for virulence in newly hatched chicks.* Infect Immun, 1998. **66**(5): p. 2099-106.

282. Gray, C.G., et al., *The identification of five genetic loci of Francisella novicida associated with intracellular growth.* FEMS Microbiol Lett, 2002. **215**(1): p. 53-6.

283. Ibrahim, Y.M., et al., *Contribution of the ATP-dependent protease ClpCP to the autolysis and virulence of Streptococcus pneumoniae.* Infect Immun, 2005. **73**(2): p. 730-40.

284. Rouquette, C., et al., *Identification of a ClpC ATPase required for stress tolerance and in vivo survival of Listeria monocytogenes.* Mol Microbiol, 1996. **21**(5): p. 977-87.

285. Rouquette, C., et al., *The ClpC ATPase of Listeria monocytogenes is a general stress protein required for virulence and promoting early bacterial escape from the phagosome of macrophages.* Mol Microbiol, 1998. **27**(6): p. 1235-45.

286. Nair, S., E. Milohanic, and P. Berche, *ClpC ATPase is required for cell adhesion and invasion of Listeria monocytogenes.* Infect Immun, 2000. **68**(12): p. 7061-8.

287. Kwon, H.Y., et al., *The ClpP protease of Streptococcus pneumoniae modulates virulence gene expression and protects against fatal pneumococcal challenge.* Infect Immun, 2004. **72**(10): p. 5646-53.

288. Cabiscol, E., J. Tamarit, and J. Ros, *Oxidative stress in bacteria and protein damage by reactive oxygen species.* Int Microbiol, 2000. **3**(1): p. 3-8.

289. Schrecke, K., S. Jordan, and T. Mascher, *Stoichiometry and perturbation studies of the LiaFSR system of Bacillus subtilis.* Mol Microbiol, 2013. **87**(4): p. 769-88.

290. Cai, S.J. and M. Inouye, *EnvZ-OmpR interaction and osmoregulation in Escherichia coli.* J Biol Chem, 2002. **277**(27): p. 24155-61.

291. Wayne, K.J., et al., *Localization and cellular amounts of the WalRKJ (VicRKX) two-component regulatory system proteins in serotype 2 Streptococcus pneumoniae.* J Bacteriol, 2010. **192**(17): p. 4388-94.

292. Langer, T., et al., *Successive action of DnaK, DnaJ and GroEL along the pathway of chaperone-mediated protein folding.* Nature, 1992. **356**(6371): p. 683-9.

293. Gamer, J., H. Bujard, and B. Bukau, *Physical interaction between heat shock proteins DnaK, DnaJ, and GrpE and the bacterial heat shock transcription factor sigma 32.* Cell, 1992. **69**(5): p. 833-42.

294. Liberek, K. and C. Georgopoulos, *Autoregulation of the Escherichia coli heat shock response by the DnaK and DnaJ heat shock proteins.* Proc Natl Acad Sci U S A, 1993. **90**(23): p. 11019-23.

295. Liberek, K., et al., *The DnaK chaperone modulates the heat shock response of Escherichia coli by binding to the sigma 32 transcription factor.* Proc Natl Acad Sci U S A, 1992. **89**(8): p. 3516-20.

296. Blaszczak, A., et al., *Both ambient temperature and the DnaK chaperone machine modulate the heat shock response in Escherichia coli by regulating the switch between sigma 70 and sigma 32 factors assembled with RNA polymerase.* EMBO J, 1995. **14**(20): p. 5085-93.

297. Chien, P., et al., *Direct and adaptor-mediated substrate recognition by an essential AAA+ protease.* Proc Natl Acad Sci U S A, 2007. **104**(16): p. 6590-5.

298. Sauer, R.T., et al., *Sculpting the proteome with AAA(+) proteases and disassembly machines.* Cell, 2004. **119**(1): p. 9-18.

299. Wortinger, M., M.J. Sackett, and Y.V. Brun, *CtrA mediates a DNA replication checkpoint that prevents cell division in Caulobacter crescentus.* EMBO J, 2000. **19**(17): p. 4503-12.

300. Ryan, K.R., E.M. Judd, and L. Shapiro, *The CtrA response regulator essential for Caulobacter crescentus cell-cycle progression requires a bipartite degradation signal for temporally controlled proteolysis.* J Mol Biol, 2002. **324**(3): p. 443-55.

301. McGrath, P.T., et al., *A dynamically localized protease complex and a polar specificity factor control a cell cycle master regulator.* Cell, 2006. **124**(3): p. 535-47.

302. Banecki, B., et al., *Structure-function analysis of the zinc finger region of the DnaJ molecular chaperone.* J Biol Chem, 1996. **271**(25): p. 14840-8.

303. Banecki, B., et al., *Structure-function analysis of the zinc-binding region of the Clpx molecular chaperone.* J Biol Chem, 2001. **276**(22): p. 18843-8.

304. Kragol, G., et al., *The antibacterial peptide pyrrhocoricin inhibits the ATPase actions of DnaK and prevents chaperone-assisted protein folding.* Biochemistry, 2001. **40**(10): p. 3016-26.

305. Cudic, M., et al., *Development of novel antibacterial peptides that kill resistant isolates.* Peptides, 2002. **23**(12): p. 2071-83.

306. McGillivray, S.M., et al., *Pharmacological inhibition of the ClpXP protease increases bacterial susceptibility to host cathelicidin antimicrobial peptides and cell envelope-active antibiotics.* Antimicrob Agents Chemother, 2012. **56**(4): p. 1854-61.

307. Bottcher, T. and S.A. Sieber, *Beta-lactones as privileged structures for the active-site labeling of versatile bacterial enzyme classes.* Angew Chem Int Ed Engl, 2008. **47**(24): p. 4600-3.

308. Brotz-Oesterhelt, H., et al., *Dysregulation of bacterial proteolytic machinery by a new class of antibiotics.* Nat Med, 2005. **11**(10): p. 1082-7.

309. Cheng, L., et al., *Discovery of antibacterial cyclic peptides that inhibit the ClpXP protease.* Protein Sci, 2007. **16**(8): p. 1535-42.

310. Worthington, R.J., M.S. Blackledge, and C. Melander, *Small-molecule inhibition of bacterial two-component systems to combat antibiotic resistance and virulence.* Future Med Chem, 2013. **5**(11): p. 1265-84.

311. Gotoh, Y., et al., *Two-component signal transduction as potential drug targets in pathogenic bacteria.* Curr Opin Microbiol, 2010. **13**(2): p. 232-9.

312. Watanabe, T., et al., *Inhibitors targeting two-component signal transduction.* Adv Exp Med Biol, 2008. **631**: p. 229-36.

313. Montville, T.J., et al., *Thermal resistance of spores from virulent strains of Bacillus anthracis and potential surrogates.* J Food Prot, 2005. **68**(11): p. 2362-6.

314. Nicholson, W.L. and B. Galeano, *UV resistance of Bacillus anthracis spores revisited: validation of Bacillus subtilis spores as UV surrogates for spores of B. anthracis Sterne.* Appl Environ Microbiol, 2003. **69**(2): p. 1327-30.

315. Hahn, B.L., S. Sharma, and P.G. Sohnle, *Analysis of epidermal entry in experimental cutaneous Bacillus anthracis infections in mice.* J Lab Clin Med, 2005. **146**(2): p. 95-102.

316. Bravata, D.M., et al., *Inhalational, gastrointestinal, and cutaneous anthrax in children: a systematic review of cases: 1900 to 2005.* Arch Pediatr Adolesc Med, 2007. **161**(9): p. 896-905.

317. Doganay, M., G. Metan, and E. Alp, *A review of cutaneous anthrax and its outcome.* J Infect Public Health, 2010. **3**(3): p. 98-105.

318. Griffith, K.S., et al., *Bioterrorism-related inhalational anthrax in an elderly woman, Connecticut, 2001.* Emerg Infect Dis, 2003. **9**(6): p. 681-8.

319. Kuehnert, M.J., et al., *Clinical features that discriminate inhalational anthrax from other acute respiratory illnesses.* Clin Infect Dis, 2003. **36**(3): p. 328-36.

320. Tepper, M. and J. Whitehead, *Clinical predictors of bioterrorism-related inhalational anthrax.* Lancet, 2005. **365**(9455): p. 214; author reply 215.

321. Borio, L., et al., *Death due to bioterrorism-related inhalational anthrax: report of 2 patients.* JAMA, 2001. **286**(20): p. 2554-9.

322. Swartz, M.N., *Recognition and management of anthrax--an update.* N Engl J Med, 2001. **345**(22): p. 1621-6.

323. Weiner, Z.P. and I.J. Glomski, *Updating perspectives on the initiation of Bacillus anthracis growth and dissemination through its host.* Infect Immun, 2012. **80**(5): p. 1626-33.

324. Gu, C., et al., *Activation of the classical complement pathway by Bacillus anthracis is the primary mechanism for spore phagocytosis and involves the spore surface protein BclA.* J Immunol, 2012. **188**(9): p. 4421-31.

325. Wang, Y., et al., *Bacillus anthracis Spore Surface Protein BclA Mediates Complement Factor H Binding to Spores and Promotes Spore Persistence.* PLoS Pathog, 2016. **12**(6): p. e1005678.

326. Candela, T. and A. Fouet, *Bacillus anthracis CapD, belonging to the gamma-glutamyltranspeptidase family, is required for the covalent anchoring of capsule to peptidoglycan.* Mol Microbiol, 2005. **57**(3): p. 717-26.

327. Sharma, S., R. Bhatnagar, and D. Gaur, *Bacillus anthracis Poly-gamma-D-Glutamate Capsule Inhibits Opsonic Phagocytosis by Impeding Complement Activation.* Front Immunol, 2020. **11**: p. 462.

328. Brezillon, C., et al., *Capsules, toxins and AtxA as virulence factors of emerging Bacillus cereus biovar anthracis.* PLoS Negl Trop Dis, 2015. **9**(4): p. e0003455.

329. Hoover, D.L., et al., *Anthrax edema toxin differentially regulates lipopolysaccharide-induced monocyte production of tumor necrosis factor alpha and interleukin-6 by increasing intracellular cyclic AMP.* Infect Immun, 1994. **62**(10): p. 4432-9.

330. Moayeri, M. and S.H. Leppla, *Cellular and systemic effects of anthrax lethal toxin and edema toxin.* Mol Aspects Med, 2009. **30**(6): p. 439-55.

331. Leppla, S.H., *Bacillus anthracis calmodulin-dependent adenylate cyclase: chemical and enzymatic properties and interactions with eucaryotic cells.* Adv Cyclic Nucleotide Protein Phosphorylation Res, 1984. **17**: p. 189-98.

332. Duesbery, N.S., et al., *Proteolytic inactivation of MAP-kinase-kinase by anthrax lethal factor.* Science, 1998. **280**(5364): p. 734-7.

333. Singh, Y., et al., *Oligomerization of anthrax toxin protective antigen and binding of lethal factor during endocytic uptake into mammalian cells.* Infect Immun, 1999. **67**(4): p. 1853-9.

334. Glomski, I.J., et al., *Noncapsulated toxinogenic Bacillus anthracis presents a specific growth and dissemination pattern in naive and protective antigen-immune mice.* Infect Immun, 2007. **75**(10): p. 4754-61.

335. Ross, J.M., *The pathogenesis of anthrax following the administration of spores by the respiratory route.* Journal of Pathology and Bacteriology, 1957. **73**(2): p. 485-94.

336. Pitt, A., et al., *Alterations in the protein composition of maturing phagosomes.* J Clin Invest, 1992. **90**(5): p. 1978-83.

337. Hackam, D.J., et al., *Regulation of phagosomal acidification. Differential targeting of Na+/H+ exchangers, Na+/K+-ATPases, and vacuolar-type H+-atpases.* J Biol Chem, 1997. **272**(47): p. 29810-20.

338. Lam, G.Y., J. Huang, and J.H. Brumell, *The many roles of NOX2 NADPH oxidase-derived ROS in immunity.* Semin Immunopathol, 2010. **32**(4): p. 415-30.

339. Bogdan, C., M. Rollinghoff, and A. Diefenbach, *The role of nitric oxide in innate immunity.* Immunol Rev, 2000. **173**: p. 17-26.

340. Sheldon, J.R. and E.P. Skaar, *Metals as phagocyte antimicrobial effectors.* Curr Opin Immunol, 2019. **60**: p. 1-9.

341. Wessling-Resnick, M., *Nramp1 and Other Transporters Involved in Metal Withholding during Infection.* J Biol Chem, 2015. **290**(31): p. 18984-90.

342. Gruenheid, S., et al., *Natural resistance to infection with intracellular pathogens: the Nramp1 protein is recruited to the membrane of the phagosome.* J Exp Med, 1997. **185**(4): p. 717-30.

343. Samanovic, M.I., et al., *Copper in microbial pathogenesis: meddling with the metal.* Cell Host Microbe, 2012. **11**(2): p. 106-15.

344. Botella, H., et al., *Mycobacterial p(1)-type ATPases mediate resistance to zinc poisoning in human macrophages.* Cell Host Microbe, 2011. **10**(3): p. 248-59.

345. de Been, M., et al., *Comparative analysis of two-component signal transduction systems of Bacillus cereus, Bacillus thuringiensis and Bacillus anthracis.* Microbiology, 2006. **152**(Pt 10): p. 3035-48.

346. Laub, M.T., *Keeping Signals Straight: How Cells Process Information and Make Decisions.* PLoS Biol, 2016. **14**(7): p. e1002519.

347. Uhl, F.E., et al., *Preclinical validation and imaging of Wnt-induced repair in human 3D lung tissue cultures.* Eur Respir J, 2015. **46**(4): p. 1150-66.

348. Alsafadi, H.N., et al., *An ex vivo model to induce early fibrosis-like changes in human precision-cut lung slices.* Am J Physiol Lung Cell Mol Physiol, 2017. **312**(6): p. L896-L902.

349. Sucre, J.M.S., et al., *Hyperoxia Injury in the Developing Lung Is Mediated by Mesenchymal Expression of Wnt5A.* Am J Respir Crit Care Med, 2020. **201**(10): p. 1249-1262.

350. Grimm, J.B., et al., *A general method to fine-tune fluorophores for live-cell and in vivo imaging.* Nat Methods, 2017. **14**(10): p. 987-994.

351. Su, S., et al., *Construction and characterization of stable, constitutively expressed, chromosomal green and red fluorescent transcriptional fusions in the select agents, Bacillus anthracis, Yersinia pestis, Burkholderia mallei, and Burkholderia pseudomallei.* Microbiologyopen, 2014. **3**(5): p. 610-29.

352. Albrink, W.S., *Pathogenesis of inhalation anthrax.* Bacteriol Rev, 1961. **25**: p. 268-73.

353. Liu, G., et al., *Use of precision cut lung slices as a translational model for the study of lung biology.* Respir Res, 2019. **20**(1): p. 162.

354. Pieretti, A.C., et al., *A novel in vitro model to study alveologenesis.* Am J Respir Cell Mol Biol, 2014. **50**(2): p. 459-69.

355. Alsafadi, H.N., et al., *Applications and Approaches for Three-Dimensional Precision-Cut Lung Slices. Disease Modeling and Drug Discovery.* Am J Respir Cell Mol Biol, 2020. **62**(6): p. 681-691.

356. Kumar, M., et al., *Integrated one- and two-photon scanned oblique plane illumination (SOPi) microscopy for rapid volumetric imaging*. Opt Express, 2018. **26**(10): p. 13027-13041.

357. Hoffmann, F.M., et al., *Distribution and Interaction of Murine Pulmonary Phagocytes in the Naive and Allergic Lung.* Front Immunol, 2018. **9**: p. 1046.

358. Abdul Hamid, A.I., et al., *A mouse ear skin model to study the dynamics of innate immune responses against Staphylococcus aureus biofilms.* BMC Microbiol, 2020. **20**(1): p. 22.

359. Blondel, C.J., et al., *CRISPR/Cas9 Screens Reveal Requirements for Host Cell Sulfation and Fucosylation in Bacterial Type III Secretion System-Mediated Cytotoxicity.* Cell Host Microbe, 2016. **20**(2): p. 226-37.

360. Shalem, O., et al., *Genome-scale CRISPR-Cas9 knockout screening in human cells.* Science, 2014. **343**(6166): p. 84-87.

361. Wang, T., et al., *Genetic screens in human cells using the CRISPR-Cas9 system.* Science, 2014. **343**(6166): p. 80-4.

362. Henkel, L., et al., *Genome-scale CRISPR screening at high sensitivity with an empirically designed sgRNA library.* BMC Biol, 2020. **18**(1): p. 174.

363. Napier, B.A. and D.M. Monack, *Creating a RAW264.7 CRISPR-Cas9 Genome Wide Library.* Bio Protoc, 2017. **7**(10).

364. Haney, M.S., et al., *Identification of phagocytosis regulators using magnetic genome-wide CRISPR screens.* Nat Genet, 2018. **50**(12): p. 1716-1727.

365. Napier, B.A., et al., *Complement pathway amplifies caspase-11-dependent cell death and endotoxin-induced sepsis severity.* J Exp Med, 2016. **213**(11): p. 2365-2382.

366. Welkos, S., et al., *Animal Models for the Pathogenesis, Treatment, and Prevention of Infection by Bacillus anthracis.* Microbiol Spectr, 2015. **3**(1): p. TBS-0001-2012.

367. Goel, A.K., *Anthrax: A disease of biowarfare and public health importance.* World J Clin Cases, 2015. **3**(1): p. 20-33.

368. Ruthel, G., et al., *Time-lapse confocal imaging of development of Bacillus anthracis in macrophages.* J Infect Dis, 2004. **189**(7): p. 1313-6.

369. Fiole, D., et al., *Two-photon intravital imaging of lungs during anthrax infection reveals long-lasting macrophage-dendritic cell contacts.* Infect Immun, 2014. **82**(2): p. 864-72.

370. Dalebroux, Z.D. and S.I. Miller, *Salmonellae PhoPQ regulation of the outer membrane to resist innate immunity.* Curr Opin Microbiol, 2014. **17**: p. 106-13.

371. Liu, J.Z., et al., *Innate Immune Interactions between Bacillus anthracis and Host Neutrophils.* Front Cell Infect Microbiol, 2018. **8**: p. 2.

372. Ascough, S., et al., *CD4+ T Cells Targeting Dominant and Cryptic Epitopes from Bacillus anthracis Lethal Factor.* Front Microbiol, 2015. **6**: p. 1506.

373. Kirchdoerfer, R.N., et al., *Variable lymphocyte receptor recognition of the immunodominant glycoprotein of Bacillus anthracis spores.* Structure, 2012. **20**(3): p. 479-86.

374. Collins, M.K., et al., *A role for TNF-alpha in alveolar macrophage damage-associated molecular pattern release.* JCI Insight, 2020. **5**(9).

375. Chen, P.M., et al., *The two-component system ScnRK of Streptococcus mutans affects hydrogen peroxide resistance and murine macrophage killing.* Microbes Infect, 2008. **10**(3): p. 293-301.

376. Hall, J.W., et al., *The Staphylococcus aureus AirSR Two-Component System Mediates Reactive Oxygen Species Resistance via Transcriptional Regulation of Staphyloxanthin Production.* Infect Immun, 2017. **85**(2).

377. Park, R.J., et al., *A genome-wide CRISPR screen identifies a restricted set of HIV host dependency factors.* Nat Genet, 2017. **49**(2): p. 193-203.

378. Han, J., et al., *Genome-wide CRISPR/Cas9 Screen Identifies Host Factors Essential for Influenza Virus Replication.* Cell Rep, 2018. **23**(2): p. 596-607.

379. Park, J.S., et al., *A FACS-Based Genome-wide CRISPR Screen Reveals a Requirement for COPI in Chlamydia trachomatis Invasion.* iScience, 2019. **11**: p. 71-84.

380. Pacheco, A.R., et al., *CRISPR Screen Reveals that EHEC's T3SS and Shiga Toxin Rely on Shared Host Factors for Infection.* mBio, 2018. **9**(3).

381. Langel, F.D., et al., *Alveolar macrophages infected with Ames or Sterne strain of Bacillus anthracis elicit differential molecular expression patterns.* PLoS One, 2014. **9**(2): p. e87201.

382. Hanna, P., *Anthrax pathogenesis and host response.* Curr Top Microbiol Immunol, 1998. **225**: p. 13-35.

383. Cote, C.K. and S.L. Welkos, *Anthrax Toxins in Context of Bacillus anthracis Spores and Spore Germination.* Toxins (Basel), 2015. **7**(8): p. 3167-78.

384. Cleret-Buhot, A., et al., *Both lethal and edema toxins of Bacillus anthracis disrupt the human dendritic cell chemokine network.* PLoS One, 2012. **7**(8): p. e43266.

385. Laub, M.T. and M. Goulian, *Specificity in two-component signal transduction pathways.* Annu Rev Genet, 2007. **41**: p. 121-45.

386. Sewell, D.L., *Laboratory safety practices associated with potential agents of biocrime or bioterrorism.* J Clin Microbiol, 2003. **41**(7): p. 2801-9.

387. Nulens, E. and A. Voss, *Laboratory diagnosis and biosafety issues of biological warfare agents.* Clin Microbiol Infect, 2002. **8**(8): p. 455-66.

388. Preisz, H., *Experimentelle studien ueber virulenz, empfaenglichkeit und immunitaet beim milzbrand.* Zeitschrift für Immunitäts-Forschung, 1909. **5**: p. 341-452.

389. Turnbull, P.C., *Anthrax vaccines: past, present and future.* Vaccine, 1991. **9**(8): p. 533-539.

390. Boyer, A.E., et al., *Kinetics of lethal factor and poly-D-glutamic acid antigenemia during inhalation anthrax in rhesus macaques.* Infect Immun, 2009. **77**(8): p. 3432-41.

391. Sanderson, M.J., *Exploring lung physiology in health and disease with lung slices.* Pulm Pharmacol Ther, 2011. **24**(5): p. 452-65.

392. Rosales Gerpe, M.C., et al., *Use of Precision-Cut Lung Slices as an Ex Vivo Tool for Evaluating Viruses and Viral Vectors for Gene and Oncolytic Therapy.* Mol Ther Methods Clin Dev, 2018. **10**: p. 245-256.

393. Liberati, T.A., M.R. Randle, and L.A. Toth, *In vitro lung slices: a powerful approach for assessment of lung pathophysiology.* Expert Rev Mol Diagn, 2010. **10**(4): p. 501-8.

394. de Graaf, I.A., et al., *Preparation and incubation of precision-cut liver and intestinal slices for application in drug metabolism and toxicity studies.* Nat Protoc, 2010. **5**(9): p. 1540-51.

395. Andreu, N., et al., *Primary macrophages and J774 cells respond differently to infection with Mycobacterium tuberculosis.* Sci Rep, 2017. **7**: p. 42225.

396. Berghaus, L.J., et al., *Innate immune responses of primary murine macrophage-lineage cells and RAW 264.7 cells to ligands of Toll-like receptors 2, 3, and 4.* Comp Immunol Microbiol Infect Dis, 2010. **33**(5): p. 443-54.

397. Kaur, G. and J.M. Dufour, *Cell lines: Valuable tools or useless artifacts.* Spermatogenesis, 2012. **2**(1): p. 1-5.

398. Pan, C., et al., *Comparative proteomic phenotyping of cell lines and primary cells to assess preservation of cell type-specific functions.* Mol Cell Proteomics, 2009. **8**(3): p. 443-50.

399. Mansilla, M.C. and D. de Mendoza, *The Bacillus subtilis desaturase: a model to understand phospholipid modification and temperature sensing.* Arch Microbiol, 2005. **183**(4): p. 229-35.

400. Porrini, L., et al., *Cerulenin inhibits unsaturated fatty acids synthesis in Bacillus subtilis by modifying the input signal of DesK thermosensor.* Microbiologyopen, 2014. **3**(2): p. 213-24.

401. Geva, G. and R. Sharan, *Identification of protein complexes from co-immunoprecipitation data.* Bioinformatics, 2011. **27**(1): p. 111-7.

402. Kerppola, T.K., *Bimolecular fluorescence complementation (BiFC) analysis as a probe of protein interactions in living cells.* Annu Rev Biophys, 2008. **37**: p. 465-87.

403. Hristozova, N., P. Tompa, and D. Kovacs, *A Novel Method for Assessing the Chaperone Activity of Proteins.* PLoS One, 2016. **11**(8): p. e0161970.

404. Lee, G.J., *Assaying proteins for molecular chaperone activity.* Methods Cell Biol, 1995. **50**: p. 325-34.

405. Kruger, E., et al., *Clp-mediated proteolysis in Gram-positive bacteria is autoregulated by the stability of a repressor.* EMBO J, 2001. **20**(4): p. 852-63.

406. Bewley, M.C., et al., *Turned on for degradation: ATPase-independent degradation by ClpP.* J Struct Biol, 2009. **165**(2): p. 118-25.

407. Peng, Q., et al., *Disruption of Two-component System LytSR Affects Forespore Engulfment in Bacillus thuringiensis.* Front Cell Infect Microbiol, 2017. **7**: p. 468.

408. Diomande, S.E., et al., *Expression of the genes encoding the CasK/R two-component system and the DesA desaturase during Bacillus cereus cold adaptation.* FEMS Microbiol Lett, 2016. **363**(16).

409. Ge, X., et al., *Ligand determinants of nisin for its induction activity.* J Dairy Sci, 2016. **99**(7): p. 5022-5031.

410. Echenique, J.R., S. Chapuy-Regaud, and M.C. Trombe, *Competence regulation by oxygen in Streptococcus pneumoniae: involvement of ciaRH and comCDE.* Mol Microbiol, 2000. **36**(3): p. 688-96.

411. Stein, T., et al., *Dual control of subtilin biosynthesis and immunity in Bacillus subtilis.* Mol Microbiol, 2002. **44**(2): p. 403-16.

412. Pi, H. and J.D. Helmann, *Sequential induction of Fur-regulated genes in response to iron limitation in Bacillus subtilis.* Proc Natl Acad Sci U S A, 2017. **114**(48): p. 12785-12790.

413. Gat, O., et al., *Characterization of Bacillus anthracis iron-regulated surface determinant (Isd) proteins containing NEAT domains.* Mol Microbiol, 2008. **70**(4): p. 983-99.

414. Jones, M.B. and M.J. Blaser, *Detection of a luxS-signaling molecule in Bacillus anthracis.* Infect Immun, 2003. **71**(7): p. 3914-9.

415. Jones, M.B., et al., *Inhibition of Bacillus anthracis growth and virulence-gene expression by inhibitors of quorum-sensing.* J Infect Dis, 2005. **191**(11): p. 1881-8.

416. Jones, M.B., et al., *Role of luxS in Bacillus anthracis growth and virulence factor expression.* Virulence, 2010. **1**(2): p. 72-83.

417. Minami, N., et al., *Regulatory role of cardiolipin in the activity of an ATP-dependent protease, Lon, from Escherichia coli.* J Biochem, 2011. **149**(5): p. 519-27.

418. Kunkle, T., et al., *Hydroxybiphenylamide GroEL/ES Inhibitors Are Potent Antibacterials against Planktonic and Biofilm Forms of Staphylococcus aureus.* J Med Chem, 2018. **61**(23): p. 10651-10664.

419. Frase, H., J. Hudak, and I. Lee, *Identification of the proteasome inhibitor MG262 as a potent ATP-dependent inhibitor of the Salmonella enterica serovar Typhimurium Lon protease.* Biochemistry, 2006. **45**(27): p. 8264-74.

420. Jiang, J., et al., *Structural basis of J cochaperone binding and regulation of Hsp70.* Mol Cell, 2007. **28**(3): p. 422-33.

421. Dougan, D.A., et al., *AAA+ proteins and substrate recognition, it all depends on their partner in crime.* FEBS Lett, 2002. **529**(1): p. 6-10.

422. Flynn, J.M., et al., *Proteomic discovery of cellular substrates of the ClpXP protease reveals five classes of ClpX-recognition signals.* Mol Cell, 2003. **11**(3): p. 671-83.

423. Oh, T.G., A.R. Kwon, and E.C. Choi, *Induction of ermAMR from a clinical strain of Enterococcus faecalis by 16-membered-ring macrolide antibiotics.* J Bacteriol, 1998. **180**(21): p. 5788-91.

424. Chang, L., *Nikon's large-format multiphoton system for intravital imaging.* Nature Methods, 2015. **12**(12): p. iii-iv.

425. Stack, E.C., et al., *Multiplexed immunohistochemistry, imaging, and quantitation: a review, with an assessment of Tyramide signal amplification, multispectral imaging and multiplex analysis.* Methods, 2014. **70**(1): p. 46-58.

426. Hofman, P., et al., *Multiplexed Immunohistochemistry for Molecular and Immune Profiling in Lung Cancer-Just About Ready for Prime-Time?* Cancers (Basel), 2019. **11**(3).

427. Tan, W.C.C., et al., *Overview of multiplex immunohistochemistry/immunofluorescence techniques in the era of cancer immunotherapy.* Cancer Commun (Lond), 2020. **40**(4): p. 135-153.

428. Oliveira, C.A., Y. Kashman, and B. Mantovani, *Effects of latrunculin A on immunological phagocytosis and macrophage spreading-associated changes in the F-actin/G-actin content of the cells.* Chem Biol Interact, 1996. **100**(2): p. 141-53.

429. Muroi, M., et al., *Folimycin (concanamycin A), a specific inhibitor of V-ATPase, blocks intracellular translocation of the glycoprotein of vesicular stomatitis virus before arrival to the Golgi apparatus.* Cell Struct Funct, 1993. **18**(3): p. 139-49.

430. Fujiwara, T., et al., *Brefeldin A causes disassembly of the Golgi complex and accumulation of secretory proteins in the endoplasmic reticulum.* J Biol Chem, 1988. **263**(34): p. 18545-52.

431. Axline, S.G. and E.P. Reaven, *Inhibition of phagocytosis and plasma membrane mobility of the cultivated macrophage by cytochalasin B. Role of subplasmalemmal microfilaments.* J Cell Biol, 1974. **62**(3): p. 647-59.